

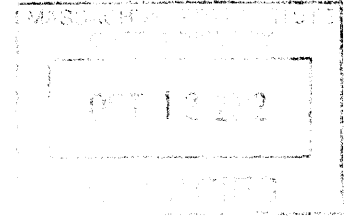
Thermal Mass Performance in Residential Construction:  
An Energy Analysis Using a Cube Model

by

Alison C. Ledwith

Bachelor of Architecture  
Bachelor of Science in Architectural Engineering  
The University of Texas at Austin, 2011

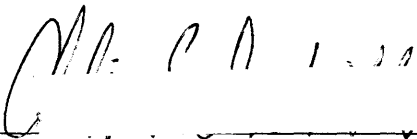
ARCHIVES





SUBMITTED TO THE DEPARTMENT OF CIVIL AND ENVIRONMENTAL ENGINEERING  
IN PARTIAL FULFILLMENT OF THE REQUIREMENTS FOR THE DEGREE OF  
MASTER OF SCIENCE IN CIVIL AND ENVIRONMENTAL ENGINEERING  
AT THE  
MASSACHUSETTS INSTITUTE OF TECHNOLOGY


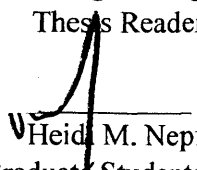
September 2012

© 2012 Massachusetts Institute of Technology. All rights reserved.

Signature of Author:   
Department of Civil and Environmental Engineering  
August 10, 2012

Certified by:   
Franz-Josef Ulm  
Professor of Civil and Environmental Engineering  
Thesis Supervisor

Certified by:   
Randa Ghattas, AIA  
Research Associate of Civil and Environmental Engineering  
Thesis Reader

Accepted by:    
Heidi M. Nepf  
Chair, Departmental Committee for Graduate Students



Thermal Mass Performance in Residential Construction:  
An Energy Analysis Using a Cube Model

by

Alison C. Ledwith

Submitted to the Department of Civil and Environmental Engineering  
on August 10, 2012 in Partial Fulfillment of the  
Requirements for the Degree of Master of Science in  
Civil and Environmental Engineering

ABSTRACT

Given the pervasiveness of energy efficiency concerns in the built environment, this research aims to answer key questions regarding the performance of thermal mass construction. The work presents the Cube Model, a simplified model of the single-family home. The model combines simplified geometry and equivalent envelope parameters with accurate climate data and internal loading assumptions. The model first addresses the notion as to whether building simplification is a valid means of analysis through a calibration and validation study. Then, the model is used to address three research areas on passive thermal mass: (1) the quantification of thermal mass performance with respect to material thermal properties; (2) the optimization of thermal mass performance for given material parameters; and (3) the sensitivity of thermal mass performance to infiltration and geometry effects. The experiments for wall and slab constructions, to address the first research area, demonstrate that the energy savings from thermal mass are both climate and season dependent. Results provide the magnitude of energy savings in fifty climates across the United States. Optimization experiments on the material thickness and conductivity, to address the second research area, show that constructions do not reach peak thermal mass performance at the same thermal properties in all climates. Sensitivity analyses, to address the third research area, indicate that passive thermal mass and tight construction practices can be mutually optimized without a trade-off of energy performance. Geometry effects demonstrate that modifications in building design can either benefit or hinder the performance of passive thermal mass. The combination of the results suggests that optimum design for thermal mass performance and the resulting energy consumption are climate-dependent and sensitive to many factors aside from material thermal properties.

Thesis Supervisor: Franz-Josef Ulm

Title: Professor of Civil and Environmental Engineering

Thesis Reader: Randa Ghattas

Title: Research Associate of Civil and Environmental Engineering



# Contents

<b>I</b>	<b>General Presentation</b>	<b>23</b>
<b>1</b>	<b>Introduction</b>	<b>24</b>
1.1	Research Premise . . . . .	24
1.2	Rationale for Research . . . . .	25
1.3	Research Approach . . . . .	27
1.4	Research Outline . . . . .	28
1.5	Chapter Summary . . . . .	29
<b>2</b>	<b>Literature Review</b>	<b>30</b>
2.1	Energy Modeling Overview . . . . .	30
2.1.1	DOE-2.1E . . . . .	31
2.1.2	EnergyPlus. . . . .	31
2.1.3	ESP-r. . . . .	32
2.1.4	TRNSYS. . . . .	32
2.1.5	Selection and Discussion . . . . .	32
2.2	Software Limitations . . . . .	33
2.3	Relevant Building Standards . . . . .	34
2.3.1	Building America House Simulation Protocol . . . . .	34
2.3.2	International Energy Conservation Code 2012 . . . . .	35
2.3.3	American Society for Heating, Refrigeration, and Air Conditioning . . . . .	35
2.4	Thermal Mass . . . . .	36
2.4.1	Effectiveness of Thermal Mass . . . . .	37
2.4.2	Reduction of Peak Demand . . . . .	38
2.4.3	Reduction of Overall Energy Consumption . . . . .	38
2.4.4	Relationship to Thermal Comfort . . . . .	40
2.5	Chapter Summary . . . . .	40

<b>II</b>	<b>Model Development, Calibration, and Validation</b>	<b>42</b>
<b>3</b>	<b>The Cube Model</b>	<b>43</b>
3.1	Model Overview . . . . .	43
3.1.1	Heat Balance. . . . .	43
3.1.2	Mass Balance . . . . .	47
3.2	Methodology . . . . .	49
3.2.1	Simplified Geometry. . . . .	50
3.2.1.1	Basic Cube Geometry Conversion . . . . .	50
3.2.1.2	Advanced Cube Geometry Conversion. . . . .	51
3.2.2	Equivalent Envelope Parameters . . . . .	52
3.2.3	Idealized HVAC System. . . . .	55
3.2.4	Accurate Loading . . . . .	56
3.2.4.1	Internal Mass . . . . .	56
3.2.4.2	People . . . . .	56
3.2.4.3	Appliances . . . . .	57
3.2.4.4	Domestic Hot Water . . . . .	57
3.2.4.5	Lighting . . . . .	58
3.3	Internal Model Assumptions and References . . . . .	58
3.3.1	Climate. . . . .	59
3.3.2	Window Parameters . . . . .	60
3.3.3	Infiltration and Ventilation. . . . .	61
3.3.4	Ground Heat Transfer . . . . .	61
3.4	Known Limitations. . . . .	61
3.5	Chapter Summary . . . . .	62
<b>4</b>	<b>Calibration and Validation</b>	<b>63</b>
4.1	Premise . . . . .	63
4.2	Envelope Calibration . . . . .	64
4.3	Geometry Calibration . . . . .	67
4.4	Calibration and Validation to Research Report R11-01 . . . . .	72
4.4.1	Experimental Simulation Setup . . . . .	74
4.4.2	Results . . . . .	76
4.5	Chapter Summary . . . . .	78
<b>5</b>	<b>Versatility</b>	<b>79</b>
5.1	Experimental Simulation Setup . . . . .	79
5.2	Results . . . . .	80
5.3	Chapter Summary . . . . .	86

<b>III</b>	<b>Application to Passive Thermal Mass</b>	<b>87</b>
<b>6</b>	<b>Thermal Mass of Equivalent Walls</b>	<b>88</b>
6.1	Introduction . . . . .	88
6.2	Experimental Simulation Setup . . . . .	89
6.3	Local Results . . . . .	90
6.3.1	Diffusivity . . . . .	90
6.3.1.1	San Francisco, CA - Mild, Marine Climate . . . . .	91
6.3.1.2	Phoenix, AZ - Hot, Dry Climate . . . . .	95
6.3.1.3	Miami, FL - Hot, Humid Climate . . . . .	99
6.3.1.4	Anchorage, AK - Cold Climate . . . . .	103
6.3.2	Seasonal Effects of Thermal Mass . . . . .	107
6.3.3	Discussion . . . . .	111
6.4	National Results . . . . .	112
6.4.1	Comparison of Normalized Energy Consumption . . . . .	112
6.4.2	Mapping the Results . . . . .	113
6.5	Chapter Summary . . . . .	120
<b>7</b>	<b>Thermal Mass of Equivalent Slabs</b>	<b>121</b>
7.1	Introduction and Experimental Simulation Setup . . . . .	121
7.2	Local Results . . . . .	121
7.2.1	Diffusivity . . . . .	122
7.2.1.1	San Francisco, CA - Mild, Marine Climate . . . . .	122
7.2.1.2	Phoenix, AZ - Hot, Dry Climate . . . . .	126
7.2.1.3	Miami, FL - Hot, Humid Climate . . . . .	130
7.2.1.4	Anchorage, AK - Cold Climate . . . . .	134
7.2.2	Seasonal Effects of Thermal Mass . . . . .	138
7.2.3	Discussion . . . . .	142
7.3	National Results . . . . .	142
7.3.1	Comparison of Normalized Energy Consumption . . . . .	143
7.3.2	Mapping the Results . . . . .	144
7.4	Chapter Summary . . . . .	150
<b>IV</b>	<b>Sensitivity Analysis of Thermal Mass Results</b>	<b>151</b>
<b>8</b>	<b>Infiltration</b>	<b>152</b>
8.1	Experimental Simulation Setup . . . . .	152
8.2	Results . . . . .	153
8.2.1	San Francisco, CA - Mild, Marine Climate . . . . .	153

8.2.2	Phoenix, AZ - Hot, Dry Climate. . . . .	155
8.2.3	Miami, FL - Hot, Humid Climate . . . . .	157
8.2.4	Anchorage, AK - Cold Climate . . . . .	158
8.2.5	Optimization and National Scale . . . . .	160
8.3	Chapter Summary . . . . .	164
<b>9</b>	<b>Geometry Effects</b>	<b>165</b>
9.1	Experimental Simulation Setup . . . . .	165
9.2	Incorporating the Attic . . . . .	166
9.2.1	San Francisco, CA - Mild, Marine Climate . . . . .	166
9.2.2	Phoenix, AZ - Hot, Dry Climate. . . . .	168
9.2.3	Miami, FL - Hot, Humid Climate . . . . .	169
9.2.4	Anchorage, AK - Cold Climate . . . . .	171
9.2.5	Discussion . . . . .	172
9.3	Testing Internal Slabs. . . . .	172
9.3.1	San Francisco, CA - Mild, Marine Climate . . . . .	173
9.3.2	Phoenix, AZ - Hot, Dry Climate. . . . .	174
9.3.3	Miami, FL - Hot, Humid Climate . . . . .	176
9.3.4	Anchorage, AK - Cold Climate . . . . .	177
9.3.5	Discussion . . . . .	179
9.4	Modeling the Basement . . . . .	179
9.4.1	San Francisco, CA - Mild, Marine Climate . . . . .	179
9.4.2	Phoenix, AZ - Hot, Dry Climate. . . . .	181
9.4.3	Miami, FL - Hot, Humid Climate . . . . .	183
9.4.4	Anchorage, AK - Cold Climate . . . . .	185
9.4.5	Discussion . . . . .	186
9.5	Height Effects . . . . .	186
9.5.1	San Francisco, CA - Mild, Marine Climate . . . . .	187
9.5.2	Phoenix, AZ - Hot, Dry Climate. . . . .	189
9.5.3	Miami, FL - Hot, Humid Climate . . . . .	191
9.5.4	Anchorage, AK - Cold Climate . . . . .	192
9.5.5	Discussion . . . . .	194
9.6	Plan Aspect Ratio Effects . . . . .	195
9.6.1	San Francisco, CA - Mild, Marine Climate . . . . .	195
9.6.2	Phoenix, AZ - Hot, Dry Climate. . . . .	197
9.6.3	Miami, FL - Hot, Humid Climate . . . . .	199
9.6.4	Anchorage, AK - Cold Climate . . . . .	200
9.6.5	Discussion . . . . .	202
9.7	Glazing Percentage Effects. . . . .	203



9.7.1	San Francisco, CA - Mild, Marine Climate . . . . .	203
9.7.2	Phoenix, AZ - Hot, Dry Climate. . . . .	205
9.7.3	Miami, FL - Hot, Humid Climate . . . . .	207
9.7.4	Anchorage, AK - Cold Climate . . . . .	208
9.7.5	Discussion . . . . .	210
9.8	Chapter Summary . . . . .	210
<b>V</b>	<b>Conclusion</b>	<b>211</b>
<b>10</b>	<b>Conclusion</b>	<b>212</b>
10.1	Main Findings . . . . .	212
10.2	Implications for Building Design . . . . .	214
10.3	Future Work . . . . .	215
<b>VI</b>	<b>Appendices</b>	<b>217</b>
<b>A</b>	<b>Detailed Model Assumptions</b>	<b>218</b>
A.1	Input Parameters for Cube Model . . . . .	218
A.2	Calculated Parameters for Cube Model . . . . .	219
A.2.1	Window Parameter Values. . . . .	219
A.2.2	Surface Albedo Values. . . . .	220
A.2.3	Thermostat Setpoint Calculations . . . . .	220
A.2.4	Internal Load Schedules . . . . .	221
A.3	EnergyPlus Code Assumptions. . . . .	226
A.4	Chapter Summary . . . . .	232
<b>B</b>	<b>References</b>	<b>233</b>

# List of Figures

1-1	Percent Energy Consumption by End Use for United States and Regions [1]. . .	26
1-2	Gross Energy Consumption for the United States by Region [1] . . . . .	26
1-3	Gross Energy Consumption per Household for the United States by Region [1]	27
3-1	Idealized Cube Model, conceptual representation . . . . .	50
3-2	Determination of Cube Footprint from Example Irregular Floor Plan. . . . .	51
3-3	Determination of Attic Height from a Sloped Roof Condition. . . . .	52
3-4	Equivalent Wall Calculation Inputs . . . . .	55
4-1	Case Study Wall Sections [70][71]. . . . .	65
4-2	Energy Comparisons for Single Cube . . . . .	69
4-3	Energy Comparisons for Multiple Cubes . . . . .	70
4-4	Variations of Geometry and Input Conditions . . . . .	75
5-1	Annual Energy Consumption per Surface ( $J/m^2$ ), ACH (1/h) vs Height (m), Anchorage, AK (above left) and Phoenix, AZ (above right) San Francisco, CA (below left) and Miami, FL (below right) . . . . .	81
5-2	Annual Energy Consumption per Volume ( $J/m^3$ ), Height (m) vs Length (m), Anchorage, AK (above left) and Phoenix, AZ (above right) San Francisco, CA (below left) and Miami, FL (below right) . . . . .	82
5-3	Annual Energy Consumption per Volume ( $J/m^3$ , left) and Surface ( $J/m^2$ , right), Width (m) vs Length (m), Anchorage, AK (row 1), Phoenix, AZ (row 2), San Francisco, CA (row 3), and Miami, FL (row 4) . . . . .	83
5-4	Annual Energy Consumption per Volume ( $J/m^3$ ), ACH (1/h) vs Wall Conductivity ( $W/m-K$ ), Anchorage, AK (above left) and Phoenix, AZ (above right) San Francisco, CA (below left) and Miami, FL (below right). . . . .	84
5-5	Annual Energy Consumption per Volume ( $J/m^3$ ), Floor Conductivity ( $W/m-K$ ) vs Wall Conductivity ( $W/m-K$ ), Anchorage, AK (above left) and Phoenix, AZ (above right) San Francisco, CA (below left) and Miami, FL (below right). . . . .	85
5-6	Annual Energy Consumption per Volume ( $J/m^3$ ), Roof Conductivity ( $W/m-K$ ) vs Wall Conductivity ( $W/m-K$ ), Anchorage, AK (above left) and Phoenix, AZ (above right) San Francisco, CA (below left) and Miami, FL (below right). . . . .	86

6-1	Specific Annual Energy Consumption ( $J/m^3$ ) vs Diffusivity ( $m^2/s$ ) and Conductivity ( $W/m-K$ ), San Francisco, CA . . . . .	92
6-2	Normalized Specific Annual Energy Consumption vs Diffusivity ( $m^2/s$ ) and Conductivity ( $W/m-K$ ), San Francisco, CA . . . . .	92
6-3	Potential Energy Savings from Thermal Mass vs Conductivity ( $W/m-K$ ), San Francisco, CA. . . . .	93
6-4	Specific Annual Energy Consumption ( $J/m^3$ ) vs Diffusivity ( $m^2/s$ ) and Wall Thickness (m), San Francisco, CA . . . . .	94
6-5	Normalized Specific Annual Energy Consumption vs Diffusivity ( $m^2/s$ ) and Wall Thickness (m), San Francisco, CA . . . . .	94
6-6	Potential Energy Savings from Thermal Mass vs Wall Thickness (m), San Francisco, CA. . . . .	95
6-7	Specific Annual Energy Consumption ( $J/m^3$ ) vs Diffusivity ( $m^2/s$ ) and Conductivity ( $W/m-K$ ), Phoenix, AZ . . . . .	96
6-8	Normalized Specific Annual Energy Consumption vs Diffusivity ( $m^2/s$ ) and Conductivity ( $W/m-K$ ), Phoenix, AZ . . . . .	97
6-9	Potential Energy Savings from Thermal Mass vs Conductivity ( $W/m-K$ ), Phoenix, AZ . . . . .	97
6-10	Specific Annual Energy Consumption ( $J/m^3$ ) vs Diffusivity ( $m^2/s$ ) and Wall Thickness (m), Phoenix, AZ . . . . .	98
6-11	Normalized Specific Annual Energy Consumption vs Diffusivity ( $m^2/s$ ) and Wall Thickness (m), Phoenix, AZ . . . . .	99
6-12	Potential Energy Savings from Thermal Mass vs Wall Thickness (m), Phoenix, AZ. . . . .	99
6-13	Specific Annual Energy Consumption ( $J/m^3$ ) vs Diffusivity ( $m^2/s$ ) and Conductivity ( $W/m-K$ ), Miami, FL . . . . .	100
6-14	Normalized Specific Annual Energy Consumption vs Diffusivity ( $m^2/s$ ) and Conductivity ( $W/m-K$ ), Miami, FL . . . . .	101
6-15	Potential Energy Savings from Thermal Mass vs Conductivity ( $W/m-K$ ), Miami, FL. . . . .	101
6-16	Specific Annual Energy Consumption ( $J/m^3$ ) vs Diffusivity ( $m^2/s$ ) and Wall Thickness (m), Miami, FL . . . . .	102
6-17	Normalized Specific Annual Energy Consumption vs Diffusivity ( $m^2/s$ ) and Wall Thickness (m), Miami, FL . . . . .	103
6-18	Potential Energy Savings from Thermal Mass vs Wall Thickness (m), Miami, FL. . . . .	103
6-19	Specific Annual Energy Consumption ( $J/m^3$ ) vs Diffusivity ( $m^2/s$ ) and Conductivity ( $W/m-K$ ), Anchorage, AK. . . . .	104

6-20	Normalized Specific Annual Energy Consumption vs Diffusivity ( $m^2/s$ ) and Conductivity ( $W/m-K$ ), Anchorage, AK . . . . .	105
6-21	Potential Energy Savings from Thermal Mass vs Conductivity ( $W/m-K$ ), Anchorage, AK . . . . .	105
6-22	Specific Annual Energy Consumption ( $J/m^3$ ) vs Diffusivity ( $m^2/s$ ) and Wall Thickness (m), Anchorage, AK . . . . .	106
6-23	Normalized Specific Annual Energy Consumption vs Diffusivity ( $m^2/s$ ) and Wall Thickness (m), Anchorage, AK . . . . .	107
6-24	Potential Energy Savings from Thermal Mass vs Wall Thickness (m), Anchorage, AK . . . . .	107
6-25	Specific Energy Consumption ( $J/m^3$ ) vs Diffusivity ( $m^2/s$ ) by Season, San Francisco, CA . . . . .	108
6-26	Specific Energy Consumption ( $J/m^3$ ) vs Diffusivity ( $m^2/s$ ) by Season, Phoenix, AZ . . . . .	109
6-27	Specific Energy Consumption ( $J/m^3$ ) vs Diffusivity ( $m^2/s$ ) by Season, Miami, FL . . . . .	109
6-28	Specific Energy Consumption ( $J/m^3$ ) vs Diffusivity ( $m^2/s$ ) by Season, Anchorage, AK . . . . .	110
6-29	Inset of Specific Summer Energy Consumption ( $J/m^3$ ) vs Diffusivity ( $m^2/s$ ), Miami, FL . . . . .	111
6-30	Comparison of Normalized Energy Consumption for Multiple Climates for a conductivity of $0.9 W/m-K$ and a thickness of $0.15 m$ . . . . .	113
6-31	Annual Thermal Mass Impact Map, percent optimization for $0.9 W/m-K$ and $0.15 m$ wall based on 30,000 of 132,500 data points for residential construction in the United States . . . . .	115
6-32	Summer Thermal Mass Impact Map, percent optimization for $0.9 W/m-K$ and $0.15 m$ wall based on 30,000 of 132,500 data points for residential construction in the United States . . . . .	116
6-33	Winter Thermal Mass Impact Map, percent optimization for $0.9 W/m-K$ and $0.15 m$ wall based on 30,000 of 132,500 data points for residential construction in the United States . . . . .	117
6-34	Optimum Conductivity ( $W/m-K$ ) for $0.15 m$ wall (green locations asymptotic, blue locations increase without bound) based on 51,000 of 132,500 data points for residential construction in the United States . . . . .	118
6-35	Optimum Thickness (m) for $0.9 W/m-K$ wall (green locations asymptotic, blue locations increase without bound) based on 38,500 of 132,500 data points for residential construction in the United States . . . . .	119
7-1	Specific Annual Energy Consumption ( $J/m^3$ ) vs Diffusivity ( $m^2/s$ ) and Conductivity ( $W/m-K$ ), San Francisco, CA . . . . .	123
7-2	Normalized Specific Annual Energy Consumption vs Diffusivity ( $m^2/s$ ) and Conductivity ( $W/m-K$ ), San Francisco, CA . . . . .	124

7-3	Potential Energy Savings from Thermal Mass vs Conductivity (W/m-K), San Francisco, CA . . . . .	124
7-4	Specific Annual Energy Consumption (J/m <sup>3</sup> ) vs Diffusivity (m <sup>2</sup> /s) and Slab Thickness (m), San Francisco, CA . . . . .	125
7-5	Normalized Specific Annual Energy Consumption vs Diffusivity (m <sup>2</sup> /s) and Slab Thickness (m), San Francisco, CA . . . . .	126
7-6	Potential Energy Savings from Thermal Mass vs Slab Thickness (m), San Francisco, CA. . . . .	126
7-7	Specific Annual Energy Consumption (J/m <sup>3</sup> ) vs Diffusivity (m <sup>2</sup> /s) and Conductivity (W/m-K), Phoenix, AZ . . . . .	127
7-8	Normalized Specific Annual Energy Consumption vs Diffusivity (m <sup>2</sup> /s) and Conductivity (W/m-K), Phoenix, AZ . . . . .	128
7-9	Potential Energy Savings from Thermal Mass vs Conductivity (W/m-K), Phoenix, AZ. . . . .	128
7-10	Specific Annual Energy Consumption (J/m <sup>3</sup> ) vs Diffusivity (m <sup>2</sup> /s) and Slab Thickness (m), Phoenix, AZ . . . . .	129
7-11	Normalized Specific Annual Energy Consumption vs Diffusivity (m <sup>2</sup> /s) and Slab Thickness (m), Phoenix, AZ . . . . .	130
7-12	Potential Energy Savings from Thermal Mass vs Slab Thickness (m), Phoenix, AZ. . . . .	130
7-13	Specific Annual Energy Consumption (J/m <sup>3</sup> ) vs Diffusivity (m <sup>2</sup> /s) and Conductivity (W/m-K), Miami, FL . . . . .	131
7-14	Normalized Specific Annual Energy Consumption vs Diffusivity (m <sup>2</sup> /s) and Conductivity (W/m-K), Miami, FL . . . . .	132
7-15	Potential Energy Savings from Thermal Mass vs Conductivity (W/m-K), Miami, FL. . . . .	132
7-16	Specific Annual Energy Consumption (J/m <sup>3</sup> ) vs Diffusivity (m <sup>2</sup> /s) and Slab Thickness (m), Miami, FL . . . . .	133
7-17	Normalized Specific Annual Energy Consumption vs Diffusivity (m <sup>2</sup> /s) and Slab Thickness (m), Miami, FL . . . . .	134
7-18	Potential Energy Savings from Thermal Mass vs Slab Thickness (m), Miami, FL. . . . .	134
7-19	Specific Annual Energy Consumption (J/m <sup>3</sup> ) vs Diffusivity (m <sup>2</sup> /s) and Conductivity (W/m-K), Anchorage, AK. . . . .	135
7-20	Normalized Specific Annual Energy Consumption vs Diffusivity (m <sup>2</sup> /s) and Conductivity (W/m-K), Anchorage, AK. . . . .	136
7-21	Potential Energy Savings from Thermal Mass vs Conductivity (W/m-K), Anchorage, AK . . . . .	136

7-22	Specific Annual Energy Consumption ( $J/m^3$ ) vs Diffusivity ( $m^2/s$ ) and Slab Thickness (m), Anchorage, AK . . . . .	137
7-23	Normalized Specific Annual Energy Consumption vs Diffusivity ( $m^2/s$ ) and Slab Thickness (m), Anchorage, AK . . . . .	138
7-24	Potential Energy Savings from Thermal Mass vs Slab Thickness (m), Anchorage, AK . . . . .	138
7-25	Specific Energy Consumption ( $J/m^3$ ) vs Diffusivity ( $m^2/s$ ) by Season, San Francisco, CA . . . . .	139
7-26	Specific Energy Consumption ( $J/m^3$ ) vs Diffusivity ( $m^2/s$ ) by Season, Phoenix, AZ . . . . .	140
7-27	Specific Energy Consumption ( $J/m^3$ ) vs Diffusivity ( $m^2/s$ ) by Season, Miami, FL . . . . .	140
7-28	Specific Energy Consumption ( $J/m^3$ ) vs Diffusivity ( $m^2/s$ ) by Season, Anchorage, AK . . . . .	141
7-29	Inset of Specific Summer Energy Consumption ( $J/m^3$ ) vs Diffusivity ( $m^2/s$ ), Miami, FL . . . . .	142
7-30	Comparison of Normalized Energy Consumption for Multiple Climates for a conductivity of 0.9 W/m-K and a thickness of 0.15 m . . . . .	143
7-31	Annual Thermal Mass Impact Map, percent optimization for 0.9 W/m-K and 0.15 m slab based on 30,000 of 132,500 data points for residential construction in the United States . . . . .	145
7-32	Summer Thermal Mass Impact Map, percent optimization for 0.9 W/m-K and 0.15 m slab based on 30,000 of 132,500 data points for residential construction in the United States . . . . .	146
7-33	Winter Thermal Mass Impact Map, percent optimization for 0.9 W/m-K and 0.15 m wall based on 30,000 of 132,500 data points for residential construction in the United States . . . . .	147
7-34	Optimum Conductivity (W/m-K) for 0.15 m slab (green locations asymptotic, blue locations increase without bound) based on 51,000 of 132,500 data points for residential construction in the United States . . . . .	148
7-35	Optimum Thickness (m) for 0.9 W/m-K slab (green locations asymptotic, blue locations increase without bound) based on 38,500 of 132,500 data points for residential construction in the United States . . . . .	149
8-1	Specific Annual Energy Consumption ( $J/m^3$ ) vs Wall Diffusivity ( $m^2/s$ ) and Infiltration (1/h), left, and Normalized Specific Annual Energy Consumption vs Wall Diffusivity ( $m^2/s$ ) and Infiltration (1/h), right, San Francisco, CA . . . . .	154
8-2	Specific Annual Energy Consumption ( $J/m^3$ ) vs Slab Diffusivity ( $m^2/s$ ) and Infiltration (1/h), left, and Normalized Specific Annual Energy Consumption vs Slab Diffusivity ( $m^2/s$ ) and Infiltration (1/h), right, San Francisco, CA . . . . .	155
8-3	Specific Annual Energy Consumption ( $J/m^3$ ) vs Wall Diffusivity ( $m^2/s$ ) and Infiltration (1/h), left, and Normalized Specific Annual Energy Consumption vs Wall Diffusivity ( $m^2/s$ ) and Infiltration (1/h), right, Phoenix, AZ . . . . .	156

8-4	Specific Annual Energy Consumption ( $J/m^3$ ) vs Slab Diffusivity ( $m^2/s$ ) and Infiltration (1/h), left, and Normalized Specific Annual Energy Consumption vs Slab Diffusivity ( $m^2/s$ ) and Infiltration (1/h), right, Phoenix, AZ . . . . .	156
8-5	Specific Annual Energy Consumption ( $J/m^3$ ) vs Wall Diffusivity ( $m^2/s$ ) and Infiltration (1/h), left, and Normalized Specific Annual Energy Consumption vs Wall Diffusivity ( $m^2/s$ ) and Infiltration (1/h), right, Miami, FL . . . . .	157
8-6	Specific Annual Energy Consumption ( $J/m^3$ ) vs Slab Diffusivity ( $m^2/s$ ) and Infiltration (1/h), left, and Normalized Specific Annual Energy Consumption vs Slab Diffusivity ( $m^2/s$ ) and Infiltration (1/h), right, Miami, FL . . . . .	158
8-7	Specific Annual Energy Consumption ( $J/m^3$ ) vs Wall Diffusivity ( $m^2/s$ ) and Infiltration (1/h), left, and Normalized Specific Annual Energy Consumption vs Wall Diffusivity ( $m^2/s$ ) and Infiltration (1/h), right, Anchorage, AK. . . . .	159
8-8	Specific Annual Energy Consumption vs Slab Diffusivity ( $m^2/s$ ) and Infiltration (1/h), left, and Normalized Specific Annual Energy Consumption vs Slab Diffusivity ( $m^2/s$ ) and Infiltration (1/h), right, Anchorage, AK. . . . .	159
8-9	Potential Energy Savings from Thermal Mass vs Infiltration (1/h), Walls (left) and Slabs (right) . . . . .	161
8-10	Optimum Infiltration (1/h) for 0.9 W/m-K, 0.15 m thick wall (green locations do not optimize at 0.6/h) based on 25,000 data points for residential construction in the United States . . . . .	162
8-11	Optimum Infiltration (1/h) for 0.9 W/m-K, 0.15 m thick slab (green locations do not optimize at 0.6/h) based on 25,000 data points for residential construction in the United States . . . . .	163
9-1	Specific Annual Energy Consumption ( $J/m^3$ ) vs Wall Diffusivity ( $m^2/s$ ) and Attic Condition, left, and Normalized Specific Annual Energy Consumption vs Wall Diffusivity ( $m^2/s$ ) and Attic Condition, right, San Francisco, CA . . . . .	167
9-2	Specific Annual Energy Consumption ( $J/m^3$ ) vs Slab Diffusivity ( $m^2/s$ ) and Attic Condition, left, and Normalized Specific Annual Energy Consumption vs Slab Diffusivity ( $m^2/s$ ) and Attic Condition, right, San Francisco, CA . . . . .	167
9-3	Specific Annual Energy Consumption ( $J/m^3$ ) vs Wall Diffusivity ( $m^2/s$ ) and Attic Condition, left, and Normalized Specific Annual Energy Consumption vs Wall Diffusivity ( $m^2/s$ ) and Attic Condition, right, Phoenix, AZ . . . . .	168
9-4	Specific Annual Energy Consumption ( $J/m^3$ ) vs Slab Diffusivity ( $m^2/s$ ) and Attic Condition, left, and Normalized Specific Annual Energy Consumption vs Slab Diffusivity ( $m^2/s$ ) and Attic Condition, right, Phoenix, AZ . . . . .	169
9-5	Specific Annual Energy Consumption ( $J/m^3$ ) vs Wall Diffusivity ( $m^2/s$ ) and Attic Condition, left, and Normalized Specific Annual Energy Consumption vs Wall Diffusivity ( $m^2/s$ ) and Attic Condition, right, Miami, FL . . . . .	170

9-6	Specific Annual Energy Consumption ( $J/m^3$ ) vs Slab Diffusivity ( $m^2/s$ ) and Attic Condition, left, and Normalized Specific Annual Energy Consumption vs Slab Diffusivity ( $m^2/s$ ) and Attic Condition, right, Miami, FL . . . . .	170
9-7	Specific Annual Energy Consumption ( $J/m^3$ ) vs Wall Diffusivity ( $m^2/s$ ) and Attic Condition, left, and Normalized Specific Annual Energy Consumption vs Wall Diffusivity ( $m^2/s$ ) and Attic Condition, right, Anchorage, AK . . . . .	171
9-8	Specific Annual Energy Consumption ( $J/m^3$ ) vs Slab Diffusivity ( $m^2/s$ ) and Attic Condition, left, and Normalized Specific Annual Energy Consumption vs Slab Diffusivity ( $m^2/s$ ) and Attic Condition, right, Anchorage, AK . . . . .	172
9-9	Specific Annual Energy Consumption ( $J/m^3$ ) vs Wall Diffusivity ( $m^2/s$ ) and Internal Slab, left, and Normalized Specific Annual Energy Consumption vs Wall Diffusivity ( $m^2/s$ ) and Internal Slab, right, San Francisco, CA . . . . .	173
9-10	Specific Annual Energy Consumption ( $J/m^3$ ) vs Slab Diffusivity ( $m^2/s$ ) and Internal Slab, left, and Normalized Specific Annual Energy Consumption vs Slab Diffusivity ( $m^2/s$ ) and Internal Slab, right, San Francisco, CA . . . . .	174
9-11	Specific Annual Energy Consumption ( $J/m^3$ ) vs Wall Diffusivity ( $m^2/s$ ) and Internal Slab, left, and Normalized Specific Annual Energy Consumption vs Wall Diffusivity ( $m^2/s$ ) and Internal Slab, right, Phoenix, AZ. . . . .	175
9-12	Specific Annual Energy Consumption ( $J/m^3$ ) vs Slab Diffusivity ( $m^2/s$ ) and Internal Slab, left, and Normalized Specific Annual Energy Consumption vs Slab Diffusivity ( $m^2/s$ ) and Internal Slab, right, Phoenix, AZ. . . . .	175
9-13	Specific Annual Energy Consumption ( $J/m^3$ ) vs Wall Diffusivity ( $m^2/s$ ) and Internal Slab, left, and Normalized Specific Annual Energy Consumption vs Wall Diffusivity ( $m^2/s$ ) and Internal Slab, right, Miami, FL. . . . .	176
9-14	Specific Annual Energy Consumption ( $J/m^3$ ) vs Slab Diffusivity ( $m^2/s$ ) and Internal Slab, left, and Normalized Specific Annual Energy Consumption vs Slab Diffusivity ( $m^2/s$ ) and Internal Slab, right, Miami, FL. . . . .	177
9-15	Specific Annual Energy Consumption ( $J/m^3$ ) vs Wall Diffusivity ( $m^2/s$ ) and Internal Slab, left, and Normalized Specific Annual Energy Consumption vs Wall Diffusivity ( $m^2/s$ ) and Internal Slab, right, Anchorage, AK . . . . .	178
9-16	Specific Annual Energy Consumption ( $J/m^3$ ) vs Slab Diffusivity ( $m^2/s$ ) and Internal Slab, left, and Normalized Specific Annual Energy Consumption vs Slab Diffusivity ( $m^2/s$ ) and Internal Slab, right, Anchorage, AK . . . . .	178
9-17	Specific Annual Energy Consumption ( $J/m^3$ ) vs Wall Diffusivity ( $m^2/s$ ) and Basement Condition, left, and Normalized Specific Annual Energy Consumption vs Wall Diffusivity ( $m^2/s$ ) and Basement Condition, right, San Francisco, CA . . . . .	180
9-18	Specific Annual Energy Consumption ( $J/m^3$ ) vs Slab Diffusivity ( $m^2/s$ ) and Basement Condition, left, and Normalized Specific Annual Energy Consumption vs Slab Diffusivity ( $m^2/s$ ) and Basement Condition, right, San Francisco, CA . . . . .	181



9-19	Specific Annual Energy Consumption ( $J/m^3$ ) vs Wall Diffusivity ( $m^2/s$ ) and Basement Condition, left, and Normalized Specific Annual Energy Consumption vs Wall Diffusivity ( $m^2/s$ ) and Basement Condition, right, Phoenix, AZ . . . . .	182
9-20	Specific Annual Energy Consumption ( $J/m^3$ ) vs Slab Diffusivity ( $m^2/s$ ) and Basement Condition, left, and Normalized Specific Annual Energy Consumption vs Slab Diffusivity ( $m^2/s$ ) and Basement Condition, right, Phoenix, AZ . . . . .	183
9-21	Specific Annual Energy Consumption ( $J/m^3$ ) vs Wall Diffusivity ( $m^2/s$ ) and Basement Condition, left, and Normalized Specific Annual Energy Consumption vs Wall Diffusivity ( $m^2/s$ ) and Basement Condition, right, Miami, FL . . . . .	184
9-22	Specific Annual Energy Consumption ( $J/m^3$ ) vs Slab Diffusivity ( $m^2/s$ ) and Basement Condition, left, and Normalized Specific Annual Energy Consumption vs Slab Diffusivity ( $m^2/s$ ) and Basement Condition, right, Miami, FL . . . . .	184
9-23	Specific Annual Energy Consumption ( $J/m^3$ ) vs Wall Diffusivity ( $m^2/s$ ) and Basement Condition, left, and Normalized Specific Annual Energy Consumption vs Wall Diffusivity ( $m^2/s$ ) and Basement Condition, right, Anchorage, AK . . . . .	185
9-24	Specific Annual Energy Consumption ( $J/m^3$ ) vs Slab Diffusivity ( $m^2/s$ ) and Basement Condition, left, and Normalized Specific Annual Energy Consumption vs Slab Diffusivity ( $m^2/s$ ) and Basement Condition, right, Anchorage, AK . . . . .	186
9-25	Specific Annual Energy Consumption ( $J/m^3$ ) vs Wall Diffusivity ( $m^2/s$ ) and Building Height (m), left, and Normalized Specific Annual Energy Consumption vs Wall Diffusivity ( $m^2/s$ ) and Building Height (m), right, San Francisco, CA. . . . .	188
9-26	Specific Annual Energy Consumption ( $J/m^3$ ) vs Slab Diffusivity ( $m^2/s$ ) and Building Height (m), left, and Normalized Specific Annual Energy Consumption vs Slab Diffusivity ( $m^2/s$ ) and Building Height (m), right, San Francisco, CA. . . . .	188
9-27	Specific Annual Energy Consumption ( $J/m^3$ ) vs Wall Diffusivity ( $m^2/s$ ) and Building Height (m), left, and Normalized Specific Annual Energy Consumption vs Wall Diffusivity ( $m^2/s$ ) and Building Height (m), right, Phoenix, AZ. . . . .	190
9-28	Specific Annual Energy Consumption ( $J/m^3$ ) vs Slab Diffusivity ( $m^2/s$ ) and Building Height (m), left, and Normalized Specific Annual Energy Consumption vs Slab Diffusivity ( $m^2/s$ ) and Building Height (m), right, Phoenix, AZ. . . . .	190
9-29	Specific Annual Energy Consumption ( $J/m^3$ ) vs Wall Diffusivity ( $m^2/s$ ) and Building Height (m), left, and Normalized Specific Annual Energy Consumption vs Wall Diffusivity ( $m^2/s$ ) and Building Height (m), right, Miami, FL. . . . .	191
9-30	Specific Annual Energy Consumption ( $J/m^3$ ) vs Slab Diffusivity ( $m^2/s$ ) and Building Height (m), left, and Normalized Specific Annual Energy Consumption vs Slab Diffusivity ( $m^2/s$ ) and Building Height (m), right, Miami, FL. . . . .	192
9-31	Specific Annual Energy Consumption ( $J/m^3$ ) vs Wall Diffusivity ( $m^2/s$ ) and Building Height (m), left, and Normalized Specific Annual Energy Consumption vs Wall Diffusivity ( $m^2/s$ ) and Building Height (m), right, Anchorage, AK . . . . .	193

9-32	Specific Annual Energy Consumption ( $J/m^3$ ) vs Slab Diffusivity ( $m^2/s$ ) and Building Height (m), left, and Normalized Specific Annual Energy Consumption vs Slab Diffusivity ( $m^2/s$ ) and Building Height (m), right, Anchorage, AK . . . . .	193
9-33	Potential Energy Savings from Thermal Mass vs Building Height (m), Constant Footprint, Walls (left) and Slabs (right). . . . .	194
9-34	Potential Energy Savings from Thermal Mass vs Building Height (m), Constant Volume, Walls (left) and Slabs (right) . . . . .	195
9-35	Specific Annual Energy Consumption ( $J/m^3$ ) vs Wall Diffusivity ( $m^2/s$ ) and Plan Aspect Ratio, left, and Normalized Specific Annual Energy Consumption vs Wall Diffusivity ( $m^2/s$ ) and Plan Aspect Ratio, right, San Francisco, CA . . . . .	196
9-36	Specific Annual Energy Consumption ( $J/m^3$ ) vs Slab Diffusivity ( $m^2/s$ ) and Plan Aspect Ratio, left, and Normalized Specific Annual Energy Consumption vs Slab Diffusivity ( $m^2/s$ ) and Plan Aspect Ratio, right, San Francisco, CA . . . . .	197
9-37	Specific Annual Energy Consumption ( $J/m^3$ ) vs Wall Diffusivity ( $m^2/s$ ) and Plan Aspect Ratio, left, and Normalized Specific Annual Energy Consumption vs Wall Diffusivity ( $m^2/s$ ) and Plan Aspect Ratio, right, Phoenix, AZ . . . . .	198
9-38	Specific Annual Energy Consumption ( $J/m^3$ ) vs Slab Diffusivity ( $m^2/s$ ) and Plan Aspect Ratio, left, and Normalized Specific Annual Energy Consumption vs Slab Diffusivity ( $m^2/s$ ) and Plan Aspect Ratio, right, Phoenix, AZ . . . . .	198
9-39	Specific Annual Energy Consumption ( $J/m^3$ ) vs Wall Diffusivity ( $m^2/s$ ) and Plan Aspect Ratio, left, and Normalized Specific Annual Energy Consumption vs Wall Diffusivity ( $m^2/s$ ) and Plan Aspect Ratio, right, Miami, FL . . . . .	199
9-40	Specific Annual Energy Consumption ( $J/m^3$ ) vs Slab Diffusivity ( $m^2/s$ ) and Plan Aspect Ratio, left, and Normalized Specific Annual Energy Consumption vs Slab Diffusivity ( $m^2/s$ ) and Plan Aspect Ratio, right, Miami, FL . . . . .	200
9-41	Specific Annual Energy Consumption ( $J/m^3$ ) vs Wall Diffusivity ( $m^2/s$ ) and Plan Aspect Ratio, left, and Normalized Specific Annual Energy Consumption vs Wall Diffusivity ( $m^2/s$ ) and Plan Aspect Ratio, right, Anchorage, AK . . . . .	201
9-42	Specific Annual Energy Consumption ( $J/m^3$ ) vs Slab Diffusivity ( $m^2/s$ ) and Plan Aspect Ratio, left, and Normalized Specific Annual Energy Consumption vs Slab Diffusivity ( $m^2/s$ ) and Plan Aspect Ratio, right, Anchorage, AK . . . . .	201
9-43	Potential Energy Savings from Thermal Mass vs N-S Plan Aspect Ratio, Walls (left) and Slabs (right). . . . .	202
9-44	Potential Energy Savings from Thermal Mass vs E-W Plan Aspect Ratio, Walls (left) and Slabs (right). . . . .	203
9-45	Specific Annual Energy Consumption ( $J/m^3$ ) vs Wall Diffusivity ( $m^2/s$ ) and Glazing Percentage, left, and Normalized Specific Annual Energy Consumption vs Wall Diffusivity ( $m^2/s$ ) and Glazing Percentage, right, San Francisco, CA . . . . .	204

9-46	Specific Annual Energy Consumption ( $J/m^3$ ) vs Slab Diffusivity ( $m^2/s$ ) and Glazing Percentage, left, and Normalized Specific Annual Energy Consumption vs Slab Diffusivity ( $m^2/s$ ) and Glazing Percentage, right, San Francisco, CA . . . . .	205
9-47	Specific Annual Energy Consumption ( $J/m^3$ ) vs Wall Diffusivity ( $m^2/s$ ) and Glazing Percentage, left, and Normalized Specific Annual Energy Consumption vs Wall Diffusivity ( $m^2/s$ ) and Glazing Percentage, right, Phoenix, AZ . . . . .	206
9-48	Specific Annual Energy Consumption ( $J/m^3$ ) vs Slab Diffusivity ( $m^2/s$ ) and Glazing Percentage, left, and Normalized Specific Annual Energy Consumption vs Slab Diffusivity ( $m^2/s$ ) and Glazing Percentage, right, Phoenix, AZ . . . . .	206
9-49	Specific Annual Energy Consumption ( $J/m^3$ ) vs Wall Diffusivity ( $m^2/s$ ) and Glazing Percentage, left, and Normalized Specific Annual Energy Consumption vs Wall Diffusivity ( $m^2/s$ ) and Glazing Percentage, right, Miami, FL . . . . .	207
9-50	Specific Annual Energy Consumption ( $J/m^3$ ) vs Slab Diffusivity ( $m^2/s$ ) and Glazing Percentage, left, and Normalized Specific Annual Energy Consumption vs Slab Diffusivity ( $m^2/s$ ) and Glazing Percentage, right, Miami, FL . . . . .	208
9-51	Specific Annual Energy Consumption ( $J/m^3$ ) vs Wall Diffusivity ( $m^2/s$ ) and Glazing Percentage, left, and Normalized Specific Annual Energy Consumption vs Wall Diffusivity ( $m^2/s$ ) and Glazing Percentage, right, Anchorage, AK. . . . .	209
9-52	Specific Annual Energy Consumption ( $J/m^3$ ) vs Slab Diffusivity ( $m^2/s$ ) and Glazing Percentage, left, and Normalized Specific Annual Energy Consumption vs Slab Diffusivity ( $m^2/s$ ) and Glazing Percentage, right, Anchorage, AK. . . . .	209
9-53	Potential Energy Savings from Thermal Mass vs Window Percentage, Walls (left) and Slabs (right) . . . . .	210

# List of Tables

- 3-1 Baseline Envelope Properties . . . . . 53
- 3-2 Envelope Properties of EnergyPlus Standard Wall Sections [23] . . . . . 54
- 3-3 Internal Load Assumptions, where FFA = Finish Floor Area, assumed in square feet by BAHSP [28]. . . . . 57
- 3-4 Domestic Hot Water Load Assumptions [28] . . . . . 57
- 3-5 Domestic Hot Water Distribution System Load Assumptions [28] . . . . . 58
- 3-6 Lighting Loads, where FFA = Finish Floor Area, assumed in square feet by BAHSP [28]. . . . . 58
- 3-7 Locations Considered in Climate Study . . . . . 59
- 4-1 Envelope Properties of Case Study Wall Sections, where CMU = Concrete Masonry Unit and EPS = Expanded Polystyrene. . . . . 66
- 4-2 Equivalent Wall Calibration Results, presented as the ratio of the test model energy to the energy predicted by the full energy model . . . . . 67
- 4-3 Geometry Calibration Results, presented as the ratio of the test model energy to the energy predicted by the full energy model . . . . . 71
- 4-4 Baseline Assumptions Present for Cube Model and R11-01 Model . . . . . 73
- 4-5 System Sensible Energy for the Basic and Advanced Cubes, presented as the ratio of the test model energy to the energy predicted by the full energy model . . . . . 77
- 4-6 System Annual Sensible Energy for the averages of variations experiments, presented as the ratio of the test model energy to the energy predicted by the full energy model . . . . . 78
- 5-1 Varied Parameters . . . . . 80
- 6-36 Ranges and Increments for Thermal Envelope Parameters . . . . . 89
- 6-37 Sub-Experiment Setup . . . . . 90
- 8-1 Levels of Infiltration According to Different Standards . . . . . 153
- 8-2 Ranges and Increments for Infiltration Study . . . . . 153
- 10-1 Ranges and Increments for Geometry Studies . . . . . 165
- A-1 Input Parameters for Cube Model . . . . . 219
- A-2 Code Required Construction Inputs by Climate Zone [29] . . . . . 220
- A-3 Surface Albedo Characteristics for Ground Heat Transfer [67] . . . . . 220
- A-4 Monthly Schedule Values for Scaling Daily BAHSP Loads [62] . . . . . 222

A-5	Daily Schedule Values for All BAHSP Loads Except Lighting [62]. . . . .	223
A-6	Daily Schedule Values for BAHSP Lighting Loads [62]. . . . .	225
A-7	EnergyPlus Code Assumptions. . . . .	227

# Acknowledgements

I would like to thank the Concrete Sustainability Hub for their generous support of my education and the opportunity to engage in this research. To my advisors, Franz-Josef Ulm and Randa Ghattas, thank you for your exhaustive comments and feedback on the research and the preparation of this document.

To the online code community, thank you for your volunteer efforts in providing a wealth of information for the purpose of enhancing public knowledge. This knowledge base was invaluable in the development of this model and report.

To my loving family and friends, thank you for your support throughout my education. I am truly blessed to have each and every one of you in my life. Thank you God for graciously providing me everything I have, including the opportunity to conduct this research.

In memory of my grandmother, Anita Ludwig, whose life, loving wisdom, and opinions on the built environment have always been an inspiration to me.

**Part I**

**General Presentation**

# Chapter 1

## Introduction

The building construction industry has narrowed its focus on key issues of sustainability and operational energy consumption in recent years. In an effort to aid these goals with clear quantitative information on the benefits of one strategy, thermal mass, this work develops a simplified model of residential construction. The model computes rough energy estimates equivalent to schematic design accuracy and generates results that can be carried further into the design realm for the purpose of optimizing energy performance. As an introduction to the problem, this chapter will discuss the rationale for the research and the scope of issues considered.

### 1.1 Research Premise

The professional and political climate at the beginning of the twenty-first century is amenable to the consideration of energy efficiency in the design of single-family residential projects. However, the availability of precise tools and information on the energy-saving potential of various strategies must be resolved before widespread implementation becomes feasible. Given requests for simplified, breadboard tools to determine broad view results of the energy benefits of key strategies, a simplified approach, the Cube Model, has been developed to discuss passive thermal mass energy savings in the typical residential home.

This Cube Model simplifies the geometry and material considerations of the building while still providing realistic approximations for energy consumption. Such a model allows for rapid comparisons of envelope materials and energy savings for improved decision making. The tool is applied to the notion of thermal mass specifically in this work to better understand the impact of the phenomenon on overall energy consumption. The results demonstrate the effectiveness of the phenomenon and generate key conclusions about the validity of passive thermal mass under



a variety of circumstances. Thus, both the model and the thermal mass results will fill expressed industry needs in an age of energy efficiency concerns.

## **1.2 Rationale for Research**

The rationale for the research is grounded in the political and cultural reality of the building stock. Trends in residential energy consumption indicate that 49% of the overall consumption is used to condition building space. This percentage can reach 60% in the Northeast region of the United States, as shown in Figure 1-1 [1]. When looking at the overall energy consumption for buildings, however, the results indicate that overall consumption by region does not follow the same trend. The regional energy consumption of buildings, as shown in Figure 1-2, shows that the South uses the most energy overall while the Midwest uses the most energy on conditioning [1]. Such results indicate that strategies benefitting those regions where heating is significant (Midwest and Northeast) or cooling is significant (South) would greatly benefit the overall energy consumption of residential homes.

Finally, looking at the per household information shown in Figure 1-3, it is clear that heating climates dominate the energy consumption per household in the United States [1]. The combination of the three figures presented here clearly indicates that different regions dominate different conditioning concerns. As a result, there is a need to find strategies that can be tailored to each climates' needs and that can reduce heating energy consumption especially. Further, the magnitudes of energy consumed indicate the need for reduction of overall energy consumption in the conditioning of a volume. As will be discussed in Section 1.3, this research departs from a set of questions, proposing the notion that thermal mass could be such a strategy for reducing the energy consumption trends presented here. Given the predominance of conditioning energy and the proposal of thermal mass as a topic of discussion, the Cube Model focuses on the energy concerns for building conditioning during the occupation phase of the building life cycle.

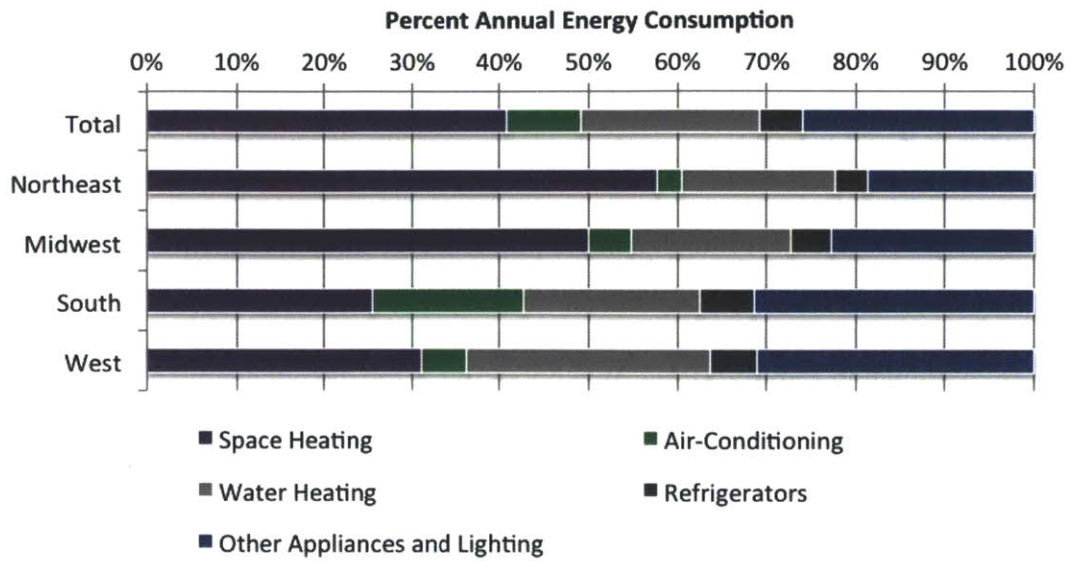


Figure 1-1 Percent Energy Consumption by End Use for United States and Regions [1]

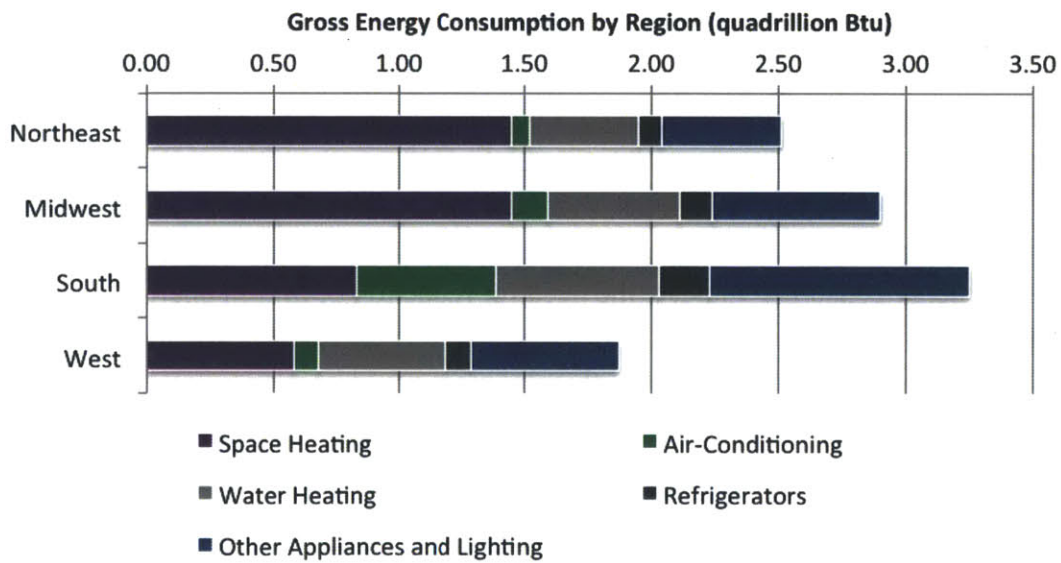


Figure 1-2 Gross Energy Consumption for the United States by Region [1]

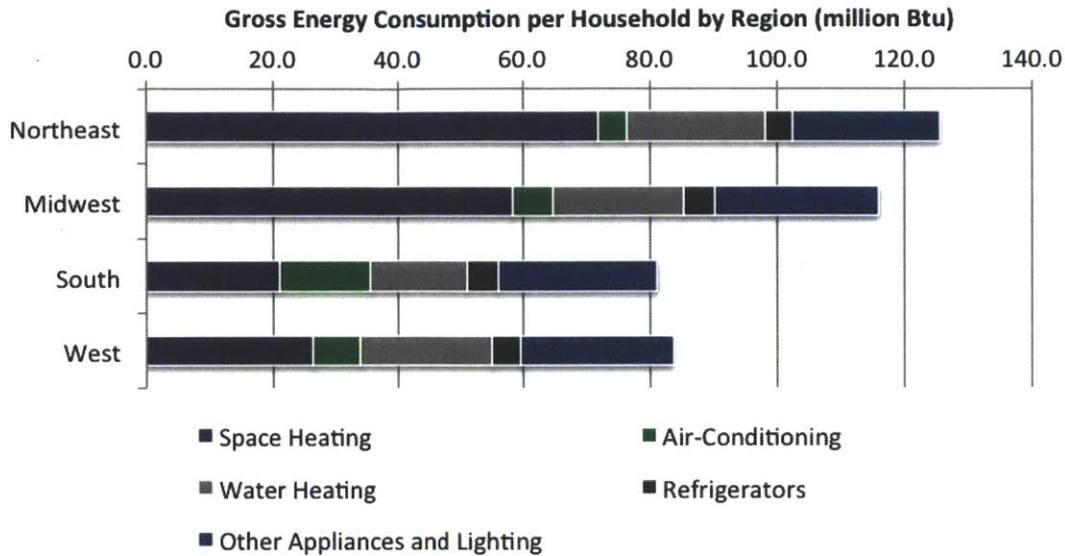


Figure 1-3 Gross Energy Consumption per Household for the United States by Region [1]

One final consideration for the research rationale is the need for energy efficiency to become a more prominent concern in the home market. In the world of developer based homes, the key considerations are location, floor plan, and aesthetics, with energy efficiency not yet making the list [2]. Addressing the need for a market for energy efficiency, Congress is focusing on a financial component of the problem. Proposed legislation will tie energy consumption to mortgage financing, rather than just operating costs. The SAVE Act has been proposed to require federal lending organizations to consider the energy efficiency of a home in determining the mortgage rate. Since these agencies are responsible for roughly 90% of the volume of home lending, the legislation may greatly impact energy efficiency considerations in construction [3]. In order to respond to an increased desire for efficiency, data on effective energy-saving strategies would be required.

### 1.3 Research Approach

The research approach is to develop a simplified model of a single-family residence for the purpose of running parametric simulations. Instead of the traditional case study approach of the results discussed in Chapter 2, this study seeks to provide information about key building assumptions to determine the ability to save energy under given circumstances. The study does not seek to represent an individual building in all its detail; rather, it uses a simulation-based experimental approach to develop energy consumption trends as they relate to thermal mass performance.

To direct the simulation-based experiments, the following questions frame the research:

1. How can the complexity of a building be reduced while maintaining similar results to a full energy model?
2. From a quantitative perspective, what is thermal mass? Of the main thermal properties of a material (thickness, conductivity, density, specific heat), which have the greatest impact on energy consumption by climate?
3. How can thermal mass of an envelope construction be optimized? Does the optimization change when considering walls versus slabs?
4. How do other parameters (infiltration, geometry) impact the thermal mass performance of a residence?

Using these questions as a baseline, a Cube Model is presented, calibrated, and validated to demonstrate that it provides the results of a full energy model. Later, this model is used to answer the key research questions regarding thermal mass performance. To demonstrate the sensitivity toward climate, detailed thermal mass results are presented for four different climates and mapping exercises will demonstrate the impact across fifty climates. The final question is answered in the form of a sensitivity analysis on the thermal mass data.

## **1.4 Research Outline**

Part I sets the general presentation of the work, including this introduction and Chapter 2, a literature review of key references on energy modeling, building standards, and previous thermal mass research. Part II of this work will discuss the model development, calibration and validation, and model versatility. Chapter 3 will present an overview of the mathematical basis of energy modeling, the Cube Model methodology, and the relevant assumptions in the analysis. Chapter 4 will present the calibration and validation of the model to justify the geometry simplifications and the relationship to full energy models. Chapter 5 will present brief experiments indicating the versatility of the model itself.

Part III of this work will present the application of the model to thermal mass considerations. Chapter 6 and Chapter 7 will discuss the findings of the cube model with respect to walls and slabs, respectively. Part IV will extend the work with a sensitivity analysis to ground the results presented for thermal mass. Chapter 8 will present an analysis of the impact of varying

infiltration on the thermal mass performance. Chapter 9 will present the impact of changing the geometry of the cube model. Finally, Part V of the work presents Chapter 10, the conclusion.

## **1.5 Chapter Summary**

In response to energy trends and initiatives for improved energy efficiency, this report aims to determine the validity of a simplified model for the purpose of modeling energy consumption. Once established, it is used to study the impact of passive thermal mass on building design. The scope has been limited to improvements on the HVAC loads, a measure of efficiency in the use phase of construction, in response to recent data and legislative initiatives. Before proceeding to describe the model developed, the literature review will be presented next to ground the work in previous scholarship.

# Chapter 2

## Literature Review

A complete investigation of the literature on either energy modeling or thermal mass is a report unto itself. Still, it is appropriate to understand some significant principles and documentation to (1) properly ground the model in prior scholarship and (2) avoid repetition by separating the model from its peers. Finally, the literature review will form the basis for the second research question, which directly addresses the need for quantification of thermal mass.

### 2.1 Energy Modeling Overview

Energy modeling aims to take inventory of all factors in a design that may impact the overall consumption of a building. The models include both the architectural design itself and provisions for including types of thermal loading that may trigger additional energy costs. Energy modeling is often used to develop a Life Cycle Assessment (LCA) of a building, but energy modeling alone does not constitute an LCA. These two tasks have fundamentally different objectives; an LCA obtains cradle-to-grave data on the environmental impact of a building while energy modeling obtains operational consumption for a building. This consumption can in turn be incorporated into a full LCA as the representation of the use phase. For comparison, one contemporary LCA is the B-PATH Model, under development at the Lawrence Berkeley National Laboratory. This model aims to provide an LCA for buildings using only a “balance of building” energy approximation for the use phase, which is much less nuanced than full energy modeling [4]. A detailed evaluation of the use energy requires either the development of a new energy modeling tool or the use of an existing one; this report does the latter.

There are many options available when considering energy modeling; the Building Technologies Program at the U.S. Department of Energy maintains a directory of software for sustainability initiatives and energy modeling comprising 408 programs, last updated in 2011 [5]. It is therefore infeasible to evaluate all available tools. This report limits its scope to tools that provide full energy modeling capabilities and

have undergone substantial validation. According to a model survey by Crawley et al [6] available from the Department of Energy, four common programs with complete validation information are DOE-2.1E, EnergyPlus, ESP-r, and TRNSYS. Further, practice in the energy modeling community is not to state that a program has been validated but to determine specifically whether a particular parameter has been validated [7]. In keeping with this theory, the following subsections will discuss noteworthy validation experiments on the subject of thermal mass, as well as any other relevant information on the program's modeling capabilities.

### **2.1.1 DOE-2.1E**

The DOE-2.1E energy simulation module has been under development since the 1960s [8]. Heat transfer is assumed to be one-dimensional and room weighting factors are used to determine how much energy is allocated to the thermal mass component [9][10]. These factors are not based on thermodynamic science but rather a set of assumptions; they have often been characterized as a weakness in the program [11]. Validation experiments from 1985 indicated that the program predicts residential buildings and thermal mass results within 20%; however, it has been noted in these validation studies that the program provides more accurate energy results for low-mass buildings than high-mass buildings. In contrast, validation experiments from 1998 indicate that the DOE-2.1E model has good agreement with the measured results for walls with low and high thermal mass [12]. The Department of Energy has since dropped support for this program in favor of EnergyPlus [13].

### **2.1.2 EnergyPlus**

EnergyPlus has been in existence since 2001 and is the successor to both DOE-2.1E and BLAST, two U.S. government models that have been under development since the 1960s and 1970s, respectively. This program combines the functionalities of both programs into a single modeling system, reducing redundancy and increasing the ease of modification. It also simultaneously solves systems and temperatures, a feature not available in its predecessors [8]. The model accounts for thermal mass effects through the use of one-dimensional conduction assumptions and a more computationally stable version of BLAST. This allows the program to determine high-mass constructions with more accuracy than some of its predecessors [14]. The ASHRAE<sup>1</sup> Standard 140-2011 procedures have been used to validate the measurement of envelope criteria, including high-mass systems, for the current version (Version 7.1). EnergyPlus accurately captured results within the same range as eight other programs for over 93% of cases; deviations in the remaining cases were on the order of 10% [15].

---

1 ASHRAE is the American Society of Heating, Refrigerating and Air-Conditioning Engineers, Inc.

### **2.1.3 ESP-r**

ESP-r is an energy modeling program whose development began in 1974. Its use is concentrated in Europe but Natural Resource Canada is also in collaboration with the tool [16]. The model can be used to consider thermal mass effects either through its standard one-dimensional conduction properties or through two- or three-dimensional properties, based on the research of Nakhi [17] into dynamic thermal performance of heat transfer in massive systems [16][17]. PASSYS<sup>2</sup> [7][18] conducted a study of predictions of passive systems using ESP-r sponsored by the European Commission. This study included high mass systems and determined that the temperature predictions for the test sites were less than 1 K different from those predicted. However, it should be noted that two- and three-dimensional conduction was used to calibrate the models to achieve this level of accuracy [7].

### **2.1.4 TRNSYS**

TRNSYS is a program originally developed in 1975 by the University of Wisconsin-Madison, though distributors including TRANSSOLAR and Thermal Energy Systems Specialists have developed some of the commercially available components due to the software's modular, adaptable nature [19]. The system can calculate high-mass components under either one-dimensional or three-dimensional calculations. Validation experiments on systems using thermal mass have shown that the one-dimensional simplifications employed in TRNSYS reasonably approximate the three-dimensional, finite element solution, even for active systems [20].

### **2.1.5 Selection and Discussion**

For this work, EnergyPlus has been selected as the energy modeling tool despite some limitations that will be covered in the following section. Since the programs tested during EnergyPlus validation include the others discussed in this literature review and showed agreement, it seems reasonable to employ the use of EnergyPlus. However, one important caveat to remember is that there have been instances where energy models are in agreement with each other but outside of alignment with actual building results. One such study by the International Energy Agency published in Annex 4 indicated that nine models were in agreement with each other but not supported by observational data [7]. While this is a dated study, data from the development of EnergyPlus indicates agreement with DOE-2, TRNSYS, and ESP, among other programs [21]. Combined with the notion that EnergyPlus is validated through the comparison to other energy simulation programs, it is important to remember that (1) these are the results from a validated

---

<sup>2</sup> PASSYS is an organization sponsored by the European Commission to investigate and validate Passive Solar Architecture [18].



but not error-proof calculation engine; and (2) limitations of the software selection will always be a consideration in a simulation study.

## 2.2 Software Limitations

Energy modeling results are only as accurate as the modeling software's algorithms allow. Whenever conducting an experiment using an existing model, it is important to interpret the results in the context of these limitations. This section is dedicated to discussing some of the known limitations of EnergyPlus that may affect the accuracy of the results presented in this report.

It is important to note that energy modeling programs which constrain heat flow through surfaces to one dimension may create a source of error [12][22]. Kossecka et al [22] discovered in a 2001 study that models conducted with simplifications generated based on three-dimensional heat transfer accurately predicted experimental data, whereas one-dimensional heat transfer programs did not accurately predict Insulating Concrete Forms (ICF) construction. Results from a comparison of energy models to validation buildings by PASSYS, sponsored by the European Commission, found that two- and three-dimensional conduction becomes important for heavily insulated wall systems [7].

EnergyPlus admits a limitation in calculating heavily insulated wall systems in an error message, visible when a wall section fails processing: "Highly conductive or highly resistive layers that are alternated with high mass layers may also result in problems" [23]. While this study seeks to analyze broad view relationships in building construction, the presence of scholarship on thermal mass conduction assumptions indicates that all results of this report must be viewed as indicative of thermal mass from a one-dimensional conduction perspective. Any energy savings arising from two- or three-dimensional conduction have not been considered.

Ground heat transfer is another possible source of error in studying residential construction. It has been shown that, while ground heat transfer can account for up to 50% of heat losses in residential construction, simulation models may vary by up to 60% in their estimates of the exact losses [13][24]. In addition, as of the report regarding the development of BESTEST<sup>3</sup> by the International Energy Agency to validate slab-on-grade modeling, there was still as much as an 18% error after improvements were made. In addition, programs such as TRNSYS use three-dimensional solutions that validate closely with other similar solution engines, meaning that these programs are used in cases where an analytic solution is unavailable. EnergyPlus is not considered a replacement for an analytical ground heat transfer solution due to its modeling assumptions [24].

---

3 BESTEST is the International Energy Agency Building Energy Simulation Test and Diagnostic Method, an international effort to establish testing and validation standards for energy modeling [24].

As a result of the use of a preprocessor and the incorporations of surface temperatures only into the final model<sup>4</sup>, it is possible that this particular type of ground heat transfer model may skew any results directly impacted by the assumption [24][25]. Studies comparing the ground heat transfer to DOE-2.1E show around a 25% discrepancy in the final reported values, with EnergyPlus providing lower heating HVAC energy and higher cooling HVAC energy [13].

Remaining model limitations primarily relate to internal assumptions and likely result in much smaller errors with respect to the analysis of thermal mass. For instance, since the R-value of mass walls is often lower than that of conventional construction, the importance of the convection terms is greater [12]. EnergyPlus sets the convection characteristics of walls through the choice of an algorithm rather than setting the rate of heat transfer itself [26]. However, since the film coefficients assumed by EnergyPlus seem to only change the overall characteristics of the building envelope by small amounts for the algorithms tested, these types of errors will likely not impede the ability of the program to generate realistic results.

## **2.3 Relevant Building Standards**

Building construction is governed in the United States by the International Building Code, which is a model code adopted into law by each jurisdiction responsible for approving building permits [27]. This document references other code documents. Energy modeling of single-family residential structures is not regulated by any code documents, but guidelines do exist for the creation of consistent results [28]. The following documents are key to the understanding of proper energy modeling.

### **2.3.1 Building America House Simulation Protocol**

The Building America House Simulation Protocol (BAHSP) is a document released by the United States Department of Energy to provide guidelines for standardization and validation of single-family energy modeling. The document has been designed with the hope of implementing new energy-efficient technologies and methods by providing a baseline set of modeling guidelines. While this document is not legally binding in any way, it has been endorsed by both the government agency and industry alike, and can be seen as a set of recommendations for obtaining reasonable energy modeling results [28].

---

<sup>4</sup> BESTEST recommended to EnergyPlus that changes be made to the method of incorporating ground temperatures, for the purpose of better integration [24].

### 2.3.2 International Energy Conservation Code 2012

The International Energy Conservation Code (IECC) is a document distributed by the International Code Council for the purpose of providing a model code for legally binding limitations of the energy efficiency of a building. Since the IECC has been adopted within the United States, and is the most standardized document available on energy codes for residential construction, it should be consulted and addressed in any energy modeling study to ensure code has been met. The document provides minimum recommended values for the construction of envelope materials, insulation, and windows. It also provides maximum acceptable limits on infiltration. Finally, the document provides reference material on the climate zones for United States locations, which can be used to determine not only code requirements but the comparability of weather conditions across different regions of the United States [29].

### 2.3.3 American Society for Heating, Refrigeration, and Air Conditioning

The American Society for Heating, Refrigeration, and Air Conditioning (ASHRAE) provides standards and handbooks designed to assist in the design and implementation of Heating, Ventilation, and Air Conditioning (HVAC) systems. Among these guidelines, three standards and one handbook are critical to the design and implementation of a best-practices, code-compliant energy model.

ASHRAE 55 is the guide, *Thermal Environmental Conditions for Human Occupancy*. This document provides the information required to determine if a space meets thermal comfort criteria by providing prediction and evaluation information [26][30][31]. It also provides recommendations for building thermostat setpoints that help ensure thermal comfort conditions are met [26][28]. Because it is the standard for thermal comfort, it is referenced by BAHSP<sup>5</sup> for the purpose of establishing reasonable energy modeling thermostat setpoints [28].

ASHRAE 62.2 is entitled *Ventilation and Acceptable Indoor Air Quality in Low-Rise Residential Buildings*. This standard includes the relevant information for indoor air ventilation requirements for low-rise residential construction. The requirements may be met through forced ventilation, natural ventilation, or infiltration in accordance with the procedures outlined. For instance, infiltration can be counted toward the ventilation requirements only if the quantity is in excess of that assumed and if the excess quantity is reduced by 50% [32]. Given the energy associated with increased infiltration versus ventilation, this requirement is essential to proper energy modeling of a residential structure.

ASHRAE 90.1 is titled *Energy Standard for Buildings Except Low-Rise Residential Buildings*. As indicated in the title, this document has no direct jurisdiction over the single-family residential home [33]. However, since this document forms the baseline for energy standards in the United States along

---

5 BAHSP is the Building America House Simulation Protocol introduced in Section 2.3.1.

with IECC, some of the information is referenced by IECC even for the residential procedures [34]. For instance, the climate zone information includes heating degree days and cooling degree days, which are referenced by IECC 2012 for climate zones not tabulated for the purpose of determining residential energy criteria [29][33].

The final document is not a technical standard but rather the *ASHRAE Handbook of Fundamentals*, 2009 Edition. It is an authoritative reference on the underlying information, principles, and values in the design of building systems and the consideration of energy usage. Its documentation on envelope construction, material assumptions, and heat transfer mechanisms forms a baseline of industry-standard information for the grounding of an energy analysis [35]. The handbook is referenced as the source for many EnergyPlus default values and data sets, though this information references the 2005 edition [23]. In turn, it also incorporates the scholarship of others. For instance, its recommendations on the internal loads of a residence are based upon the Building America House Simulation Protocols 2004 edition; these values have been ignored in favor of the procedures in the 2010 edition cited in this report [35].

## 2.4 Thermal Mass

The literature on thermal mass is extensive, but few available sources discuss the precise topic that this work addresses. While thermal mass can either be a passive or an active system, depending on whether building systems modifications such as radiant heating or cooling have been incorporated, this review will concentrate on the subject of this report: passive thermal mass. In general, thermal mass is the building industry term for the consideration of transient effects in conduction heat transfer, either within a space or through the building envelope. It can also be referred to as the capacitance of the building envelope, which is mathematically defined as the product of material thickness  $t$ , specific heat capacity  $C_p$ , and density  $\rho$  [36]:

$$C = t \cdot C_p \cdot \rho \quad (2-1)$$

The relevant modeling parameters to accurately capture thermal mass are extensive, extending well past the material's defined storage capacity. First, one must consider the many different parameters that can impact the density and specific heat of a material, as all of these parameters can impact a building's ability to capitalize on the effect. For instance, temperature and humidity effects alter the heat transfer properties of a material, leading to interest in the time-dependent material properties in the study of thermal mass [17]. The default of EnergyPlus is to model constant material properties; this appears to be a common assumption used in other simulation engines [10][14].

In addition to the impact of simulation parameters on the materials themselves, there is the impact of environmental factors and the interaction of various heat transfer mechanisms. It is the impact of all of

these terms, each responsible for a unique heat flux term, that complicates the quantification of thermal mass. Even in the methods developed for DOE-2 dating back to 1981, each separate term's contribution to overall energy storage was scaled according to its effect on thermal storage and accounted for separately [10]. In a survey of seventeen different mathematical models studying thermal mass, Balaras found that models generally considered some or all of the following: building geometry, material properties, detailed climate data, solar radiation, internal loads, infiltration, ventilation, and wind properties [37]. These parameters indicate that thermal mass performance is dependent on many factors in addition to the material property itself, leading to the use of energy simulation software that accounts for transient effects [38][39]. Even when considered in isolation, the implication of transient effects is that R-values alone do not represent the energy savings potential of thermal mass [40]. Still, there is precedent for the simplified modeling of geometry and material to study thermal mass, provided the essential properties are maintained in the study [22][41].

### **2.4.1 Effectiveness of Thermal Mass**

Researchers have generally determined that thermal mass is not effective in all cases. One of the factors that has a strong impact on the benefit of thermal mass is climate. One climate-dependent study of passive thermal mass indicated that, of the climates tested, Phoenix performed best in energy reduction while Minneapolis performed worst [22]. This difference in performance is not solely a function of climate but of the variation between day and night temperature, or the diurnal cycle of heat transfer [37][42] [43]. Sources indicate that good candidates for thermal mass implementation have diurnal temperature variations of at least 5 - 10 K. Often, these variations are suggested due to the ability to combine night ventilation with the use of high mass materials [37][42].

Another important consideration of thermal mass is the location of the high-mass materials. Often described as "thermal linking" or "thermal coupling," thermal mass performs better when the construction have direct exposure to the space meant to be tempered [38][42][44]. In other words, adding finish materials on top of concrete constructions often reduces or eliminates the impact of thermal mass [38] [42]. The impact of the location of insulation within a wall is also an important consideration in the effectiveness of the phenomenon [38]. A study by Kossecka and Kosny [42] using thermal structure factors to modify the standard transient heat equations determined from a mathematical and energy modeling perspective that direct mass exposure on the inside surface had better performance than mass encapsulated in insulation [43].

The concept of an optimum thermal mass material begins with a discussion of high density and high specific heat. Additional sources will often discuss conductivity as being key and existing in a proper balance with outside thermal loading conditions [42]. This information is often summarized either with new thermal mass parameters or with the use of diffusivity to represent the impact of the depth of

penetration and the effectiveness of the parameter [37][38]. In addition, one study indicated that R-values must be reasonably high to achieve the energy savings associated with thermal mass [40].

Finally, thermal mass effectiveness is determined by building design decisions. Window location and size has also been found to be crucial; one study in Australia determined that thermal mass and window size should be increased proportionally for optimum performance [45]. This research builds upon the work conducted in the 1970s and 1980s at Los Alamos National Laboratory, where research into mass material properties for energy storage coupled with windows used for passive solar led to two building references, *Passive Solar Handbook* and *Passive Solar Construction Handbook* [40].

### **2.4.2 Reduction of Peak Demand**

A large portion of the research into the benefits of thermal mass pertains to the reduction of peak demands by using thermal mass in conjunction with building setpoints. For instance, by using setpoints such as daytime 22.2°C and night 29.4°C, a building-specific thermostat model reduced the peak by 25-60% [46][47][48]. Since residences are occupied at night, such a strategy is only applicable to commercial buildings. Also, larger commercial buildings are considered better candidates for this type of system because there is generally more mass for a given external surface area [49]. Geometry is not the only limitation on setpoint strategies; improper calibration of a setpoint system can result in rebound effects, where additional money and/or energy is used over the baseline, low mass scenario [50][51].

A key omission in many discussions of peak demand reduction is the overall energy reduction. One study indicated the ability to use reduced peak demand to obtain a conditioning system with lower capacity, reducing energy efficiency loss caused by equipment oversizing [52]. Another study indicated that cooling system loads could be reduced by 10-15% through one of these demand-limiting strategies; note the reduction from the values quoted for peak reduction [47]. In general, the discussions of peak demand reduction are a means to reduce operating costs rather than operating energy. The cost reduction arises from the use of off-peak energy billed at a lower rate, not from the use of less energy [49][51].

### **2.4.3 Reduction of Overall Energy Consumption**

Studies have generally indicated that there is a reduction of annual energy consumption through the passive use of thermal mass. Before proceeding, however, a clear distinction must be drawn between the available literature on energy savings versus the available literature on financial benefits. The preceding section discussed strategies primarily aimed at financial gains through using energy during off-peak, lower billing periods [49]. Considering night cooling rather than thermostat setpoints, a test chamber

containing a residential test building experienced a 50% drop in electricity usage due to thermal mass, whereas a 20% reduction in energy consumption in commercial buildings has also been observed [37].

Specifically, many night cooling schemes are most promising in mild climates or climates with large diurnal temperature variations. A sensible load reduction of 40% has been achieved through the use of night ventilation with these conditions, but this reduction does not consider the additional latent loads from the ventilation [37]. A study performed on a building in Cyprus optimized roof overhang, wall thickness, and infiltration to obtain a 47% reduction in the heating energy consumption through simulation of a mass wall on the south facade. Notably in this study, cooling loads showed a small increase due to the addition of thermal mass [38].

Many studies have been conducted in multiple climates without consideration of diurnal variations and for buildings where neither night ventilation nor setpoint modification have been employed. One study looking to provide recommendations for LEED<sup>6</sup> credits for energy reduction determined that climates such as Miami would receive no LEED points, whereas other climates tested (Phoenix, Denver, Chicago, Memphis, Salem OR) would likely obtain 2-4 LEED points, corresponding to an overall energy reduction ranging from 6-9% [53]. Notably, this report has been used by others in the formulation of recommendations regarding thermal mass, including its incorporation into the B-PATH model as the operational energy savings for concrete construction [4].

Studies conducted by the U.S. Department of Energy between 1983 and 1985 indicated a 5% annual energy savings in New Mexico for windowless test buildings, despite comparing an R-13 wood wall to R-2 to R-5 mass walls. Researchers believe that the failure to compare like R-values negatively impacted the energy saving results. A supplemental DOE study in Tennessee during this time period found 10-13% energy savings from employing thermal mass [40]. NAHB field experiments combined with Oak Ridge National Laboratory energy simulations concluded that the difference in R-value between standard wood construction (R-13) and a test ICF wall (R-20) should result in 8-9% energy reduction while the thermal mass savings amount to 11%, for a combined 20% reduction in annual energy use [40].

One of the most notable series of investigations on the energy consumption of thermal mass has been performed by Kossecka and Kosny et al [40][55][56], which complemented building monitoring with rigorous mathematical investigation. This investigation has led to a revised representation of one-dimensional constructions for the purpose of thermal mass, where structure factors consider whether the thermal mass is exposed in the calculation of energy consumption [55][56]. The result of this ten-climate study indicated a national average savings of 6-8% with benefits reaching 12% under select circumstances. In contrast, low R-value walls in some climates showed increased energy performance versus lightweight construction [40]. Finally, the use of the structure factors indicated that exposed

---

6 LEED is Leadership in Energy and Environmental Design, a sustainable building certification program sponsored by the United States Green Building Council [54].

internal mass construction showed better benefits than mass isolated from the internal environment by insulation [22][56]. The net result of these experiments is an indication that climate, wall construction, and overall R-value play important roles in the determination of thermal mass benefit.

#### **2.4.4 Relationship to Thermal Comfort**

Thermal mass can have either a strong positive or a strong negative impact on thermal comfort, as sources on thermal mass's relationship to internal temperature are varied and climate plays an important role. One of the strongest claims behind thermal mass is its ability to provide interior temperature stability [37][38][40]. However, other sources claim that a variable interior temperature is a critical component of capitalizing on thermal mass [42]. This can likely be attributed to the difference between the moderating effect of the surface temperature, and the tolerated internal temperature range before environment conditioning systems are triggered [38].

These impacts on the internal temperature, in turn, affect the thermal comfort of occupants. While the stable concrete temperature can be used to improve thermal comfort, overheating can also result [37][42]. In general, the benefit to thermal comfort comes from its consideration both of air temperature and surface temperature [26]. Therefore, in a building employing thermal mass effectively, the mass will reduce temperature fluctuations in the surface temperature, which stabilizes the effective temperature felt by the occupant and improves thermal comfort [45]. Mild climates such as California and Nairobi, Kenya have both been shown to employ thermal mass without overheating effects [57]. In contrast, research in Thailand has aimed to use hollow concrete construction materials, reducing thermal mass due to its tendency to overheat in this climate [58].

## **2.5 Chapter Summary**

This chapter provides a brief overview of the available, relevant literature on energy modeling, energy standards, and thermal mass. The energy modeling information shows that, while EnergyPlus may have a few key limitations, it provides validated energy results for thermal mass inputs. The building standards are a reminder that energy modeling should not exist in a vacuum; building use is subject to distinct patterns and requirements, which should be incorporated into any working model. The thermal mass research indicated that, while there is substantial information on the heat transfer mechanisms, building controls implementation, and thermal comfort concerns, the information on the actual energy savings from thermal mass appears to be the weakest link. This finding has been used as the primary impetus for the second research question and primary charge of the report:



2. From a quantitative perspective, what is thermal mass? Of the main thermal properties of a material (thickness, conductivity, density, specific heat), which have the greatest impact on energy consumption by climate?

No study can conduct every possible simulation; this report will aim to determine if the typical developer concrete home will have thermal mass benefits from the incorporation of heavier construction materials. It will not aim to repeat the work above, nor will it aim to validate the impact of thermal mass in highly specialized, high performance homes, such as those designed using the siting and orientation procedures of Passive House. This work is separated from its peers by the use of simplification and the development of a wide-angle view across many material properties and locations. In the next part of this report, the design, calibration, and validation of the Cube Model will be presented to provide a framework for the simplified analysis of thermal mass through the use of energy modeling tools.

**Part II**

**Model Development, Calibration, and**

**Validation**

# Chapter 3

## The Cube Model

The Cube Model has been developed as an approximation of a full energy model with the intent of studying thermal mass impact through many possible material combinations. This model responds to the first research question, which addresses the need for a model which can predict the energy consumption of a home with a reduced number of parameters. The underlying mathematical basis for building analysis is similar for all typologies, allowing this representation to be potentially adapted to other building types by appropriately changing the constant parameters, such as the internal loads. The goal of the model is to use accurate representations of the heat flux terms and a simplified representation of building geometry and envelope design. This model provides schematic design level energy predictions requiring the level of knowledge available at the early phase of building design. This chapter will present the relevant mathematical basis of building energy consumption, the methodology of the cube model itself, and the detailed model inputs used to set the constant values in the building.

### 3.1 Model Overview

The Cube Model is a model based on a combined heat and moisture balance modeled by EnergyPlus, the energy modeling software provided by the United States Department of Energy. In addition to the solution of both phenomena, the program simultaneously solves the envelope, the system energy, and the air balance by considering multiple different regions. This model overview will explain the fundamental mechanics of the solution engine and how these mechanics are applied to generate a full energy model of a building and the total energy used by the system.

#### 3.1.1 Heat Balance

The underlying principle of energy consumption is the heat equation, and this comprises the majority

of energy consumption in most climates. The principle of this heat balance is that, for any given entity in a building, the heat stored, heat generated, and heat imposed by flux terms must be in equilibrium. Such equations can be written for the energy balance in envelope materials and zone air. Since these components are in contact with one another, the relationships between the terms form the boundary conditions of an adjacent element. Finally, the climate conditions and ground heat transfer form the exterior boundary conditions of the building.

Taking the envelope as the target material, the energy balance can be expressed by [59]:

$$\frac{dU}{dt} = Q_1(t) + Q_2(t) \quad (3-1)$$

In this expression, the term  $dU/dt$  defines the change of the internal energy stored in the wall with respect to time, the term  $Q_1(t)$  represents the movement of heat inside or outside of the volume, and the final term  $Q_2(t)$  represents any sources that exist inside of the volume itself [59].

In order to properly use this equation, each of the terms described above should be better defined. The first term,  $dU/dt$ , is the one most important to the study of thermal mass, as it mathematically defines the energy stored within the envelope material. This material property is defined based on the specific internal energy  $du$ , a function of specific heat  $C_p$ , and the density of the material  $\rho$ , as described by [59]:

$$du = C_p(\vartheta) d\vartheta \quad (3-2)$$

$$\rho = \rho(\vartheta) \quad (3-3)$$

$$\frac{dU}{dt} = \int_{(V)} \rho(\vartheta) C_p(\vartheta) \frac{\partial \vartheta}{\partial t} dV \quad (3-4)$$

The second term in Equation (3-1) represents the rate of heat transfer into the envelope from either the inside or outside of the building. The time-dependent representation of this term is defined by the heat flux through the envelope  $\mathbf{q}$ , the orientation of the envelope surface is defined by its unit normal vector  $\mathbf{n}$ , and the differential surface area is shown as  $dA$  [59]:

$$Q_1(t) = - \int_{(A)} \mathbf{q}(\mathbf{x}, t) \cdot \mathbf{n} dA \quad (3-5)$$

The final term in Equation (3-1) is the internal source term,  $Q_2(t)$ . This term assumes that either there is an energy change due to volume changes, internal energy generation, or internal source loads. Considering the passive envelope which does not incur volume changes, this term can be assumed to be zero. When applying these equations to a fluid as the medium, internal point source loads result in a non-zero term. The point source loads include the energy contribution from the conditioning system for the room air balance [14][59].

The only term in these heat equations left to define is the magnitude of the heat flux acting on the system. For conduction, heat flux is defined by the relationship between the temperature profile and the flux; that is, either temperature or flux can be imposed on a conduction driven system while the other term is the resultant of the equation. This relationship is given in equation form by Fourier's Law for conduction through a solid [59]:

$$\mathbf{q}(\mathbf{x},t) = -\lambda \text{grad } \vartheta(\mathbf{x},t) \quad (3-6)$$

Once the balance of heat has been established, the boundary conditions of the heat transfer problem must be established for the energy model to be well posed. Either the continuity of temperature or the continuity of flux must be imposed. For the continuity of temperature to be satisfied, for solid-solid, solid-fluid, or fluid-fluid contact conditions must have equal temperatures at the interface of the media [59]:

$$\vartheta_i^{(1)} = \vartheta_i^{(2)} \quad (3-7)$$

For the flux condition, there must be a continuous heat flux or a deviation in heat flux specified by a specific resistance. The continuity equation for solid-solid contact is given by the balance of the partial derivative of the temperature function with respect to the surface, scaled by the conductivity of the medium [59]:

$$\lambda^{(1)} \left( \frac{\partial \vartheta^{(1)}}{\partial \mathbf{s}} \right)_i = \lambda^{(2)} \left( \frac{\partial \vartheta^{(2)}}{\partial \mathbf{s}} \right)_i \quad (3-8)$$

Should the contact condition be between a solid and a fluid, such as the interaction of the wall with the room air, then the balance is governed by a linear exchange condition. This equation includes the product of conductivity and the partial derivative with respect to surface, balanced by the product of the contact heat transfer coefficient and the temperature difference at the point of contact [59]:

$$-\lambda \left( \frac{\partial \vartheta}{\partial \mathbf{s}} \right)_{\text{SOLID}} = \alpha (\vartheta_{\text{SOLID}} - \vartheta_{\text{FLUID}}) \quad (3-9)$$

These heat transfer equations act as the governing principles of energy modeling. The art of energy modeling moves beyond the mathematics to the determination of key magnitudes of the terms. The magnitudes of these loads will be presented in Section 3.2.4 for the internal loads and Section 3.3.1 for the external loads. Generally, internal loads are assumed to have both a radiant and convective portion, solar impacts have a radiant heat gain, and weather effects impact the building through direct air contact and air movement shown in the conduction and convection equations [14][26].

As a conclusion to this derivation, it is important to note that EnergyPlus does not use the full continuum theory representation of heat transfer; instead, it uses a space-state formulation and numerical methods to approximate the solution. In addition, a few key simplifying assumptions are made to these equations.

First, the thermal properties of a material are assumed to be independent of the temperature profile, resulting in constant density, conductivity, and specific heat. This assumption is valid under steady-state conditions but can break down under situations such as solar radiation acting on a surface, resulting in a localized change in thermal properties on that surface from the induced temperature increase. To illustrate the means of reducing the equations, only the conduction component will be considered here. With this assumption, substituting Equations (3-4), (3-5), and (3-6) into (3-2), and applying the Gauss divergence theorem, the equation for transient heat conduction emerges [14][36][59]:

$$\int_{(v)} \left[ \rho C_p \frac{\partial \vartheta}{\partial t} + \lambda \nabla^2 \vartheta \right] dV = 0 \quad (3-10)$$

For this relationship to hold, the integrand must be equal to zero. Dividing the relationship by  $\rho C_p$ , the linear conduction component of the heat equation can be written as [59][60]:

$$\frac{\partial \vartheta}{\partial t} = a \frac{\partial^2 \vartheta}{\partial x^2} \quad (3-11)$$

This equation holds with the diffusivity of a material defined by [59][60]:

$$a = \frac{\lambda}{\rho C_p} \quad (3-12)$$

This relationship is significant in that it shows diffusivity,  $a$ , as the measure of the rate of temperature change. Such a measure will be an important quantity in discussing the thermal mass of building systems [59][60].

The other main simplifying assumption is the reduction of the conduction problem to a one-dimensional system with the surface area assumed constant. In addition, this means that the material properties are assumed constant throughout the surface area, and all heat transfer occurs through the thickness of the envelope. This can result in improper estimation of complex systems with multi-dimensional thermal bridging phenomena [14][36][59]. The result of these simplified assumptions are the equations presented in the Engineering Reference for EnergyPlus for the heat balance terms [14]. While these equations have been particularized to the one-dimensional and building cases, they represent the interactions of the conduction, convection, and radiation flux terms presented in this section, namely:

$$C_z \frac{dT_z}{dt} = \sum_{i=1}^{N_{sl}} \dot{Q}_i + \sum_{i=1}^{N_{surfaces}} h_i A_i (T_{si} - T_z) + \sum_{i=1}^{N_{zones}} \dot{m}_i C_p (T_{zi} - T_z) + \dot{m}_{inf} C_p (T_{\infty} - T_z) + \dot{Q}_{sys} \quad (3-13)$$

The left side of the equation represents the change in temperature with respect to time,  $dT_z/dt$ . This term is scaled by the factor  $C_z$ , an optional parameter for modeling stability with no physical significance. For the purpose of this report, it has been set to 1 to remove it from consideration. The first term on the right side of the equation is the sum of internal point load contributions, input at rate terms. The second term is the contribution of the building envelope, whose magnitude is defined by the heat transfer coefficient

$h_p$ , the surface area  $A_p$ , and the difference in temperature between the surface  $T_{si}$  and ambient room  $T_z$ . This term is summed over the total number of surfaces in the model. The third term in the equation is the contribution of inter-zone mixing, which is defined by the mass transfer rate  $\dot{m}_p$ , the specific heat of air  $C_p$ , and the difference of temperature between the adjacent zone  $T_{zi}$  and the ambient room  $T_z$ . This contribution is summed over the total number of zones in the model. The fourth term in the equation is the contribution of infiltration, represented by the mass flow rate  $\dot{m}_{in}$ , the specific heat of air  $C_p$ , and the difference of temperature between the outdoor air  $T_o$  and the ambient room  $T_z$ . The final term is the source term due to the HVAC system [14].

From this equation, the sensible conditioning energy can be determined through the use of  $\dot{Q}_{sys}$  through the summation expression:

$$Q_{sys} = \int \dot{Q}_{sys} dt \quad (3-14)$$

For the purpose of this report, the continuous approximation of the summation is used to generate the hourly energy quantities as outputs. These terms are then totaled to achieve the final sensible energy consumption:

$$Q_{sensible} = \sum Q_{sys} \quad (3-15)$$

### 3.1.2 Mass Balance

The second major phenomena to act upon a building is the mass balance of moisture content in the system. This is a balance of the quantity of moisture in the air and inside materials, which is governed by mass diffusion and transport equations. Many of these equations are analogous to heat transfer concepts, resulting in very similar formulations. Beginning with the movement of moisture through the envelope, the diffusion is the change in flux through the envelope, given by [36][59]:

$$\int_{(V)} \frac{\partial \rho}{\partial t} dV = - \int_{(A)} j_A^* n dA \quad (3-16)$$

In this equation, the partial derivative of moisture content with respect to time, integrated over volume, equals the area integral of flux moving through the envelope in the direction of the unit normal  $\mathbf{n}$ . For this equation to hold, the flux is governed by Fick's Law, the mass balance analog to Fourier's Law [36][59]:

$$j_A^* = -\rho D \text{grad } \xi_A \quad (3-17)$$

While this is considered the quiescent solution, it is the one employed by the energy balance equation due to the relative insignificance of this term in comparison to larger latent loads [36][59]. Most of the impact

of mass transport is in the contribution of air movement, including infiltration, ventilation, gains from domestic hot water systems, and building air circulation. While the hot water gains can be represented as point loads in the system, the other air movement results in a net increase or decrease of the mass of moisture present. The change in concentration due to convective mass transfer equals the sum of the volume integral of the density change with respect to time and the volume integral of the density change with respect to position. Here,  $w_i$  is a measure of the volume and  $x$  is the direction of transport. This is known as the Reynolds transport theorem [59]:

$$\frac{dM}{dt} = \int_{V(t)} \frac{\partial \rho}{\partial t} dV + \int_{V(t)} \frac{\partial \rho w_i}{\partial x_i} dV \quad (3-18)$$

Similarly to the heat balance, EnergyPlus does not solve the differential version of the mass balance but rather the one-dimensional simplification assuming independence of all material properties with respect to concentrations, position, and temperature. This results in the final equations presented by EnergyPlus [14]:

$$\rho_{\text{air}} V_z C_w \frac{dW_z}{dt} = \sum_{i=1}^{N_{\text{sl}}} k g_{\text{mass,bed load}} + \sum_{i=1}^{N_{\text{surfaces}}} A_i h_{\text{mi}} \rho_{\text{air},z} (W_{\text{surfs}_i} - W_z^t) + \sum_{i=1}^{N_{\text{zones}}} \dot{m}_i (W_{z_i} - W_z^t) + \dot{m}_{\text{inf}} (W_{\infty} - W_z^t) + \dot{m}_{\text{sys}} (W_{\text{sup}} - W_z^t) \quad (3-19)$$

The left side represents the change in moisture content with respect to time  $dW_z/dt$ , scaled by the zone volume  $V_z$ , the density  $\rho_{\text{air}}$ , and the non-physical scaling constant  $C_w$ . The first term on the right side represents source term moisture loads that exist within the system by their sum. The second term represents the transfer of moisture through the envelope by the surface area  $A_i$ , the transfer coefficient  $h_{\text{mi}}$ , the air density  $\rho_{\text{air},z}$ , and the difference in moisture content between the surface  $W_{\text{surfs}_i}$  and the room  $W_z$  at time  $t$ . The total contribution is the sum from all surfaces. The third term is the contribution of moisture content from other zones, represented as the summation from all zones. This term is dependent on the mass transfer rate  $\dot{m}_i$  and the difference in moisture content between the adjacent zone  $W_{z_i}$  and the room  $W_z$  at time  $t$ . The fourth term is the contribution from infiltration, dependent on the mass transfer rate  $\dot{m}_{\text{inf}}$  and the difference in moisture content between the outdoor air  $W_{\infty}$  and the room  $W_z$  at time  $t$ . The final term is the contribution of moisture content from the system, represented by the product of the mass transfer rate  $\dot{m}_{\text{sys}}$  and the difference in moisture content between the supply air  $W_{\text{sup}}$  and the room  $W_z$  at time  $t$  [14].

From the equation, the latent load contribution can be calculated using the system energy component:

$$Q_{\text{sys,w}} = \int \dot{m}_{\text{sys}} (W_{\text{sup}} - W_z^t) dt \quad (3-20)$$

Taking this expression to represent the hourly output of EnergyPlus for the energy consumption, the final latent energy consumption for the building can be defined by:



$$Q_{\text{latent}} = \sum Q_{\text{sys,w}} \quad (3-21)$$

The energy consumption values presented in this report section will be the sum of the latent and sensible components. Specific energy consumption represents this sum of latent and sensible load divided by the volume of the building.

## 3.2 Methodology

The previous section considered heat and moisture transfer as it applies to all buildings. This section will introduce the key assumptions regarding the simplification of buildings to the cube geometry proposed. The Cube Model includes a reductionist geometry approximation as a prismatic solid defined only by equivalent length, width, and height, as illustrated in Figure 3-1. The model is designed to provide relationships regarding the thermal performance of a building. In contrast with the reductionist building geometry, the model has been constructed with the goal of creating accurate estimations of heat flux terms. These driving forces are treated as constants but must be set based on available data and protocols to ensure that the model accurately reflects the nature of a true building. Assumptions for these loads have been based on available EnergyPlus weather data for exterior heat flux and Building America House Simulation Protocols (BAHSP), a publication from the National Renewable Energy Laboratory, for the internal flux loads [23][28]. Finally, ground heat transfer flux assumptions have been generated through the preprocessors available in EnergyPlus, with accurate modeling constants from scholarly publications.

The effect of this methodology is to limit the number of inputs to determine by the user. In addition, the model's experiments are conducted using baseline values for the constant parameters. This discussion will refer to a basic cube and its extensions; the basic cube contains only a slab-on-grade, walls, and a roof while the advanced extensions adjust the model to incorporate internal slabs, an attic, and additional ground conditions. The remainder of this section discusses the specific modeling assumptions and baseline values for the most important components of the Cube Model framework: simplified geometry, equivalent envelope parameters, idealized HVAC system, and accurate loading. The following section will address additional constant inputs used in the model.

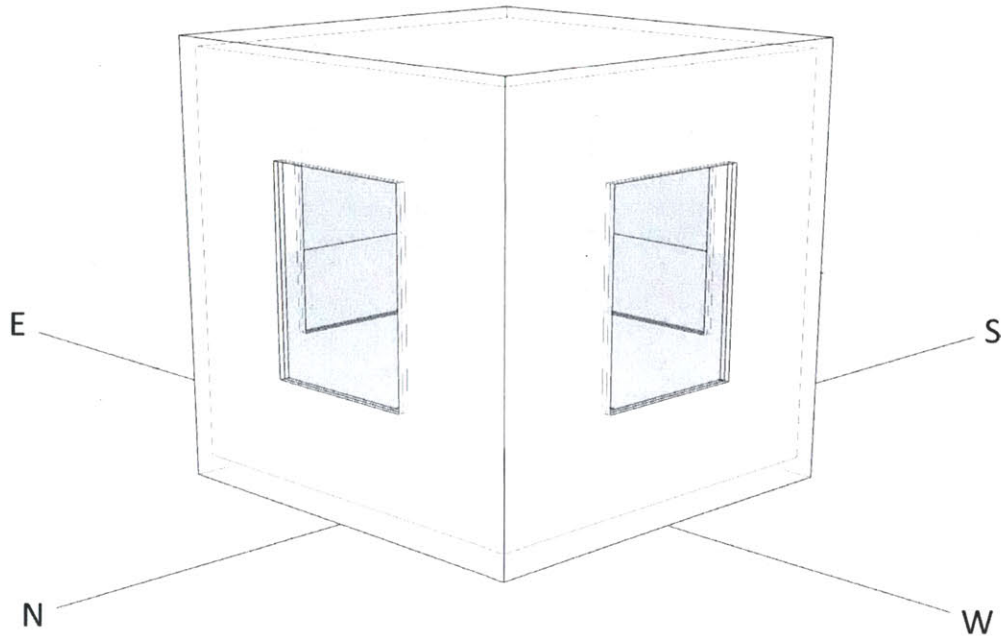


Figure 3-1 Idealized Cube Model, conceptual representation

### 3.2.1 Simplified Geometry

The Cube Model has a simplified, rectilinear prismatic geometry for the purpose of developing a set of relevant simulation experiments. The cube can be controlled by volume, by plan aspect ratio, or by individual dimension assumptions to better standardize to modeling objectives and illuminate size effects in physical phenomena. The parametric nature of the dimensioning of the building allows many building geometry options to be explored quickly. The basic cube model can be seen as a single cube model, while the advanced cube model can contain up to three stacked cubes: one for the main zone, and two additional cubes to represent attic and basement conditions. Where no values are specified, the baseline dimensions include no attic, no basement, and a 4 m tall cube that is 10 m x 10 m in plan. This is representative of a modestly sized house of between one and two stories. In order to compare the results of the Cube Model to a complete energy model, a standardized procedure must be devised to convert the properties of an actual home to the cube model. The following sections will discuss the conversion procedure from an actual building to the Cube Model.

#### 3.2.1.1 Basic Cube Geometry Conversion

Building dimensions are approximated to determine the prismatic equivalent of the building. Note that the walls are orientation-specific with north shown in Figure 3-2 along with the graphic description of this procedure. For all calculations, overhangs and protrusions that substantially deviate from the footprint of

the building are neglected. To determine the building length and width, a weighted average of the length and width of the building is obtained. The relevant parameters are the set of  $n$  widths  $W_i$  and  $n$  lengths  $L_i$ , which can be averaged using:

$$L_{eq} = \frac{\sum_{i=1}^n L_i \cdot W_i}{\sum_{i=1}^n W_i} \quad (3-22)$$

$$W_{eq} = \frac{\sum_{i=1}^n L_i \cdot W_i}{\sum_{i=1}^n L_i} \quad (3-23)$$

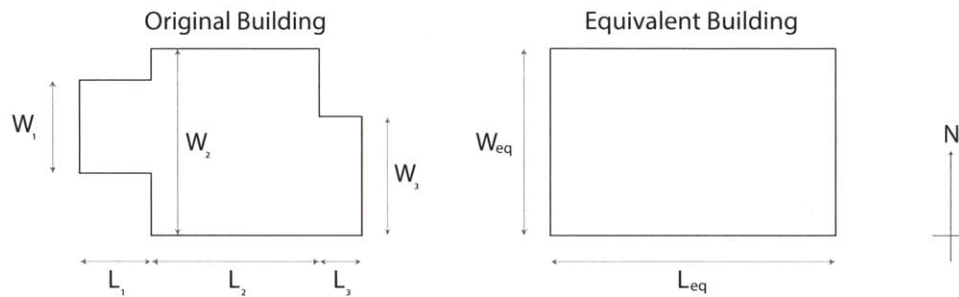


Figure 3-2 Determination of Cube Footprint from Example Irregular Floor Plan

For the basic cube, the height is defined as the dimension from the slab-on-grade to the ceiling on the upper floor of the conditioned space. The roof geometry need not be considered if all slopes are contained in an unconditioned attic. For buildings with sloped condition space, the procedure for determining the dimensions of the attic, explained below, can be adapted for the determination of the conditioned volume.

### 3.2.1.2 Advanced Cube Geometry Conversion

The conditioned space of the building is calculated in the same manner as the basic cube. Internal slabs can only be specified by the number of internal levels, and it is assumed that floors extend over the entire footprint. If a basement is desired, it is assumed to extend under the entire footprint and is defined only by its height. Since the height is variable, this feature can be used to approximate either a crawlspace or a full basement. It does not model walk-out basements or building geometries where the grade level changes substantially over the floor plan of the building.

The attic cube is also assumed to cover the floor plan of the entire building and is defined only by a constant height. Figure 3-3 shows a graphic representation and a sample model conversion for a gable roof. To determine the attic height, a volumetric average of the attic should be taken. That is, the model assumes that the attic for the equivalent model has the same volume as an attic for the full energy model,

but that the volume is configured as a cube. The height  $H_a$  of the equivalent attic is obtained from volume  $V_a$  and equivalent dimensions  $L_{eq}$  and  $W_{eq}$  using:

$$H_a = \frac{V_a}{L_{eq} \cdot W_{eq}} \quad (3-24)$$

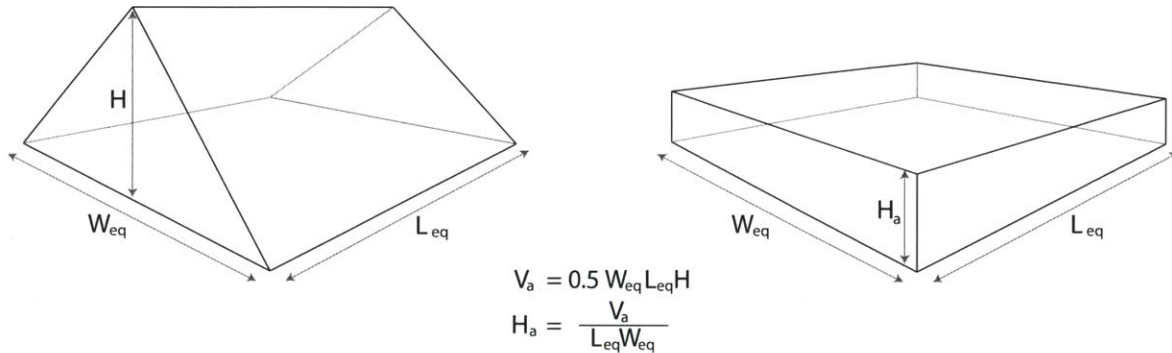


Figure 3-3 Determination of Attic Height from a Sloped Roof Condition

### 3.2.2 Equivalent Envelope Parameters

The Cube Model uses an equivalent envelope rather than modeling the full construction details of the envelope. Therefore, there is only one layer to the floor, walls, roof, and constructions for the advanced extensions of the model. Each layer comprises the effective thickness, thermal conductivity, density, and specific heat capacity of the overall construction. Material property assumptions have been obtained from ASHRAE Handbook of Fundamentals 2009 and the materials data set available with EnergyPlus, based on the ASHRAE Handbook of Fundamentals 2005 [23][35]. Specifically, the four effective properties discussed above (thickness, thermal conductivity, density, and specific heat capacity) have been obtained directly from ASHRAE, while the qualitative parameters such as surface roughness have been set to the EnergyPlus standard approximations of ASHRAE materials. Finally, thermal, solar, and visible absorptance have been set to BAHSP standard inputs for walls and roofs, where the wall values have been used for non-specified envelope constructions.

A baseline material cube has been programmed to be pure concrete for walls, roofs, and slabs, with no additional geometric constructions. Where the attic floor, basement walls, basement slab, or internal slabs are used to extend the Cube Model, these constructions are created in the same way but can each be varied independently from the main cube materials. Numbers have been rounded during the course of experiments; the baseline values used can be found in Table 3-1.

Table 3-1 Baseline Envelope Properties

Surface	Thickness	Conductivity	Density	Specific Heat
Roof	0.15 m (6 in)	0.9 W/m-K	2300 kg/m <sup>3</sup>	650 J/kg-K
Walls	0.15 m (6 in)	0.9 W/m-K	2300 kg/m <sup>3</sup>	650 J/kg-K
Slab	0.15 m (6 in)	0.9 W/m-K	2300 kg/m <sup>3</sup>	650 J/kg-K

To convert from actual building materials to the equivalent envelope parameters, the following procedure should be used. There are four parameters that must be determined: thickness, thermal conductivity, density, and specific heat capacity. Thickness is the simplest; the equivalent thickness  $t_{eq}$  is the total thickness of the  $n$  construction layers, each of thickness  $t_i$ :

$$t_{eq} = \sum_{i=1}^n t_i \quad (3-25)$$

Next, the equivalent R-value of the wall section needs to be calculated. This value can be obtained by summing the R-values of each individual layer using one-dimensional conduction assumptions. Note that EnergyPlus automatically adds the film coefficients for convection on either side of the wall section, so the R-value obtained here only needs to include the geometry of the wall section [14]. The equation for determining the R-value of a given material  $R_i$  based on its thickness  $t_i$  and thermal conductivity  $\lambda_i$  is given by:

$$R_i = \frac{t_i}{\lambda_i} \quad (3-26)$$

The expression for the equivalent R-value of the construction  $R_{eq}$  is given as the summation of a wall composed of  $n$  materials whose R-values are given by  $R_i$ :

$$R_{eq} = \sum_{i=1}^n R_i \quad (3-27)$$

The R-value of the section can then be used to calculate the thermal conductivity of the equivalent wall section. This calculation uses the previously calculated equivalent thickness and equivalent R-value in its formulation:

$$\lambda_{eq} = \frac{t_{eq}}{R_{eq}} \quad (3-28)$$

Following the R-value, a measurement of the thermal mass must be calculated, sometimes referred to as the capacitance or C-value of the wall section [22][36]. The equations for determining the C-value of a given material  $C_i$  depends on its thickness  $t_i$ , density  $\rho_i$  and specific heat  $C_{p,i}$ :

$$C_i = t_i \cdot \rho_i \cdot C_{p,i} \quad (3-29)$$

Then the equivalent C-value is the summation for n layers in the system:

$$C_{eq} = \sum_{i=1}^n C_i \quad (3-30)$$

The equivalent density of the material is calculated by obtaining a weighted average of the densities of the individual materials, where the densities  $\rho_i$  of the material are weighted by the individual thicknesses  $t_i$ :

$$\rho_{eq} = \frac{\sum_{i=1}^n t_i \cdot \rho_i}{\sum_{i=1}^n t_i} \quad (3-31)$$

Lastly, the C-value  $C_{eq}$  and the equivalent density  $\rho_{eq}$  are used to determine the equivalent specific heat of the construction:

$$C_{p,eq} = \frac{C_{eq}}{t_{eq} \cdot \rho_{eq}} \quad (3-32)$$

Through this procedure, the equivalent properties of the wall section have been obtained. Table 3-2 shows the properties of standard wall sections provided with EnergyPlus [23]. These properties show the magnitudes of input parameters for an equivalent wall section that should be considered in an analysis. Figure 3-4 provides an illustration of the referenced values used in the calculation performed above.

Table 3-2 Envelope Properties of EnergyPlus Standard Wall Sections [23]

Construction Name	Thickness (m)	Conductivity (W/m-K)	Density (kg/m <sup>3</sup> )	Specific Heat (J/kg-K)
Composite 2x4 Wood Stud R11	0.127	0.0636	274	1048
Composite 2x6 Wood Stud R19	0.177	0.0577	209	1006
Composite ICF Wall With Steel Ties	0.273	0.138	1173	971
Composite Concrete/Foam/Concrete With Steel Connectors	0.204	0.151	1395	1069
Composite Concrete/Foam/Concrete With Plastic Connectors	0.204	0.108	1521	975
Composite 2x4 Steel Stud R11	0.127	0.0816	230	1048
Composite Brick Foam 2x4 Steel Stud R11	0.223	0.0989	824	814
Composite 2x6 Steel Stud R19	0.177	0.0886	175	1006
Composite Foam 2x6 Steel Stud R19	0.210	0.0786	329	876
Composite Brick Foam 2x6 Steel Stud R19	0.273	0.100	695	964
Composite 2-Core Filled Concrete Block Uninsulated	0.295	1.24	1405	706
Composite 2-Core Filled Concrete Block Insulated	0.295	0.732	1186	838

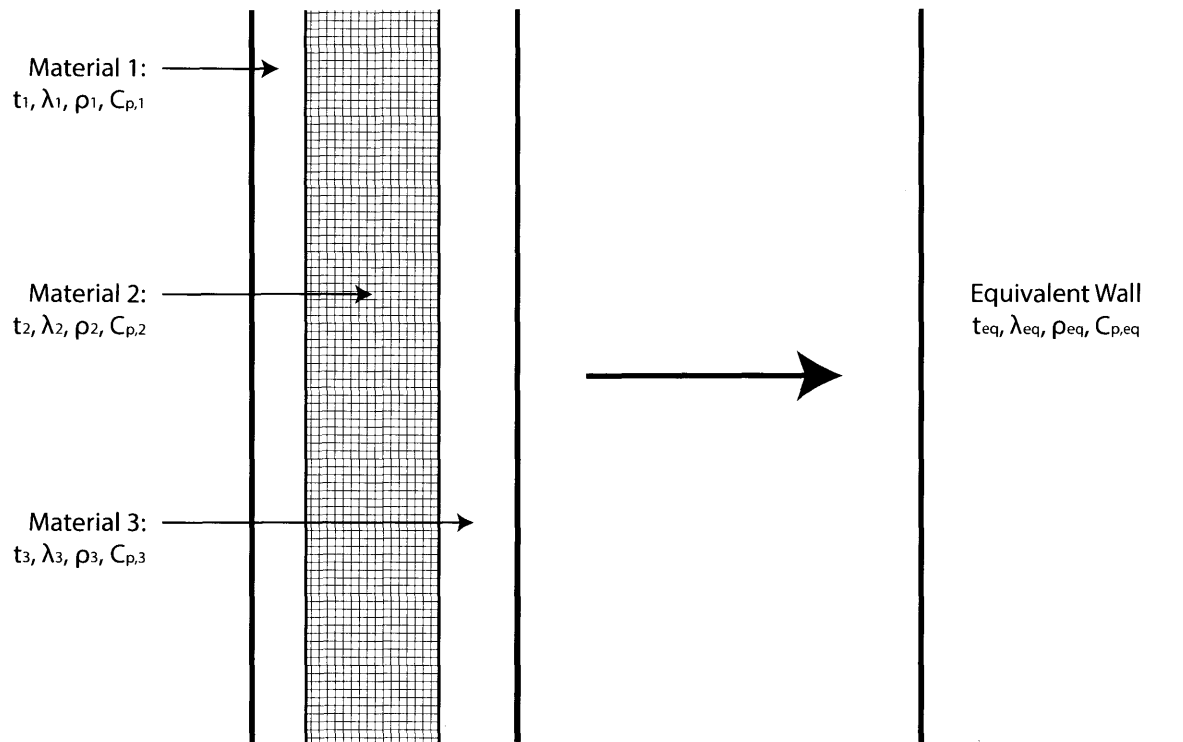


Figure 3-4 Equivalent Wall Calculation Inputs

### 3.2.3 Idealized HVAC System

The Cube Model utilizes the Ideal Loads Air System in EnergyPlus. This system calculates the combined sensible and latent cooling and heating loads as a result of design decisions, but it does not obtain energy values in electricity or fuel consumed. This system is intended for applications where building performance is the target of the study, not HVAC performance. The system has been programmed with infinite capacity, no economizer, no heat recovery, and EnergyPlus default inputs for supply air temperature and humidity [26]. The system supplies ventilation according to the strategy discussed in Section 3.3.3. For the advanced extensions of the cube, the attic is never conditioned, and the basement includes the option to be conditioned as a separate zone.

Building setpoints have been set in accordance with the procedure outlined from BAHSP. That is, there is a heating setpoint of 21.67 C (71°F) and a cooling setpoint of 24.44 C (76°F), which are based on ASHRAE 55. Heating and cooling availability and the switch between the setpoints has been established using the BAHSP procedure based on the monthly average temperatures, 99% design days provided by ASHRAE, and adjustment parameters exclusive to BAHSP. Finally, the setpoint for dehumidification in the winter is set at 60% relative humidity [28]. Natural ventilation is not provided, as allowed by BAHSP and to accommodate the simplified air flow network in the idealized HVAC system [26][28].

### 3.2.4 Accurate Loading

The need for accurate weather and scheduled loading is recognized in the energy simulation community as key to obtaining realistic results [12]. For the Cube Model, the types of loads considered are internal mass, occupation gains, lighting, appliances, and domestic hot water. The magnitudes of these loads have been established through BAHSP methods. According to these methods, some loads are fixed in magnitude, some vary by the finish floor area, and others vary by the number of bedrooms in the residence [28]. For the finish floor assumptions, the square footage of the cube and any additional internal slabs are considered for the main living area. Since no bedrooms are modeled, the number of bedrooms is calculated using the BAHSP formula for occupants per bedroom [28]:

$$Occupants = 0.59 \cdot N_{br} + 0.87 \quad (3-31)$$

The number of occupants has been set as the average household size from the 2010 U.S. Census: 2.58 [61]. The result of the above equation reveals that a residence should have 2.90 bedrooms. Finally, the internal loads have been programmed with the BAHSP vacation schedule off, due to the desire to have a fully occupied year-round cube.

To model internal loads with the existence of attics and basements, the following assumptions are made: all loads are assumed to occur in the main living zone, with one important exception. In the case of a finished basement, those loads that are increased by BAHSP as a result of the increase in finish floor area (internal mass, lighting, and miscellaneous plug loads) are assumed to act in the basement. The following subsections list the magnitudes of the internal loads. Details on the schedules and their calculation can be found in Appendix A, as each variable internal load is modified by a set of 288 values.

#### 3.2.4.1 Internal Mass

BAHSP requires the internal mass of the building to be 8 lb/ft<sup>2</sup> [28]. From an EnergyPlus standpoint, this translates to a typical wood material with an exposed surface area of 65% of the finished floor area. The use of wood is recommended by the EnergyPlus data set, whose inputs for surface roughness have also been used [23].

#### 3.2.4.2 People

While the number of people has been fixed to the 2010 Census data, the magnitude of the load has been set from BAHSP assumptions for occupancy [28][61]. The baseline sensible internal load for occupation



is 220 Btu/person/h and the baseline latent internal load is 164 Btu/person/h [28]. Schedule assumptions have also been obtained from BAHSP and are available in Appendix A [62].

### 3.2.4.3 Appliances

Appliance loads have been obtained from BAHSP assuming that the Cube Model is an electric home. Only those loads used in the benchmark home have been included [28]. The calculated values used in the model for the appliance equipment are shown in Table 3-4.

Table 3-3 Internal Load Assumptions, where FFA = Finish Floor Area, assumed in square feet by BAHSP [28]

Equipment Type	Load (kWh/yr)
Refrigerator	434
Range	490.56
Clothes Washer	76.19
Clothes Dryer	1058.16
Dishwasher	172.23
Miscellaneous Electric Load	$2473.95 + FFA \cdot 0.454$

### 3.2.4.4 Domestic Hot Water

The provision of domestic hot water also increases the internal loads within the typical residence. The baseline values from BAHSP are used for the Cube Model and are listed in Table 3-4. In addition, the hot water distribution system increases the overall loads in the building. Due to the substantial seasonal variation, BAHSP recommends calculating a different value per month and then modifying these values through schedules [28]. The monthly loads from the distribution system have been included in Table 3-5, and the schedules for both the distribution system and fixtures are provided in Appendix A.

Table 3-4 Domestic Hot Water Load Assumptions [28]

Source of Gain	Load (kWh/yr)
Shower	303.90
Bath	39.01
Sinks	94.64

Table 3-5 Domestic Hot Water Distribution System Load Assumptions [28]

Month	Load (kWh/month)
January	39.37
February	37.93
March	36.32
April	34.97
May	34.24
June	34.32
July	35.20
August	36.63
September	38.24
October	39.60
November	40.33
December	40.24

### 3.2.4.5 Lighting

The lighting is modeled based on Option 1 provided by the BAHSP protocol, which assumes a standard quantity of lighting based on finished floor area. One important exception is that no garage lighting has been modeled for the cube [28]. Due to the small magnitude of the garage lighting, this load can be reasonably neglected. In addition, the lighting values are not considered replaceable; only the heat transfer from the radiation of daylight is included in the model. The magnitude of lighting is indicated in Table 3-6, based on finished floor area in square feet, and the schedules are described in Appendix A.

Table 3-6 Lighting Loads, where FFA = Finish Floor Area, assumed in square feet by BAHSP [28]

Lighting Type	Lighting Load (kWh/yr)
Internal hard-wired lighting	$0.8(FFA \cdot 0.542 + 334)$
Internal plug-in lighting	$0.2(FFA \cdot 0.542 + 334)$
External lighting	$FFA \cdot 0.145$

## 3.3 Internal Model Assumptions and References

This section accounts for the remaining essential assumptions in the Cube Model, which are entirely internal to the model code. A more detailed overview of these assumptions for specific code modules can be found in Appendix A. As a general rule, the order of preference for modeling standards is: BAHSP, IECC 2012, ASHRAE Publications, EnergyPlus default settings, and other scholarly research.

### 3.3.1 Climate

The climate data is obtained from the available information on the EnergyPlus website. All United States data comes from the Typical Meteorological (TMY3) data set, maintained by the National Renewable Energy Laboratory [23]. Fifty locations were selected to provide a representative sample of climate information. Locations have been selected from a map to be geographically well-spaced (for instance, see Figure 6-31). Otherwise, the goal of the choices is to include a variety of climates, though the actual city selections are somewhat arbitrary. The locations tested are listed in Table 3-7 along with their climate zones as indicated in IECC 2012 [29].

Table 3-7 Locations Considered in Climate Study

Location	Climate Zone [29]
Anchorage, AK	7
Tuscaloosa, AL	3A
Little Rock, AR	3A
Phoenix, AZ	2B
Los Angeles, CA	3B
San Diego, CA	3B
San Francisco, CA	3C
Denver, CO	5B
Hartford, CT	5A
Miami, FL	1A
Orlando, FL	2A
Atlanta, GA	3A
Honolulu, HI	1A
Des Moines, IA	5A
Boise, ID	5B
Chicago, IL	5A
Indianapolis, IN	5A
Wichita, KS	4A
New Orleans, LA	2A
Boston, MA	5A
Bangor, ME	6A
Detroit, MI	5A
Sault Ste. Marie, MI	7
Minneapolis, MN	6A
St. Louis, MO	4A
Bozeman, MT	6B
Greensboro, NC	4A

Location	Climate Zone [29]
Bismarck, ND	6A
Omaha, NE	5A
Albuquerque, NM	4B
Las Vegas, NV	3B
Buffalo, NY	5A
New York, NY	4A
Columbus, OH	5A
Oklahoma City, OK	3A
Portland, OR	4C
Philadelphia, PA	4A
Pittsburgh, PA	5A
Charleston, SC	3A
Pierre, SD	6A
Nashville, TN	4A
Austin, TX	2A
Dallas, TX	3A
Houston, TX	2A
Midland, TX	3B
Salt Lake City, UT	5B
Richmond, VA	4A
Seattle, WA	4C
Spokane, WA	5B
Cheyenne, WY	6B

### 3.3.2 Window Parameters

While doors and protrusions are neglected, window openings are critical to proper energy modeling of a building. One equivalent window has been modeled per wall, centered with respect to the height and width. The window has the same aspect ratio as the wall to prevent geometric irregularities. The window size is set based on the BAHSP standard of 15% glazing per wall [28]. The material composition of the window is modeled based on its equivalent U-factor, solar heat gain coefficient, and visible transmittance, as defined by IECC 2012 code requirements [29]. The building has been modeled to meet BAHSP solar neutrality criteria by incorporating equal percentages of windows on all faces. Therefore, one model run in the base orientation is sufficient to capture energy results from a solar neutral standpoint [28].

### 3.3.3 Infiltration and Ventilation

Infiltration is modeled based on the air changes per hour of the structure. The baseline values have been obtained from IECC 2012 requirements and set by climate zone. Note that these values are denoted in  $ACH_{50}$ , which is the exchange rate from a door blower test conducted at 50 Pascals [29]. Values in the Cube Model have been incorporated to standard ACH using the industry approximation of 1:20, as opposed to the more complex transformation using LBL factors [63][64]. Infiltration is assumed to occur in all zones, conditioned and unconditioned.

Ventilation in excess of infiltration was determined using ASHRAE 62.2, the relevant standard for the information. The required ventilation has been scaled by the floor area and fixed with respect to the number of bedrooms. The model credits half the infiltration over the standard allotment<sup>1</sup> of 2 CFM/100ft<sup>2</sup>, as is standard practice for providing residential ventilation [32]. Therefore, especially leaky buildings will have no forced ventilation, while tight buildings will be provided the full requirement. Ventilation is assumed to be provided only to conditioned zones.

### 3.3.4 Ground Heat Transfer

Ground heat transfer has been modeled using either the slab preprocessor or the basement preprocessor available with EnergyPlus. Experimental data is used for surface albedo, while assumptions from Bahnfleth, whose work forms the core of the preprocessors, are used for the surface emissivity, surface roughness, and convection values [65][66][67]. Outside data is used here due to discrepancies between various EnergyPlus documents regarding reasonable values [23][25]. EnergyPlus native equivalent geometries and auto-grid features are used, as deviations from these defaults are not recommended for stable modeling [25]. Also notably, evapotranspiration, or the impact of plants placed close to the foundation, has been neglected for this study due to its tendency to cause instabilities in the model.

## 3.4 Known Limitations

Since the purpose of this model is to idealize the single-family residence into an equivalent building, there are known limitations in the resulting predictions. First, the model accepts the BAHSP standards for human behavior which can vary widely and greatly affect energy performance. One key limit for the Cube Model and its application to the study of thermal mass is the omission of natural ventilation. The Ideal Loads Air System is incompatible with natural ventilation, so even the BAHSP typical schedule must be omitted. While the use of this system makes the cube more widely applicable, it may hinder its predictions insofar as thermal mass performance depends on natural ventilation.

---

<sup>1</sup> The standard allotment is given in English unit CFM, which stands for cubic feet per minute.

The idealization of the building systems is substantial, and therefore the model only predicts system loads, not final energy values. It should also be noted that duct losses, machine efficiencies, economies of scale, and heating or cooling limits are not taken into account since only the loads are calculated. The Cube Model predicts the performance of the building envelope; it does not provide recommendations on HVAC system design.

The idealization of the building envelope is effective so long as the assumption of an equivalent wall experiencing one-dimensional conduction is valid. This idealization provides the opportunity to generate key relationships for building design, but it may not predict phenomena for all constructions. Chapter 4 includes a demonstration of the effectiveness of the equivalent wall in predicting energy performance for a variety of wall sections insofar as EnergyPlus models them.

Finally, the model is limited by the use of existing energy modeling software. As Chapter 2 discussed, there are known limitations to EnergyPlus and its ability to accurately capture building performance. Any limitation of EnergyPlus can be seen as a limitation of the Cube Model, as correcting the simulation engine is beyond the scope of this work.

## **3.5 Chapter Summary**

This chapter has established the methodology and assumptions behind the Cube Model, which is developed in response to the first research question targeting building simplification. The model incorporates simplified geometries, equivalent envelope parameters, and an idealized HVAC system with accurate loading conditions. Assumptions are based on relevant modeling standards and building codes. From these assumptions, a parametric model using Unix shell script has been created. Due to the known limitations of EnergyPlus discussed here and in Chapter 2, the calibration and validation discussions in the chapters that follow will be conducted with respect to full energy models. The goal of the Cube Model is to provide predictions reasonably close to a full model using similar key assumptions rather than to validate the software engine.

# Chapter 4

## Calibration and Validation

To justify the use of the Cube Model as a solution to the first research question regarding simplification of building parameters, a calibration process is necessary. Calibration is the process of comparing a model's simplifications to more advanced features to verify the assumptions. This calibration process will provide useful information regarding: (1) the level of detail required to produce accurate results, (2) the level of accuracy of the results themselves, and (3) the need for any post-processing or scaling based on reasonable engineering judgment. Once the calibration of the model is complete, a validation process will help ensure that the energy results from this model approximate more complex buildings. Thus, validation is the process of comparing a new model to real data or previously created models. The combination of the calibration and validation information will provide information about key modeling parameters to be considered and verify that the Cube Model can reasonably represent the information from a full energy model of similar assumptions.

### 4.1 Premise

The calibration and validation of energy modeling procedures is the subject of extensive literature. The literature review in Chapter 2 indicates that there are known discrepancies between energy models and actual building energy results. The simplified model did not seek to remedy any of the issues with buildings representing reality but rather to generate relationships that are otherwise hidden in the course of case study analysis. As a result, the notion of interest is that the simplified model is generating reasonably similar results to more complex models. Since the goal is to provide a breadboard tool for use in the early phases of building design, some deviation is acceptable so long as the trends are replicated. Therefore, this procedure of calibration and validation will demonstrate that the envelope, geometry, and loading assumptions are reasonable, within the context of the known limitations of EnergyPlus.

## 4.2 Envelope Calibration

The first step in the calibration is to demonstrate the validity of the assumption of equivalent envelope materials. Since buildings are constructed from complex multi-layered systems, not equivalent systems, this section will test the equivalency assumption by comparing full wall sections to their equivalent properties. While EnergyPlus provides accompanying sets of wall construction assumptions, these wall sections have not been normalized using one-dimensional conduction assumptions (see Section 3.1) and therefore should not be used to test the simplification of the Cube Model. Therefore, to conduct this test, wall sections from case study buildings have been modeled in EnergyPlus using the procedures described in Section 3.2.2.

The selected wall sections provide either a high level of complexity or a test of high performance design, which will test the robustness of the assumption that one equivalent material can be modeled in lieu of a composite structure. In addition, each wall section has a high-mass concrete component for verification that the equivalent envelope represents thermal mass design. This calibration analysis will not make judgments on the performance of these systems, only verify the robustness of the model. To this end, properties have been generated using the procedure outlined in Chapter 3 with each wall section incorporated on the standard geometry slab-on-grade cube. This will remove geometry effects from the calibration procedure and test only the validity of the envelope equivalency. The equivalent wall sections and their full construction models have been tested for the list of climates presented in Table 3-7. The goal of this study is to determine the effects of the normalization procedure on the overall energy predictions for the wall section. The remainder of this section will provide details of the wall sections considered and the calibration results.

The first system is a combination of concrete block exterior and R-19 wood interior, which tests the ability of the model to incorporate high levels of complexity. The second wall section is an R44 precast concrete sandwich panel construction. Both a load bearing and a non-load bearing version of this construction type have been tested. The remaining two wall systems are examples of two modified ICF constructions. The first is a “stick-framed” ICF construction using studs, headers, and grade beams rather than a full concrete layer [68]. The second is an ICF wall construction with exterior insulation and minimal interior insulation and framing [69]. Wall sections are presented in Figure 4-1. Material properties are presented in Table 4-1, gathered from manufacturer literature when an exact manufacturer or reasonable alternative could be discovered. In other cases, reasonable assumptions from ASHRAE, EnergyPlus, or commonly available material properties have been used.



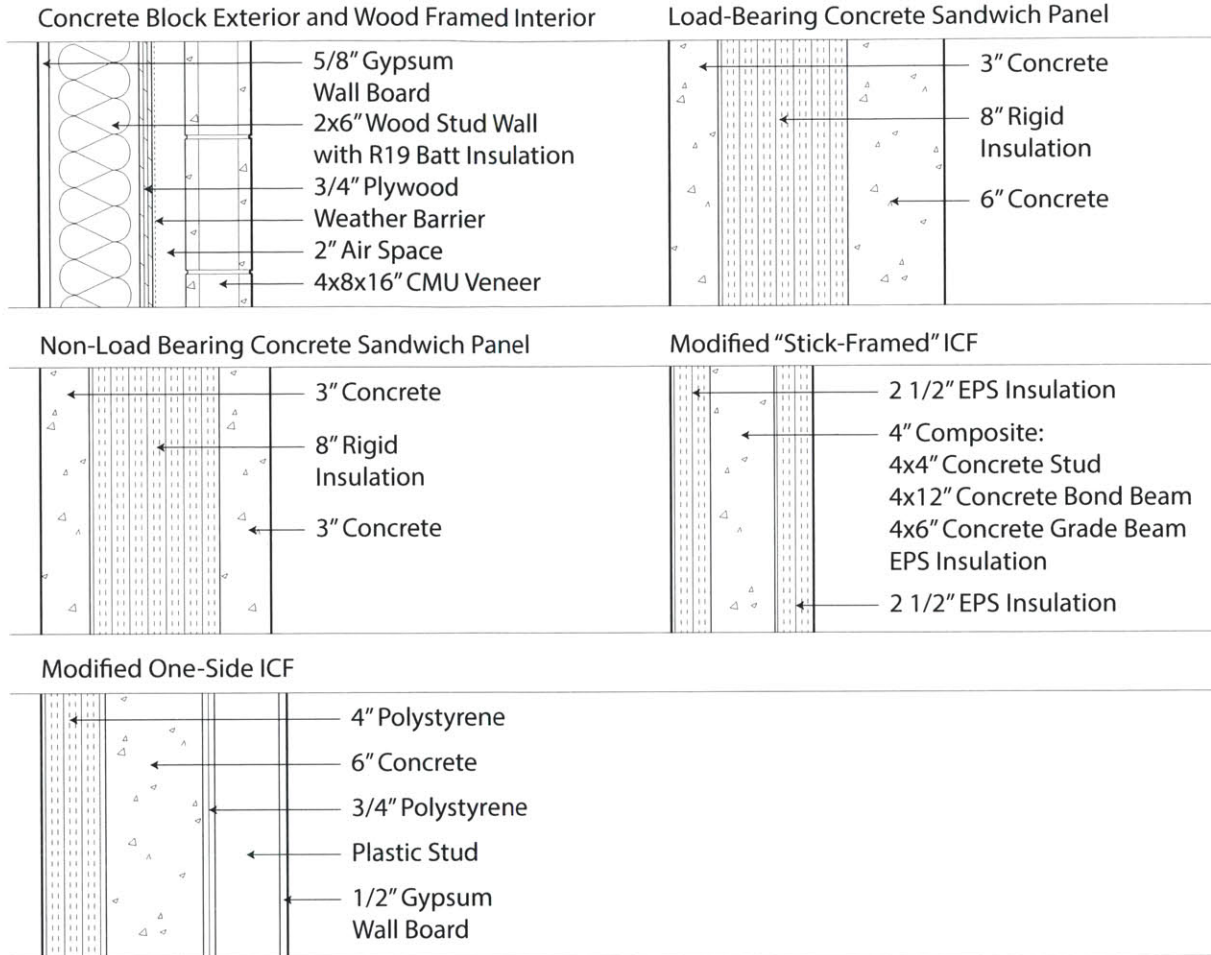


Figure 4-1 Case Study Wall Sections [70][71]

Table 4-1 Envelope Properties of Case Study Wall Sections,  
 where CMU = Concrete Masonry Unit and EPS = Expanded Polystyrene

Material	Thickness (m)	Conductivity (W/m-K)	Density (kg/m <sup>3</sup> )	Specific Heat (J/kg-K)	R-Value (m <sup>2</sup> -K/W)
<b>Concrete Block Exterior and Wood Framed Interior</b>					
CMU Outside [72][73][74]	0.0254	0.968	2326	695	0.0263
CMU Middle [72][73][74]	0.0508	0.319	609	1009	0.159
CMU Inside [72][73][74]	0.0254	0.968	2326	695	0.0263
Air Space [74]	0.0508	0.0442	0.616	1044	1.150
Weather Barrier [75]	0	0	0	0	0.326
Plywood [23]	0.0190	0.120	540	1210	0.158
Studs and Insulation [23]	0.140	0.0543	87.4	1038	2.572
Gypsum Wall Board [23]	0.0159	0.160	800	1090	0.0994
<b>Equivalent Wall</b>	<b>0.327</b>	<b>0.0724</b>	<b>564</b>	<b>826</b>	<b>4.517</b>
<b>Load Bearing Concrete Sandwich Panel</b>					
Structural Concrete [35]	0.1524	0.930	2300	653	0.164
EPS Insulation [76]	0.2032	0.0262	29	1210	7.76
Concrete [35]	0.0762	0.930	2300	653	0.0819
<b>Equivalent Wall</b>	<b>0.432</b>	<b>0.0539</b>	<b>1231</b>	<b>659</b>	<b>8.001</b>
<b>Non-Load Bearing Concrete Sandwich Panel</b>					
Concrete [35]	0.0762	0.930	2300	653	0.0819
EPS Insulation [76]	0.2032	0.0262	29.0	1210	7.76
Concrete [35]	0.0762	0.930	2300	653	0.0819
<b>Equivalent Wall</b>	<b>0.3556</b>	<b>0.0449</b>	<b>1002</b>	<b>662</b>	<b>7.924</b>
<b>Modified "Stick-Framed" ICF [68]</b>					
EPS Insulation [23][76]	0.0635	0.043268	24.0	1210	1.468
Concrete and EPS [23][35][76]	0.1016	0.47398	1130	924	0.214
EPS Insulation [23][76]	0.0635	0.043268	24.0	1210	1.468
<b>Equivalent Wall</b>	<b>0.229</b>	<b>0.0726</b>	<b>515</b>	<b>931</b>	<b>3.150</b>
<b>Modified One-Sided ICF [69]</b>					
Exterior Polystyrene [23][69]	0.102	0.0288	32.0	1210	3.52
Concrete [35]	0.152	0.930	2300	653	0.164
Interior Polystyrene [23][69]	0.0191	0.0865	32.0	1210	0.220
Uninsulated Plastic Stud [69][77]	0.117	0.0455	18.0	1048	2.563
Gypsum Wall Board [23]	0.0127	0.160	800	1090	0.0794
<b>Equivalent Wall</b>	<b>0.402</b>	<b>0.0615</b>	<b>911</b>	<b>673</b>	<b>6.546</b>

The results of the simulations from these wall sections indicate that in all cases, the equivalent wall system accurately represents the material properties of the building. The results in Table 4-2 show the average of all climates tested for the annual and seasonal energy totals for each wall construction. For this investigation, winter energy is the sum of October to March energy consumption and summer energy is the remainder of the year. All energy values have been calculated using the procedure in Section 3.1. No significant difference in calibration has been observed between the climate zones. Given the close approximation of the energy values, the notion of the equivalent envelope can be safely used to consider real wall sections. It should be noted finally that the procedure used to calculate the equivalent properties provides the same values for the U-value and C-value of the full wall construction, which serves as an additional validation of the equivalent systems. Still, this test has demonstrated with confidence that the Cube Model accounts for the full wall section’s energy properties.

Table 4-2 Equivalent Wall Calibration Results, presented as the ratio of the test model energy to the energy predicted by the full energy model

Wall Type	Annual Energy	Winter Energy	Summer Energy
Concrete Block Exterior and Wood Framed Interior	0.996	0.995	0.993
Load Bearing Concrete Sandwich Panel	1.013	1.021	1.023
Non-Load Bearing Concrete Sandwich Panel	1.015	1.023	1.025
Modified “Stick-Framed” ICF	0.995	0.989	0.995
Modified One-Sided ICF	0.996	0.992	0.994

### 4.3 Geometry Calibration

Before moving to discuss the full energy models, this section will analyze the reduced geometry of the Cube Model. The following tests will question the need for an attic, a basement, and internal slabs. In addition, this analysis will consider stacked cubes, adjacent cubes, and buildings of more complex geometry. In total, thirteen comparisons in geometry reduction have been considered in order to better understand the important elements of energy modeling. These comparisons have been graphically represented in Figure 4-2 and Figure 4-3.

For each simulation experiment, the annual, summer, and winter energy totals have been calculated for all fifty locations in Table 3-7. The base geometry values are a 10m x 10m x 4m cube, a 2.5m basement, an attic based on the normalized height of a 5:12 gable roof, and the baseline material properties presented in Table 3-1. The hip roof also has a 5:12 slope but a different volume due to the change in geometry. The stacked and adjacent cube experiments are exactly double the size of the base geometry in total conditioned area. The split or separate loads relates to whether the two-cube models are meant to represent a divided single home or a two-family structure; whereas a single home does not increase

appliances based on zone descriptions, two separate residences would have twice the internal occupant loads as the single-family prototype. Both the split and separately loaded systems are compared to base systems with equivalently sized loads. In other words, the single cube model for comparison has the same magnitude of internal loads as the two-zone model, ensuring that the boundary conditions are fixed. The plan normalization experiments describe two different buildings whose total floor area equals the 10m x 10m cube but is arranged differently. The cross building is 14m x 8m with 3m<sup>2</sup> corners removed. The U-shape plan is 12m x 10m with a 5m x 4m interior section removed.

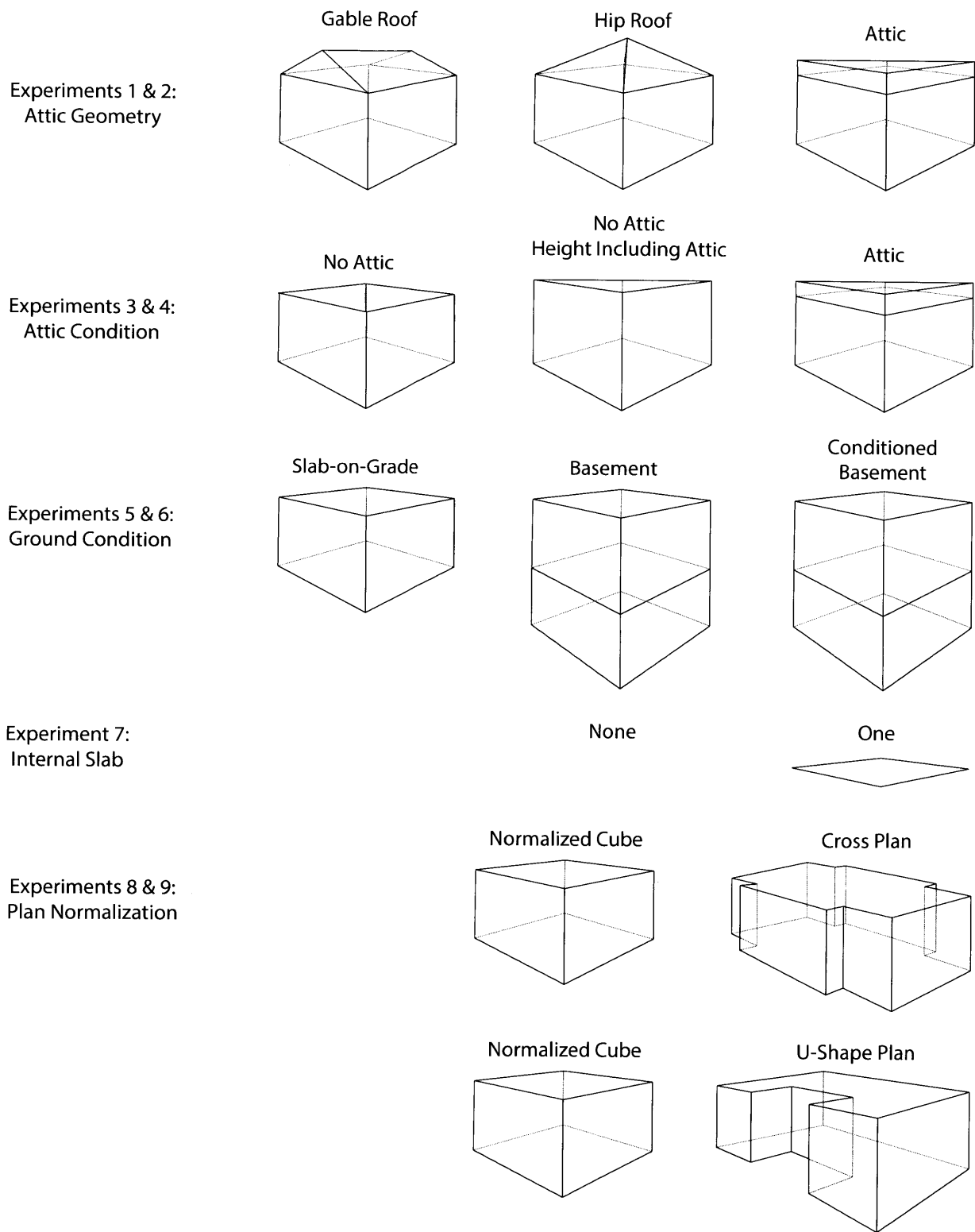
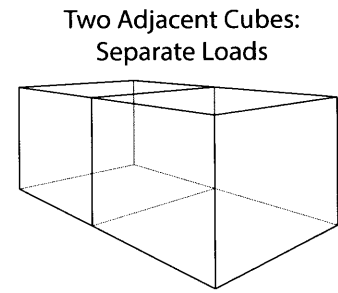
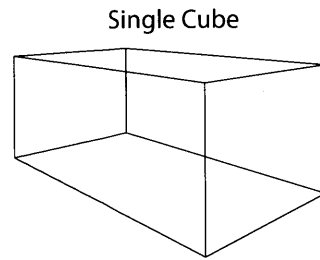
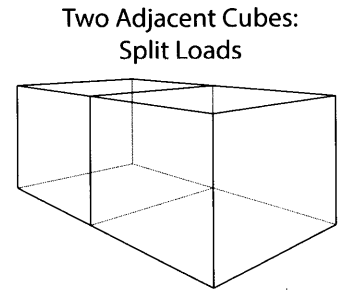
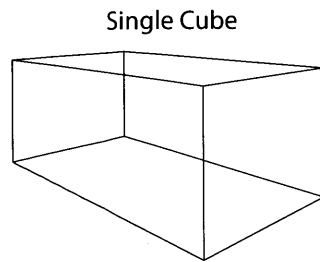


Figure 4-2 Energy Comparisons for Single Cube

Experiments 10 & 11:  
Adjacent Cubes



Experiments 12 & 13:  
Stacked Cubes

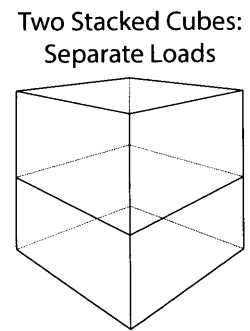
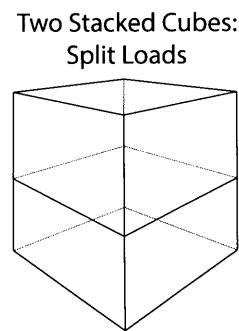
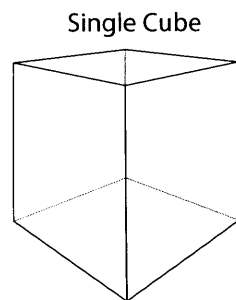


Figure 4-3 Energy Comparisons for Multiple Cubes

The geometry calibration procedure demonstrates that the geometry simplifications can be applied while still obtaining realistic energy consumption results. The ratios of simplified geometry to complex geometry are shown in Table 4-3. These ratios have been averaged over all climates, as few geometry simplifications show a climate dependence. The notable exception, however, is the incorporation of the attic, which primarily impacts the magnitude of the cooling load and therefore results in more significant error in warm climates than cold climates.

Table 4-3 Geometry Calibration Results, presented as the ratio of the test model energy to the energy predicted by the full energy model

<b>Experiment</b>	<b>Annual Energy</b>	<b>Winter Energy</b>	<b>Summer Energy</b>
Experiment 1: Gable Roof to Cube Attic	1.001	1.004	0.996
Experiment 2: Hip Roof to Cube Attic	1.006	1.012	0.997
Experiment 3: Attic to No Attic	1.216	1.190	1.300
Experiment 4: Attic to No Attic, adjusting Cube Height for Attic	1.380	1.375	1.440
Experiment 5: Unconditioned Basement to Slab-on-Grade	0.961	0.970	0.950
Experiment 6: Conditioned Basement to Slab-on-Grade	0.794	0.764	0.839
Experiment 7: Internal Slab to No Internal Slab	0.862	0.880	0.860
Experiment 8: Cross Plan to Normalized Plan	0.962	0.942	0.993
Experiment 9: U-Shaped Plan to Normalized Plan	0.872	0.852	0.901
Experiment 10: Adjacent Cubes with Split Internal Loads to Single Cube	0.921	0.928	0.915
Experiment 11: Adjacent Cubes with Separate Internal Loads to Single Cube	0.923	0.930	0.917
Experiment 12: Stacked Cubes with Split Internal Loads to Single Cube	0.877	0.889	0.873
Experiment 13: Stacked Cubes with Separate Internal Loads to Single Cube	0.880	0.891	0.880

The calibration procedure demonstrates that it is essential to consider certain elements, such as attics, basements, or heavyweight interior constructions. In contrast, exact geometry does not need to be considered provided the volume of the cube, window percentage, and other parameters have been adjusted to the idealized cube building. Omitting an attic, including attic or other unconditioned elements in the conditioned cube, or neglecting conditioned areas such as basements will invalidate the overall energy consumption results.

Finally, in comparison combinations of cubes, it should be noted that the results presented above indicate that internal partitions between two building systems are not important. However, as an aside, when the internal loads are not consistent between the system, the aggregate average for the United States is acceptable but the spread of the values is much larger. This indicates that the Cube Model can be applied to different loading cases provided the assumptions are properly reformulated, as these assumptions form an essential boundary condition of the system. When the model is applied to situations that are substantially different without substantial changes in assumptions, the predictability of the results decreases. Therefore, the assumptions of the model should be adjusted before applying the model to substantially different loading conditions such as multi-family or commercial.

## 4.4 Calibration and Validation to Research Report R11-01

The first set of full energy models has been used both to calibrate and validate the Cube Model. That is, geometry experiments have been run to determine which set of parameters most accurately capture a full building model, in addition to ensuring that the energy quantities obtained are reasonable. The data source that has been used is the work previously published at MIT in Research Report R11-01, Department of Civil and Environmental Engineering. This report by J. Ochsendorf, et al, completes a Life-Cycle Assessment (LCA) and Life-Cycle Cost Assessment (LCCA) of single-family residential, multi-family residential, and commercial buildings. The single-family residential analysis is relevant to this work. The report compares buildings in Chicago and Phoenix constructed either of Insulated Concrete Form (ICF) or traditional light-frame wood construction. The result of this analysis is the conclusion that thermal resistance has a greater impact on energy usage than thermal mass [78]. Given its use of specific buildings and climates, this report can be considered a case-study analysis, producing accurate LCA results for a specific set of buildings, materials, and locations.

This analysis is comprehensive in scope due to the nature of LCA, but only a small portion is necessary for comparison to the present work. EnergyPlus models framed around the International Energy Conservation Code (IECC) 2009, Building America House Simulation Protocols (BAHSP), BEOpt standard information, experimental infiltration data, and local building codes and standards were used to evaluate the occupation phase [78][79]. These assumptions result in methodology differences in the estimation of window properties, availability of heating and cooling, and calculation of infiltration. Engineering judgment has been used by both the R11-01 models and the Cube Model for the purpose of ground heat transfer assumptions, leading to different means of approximating ground contact between the phases. The details of these baseline assumptions are presented in Table 4-4 and are fixed throughout the experimental simulation runs.



Table 4-4 Baseline Assumptions Present for Cube Model and R11-01 Model

Parameter	Cube Model	R11-01 Model <sup>a</sup>
<b>Baseline Assumptions</b>		
Model Protocol	Building America House Simulation Protocol (BAHSP)	Building America House Simulation Protocol (BAHSP)
Energy Code	International Energy Conservation Code (IECC) 2012	International Energy Conservation Code (IECC) 2009
Ground	Phoenix: slab-on-grade Chicago: basement & slab-on-grade	Slab-on-grade <sup>b</sup>
Infiltration	IECC 2012	Experimental Data
Heating / Cooling Availability	Availability Matches Setpoints Found from BAHSP	Always Available
Internal Loads	BAHSP for lighting, occupation, appliances, and domestic hot water	BAHSP lighting and occupation BEOpt appliances
<b>Internal Load Parameters <sup>c</sup></b>		
Occupation	2.58 people at 986.50 kWh/yr	2.64 people at 986.60 kWh/yr
Lighting	(1158.09 + 824.09 * Slabs) kWh/yr <sup>d</sup>	3213.95 kWh/yr
Refrigerator	434 kWh/yr	798.57 kWh/yr
Range	490.56 kWh/yr	1805.76 kWh/yr
Clothes Washer	76.19 kWh/yr	191.09 kWh/yr
Clothes Dryer	1058.16 kWh/yr	2507.02 kWh/yr
Dishwasher	172.23 kWh/yr	509.23 kWh/yr
Miscellaneous Electric Load	(3018.55 + 544.6 * Slabs) kWh/yr <sup>d</sup>	5005.30 kWh/yr
Miscellaneous Gas Load	None	1157.09 kWh/yr
Domestic Hot Water	Table 3-4 and Table 3-5 for Imposed kWh/yr Values	Full Domestic Hot Water System, specifying water flow and equipment, Loads calculated by EnergyPlus
<sup>a</sup> Data from Concrete Sustainability Hub, Massachusetts Institute of Technology [78][79][80][81][82][83] <sup>b</sup> Models run as slab-on-grade whether basement present or not [84] <sup>c</sup> For both models, schedules modify these base loads [80][81][82][83] <sup>d</sup> Slabs contribute to overall finish area and scale these loads in experiments where they are present		

#### **4.4.1 Experimental Simulation Setup**

This simulation experiment has been used to validate the energy prediction of the models and to verify the procedure established in Section 3.2.1 for reducing the geometry of the building to a simplified cube. To accomplish this goal, many more options for the Cube Model geometry have been tested than simply the basic cube and the full advanced cube. Variations in the attic condition, basement condition, and internal slab condition have been considered. In addition, the ground condition has been initially calculated by combining the Winkelmann method of including soil in the slab construction; this assumption has been tested by running the data with and without the soil layer to judge the importance of considering soil as part of the ground contact system [85]. Finally, since models were available in two locations and for two wall systems, these variations were also tested. The result is 14 experiments for Phoenix and 28 experiments for Chicago, with the difference in number due to the presence of a basement in the Chicago home and absence of one in the Phoenix home. Figure 4-4 summarizes the parameters that vary throughout the comparison.

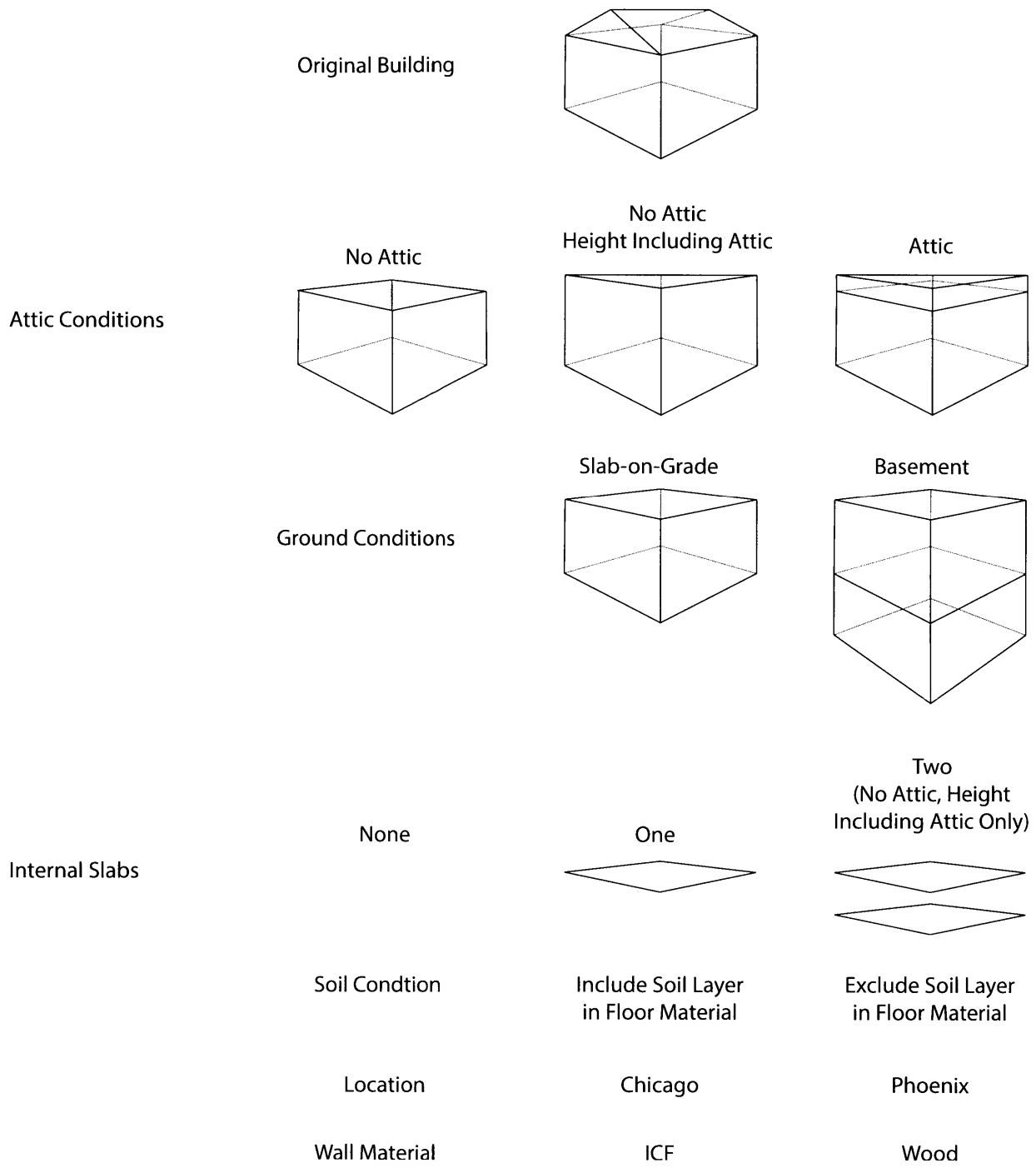


Figure 4-4 Variations of Geometry and Input Conditions

The parameters shown in Figure 4-4 represent the variables in the comparison. The building itself is 9.75 m in the N-S direction and 11.43 m in the E-W direction with a 6:12 gable roof. To conduct the experiment, the properties of the ICF and wood construction were converted into the equivalent wall using the procedure in Section 3.2.2. The ICF consists of six inches of concrete and 2.5 inches of insulation on either side, while the wood framing is a code-insulated 2x4 stud wall in Phoenix and 2x6 stud wall in Chicago. Basement construction in Chicago was concrete for the wood home and ICF with an eight inch core. Internal slabs are uninsulated wood construction, and the attic floor is an insulated wood construction. Roofing is asphalt and the exterior slab is concrete. Structural drawings provided in the report have been used to approximate the basement geometry for the comparison, since no code module was available; all other components have been converted directly from the EnergyPlus input information [78][79][80][81][82][83].

#### 4.4.2 Results

Analysis of the results demonstrates that a single cube alone cannot accurately represent the full output from a real building, but that a single cube is reasonable for envelope phenomena not impacted by a few key assumptions. Since energy modeling is a science of complex interactions, the data here will not be scaled but rather analyzed to determine which modeling parameters are necessary to capture a real building. Before proceeding, the following terms will be used to describe the output. The term “Basic Cube” is used to refer to a cube model that has no attic, a slab-on-grade, and no internal slabs. The term “Advanced Cube” is used to refer to the cube model that closest resembles the actual building by including internal slabs, an attic, and accurate ground conditions. Other models described in the experiment setup are referred to by their specific settings. Averages are presented of all cubes featuring a certain modeling parameter, such as an attic or internal slabs, though their other parameters differ.

To properly compare the energy outputs of the building, an output variable must be used to compare like information. The Ideal Loads Air System has its own measurements of combined sensible and latent loads assuming building systems operate at perfect efficiency, which are the best indicators of energy consumption for the Cube Model [26]. However, such outputs are not available on full energy models, which calculate electricity or source fuel demand instead of loads as a final output. Therefore, the sensible energy loads for heating and cooling have been exported due to their availability regardless of HVAC system. This will allow a validation of the cube simplification.

The annual and seasonal sensible energy loads for the Basic Cube and the Advanced Cube are presented in Table 4-5 as the ratio of the test model energy to the full model. In this table, note that the Advanced Cube obtains reasonable results for all buildings modeled while the Basic Cube obtains such reasonable results for none of the test buildings. This indicates that the basic cube model does not accurately capture the energy consumption of the building. In addition, the experimental average has been presented to

further underscore the need to select the correct set of input parameters for the cube model rather than select any of the geometries presented in the experimental setup. Finally, it is notable in the seasonal results that generally the off-peak seasons are modeled with slightly less accuracy than the peak seasons. Since the overall annual energy is not substantially affected by these seasons, it seems likely that the deviation is higher simply because the gross energy is lower and variations in predicted energy amount to higher percents of overall consumption.

Table 4-5 System Sensible Energy for the Basic and Advanced Cubes, presented as the ratio of the test model energy to the energy predicted by the full energy model

Parameter	Chicago		Phoenix	
	ICF	WOOD	ICF	WOOD
<b>Basic Cube</b>				
Annual System Sensible Energy	2.30	2.20	2.24	2.09
Winter System Sensible Energy	2.46	2.34	2.19	2.00
Summer System Sensible Energy	2.02	1.97	2.25	2.11
<b>Advanced Cube</b>				
Annual System Sensible Energy	0.92	0.92	0.98	0.99
Winter System Sensible Energy	0.97	0.97	0.78	0.78
Summer System Sensible Energy	0.85	0.84	1.03	1.05
<b>Experiment Average</b>				
Annual System Sensible Energy	2.13	2.01	2.02	1.91
Winter System Sensible Energy	2.31	2.16	1.88	1.73
Summer System Sensible Energy	1.78	1.76	2.05	1.95

While the Advanced Cube obtains reasonable results, another benefit of the setup of this analysis is to determine which geometry features are most responsible for these energy results. To demonstrate this, the averages have been calculated for each of the varying parameters to determine which have the greatest impact on energy consumption. These averages are presented in Table 4-6. These results indicate that the attic is the single most important modeling change to result in reasonable energy predictions. The ground condition also provides some change in the mean, but much less substantial. In this experiment, the internal slabs are negligible due to their lightweight construction. This suggests that before reducing interior geometry one must know something about the material properties and use engineering judgment regarding the relative importance of those masses. Finally, the results indicate that the incorporation or absence of the soil layer in the slab construction do not affect the energy values in any substantial manner, meaning that this additional complexity in the model can be safely neglected. This allows the equivalent slab to represent constructed materials rather than needing to incorporate the soil thermal properties in the slab itself. All soil conditions are taken into account by the preprocessor.

Table 4-6 System Annual Sensible Energy for the averages of variations experiments, presented as the ratio of the test model energy to the energy predicted by the full energy model

Parameter	Chicago		Phoenix	
	ICF	WOOD	ICF	WOOD
<b>Attic Condition</b>				
Attic Modeled	1.02	0.99	0.96	0.98
No Attic Modeled	2.39	2.25	2.31	2.14
Height Including Attic but No Attic Modeled	2.69	2.55	2.53	2.37
<b>Ground Condition</b>				
Slab-on-Grade	2.05	1.98	2.02	1.91
Basement	2.21	2.06	N/A	N/A
<b>Internal Slab Condition</b>				
No Slabs Modeled	2.03	1.92	1.87	1.77
One Slab Modeled	2.04	1.93	1.97	1.86
Two Slabs Modeled	2.70	2.56	2.61	2.45
<b>Soil Condition</b>				
Including Soil Layer in Equivalent Slab	2.12	2.01	2.02	1.90
Excluding Soil Layer in Equivalent Slab	2.13	2.02	2.02	1.91

## 4.5 Chapter Summary

This chapter presents a summary of the calibration and validation experiments used to determine if the Cube Model provides similar results to full energy models and geometries. The results indicate that it is not the simplification of geometry that results in modeling errors, provided a sufficient level of complexity, such as an attic, is added where required. In the end, the Cube Model will produce similar results as a full building model when the building uses reasonably similar assumptions. Thus, the calibration and validation results provide an indication that the Cube Model is one answer to the first research question:

1. How can the complexity of a building be reduced while maintaining similar results to a full energy model?

Where data sets use substantially different assumptions, a redesign of the Cube Model is required to take those assumptions into account. It is for this reason that standard energy modeling baselines and building codes have been used to set the assumptions; without these assumptions, the model exists in a vacuum and cannot be a valid representation of a building. The next section will begin to demonstrate the versatility of a scaling relationships using the Cube Model, and the remaining chapters will address the subsequent research questions.

# Chapter 5

## Versatility

While the Cube Model developed will be used to study thermal mass, the infrastructure is sufficiently general to study many other parameters. This section will provide an overview of some of the relationships that can be generated by the model. This chapter introduces the notion of geometry scaling effects, which will be revisited when the sensitivity of the thermal mass data is tested in Part IV.

### 5.1 Experimental Simulation Setup

This section will setup simulation experiments to test the inter-relationship between two given parameters for its impact on annual or seasonal energy consumption. The parameters that have been varied and their range of values are listed in Table 5-1. All other values remain constant at the baseline Cube Model parameters that are presented in Chapter 3. Using this setup, 400 experiments have been run per climate.

Table 5-1 Varied Parameters

Parameter	Minimum	Maximum	Increment
<b>Experiment One: Height versus Infiltration</b>			
Height (m)	1 m	20 m	1 m
Infiltration (ACH)	0.025 1/h	0.5 1/h (ACH <sub>50</sub> =10)	0.025 1/h
<b>Experiment Two: Length+Width (constrained equal) versus Height</b>			
Length (m) + Width (m)	1 m	20 m	1 m
Height (m)	1 m	20 m	1 m
<b>Experiment Three: Length versus Width</b>			
Length (m)	1 m	20 m	1 m
Width (m)	1 m	20 m	1 m
<b>Experiment Four: Wall Conductivity versus Infiltration</b>			
Wall Conductivity (W/m-k)	0.1 W/m-K	2.0 W/m-K	0.1 W/m-K
Infiltration (1/h)	0.025 1/h	0.5 1/h (ACH <sub>50</sub> =10)	0.025 1/h
<b>Experiment Five: Wall Conductivity versus Floor Conductivity</b>			
Wall Conductivity (W/m-K)	0.1 W/m-K	2.0 W/m-K	0.1 W/m-K
Floor Conductivity (W/m-K)	0.1 W/m-K	2.0 W/m-K	0.1 W/m-K
<b>Experiment Six: Wall Conductivity versus Roof Conductivity</b>			
Wall Conductivity (W/m-K)	0.1 W/m-K	2.0 W/m-K	0.1 W/m-K
Roof Conductivity (W/m-K)	0.1 W/m-K	2.0 W/m-K	0.1 W/m-K

## 5.2 Results

The results of the above studies suggest that numerous scaling relationships and correlations exist between building parameters, indicating that there may be means of optimizing building design with regard to these relationships. The following analysis will consider the annual energy consumption per volume or per surface for each set of analyses.

The first experiment varied the height of the Cube Model and the infiltration, measured in overall air changes per hour. Figure 5-1 displays the results for the energy consumption per surface, which indicate that there is an interplay between the two parameters that varies by climate. In Anchorage, AK, the results show that for higher values of infiltration, there is an optimum height at which minimum energy consumption per surface occurs. The results for Phoenix, AZ and Miami, FL indicate that the impact of



height is much greater than the impact of infiltration for the energy consumption per surface. Finally, the results for San Francisco, CA show a trend where low values of infiltration and height have lowest energy and the corresponding upper values have the highest energy. The difference in these trends suggests that there may be different optimum aspect ratios of buildings when considering the interaction of form with mechanisms of energy loss.

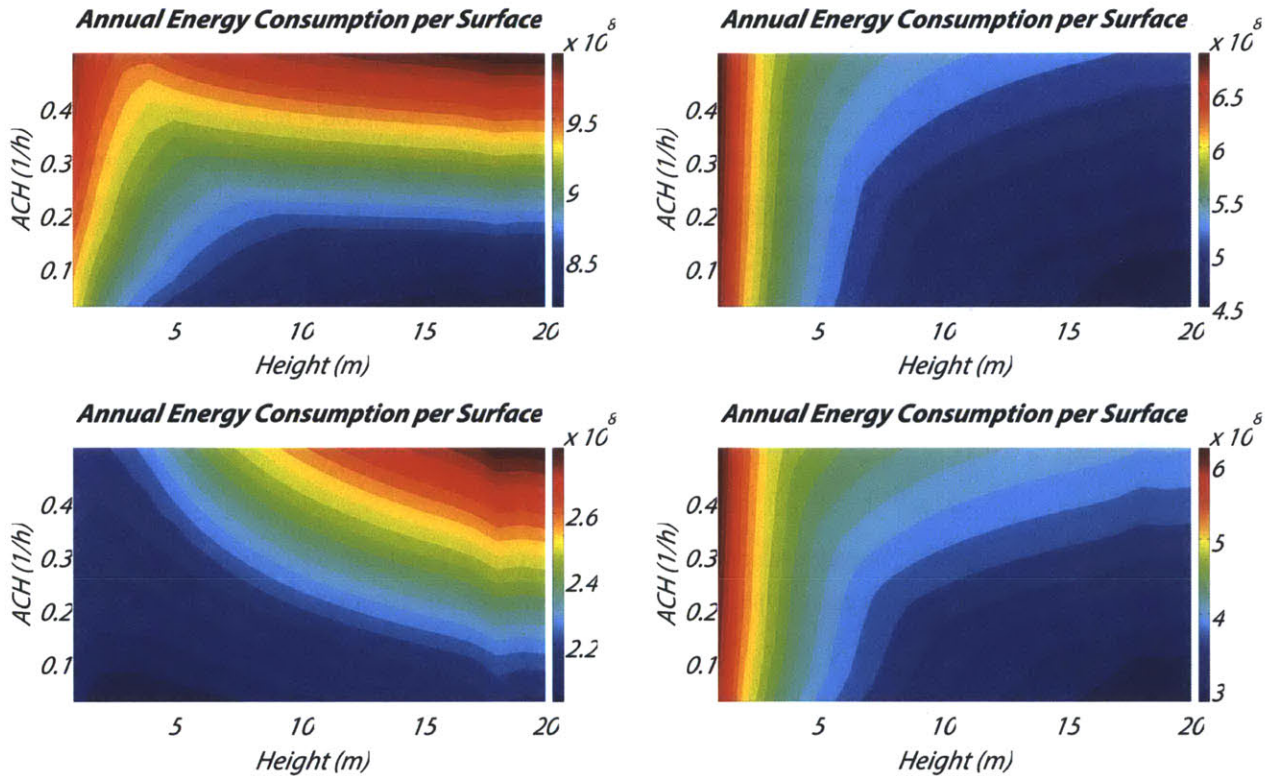


Figure 5-1 Annual Energy Consumption per Surface ( $J/m^2$ ), ACH (1/h) vs Height (m),  
 Anchorage, AK (above left) and Phoenix, AZ (above right)  
 San Francisco, CA (below left) and Miami, FL (below right)

The results of building aspect ratio for the four climates are similar for surface and volume; therefore, the results for the annual energy consumption per volume are shown in Figure 5-2. While the magnitudes of the energy values vary by climate, the energy trend for all climates is similar. The greatest amount of energy per volume is consumed for the buildings of the smallest length and height. This is due to the increased amount of surface area for a given conditioned volume. Since conduction, convection, and radiation through the envelope are surface-driven effects, additional surface area for the same volume will increase specific energy consumption. The graphs are also roughly mirrored about an aspect ratio on the order of one, which suggests that this is likely a peak energy consumption ratio that varies slightly by climate conditions. This suggests that there may be aspect ratios to use or avoid, depending on the chosen climate of construction.

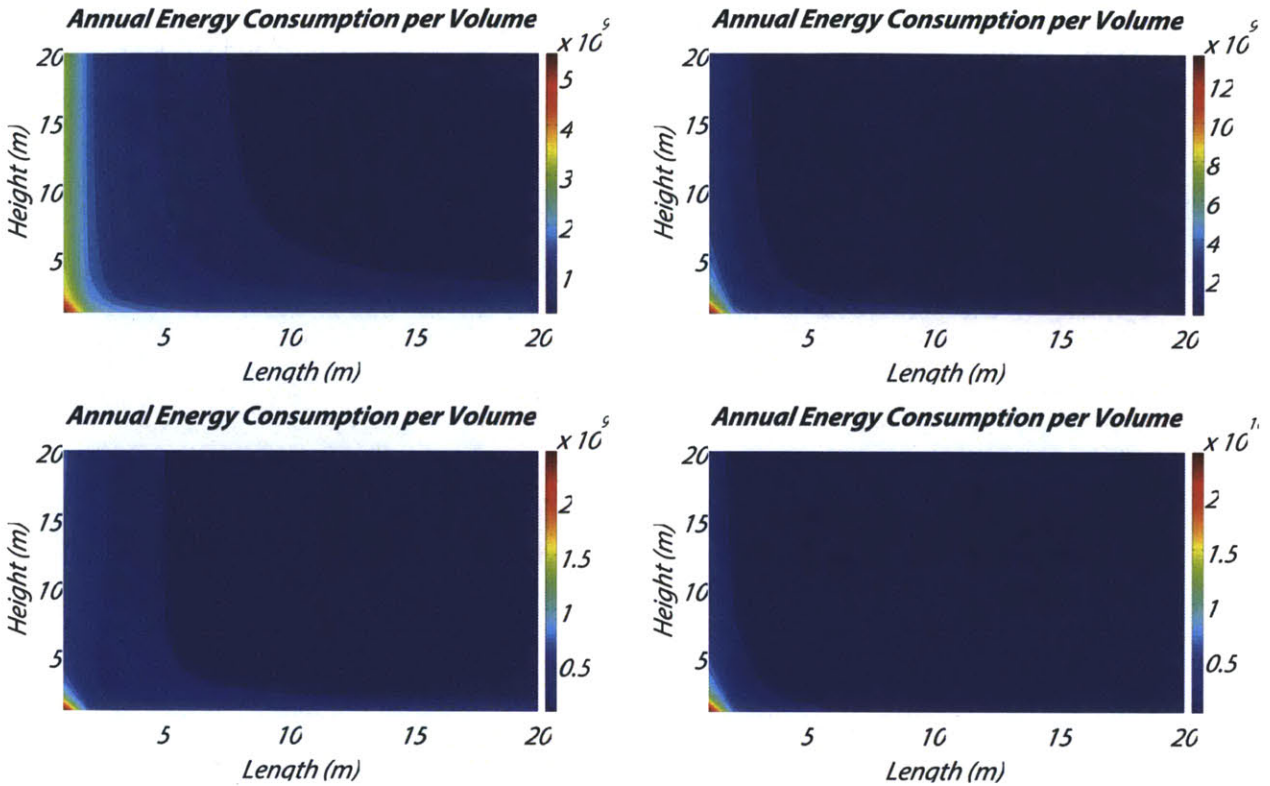


Figure 5-2 Annual Energy Consumption per Volume ( $\text{J/m}^3$ ), Height (m) vs Length (m),  
 Anchorage, AK (above left) and Phoenix, AZ (above right)  
 San Francisco, CA (below left) and Miami, FL (below right)

The results of the length versus width experiment in Figure 5-3 show similar results per volume across the climates but different relationships per surface. The volume relationship indicates that the smallest buildings use the most energy per volume, with energy consumption decreasing as building size increases. This is similarly due to the surface-driven effects on the building; smaller buildings have more surface area for their volume size, amounting to a greater contribution of conduction, convection, and radiation through the envelope. There is a pivot point in the graph at around a plan aspect ratio of one, indicating that square buildings consume less energy than their rectangular counterparts. For the relationships per surface, in Anchorage and San Francisco the highest energy per surface is found for the largest size, while in Phoenix and Miami the highest energy per surface is found for the smallest size. This pattern indicates that in warm climates, compact building is generally optimum. In contrast, there appears to be an optimum size as a result of the relationship between surface area and volume for Anchorage and San Francisco.

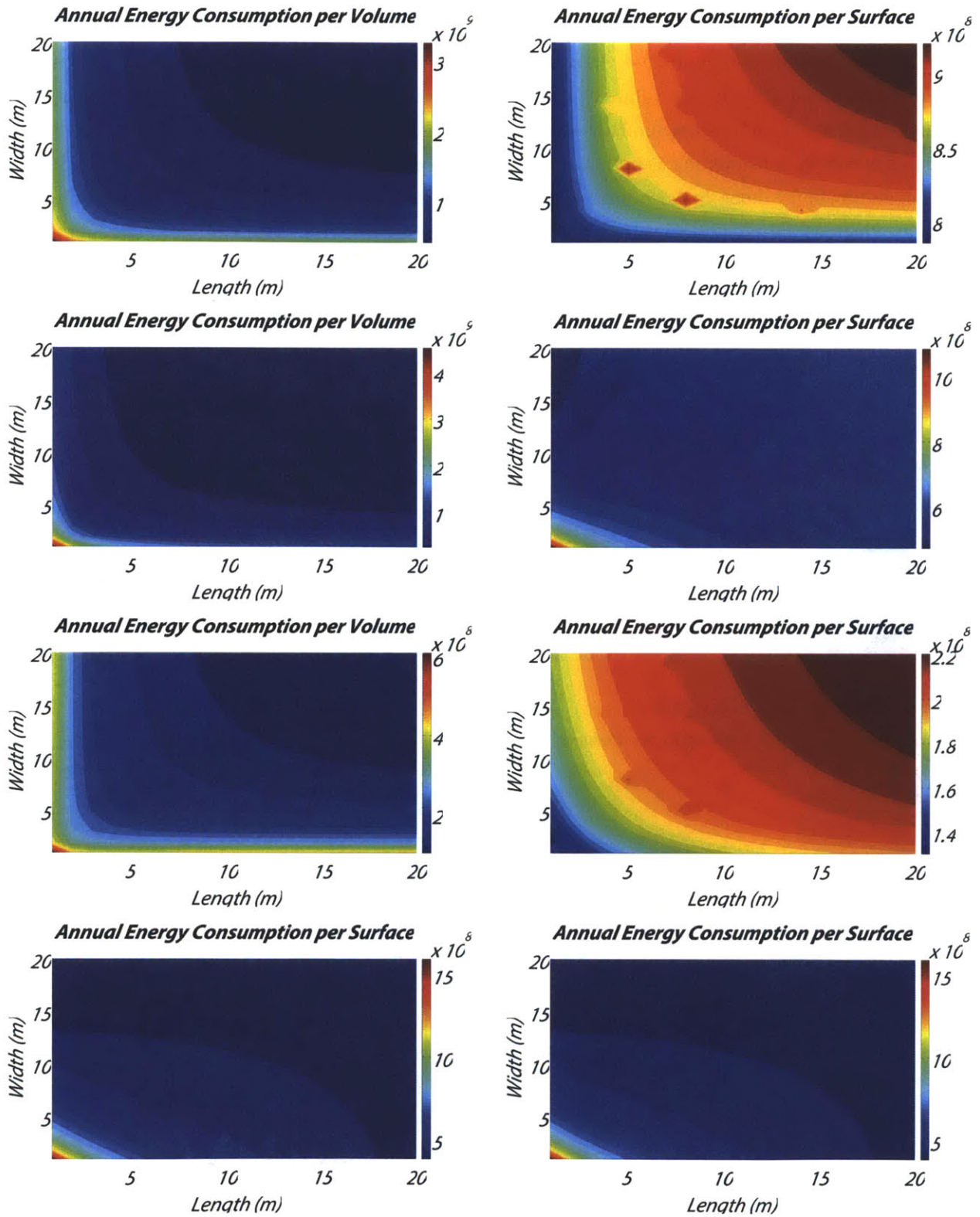


Figure 5-3 Annual Energy Consumption per Volume ( $J/m^3$ , left) and Surface ( $J/m^2$ , right), Width (m) vs Length (m), Anchorage, AK (row 1), Phoenix, AZ (row 2), San Francisco, CA (row 3), and Miami, FL (row 4)

The results for annual consumption per volume for the relationship between wall conductivity and infiltration are presented in Figure 5-4. As expected, the results show that in all four climates, the lowest energy is consumed at the lowest values of both parameters while the highest energy is consumed at the highest values of each parameter. However, it is notable that the relationships do not show steady increases in energy consumption as both parameters increase. Instead, the data show that one parameter tends to dominate the other. In Anchorage, conductivity dominates most buildings, with infiltration playing an increasingly important role as conductivity increases. The results are similar in Phoenix and San Francisco. In Miami, on the other hand, infiltration plays a much stronger role, which can be seen by the movement toward more horizontal trend lines in the graph, especially for higher conductivities. These results suggest that a focus on increasing wall insulation or increasing air-tightness should be a climate-based decision for achieving maximum energy savings.

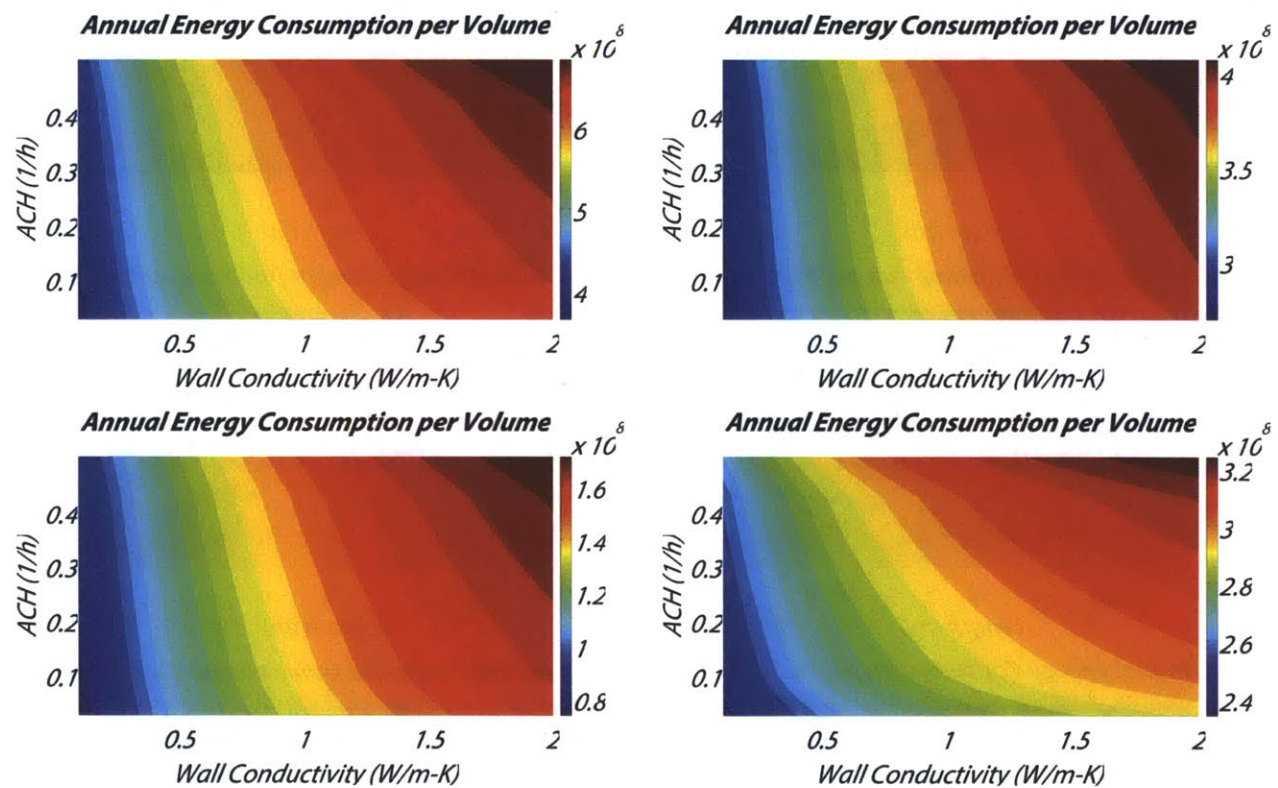


Figure 5-4 Annual Energy Consumption per Volume ( $J/m^3$ ), ACH (1/h) vs Wall Conductivity (W/m-K), Anchorage, AK (above left) and Phoenix, AZ (above right) San Francisco, CA (below left) and Miami, FL (below right)

The annual energy consumption per volume for the comparison of floor conductivity and wall conductivity in Figure 5-5 can be seen as a measure of the relative benefit of providing increased insulation in the slab or in the walls. All climates show that the least energy is consumed at the lowest values of wall conductivity, while the most energy is consumed at the highest value of wall conductivity and the lowest value of slab conductivity. However, the trends between these values are not identical.

The results for Anchorage and San Francisco indicate that wall conductivity is the dominant parameter governing energy consumption, while the behavior in Phoenix and Miami indicates that both floor and wall behavior contribute substantially toward the overall energy consumption. These results address the relative importance of ground contact by climate; in some climates the ground optimization problem is less important due to mild surface contact temperatures.

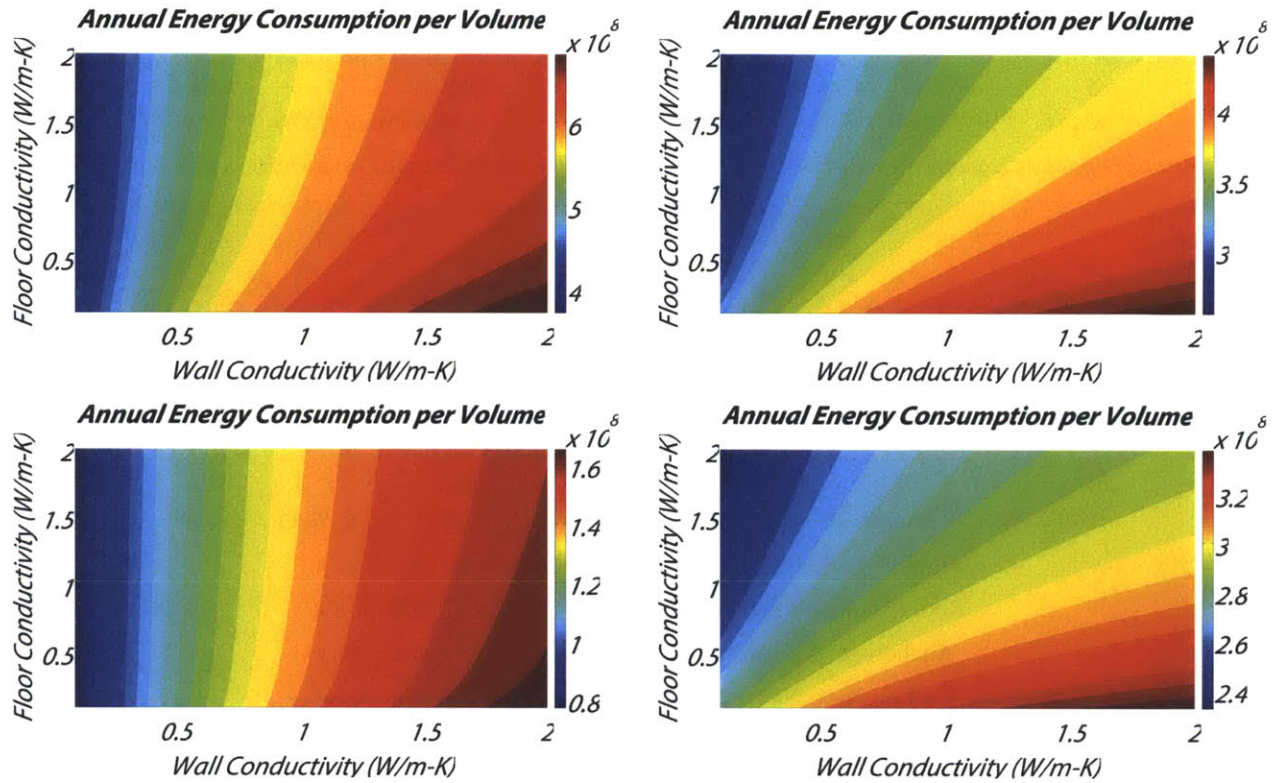


Figure 5-5 Annual Energy Consumption per Volume ( $J/m^3$ ), Floor Conductivity (W/m-K) vs Wall Conductivity (W/m-K), Anchorage, AK (above left) and Phoenix, AZ (above right) San Francisco, CA (below left) and Miami, FL (below right)

The final set of simulation experiments studies the relationship between wall conductivity and roof conductivity to determine if there are benefits to minimizing one or the other in building construction. The annual energy consumption per volume for the four climates is presented in Figure 5-6. The results indicate that roughly the same trend is observed in all climates modeled. The lowest energy consumption is observed where both wall and roof conductivity is at a minimum, while the highest energy is observed at their mutual maxima. The curved bands suggest that roof conductivity dominates energy consumption where wall conductivity is at its minimum and vice versa. As such, these results do not demonstrate a benefit of providing lower conductivities in one location versus another.

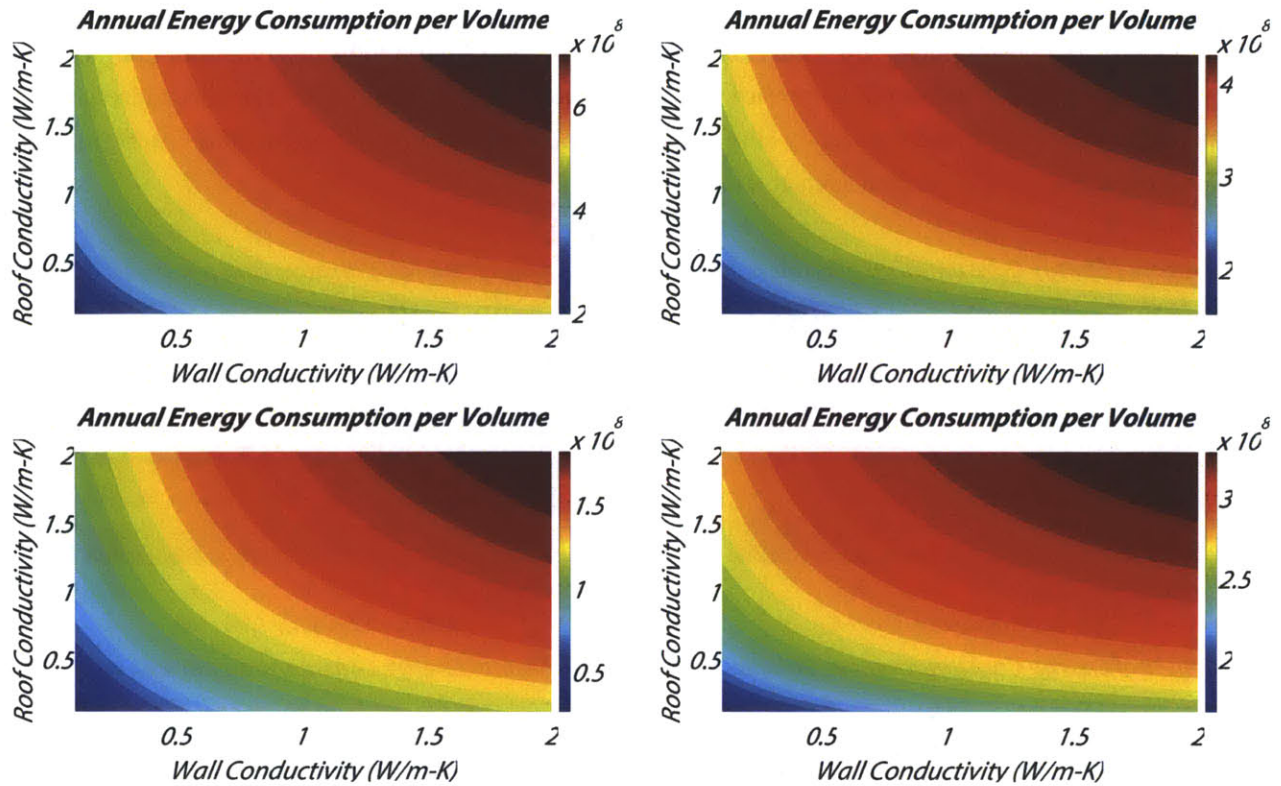


Figure 5-6 Annual Energy Consumption per Volume ( $J/m^3$ ), Roof Conductivity (W/m-K) vs Wall Conductivity (W/m-K), Anchorage, AK (above left) and Phoenix, AZ (above right) San Francisco, CA (below left) and Miami, FL (below right)

### 5.3 Chapter Summary

This chapter demonstrates that the Cube Model can be used to explore significant relationships between parameters. The results show that the relationships for height versus infiltration and length versus width vary widely between climates, while the relationships for studies of conductivity, height versus length, and conductivity versus infiltration show similar behavior for all climates. Finally, these results show that many additional topics of study could be addressed using the Cube Model. For the remainder of this report, the cube model will be used to study the thermal mass effect. Some of the scaling topics addressed here will be revisited in Part IV where sensitivity analyses will be conducted to determine if scaling relationships impact the performance of thermal mass. Before scaling effects can be considered, the main relationships governing thermal mass performance will be developed in the following chapters.

## **Part III**

# **Application to Passive Thermal Mass**

# Chapter 6

## Thermal Mass of Equivalent Walls

Chapter 2 presented an overview of the wide range of thermal mass literature. Still, while many of these studies involve qualitative building design or quantitative building control discussions, few seek to quantify the energy saving potential of passive thermal mass within the building envelope. This chapter will analyze the potential of passive thermal mass use in walls to benefit the energy consumption of a building. Chapter 7 will present the potential for thermal mass use in slabs. The focus of this chapter is to answer the second and third research questions by simultaneously addressing both the quantification and optimization of thermal mass performance.

### 6.1 Introduction

Thermal mass is, fundamentally, the ability of a material to store energy at one point in time and release this energy at another. Climate is inextricably tied to the benefits of thermal mass for two reasons. First, the climate determines the ambient temperature and the latitude and altitude determine the available solar radiation. Second, climate determines whether the storage of energy in a material is desirable. It is undesirable for heat to be released into a building during a cooling season or out of a building during heating season. This common sense principle, taken to its conclusion, indicates that thermal mass should be considered both by climate and by season.

For the purpose of this discussion, only passive thermal mass will be considered. Passive thermal mass means the ability of the envelope to store and release energy for the benefit of overall consumption, without the aid of controls or system intervention. Active thermal mass involves the use of radiant systems or other clear interventions into the storage system of the envelope. These systems are beyond the scope of this report.



## 6.2 Experimental Simulation Setup

A simulation experiment to test the thermal mass of a material must necessarily involve the properties that define its heat transfer characteristics. The cube model allows the modification of thickness, thermal conductivity, density, and specific heat capacity. Rather than conduct a case study analysis of specific wall sections, this experiment seeks to target the material properties that a wall section should obtain. Therefore, each property is varied across a range of reasonable values. It should be noted, therefore, that some combinations of material properties, especially those on the extremes of an experiment, may not accurately represent a constructible wall section. However, the broad scope of data better allows for the identification of trends. The ranges and increments used for the experiment are shown in Table 6-1.

Table 6-1 Ranges and Increments for Thermal Envelope Parameters

Parameter	Minimum Value	Maximum Value	Increment
Thickness	0.05 m	0.75 m	0.05 m
Thermal Conductivity	0.1 W/m-K	2.0 W/m-K	0.1 W/m-K
Density	100 kg/m <sup>3</sup>	3000 kg/m <sup>3</sup>	100 kg/m <sup>3</sup>
Specific Heat Capacity	100 J/kg-K	2000 J/kg-K	100 J/kg-K

Basic permutation of the parameters, however, indicates that a complete set of combinations of these parameters would result in 180,000 simulations per climate location. Clearly, such an experimental setup would require a computational expense that is unreasonable for the benefits: To simplify the experiment, six sub-experiments have been run where two parameters are varied and two remain constant. This reduces the final scope of the experiment to 2,650 experiments per climate location. The use of sub-experiments allows the trends associated with each parameter to be illuminated while maintaining a reasonable scope of the experiment. The constant parameters remain at typical values for a concrete wall, testing the assumption that the material has beneficial thermal mass characteristics. Table 6-2 presents the subexperiments and the constant parameters assumed for each case.

Table 6-2 Sub-Experiment Setup

Parameters Varied	Constant 1	Constant 2
Thermal Conductivity versus Specific Heat Capacity	Thickness = 0.15 m	Density = 2300 kg/m <sup>3</sup>
Thermal Conductivity versus Density	Thickness = 0.15 m	Specific Heat Capacity = 650 J/kg-K
Thermal Conductivity versus Thickness	Density = 2300 kg/m <sup>3</sup>	Specific Heat Capacity = 650 J/kg-K
Thickness versus Density	Thermal Conductivity = 0.9 W/m-K	Specific Heat Capacity = 650 J/kg-K
Thickness versus Specific Heat Capacity	Thermal Conductivity = 0.9 W/m-K	Density = 2300 kg/m <sup>3</sup>
Specific Heat Capacity versus Density	Thermal Conductivity = 0.9 W/m-K	Thickness = 0.15 m

## 6.3 Local Results

Understanding thermal mass begins at the scale of the individual cube model in a single location. For brevity, only a few locations will be discussed in detail as case studies. These results present the annual energy consumption, as determined from the Ideal Loads Total Energy (see Section 3.2.3). These are the total sensible and latent loads for the building, not a measure of electricity or fuel consumption. Therefore, the results that follow can be applied to buildings with most traditional systems. Section 6.4 will present the results on a national scale, and the lessons learned from a larger scale experimental run.

### 6.3.1 Diffusivity

Diffusivity is the ratio of heat transmittance to heat storage. This parameter is used to present the thermal properties of a material as a single parameter and can be used to better understand the relationship between thermal mass and resistance of a material. The diffusivity of the equivalent envelope material,  $a$ , is defined as the ratio of equivalent thermal conductivity  $\lambda$  to the product of equivalent density  $\rho$  and equivalent heat capacity  $C_p$  (see Section 3.1) [60].

$$a = \frac{\lambda}{\rho C_p} \quad (6-1)$$

The results from the experiments on the envelope of the cube indicate that there are competing effects on the energy consumption of a building. First, the impact of increased conductivity, or the transmission of heat through the system, increases the system energy. This is the rationale behind the industry practice of using higher R-value products in wall construction: keep the heat from transmitting in or out of the

envelope. In contrast, increases in thermal mass storage, as represented by the product of the specific heat capacity and density, tend to decrease the overall energy consumption of the building. Finally, there is the impact of wall thickness, which tends to increase or decrease the ability of thermal mass to function effectively in a given climate. The following subsections will analyze the output graphs from four climates to show how the results differ by climate.

### **6.3.1.1 San Francisco, CA - Mild, Marine Climate**

The first case study climate to be discussed is San Francisco, CA, which is classified as climate zone 3C: a mild, marine climate [29]. The three sub-experiments conducted on a fixed thickness (0.15 m) wall are plotted versus their annual specific energy consumption in Figure 6-1. As can be seen in the figure, variations in density and specific heat capacity form smooth curves, which are shifted by the impact of the conductivity of the material. This reinforces the notion that decreasing the thermal conductivity decreases the amount of energy consumed. From the experiment varying specific heat capacity and density only, there is a 22% optimization possible from the maximum value over the range of material properties measured.

While the whole impact of building energy consumption is an effective parameter to study, the normalized energy consumption illuminates another key relationship for thermal mass performance. To normalize the data, results were separated by wall thickness and conductivity groupings. Then, each value has been scaled by the maximum energy consumption in its group. The result of this normalization for the 0.15 m wall is shown in Figure 6-2. The diffusivity values at which peak energy consumption occurs range between  $5E-7$  m<sup>2</sup>/s and  $1E-5$  m<sup>2</sup>/s, with smaller conductivities having lower peak diffusivities. This result indicates that, as conductivity decreases, one requires a wall with a much lower diffusivity in order to benefit from thermal mass. In the terms of practical building construction, as the R-value of a wall increases, the relative density and/or specific heat capacity of mass materials necessary to benefit from thermal mass must increase as well.

When looking at Figure 6-2, one should note that the maximum ability to reduce energy consumption is not equal for all conductivities of wall materials. There are 51 cube models common to all conductivity experiments run on this graph. These include variations of conductivity for a specific heat capacity of 650 and a variable density, variations of conductivity for a density of 2300 kg/m<sup>3</sup> and a variable specific heat capacity, and a base case with constant density and specific heat at their baseline values. Taking these points and finding the potential energy savings along each curve, Figure 6-3 results. This figure indicates that, for a 0.15 m wall, the optimum conductivity of a wall from a thermal mass perspective is 0.4 W/m-K. This can be readily translated into an R-value of 0.375 m<sup>2</sup>-K/W (2.13 hr-ft<sup>2</sup>-°F/Btu) [86]. Note that this is an R-value for an entire wall construction, not an R-value for insulation.

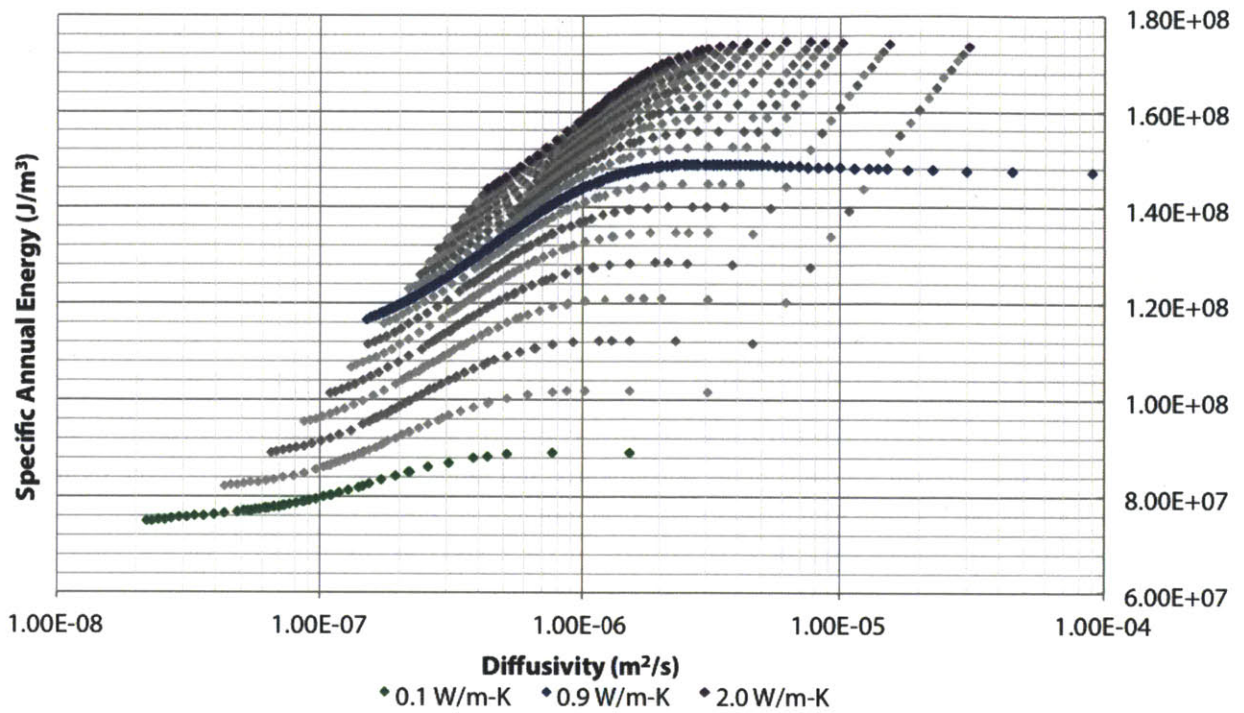


Figure 6-1 Specific Annual Energy Consumption (J/m³) vs Diffusivity (m²/s) and Conductivity (W/m-K), San Francisco, CA

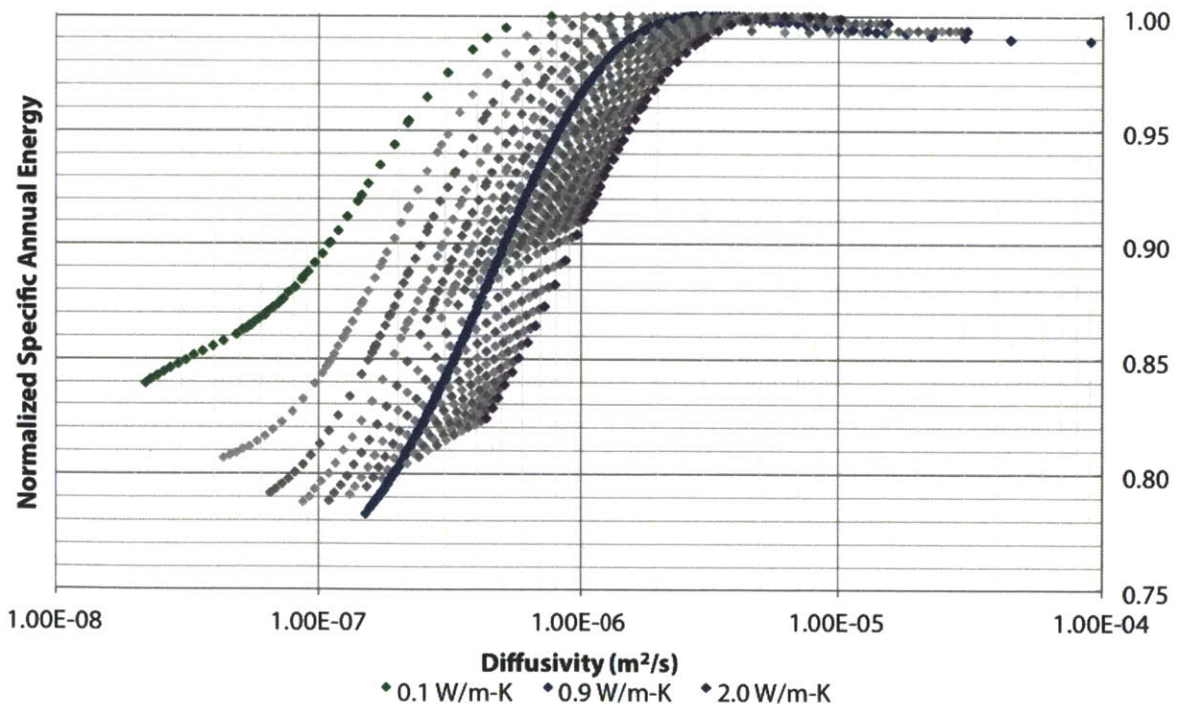


Figure 6-2 Normalized Specific Annual Energy Consumption vs Diffusivity (m²/s) and Conductivity (W/m-K), San Francisco, CA

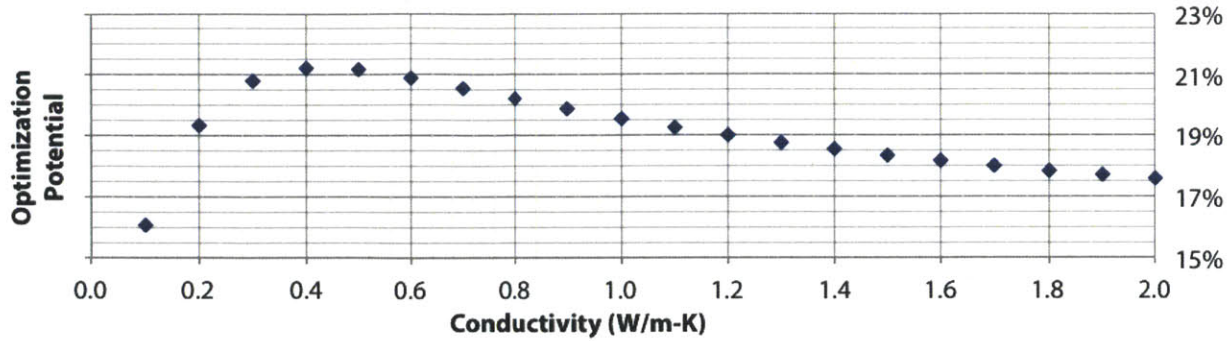


Figure 6-3 Potential Energy Savings from Thermal Mass vs Conductivity (W/m-K), San Francisco, CA

Looking at the diffusivity results from a different perspective, one can analyze the impact of changes of wall thickness on the ability of thermal mass to perform in San Francisco, CA. Figure 6-4 shows the graph for the three sub-experiments that consider variations of wall thickness with respect to their thermal mass impact. Once again, a family of curves is generated for the wall sections considered. However, in contrast with the results for the conductivity curves, these results are not all essentially parallel. There is a noticeable change in concavity for the curves above around 0.20 m. This indicates that there is a difference between the manner in which thermal storage functions in thin walls versus thick walls. The graph also indicates that thinner walls result in higher energy consumption than thick walls, though the benefit of increasing thickness is met with diminishing returns after around 0.50 m.

Performing a normalization for each curve individually, Figure 6-5 results. The curves have maxima in the range of  $9E-7 \text{ m}^2/\text{s}$  to  $2E-5 \text{ m}^2/\text{s}$ , with thinner wall sections experiencing peaks at lower values of diffusivity. These results indicate that thin wall sections have much lower potential to be optimized for thermal mass than thicker wall sections. However, the overlap of curves for the upper values of wall thickness again indicates that there is a point at which marginal performance improvements diminish. Finally, especially considering the change in concavity for the function, for middle range diffusivities one benefits marginally more from increasing wall thickness than for lower diffusivities.

Similar to the results for conductivity, it is clear that there is not an equal benefit for thermal mass with respect to all values of wall thickness. Assembling the 51 experiments versus wall thickness that are identical for all thicknesses, one can obtain the results in Figure 6-6. This plot clearly demonstrates the diminishing returns of optimizing thermal mass past a certain wall thickness. While the graph has a peak at 0.3 m, the results are essentially flat for the region 0.25 m to 0.55 m before the ability to save energy from thermal mass benefits actually decreases for very thick wall sections. When taking cost into account, this would suggest that, for a 0.9 W/m-K wall, there is no benefit to justify added material cost for a wall thicker than 0.25 m functioning along thermal mass optimization principles. This result translates to a total wall R-value of  $0.278 \text{ m}^2\text{-K/W}$  ( $1.58 \text{ hr-ft}^2\text{-}^\circ\text{F/Btu}$ ) [86].

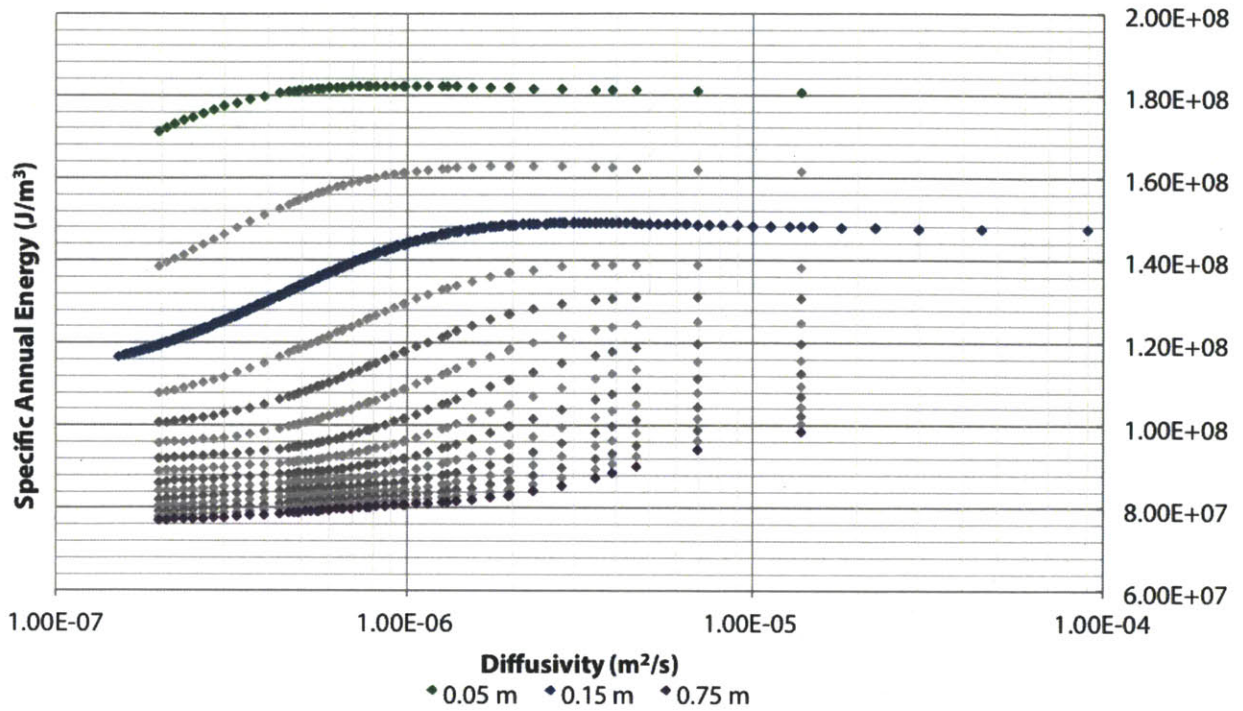


Figure 6-4 Specific Annual Energy Consumption (J/m³) vs Diffusivity (m²/s) and Wall Thickness (m), San Francisco, CA

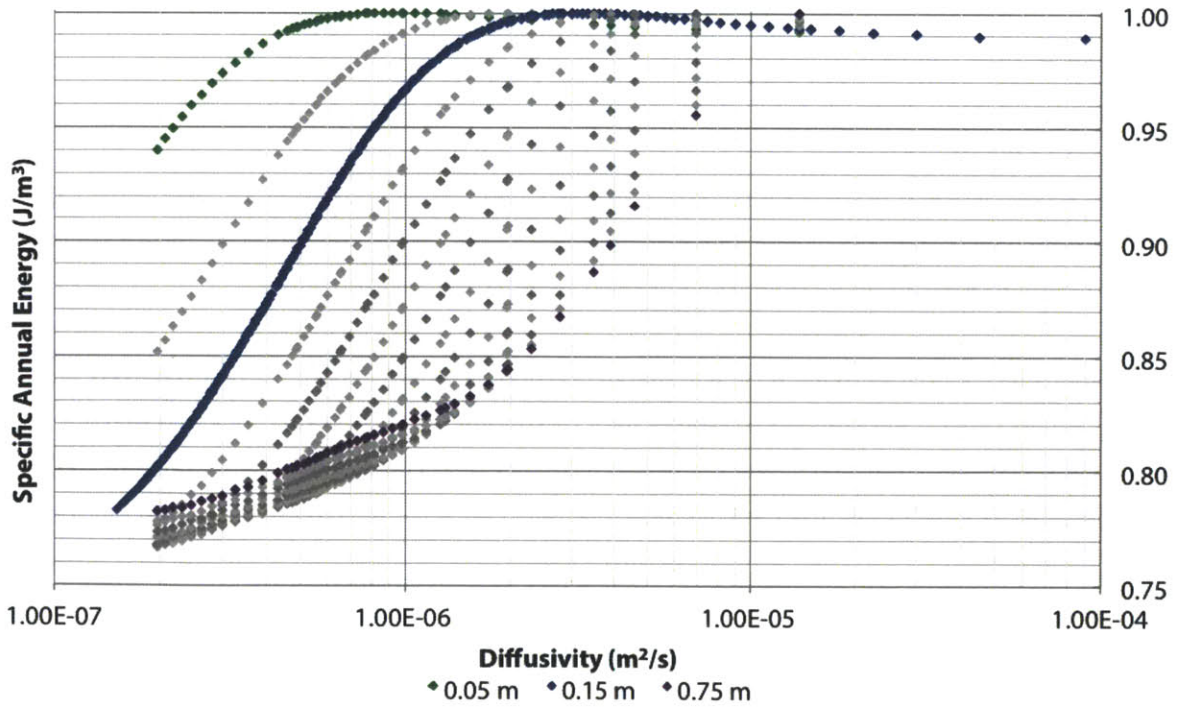


Figure 6-5 Normalized Specific Annual Energy Consumption vs Diffusivity (m²/s) and Wall Thickness (m), San Francisco, CA

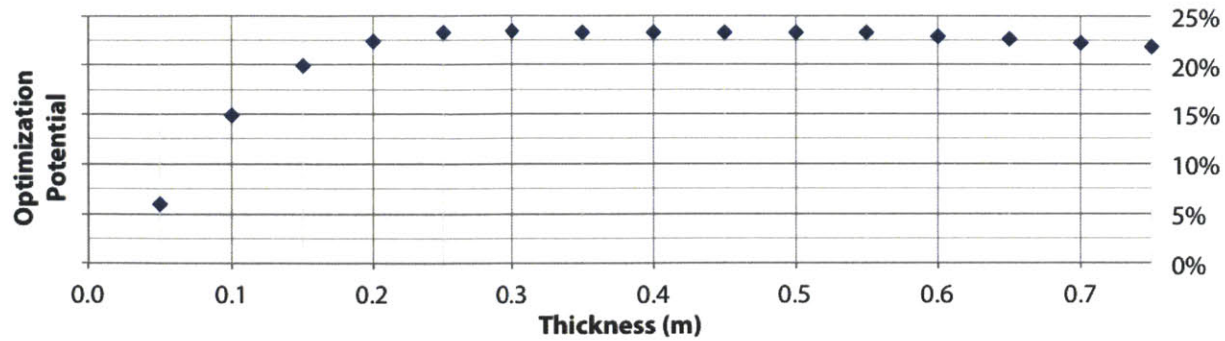


Figure 6-6 Potential Energy Savings from Thermal Mass vs Wall Thickness (m), San Francisco, CA

### 6.3.1.2 Phoenix, AZ - Hot, Dry Climate

The second case study to be discussed is Phoenix, AZ, which is classified as climate zone 2B, or a hot, dry climate [29]. The sub-experiments conducted on the 0.15 m wall versus specific annual energy consumption are presented in Figure 6-7. This figure indicates that higher energy consumption occurs with increasing thermal conductivity and presents a similar set of curves to the ones indicated for San Francisco, CA (see Figure 6-1). Differing from San Francisco, however, is the change in energy consumption as a result of increasing thermal mass (density and/or specific heat capacity). It can be seen that the curves show less improvement in energy consumption, to the extent where for some conductivities, there is no overlap in energy magnitudes for the extent of one curve versus another. This indicates that, if one uses a wall section with this equivalent conductivity, no amount of improvement of thermal mass will result in lower energy consumption than a decrease in conductivity.

Conducting a normalization of the curves, one can see in Figure 6-8 that, while the shape of the curves is similar to the results for San Francisco (see Figure 6-2), the magnitude of impact is significantly lower. Using the density-specific heat curve generated for 0.9 W/m-K and 0.15 m, there is a 4.9% potential energy reduction possible for this location. In keeping with the results from San Francisco, the peak energy consumptions occur in the same range of diffusivities, and lower conductivities peak at lower values of diffusivity. That is, for a given diffusivity, higher conductivities have greater benefit for thermal mass. However, it is important to offset this effect against the results of Figure 6-7, to ensure that in the process of optimizing thermal mass one does not inadvertently increase the conductivity such that a negative impact on overall energy performance occurs.

Finally, looking at the experimental set constant to all conductivities and plotting the energy savings potential versus conductivity, one obtains the results shown in Figure 6-9. In contrast with the results for San Francisco (see Figure 6-3), which had an optimum value of conductivity, this climate has an asymptotic behavior, whereby the maximum energy savings has little marginal increase as conductivity grows larger. The impact of conductivity to improve thermal mass performance levels off at about 1.0

W/m-K, indicating that little gain occurs for improving the conductivity of the wall section. Also, one must bear in mind the results of the overall energy graph, which shows that increasing conductivity increases the base overall consumption value. Comparing Figure 6-7 and Figure 6-9, one can see that even though only 2.4% benefit from thermal mass has been registered for a 0.1 W/m-K conductive wall, the entire curve lies below the next highest conductivity value. These results would seem to indicate that, for the conditions tested, it would be wise to optimize lower conductivity than to optimize the curve in Figure 6-9. Therefore, the optimum wall among those tested would have an R-value of 1.5 m<sup>2</sup>-K/W (8.52 hr-ft<sup>2</sup>-°F/Btu), with the likelihood that an even higher R-value would further improve performance [86].

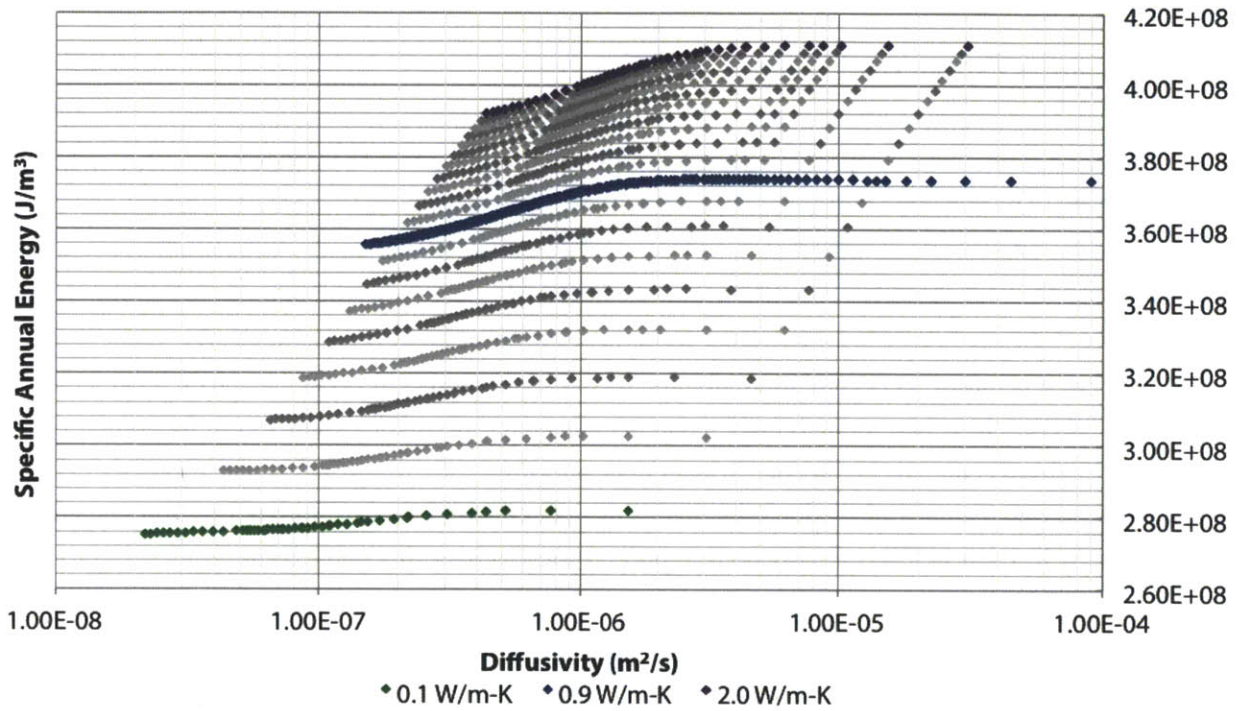


Figure 6-7 Specific Annual Energy Consumption (J/m<sup>3</sup>) vs Diffusivity (m<sup>2</sup>/s) and Conductivity (W/m-K), Phoenix, AZ



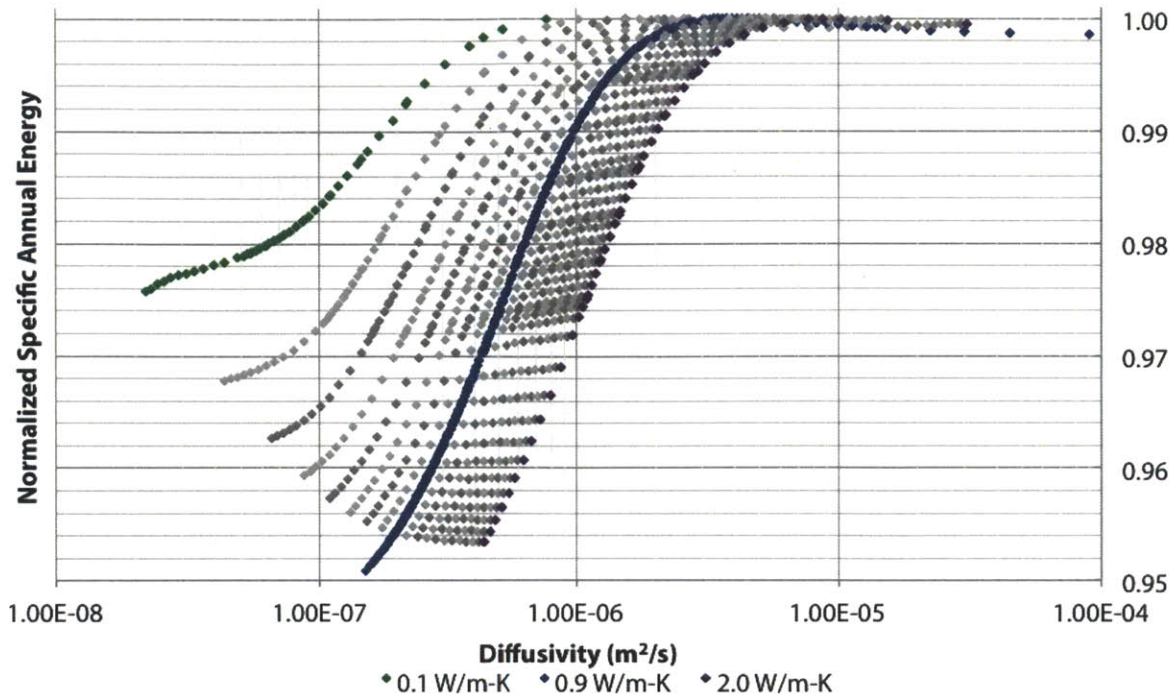


Figure 6-8 Normalized Specific Annual Energy Consumption vs Diffusivity ( $m^2/s$ ) and Conductivity ( $W/m-K$ ), Phoenix, AZ

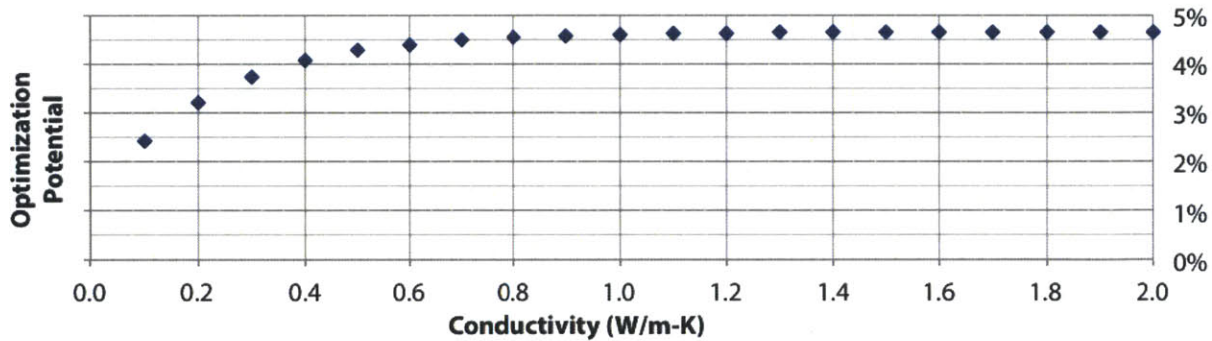


Figure 6-9 Potential Energy Savings from Thermal Mass vs Conductivity ( $W/m-K$ ), Phoenix, AZ

Shifting to a discussion of the relationships between energy and wall thickness, plotted in Figure 6-10 is the data for a conductivity of  $0.9 W/m-K$  and a variety of wall thicknesses to generate the master curve relationships of the density-specific heat term. This graph shows similar results to San Francisco, CA (see Figure 6-4), indicating that thicker walls shift the master curve of thermal mass potential downward. There is the same change in concavity of curves, also observed at around  $0.20 m$  thick walls. Finally, the results also indicate that there may be diminishing returns to energy performance from increasing wall thickness beyond  $0.50 m$ .

Normalizing the master curves to their maxima, one can see in Figure 6-11 that the relationships are similar to San Francisco (see Figure 6-5) from this standpoint as well, with the exception that there is less potential to normalize thermal mass. The maxima of the curves occur in the same range, between  $9E-7$  to  $2E-5$ , and the curves show the same trends in concavity. Finally, there are similar results in the benefit of increasing wall thickness, except in Phoenix the ability to optimize thermal mass diminishes beyond a certain wall thickness. This is likely due to the fact that the hot climate is governed by cooling loads, where thermal storage radiating into the building is not desired.

Finally, plotting the maximum percent energy savings from the set of points common to all wall thicknesses versus wall thickness, one can see in Figure 6-12 that there is a clear maximum value for optimizing energy savings due to thermal mass. The system shows that 0.20 m is the wall thickness to have the best potential to optimize thermal mass performance. This can be converted to an R-value of  $0.222 \text{ m}^2\text{-K/W}$  ( $1.26 \text{ hr-ft}^2\text{-}^\circ\text{F/Btu}$ ) [86]. As the walls become thicker than this point, more energy per volume can be saved for a given weight of material, though the ability to attribute these savings to the material mass becomes more limited. Still, the overlap in the energy curves for thickness presented in Figure 6-10 indicates that one could achieve same or lower energy performance from a thinner mass wall than a low mass construction.

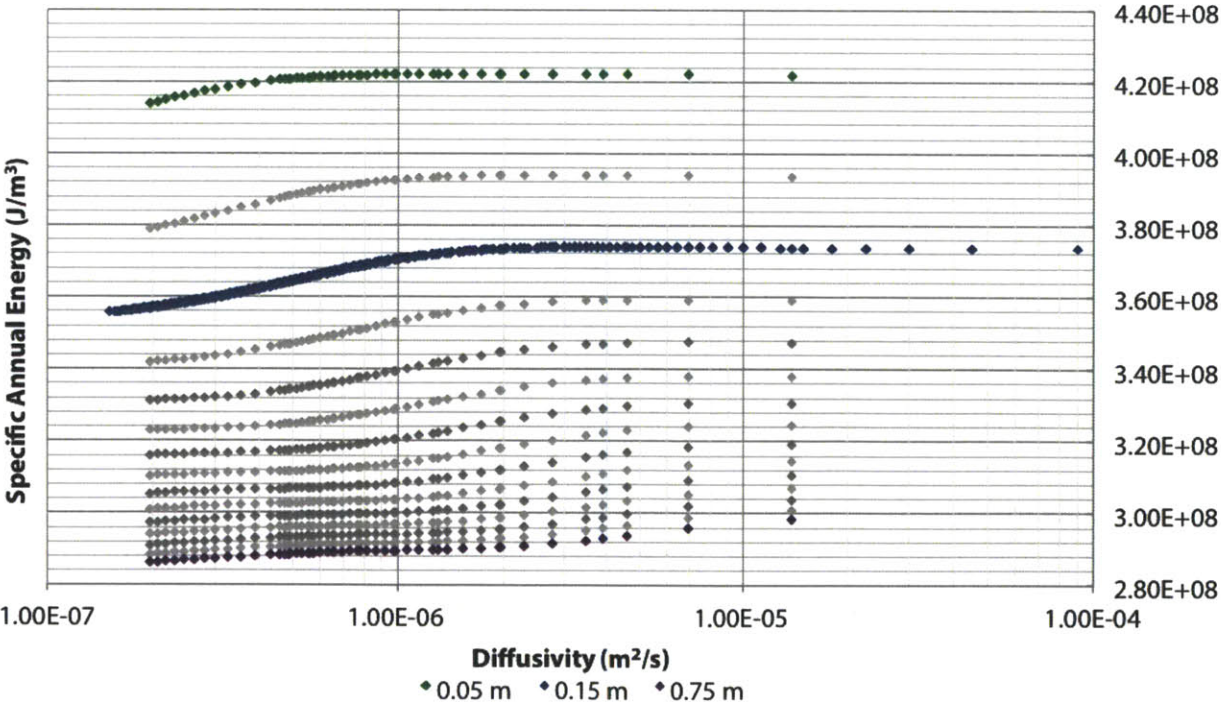


Figure 6-10 Specific Annual Energy Consumption ( $\text{J/m}^3$ ) vs Diffusivity ( $\text{m}^2/\text{s}$ ) and Wall Thickness (m), Phoenix, AZ

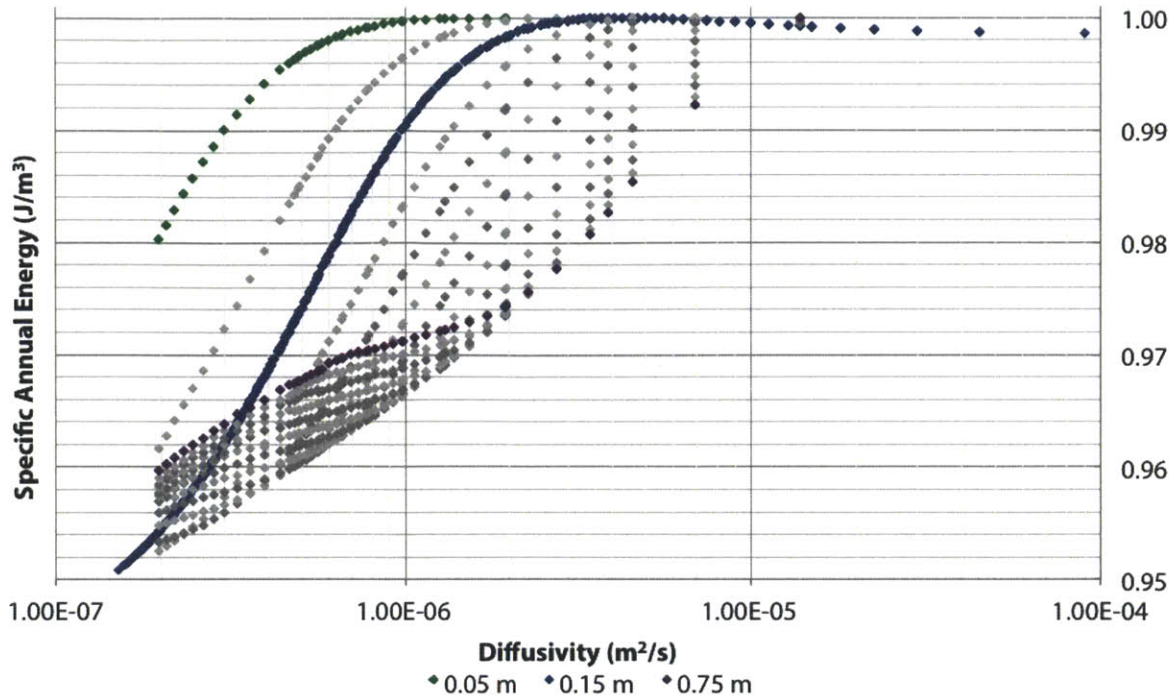


Figure 6-11 Normalized Specific Annual Energy Consumption vs Diffusivity ( $m^2/s$ ) and Wall Thickness (m), Phoenix, AZ

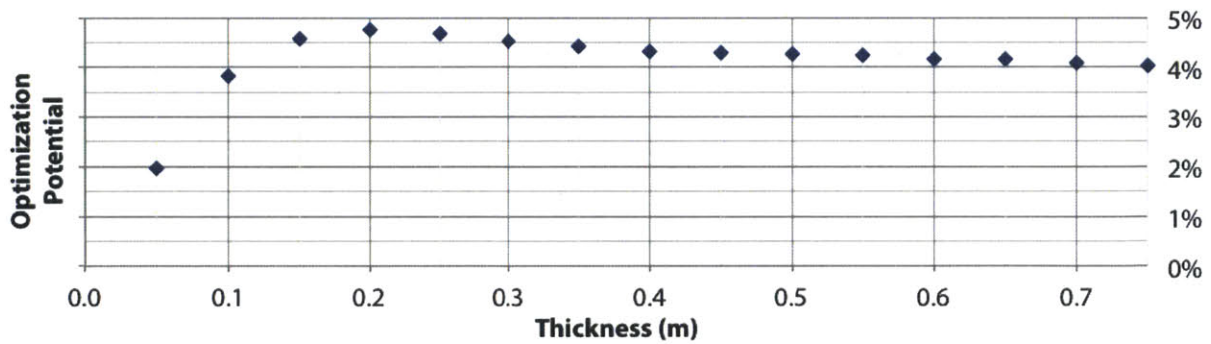


Figure 6-12 Potential Energy Savings from Thermal Mass vs Wall Thickness (m), Phoenix, AZ

### 6.3.1.3 Miami, FL - Hot, Humid Climate

The third case study is Miami, FL, located in climate zone 1A and characterized as a hot, humid climate [29]. Beginning with an analysis of the three sub-experiments comprising constant (0.15 m) wall thickness and variable conductivity, one can see in Figure 6-13 that there is a similar family of curves to the other two climates considered. Here, the lower conductivities are more widely spaced than the higher conductivities, indicating that the improvement of energy efficiency becomes much greater as conductivity becomes progressively lower. Also, it should be noted for the lower conductivities that,

like Phoenix, AZ (see Figure 6-7), there is no overlap in the curves. This means that, for instance, no optimization of thermal mass of a wall with 0.2 W/m-K conductivity could be used to obtain better results than a 0.1 W/m-K wall.

Normalizing the values for each master curve, Figure 6-14 shows that the ability to benefit from thermal mass increases with increasing conductivity. However, the magnitude of the benefit is not very large; for the standard 0.9 W/m-K master curve of density and specific heat, there is an optimization potential of 3.1%. In comparison with the other climate curves, the maxima fall between  $5E-7$  m<sup>2</sup>/s and  $4E-5$  m<sup>2</sup>/s, which is a slight extension of the range observed in the previous climates but nonetheless shows reasonable overlap. While there is an increase in ability to optimize thermal mass, the results of Figure 6-13 indicate that greater overall energy will be consumed by using a high conductivity, high mass wall.

Looking at the relationship of energy savings to conductivity of a wall shown in Figure 6-15, the potential for optimizing thermal storage increases with conductivity with no visible asymptotic behavior. Therefore, it is possible that increasing thermal conductivity further would result in even greater energy savings potential. However, keeping in mind the results of Figure 6-13, it is unwise to use passive thermal mass in this climate at a high conductivity, as the amount of overall energy increases. Among those conditions tested, this climate would be best served by a wall with overall R-value of 1.5 m<sup>2</sup>-K/W (8.52 hr-ft<sup>2</sup>-°F/Btu) or higher [86].

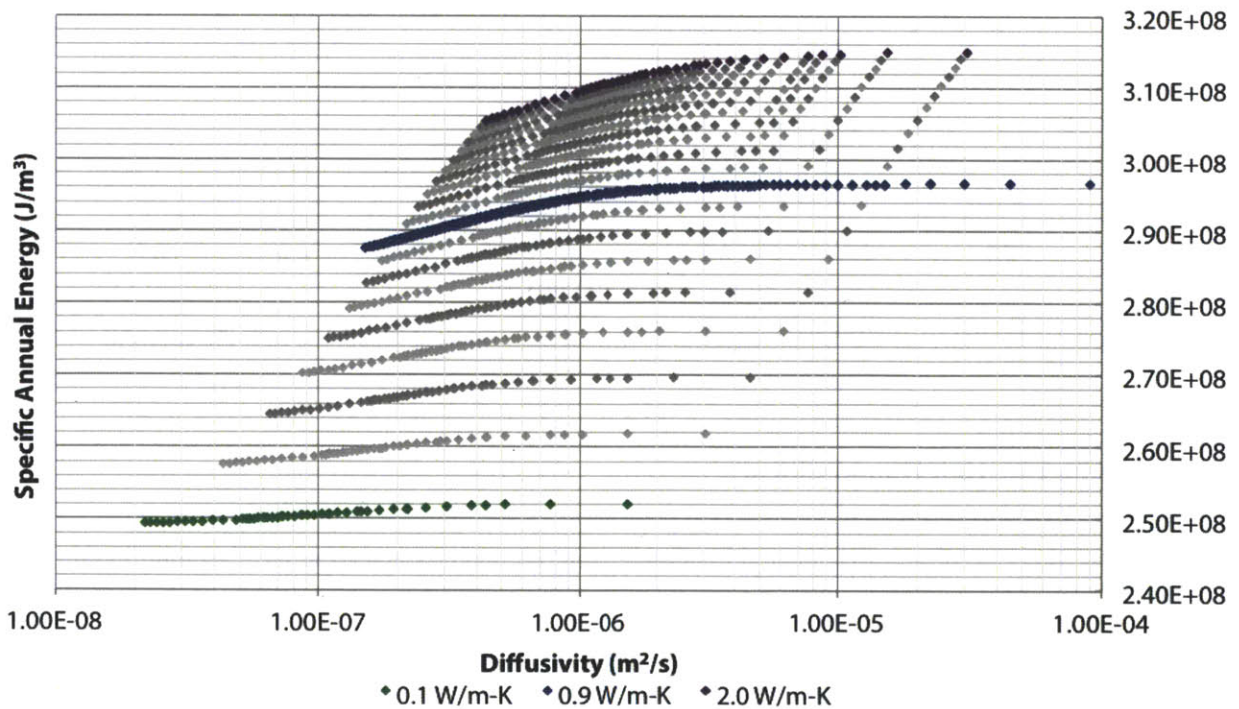


Figure 6-13 Specific Annual Energy Consumption (J/m<sup>3</sup>) vs Diffusivity (m<sup>2</sup>/s) and Conductivity (W/m-K), Miami, FL

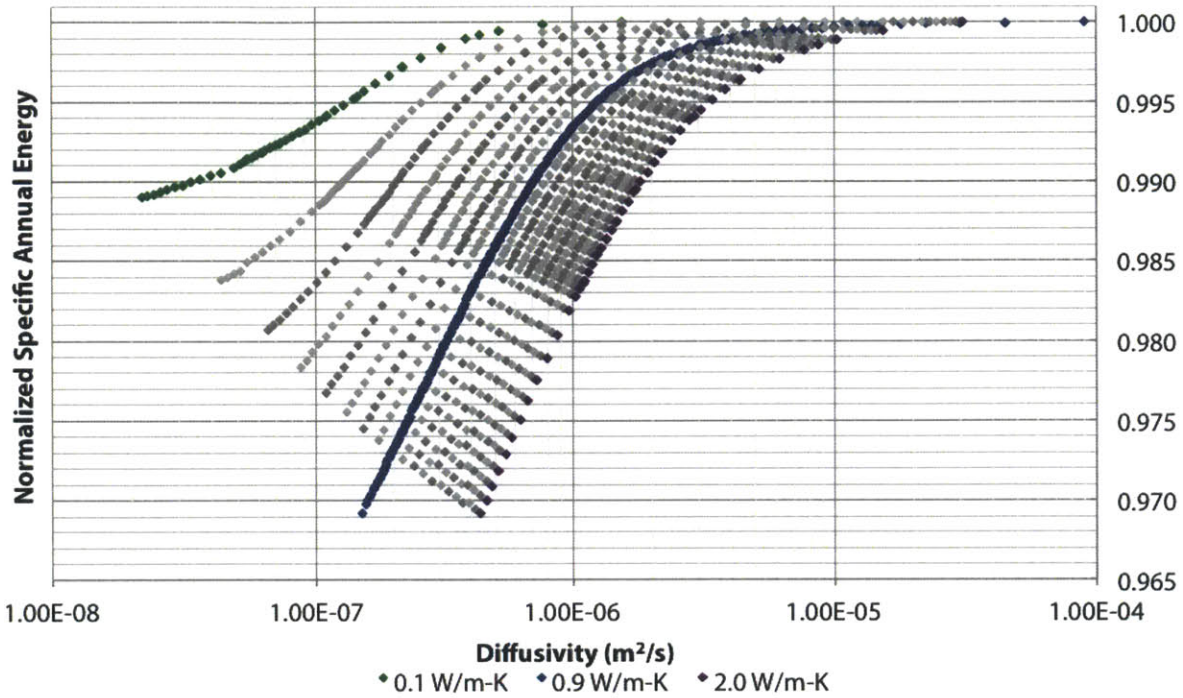


Figure 6-14 Normalized Specific Annual Energy Consumption vs Diffusivity ( $m^2/s$ ) and Conductivity ( $W/m-K$ ), Miami, FL

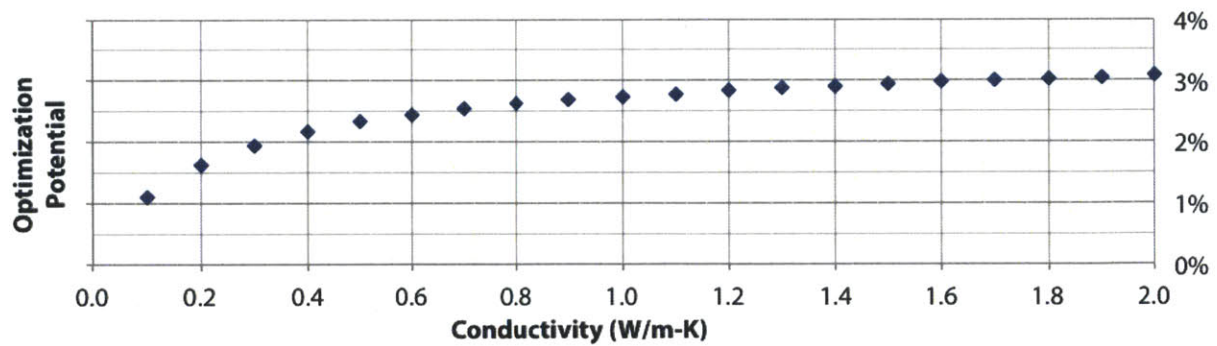


Figure 6-15 Potential Energy Savings from Thermal Mass vs Conductivity ( $W/m-K$ ), Miami, FL

Looking at the relationships of diffusivity to wall thickness for Miami, Figure 6-16 shows that increases in wall thickness will decrease overall energy performance, though the benefits of this trend diminish as the wall thickness increases. This graph also shows a change in trend concavity above around 0.20 m and diminishing returns after around 0.50 m, indicating that these trends occur in multiple climate types. There is overlap among the energy consumption values for the curves, indicating that in Miami, FL, one could achieve the same or better energy performance using thermal mass with a thinner wall section than using a low-mass wall construction.

Normalizing the energy consumption with respect to each curves' maximum value, it is clear from Figure 6-17 that in Miami, thermal mass becomes much more difficult to optimize for thicker wall sections. This is evident due to the upward swing of the graph for 0.75 m in comparison to thinner wall sections such as the 0.15 m. In fact, for those wall sections tested, only the 0.05 m wall section has less potential energy savings from thermal mass than the 0.75 m wall section. Therefore, these results indicate that in climates similar to Miami, it is unwise to construct thick walls for the purpose of optimizing thermal mass as thinner walls achieve better performance. Looking at the main 0.15 m thick curve, there is a 2.7% reduction in energy possible by improving the mass of the construction.

Considering the graph of the normalized energy reduction potentials shown in Figure 6-18, the best opportunity to optimize the thermal mass performance of a wall section occurs at 0.20 m. Given the conductivity tested for this experiment, this result translates to an R-value of 0.222 m<sup>2</sup>-K/W (1.26 hr-ft<sup>2</sup>-°F/Btu) [86]. This graph also clearly shows that the energy usage of wall sections strictly greater than 0.50 m, from a thermal mass perspective, only outperform the 0.05 m wall construction. This clearly indicates the potential for thermal mass to hurt energy saving potential in warm climates where thermal storage can be a detriment during the cooling season.

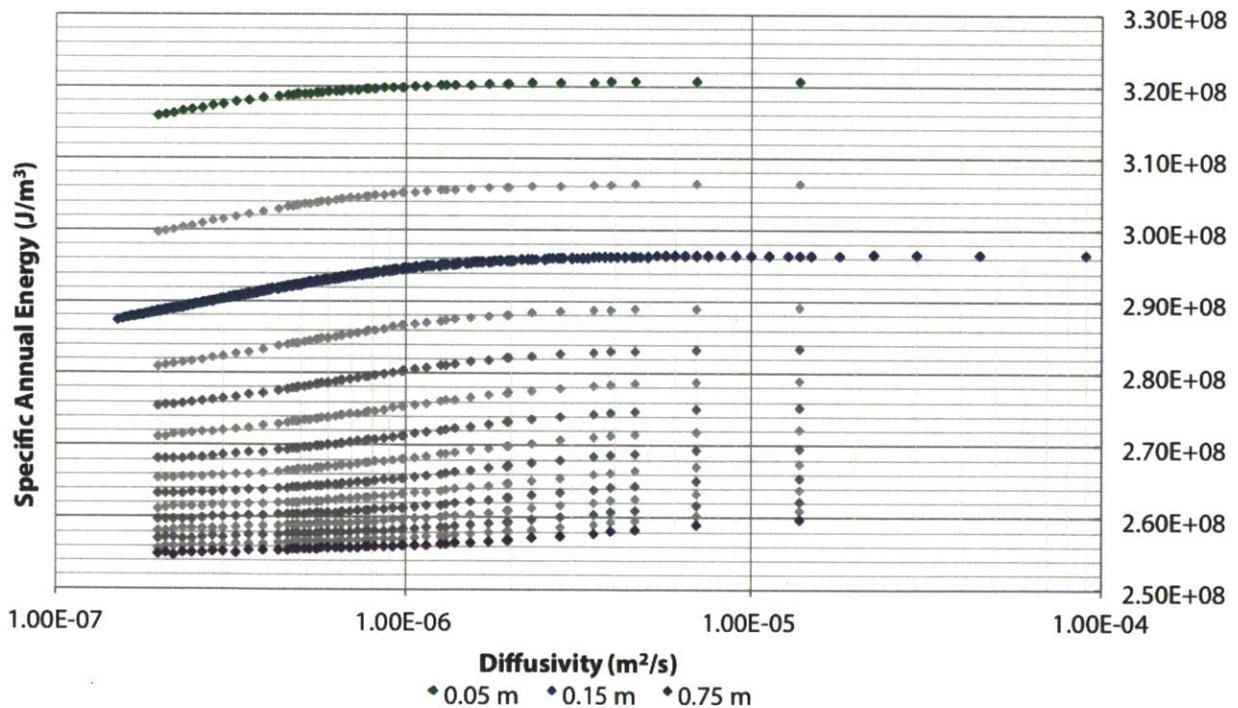


Figure 6-16 Specific Annual Energy Consumption (J/m<sup>3</sup>) vs Diffusivity (m<sup>2</sup>/s) and Wall Thickness (m), Miami, FL

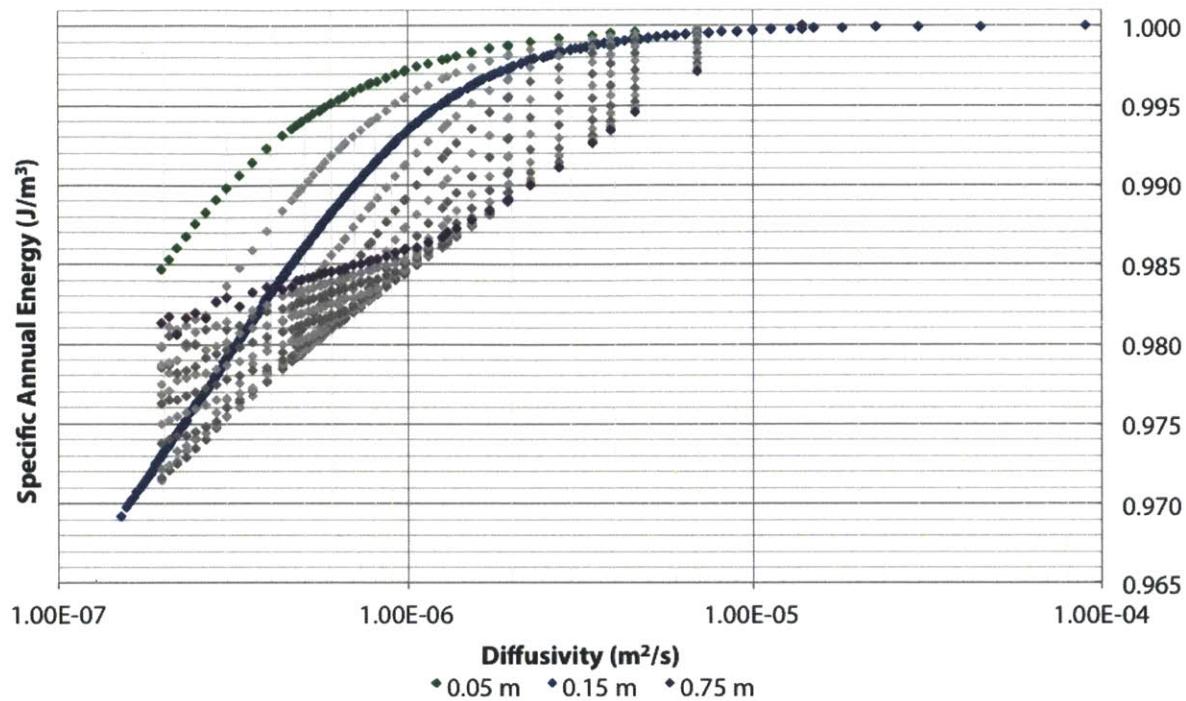


Figure 6-17 Normalized Specific Annual Energy Consumption vs Diffusivity ( $m^2/s$ ) and Wall Thickness (m), Miami, FL

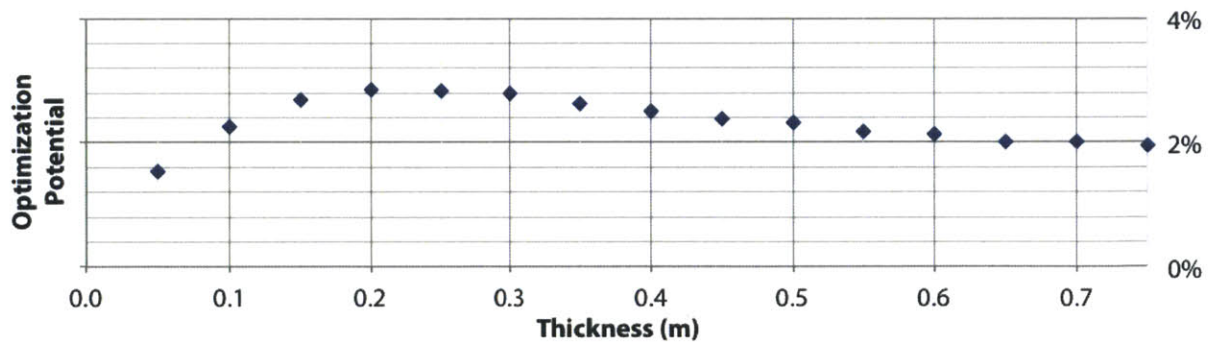


Figure 6-18 Potential Energy Savings from Thermal Mass vs Wall Thickness (m), Miami, FL

### 6.3.1.4 Anchorage, AK - Cold Climate

The last case study to be discussed is Anchorage, AK, a cold climate located in zone 7 [29]. Looking first at the relationship between diffusivity, conductivity, and specific annual energy shown in Figure 6-19, the density-specific heat curves are mostly flat. This indicates that changes in the mass of the material have very little benefit for thermal performance. Further, for most low conductivities there is no overlap in the energy performance of any of these curves. This means that, for instance, increasing the conductivity of a wall system will generally result in greater energy consumption regardless of the thermal mass of the

structure. Such a result indicates that thermal mass optimization of the equivalent walls tested here is not beneficial for energy performance.

The normalized energy consumption shown in Figure 6-20 indicates that the changes in the conductivity curves match the results of other climates; that is, as conductivity increases, the diffusivity at which maximum energy consumption occurs also increases. The maxima fall in the same range of diffusivities as the previously explored climates. However, the overall optimization potential is quite low. For the 0.9 W/m-K master curve only a 1.5% optimization potential exists.

Finally, considering the graph of the normalized results of thermal mass benefit shown in Figure 6-21, if thermal mass were to be used the optimum conductivity of the wall section is 0.4 W/m-K. However, the results of Figure 6-19 must be recalled; the graph of energy consumption indicates that such a wall consumes far more energy than the lower conductivity wall section. Therefore, the best recommendation for this climate is to optimize with respect to conductivity, indicating an R-value of approximately 1.5 m<sup>2</sup>-K/W (8.52 hr-ft<sup>2</sup>-°F/Btu) or higher [86].

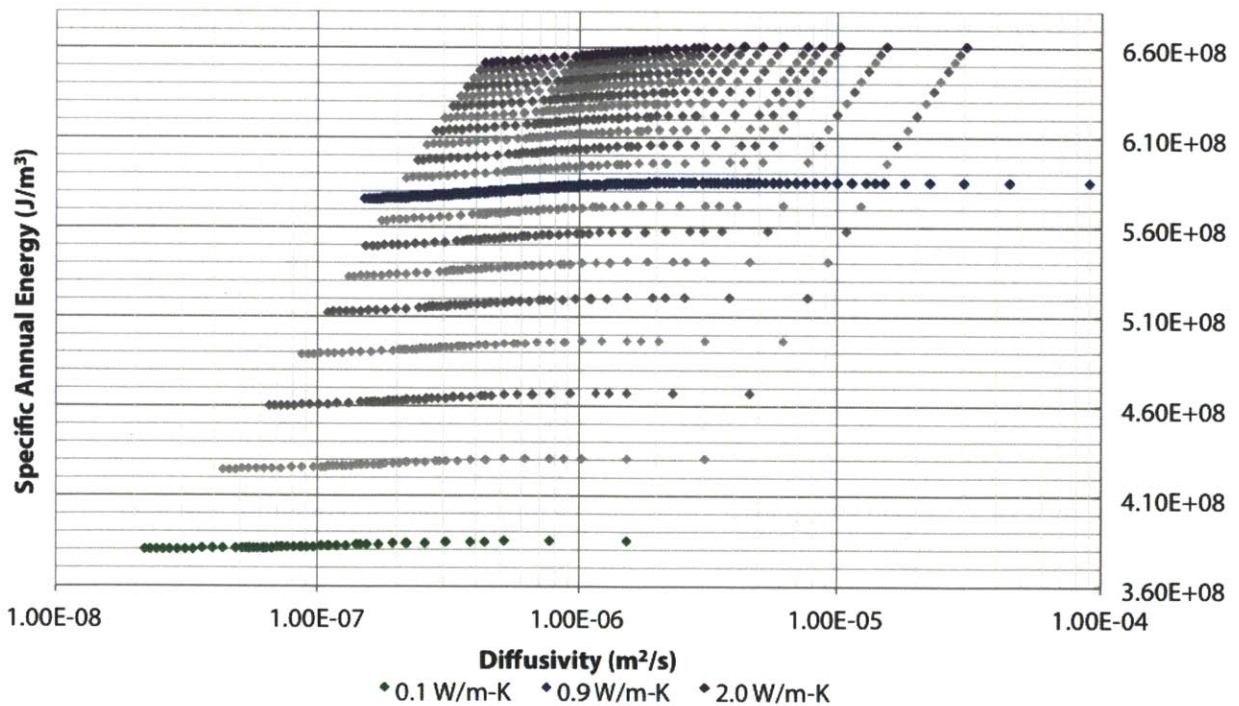


Figure 6-19 Specific Annual Energy Consumption (J/m<sup>3</sup>) vs Diffusivity (m<sup>2</sup>/s) and Conductivity (W/m-K), Anchorage, AK



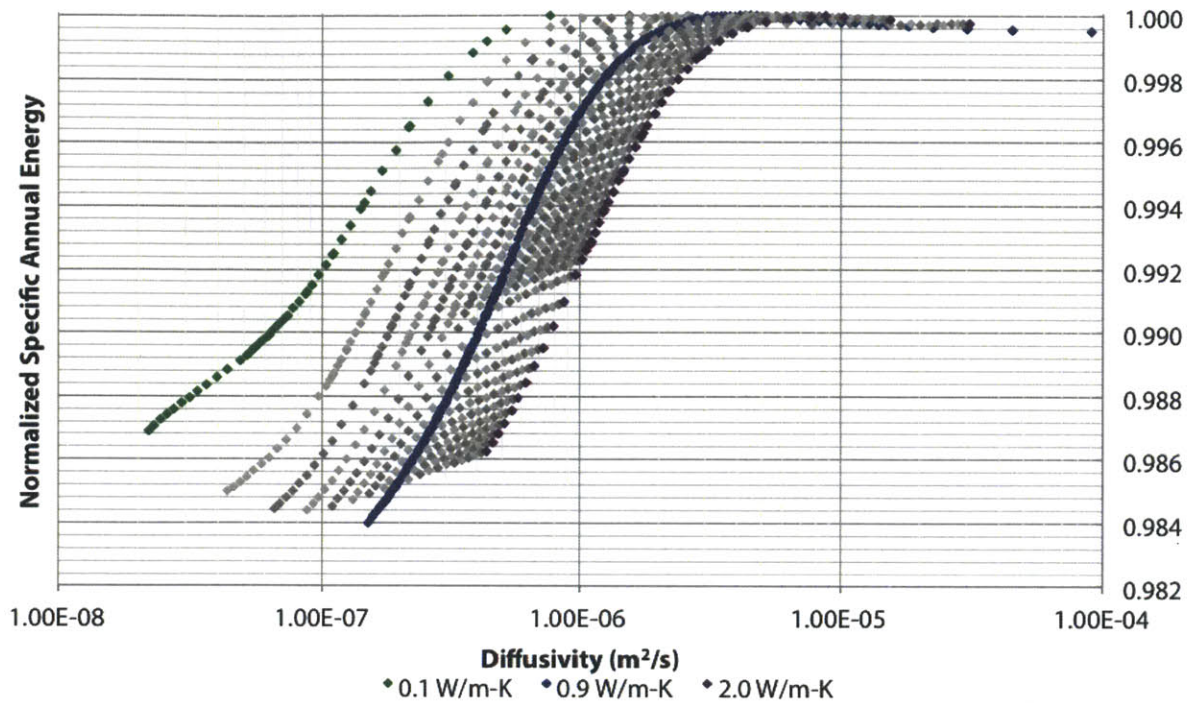


Figure 6-20 Normalized Specific Annual Energy Consumption vs Diffusivity ( $m^2/s$ ) and Conductivity ( $W/m-K$ ), Anchorage, AK

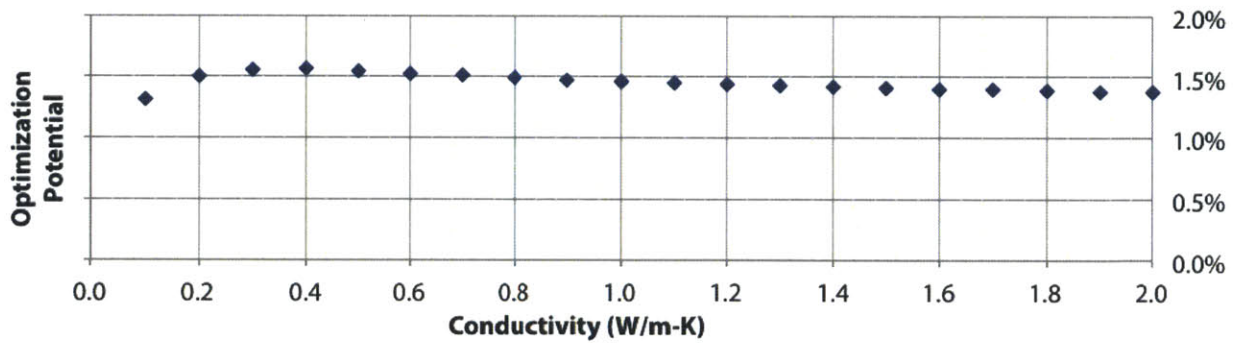


Figure 6-21 Potential Energy Savings from Thermal Mass vs Conductivity ( $W/m-K$ ), Anchorage, AK

Looking at the relationships of density-specific heat curves for varying thicknesses shown in Figure 6-22, the curves show similar behavior to other climates, with the exception of the magnitude of energy reduction for varying the weight of materials. As a result, for most typical wall thicknesses, there is no overlap of values from one curve to another. Therefore, one cannot achieve the same or better energy performance using a mass wall of different thickness. These results are also in agreement with other climates in that the return from increasing wall thickness becomes lower for larger wall sections, indicating that little additional performance is obtained for walls thicker than around 0.50 m.

Studying the normalized energy curves shown in Figure 6-23, one can see that the same phenomena occur in Anchorage as other climates, but on a much smaller scale. There is a similar shift in concavity of the curve occurring around 0.15 m thickness, and very thick wall sections show less ability to be optimized than thinner wall sections. The locations of the maxima also occur in similar ranges as for other climates. Therefore, it can be seen that, while the mechanisms of thermal mass seem unaffected by change in climate, the magnitude of the energy impact diminishes greatly in climates such as Anchorage.

Finally, looking at the optimization potential shown in Figure 6-24, it can be seen that the curve is mostly flat after 0.30 m, indicating that no additional benefit to the thermal mass effect occurs past this thickness. No R-value or design recommendations should be made from this behavior, however, because of the results of Figure 6-22, which indicate that this energy savings from optimizing thermal mass is too minor in Anchorage to be a recommended design route.

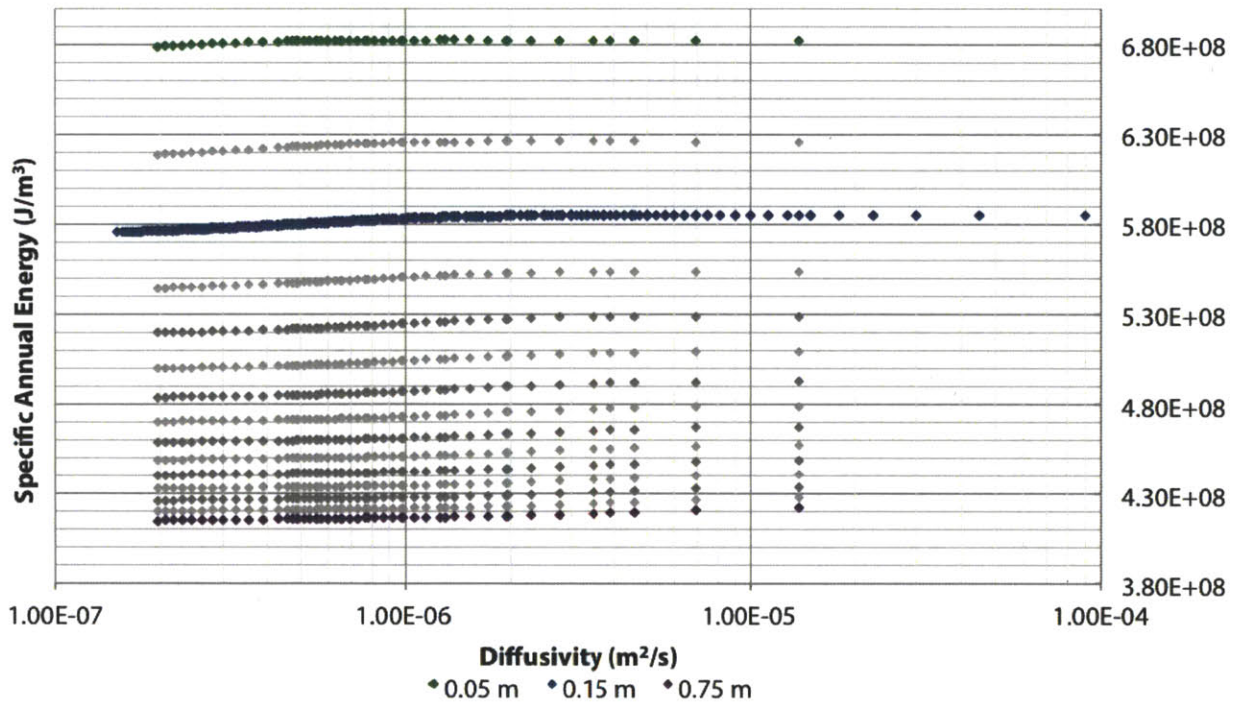


Figure 6-22 Specific Annual Energy Consumption (J/m<sup>3</sup>) vs Diffusivity (m<sup>2</sup>/s) and Wall Thickness (m), Anchorage, AK

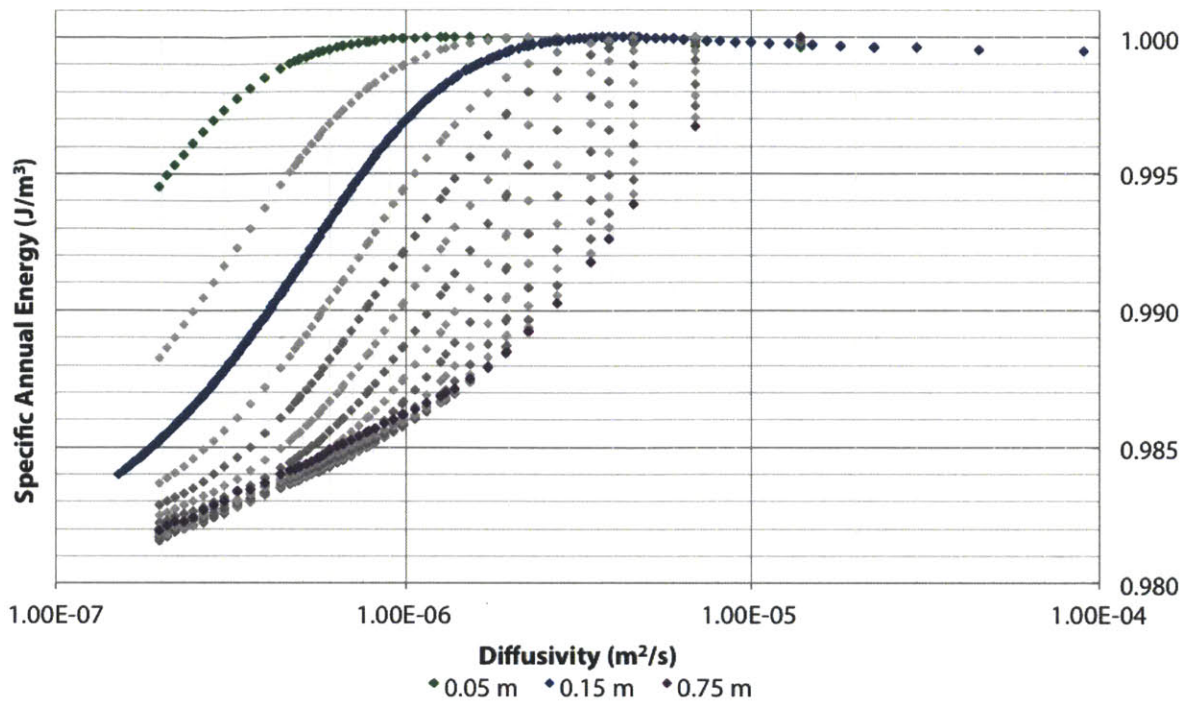


Figure 6-23 Normalized Specific Annual Energy Consumption vs Diffusivity ( $m^2/s$ ) and Wall Thickness (m), Anchorage, AK

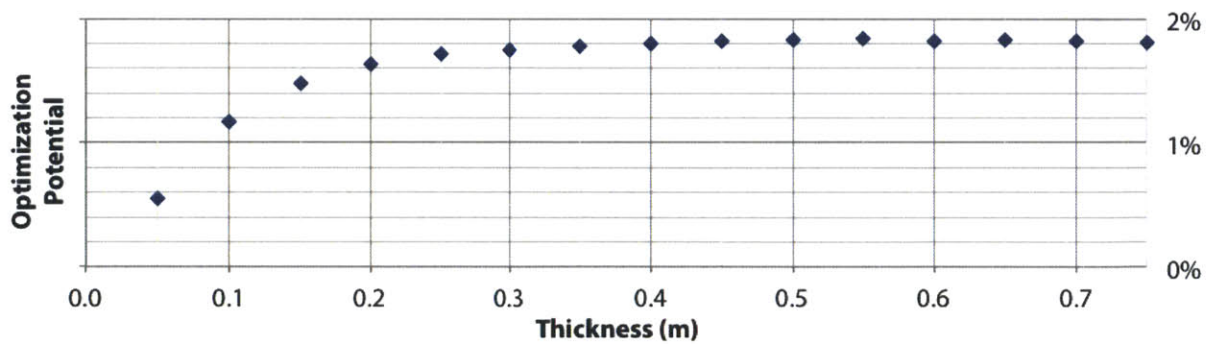


Figure 6-24 Potential Energy Savings from Thermal Mass vs Wall Thickness (m), Anchorage, AK

### 6.3.2 Seasonal Effects of Thermal Mass

The results above have mainly focused on the ability of thermal mass to save energy on an annual basis. However, the seasonal effects of thermal mass are also critical to understanding the energy use of the single-family residence incorporating thermal mass. Figure 6-25 through Figure 6-28 show the seasonal variation of the density-specific heat curve for a  $0.9 \text{ W/m-K}$  conductivity and  $0.15 \text{ m}$  thick wall. For the purpose of this graph, summer data is the total energy consumption from April to September, while winter data is the total energy consumption from October to March.

Figure 6-25 and Figure 6-28, showing San Francisco and Anchorage, respectively, indicate that for these climates, there is better performance of thermal mass in the summer than in the winter. In contrast, Figure 6-26 and Figure 6-27 demonstrate that Phoenix and Miami have the opposite behavior. Recalling that Anchorage is primarily a heating climate while Phoenix and Miami are cooling climates, it can be seen that for most climates better thermal mass performance is observed in off-peak seasons. San Francisco is mild throughout the year, and therefore the better performance in the summer is likely because the summers are even more mild than the winters observed.

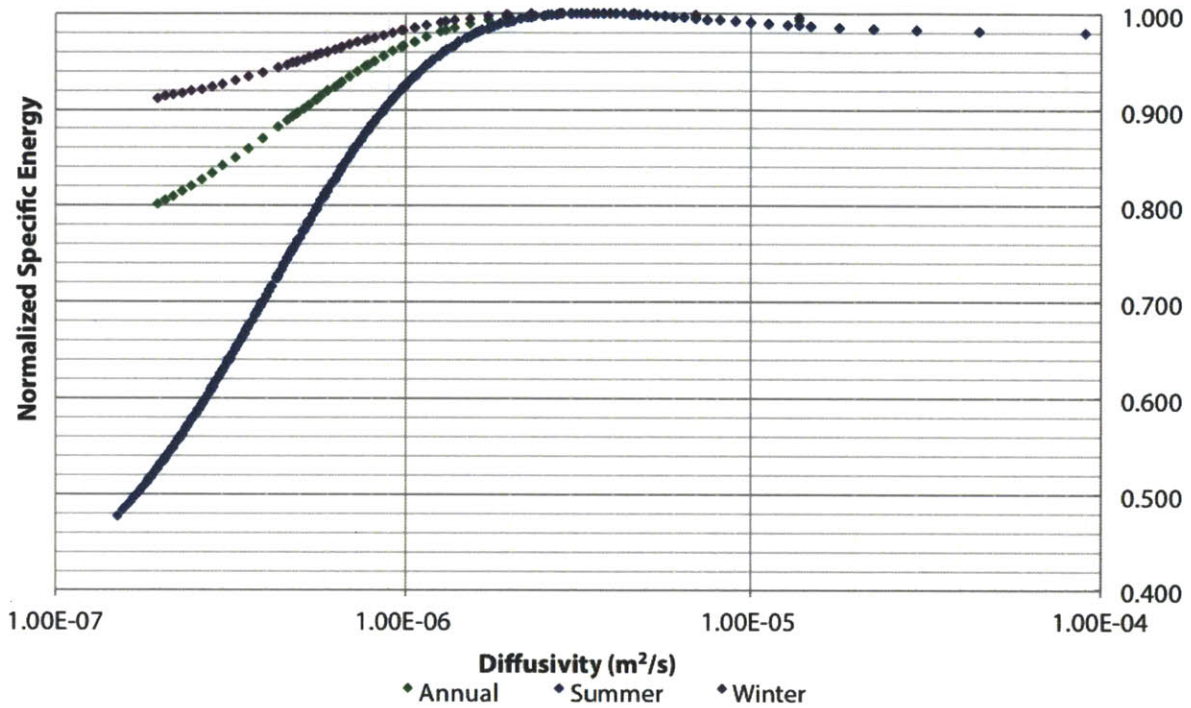


Figure 6-25 Specific Energy Consumption (J/m<sup>3</sup>) vs Diffusivity (m<sup>2</sup>/s) by Season, San Francisco, CA

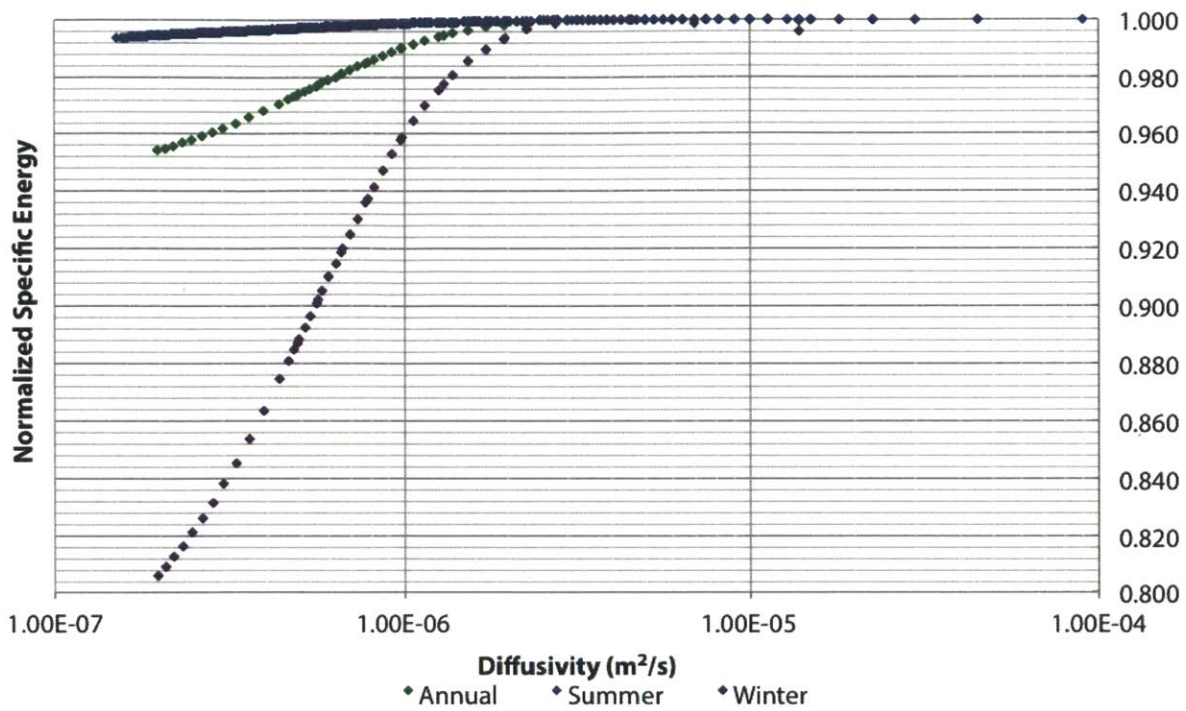


Figure 6-26 Specific Energy Consumption (J/m<sup>3</sup>) vs Diffusivity (m<sup>2</sup>/s) by Season, Phoenix, AZ

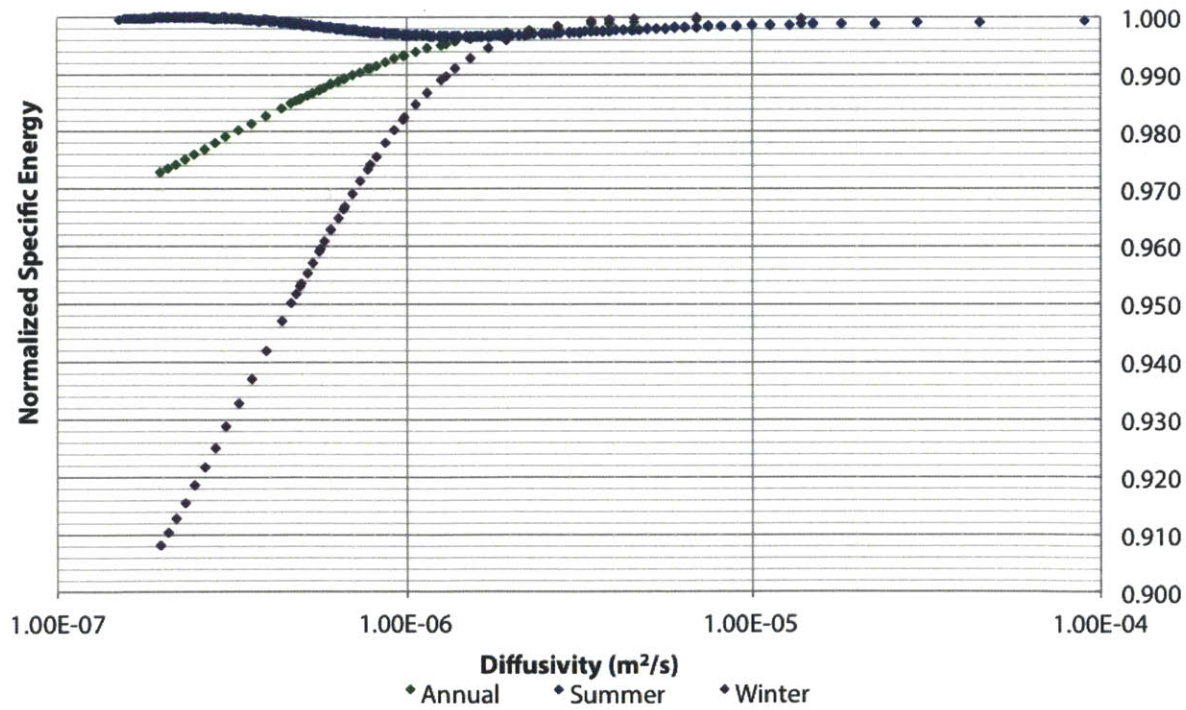


Figure 6-27 Specific Energy Consumption (J/m<sup>3</sup>) vs Diffusivity (m<sup>2</sup>/s) by Season, Miami, FL

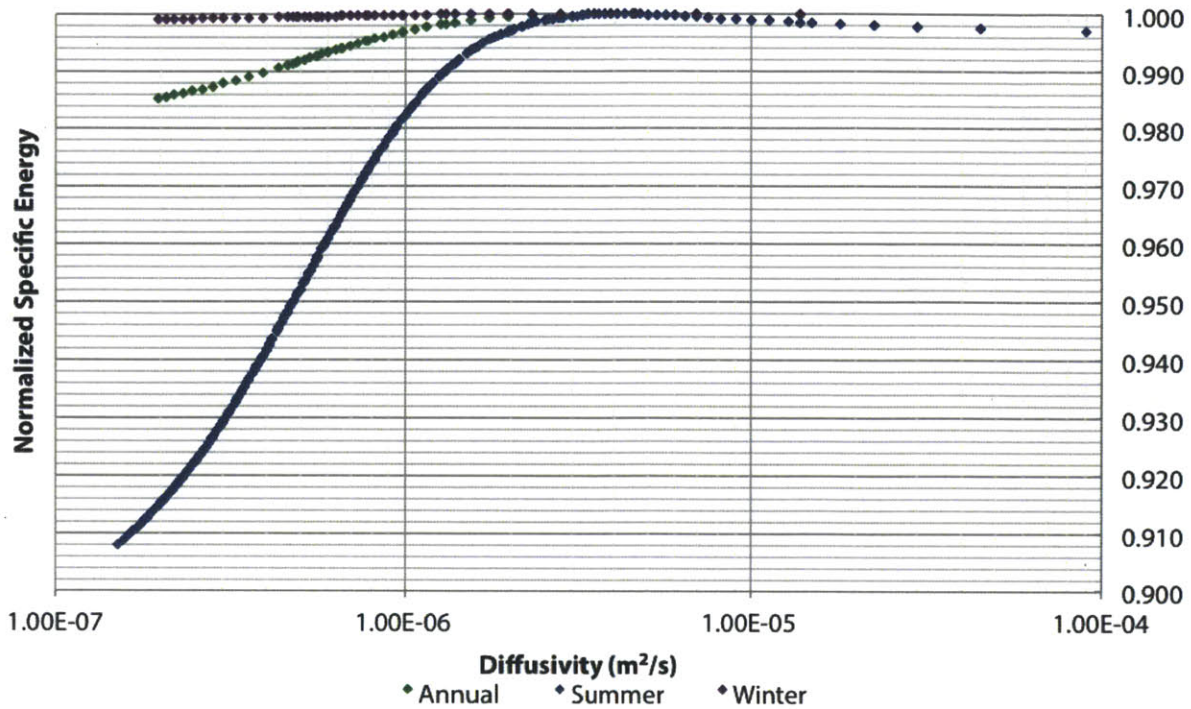


Figure 6-28 Specific Energy Consumption (J/m<sup>3</sup>) vs Diffusivity (m<sup>2</sup>/s) by Season, Anchorage, AK

Beyond the observed trends for seasonal effects as a whole, it is important to focus on the effect demonstrated in Miami, FL. An inset of the graph of the summer specific energy has been provided in Figure 6-29. This figure shows unequivocally that increasing thermal mass in Miami results in additional energy consumption during the summer, likely due to the effects of overheating of the thermal mass. The value of minimum energy consumption is at a diffusivity of 1.5E-6 m<sup>2</sup>/s, which is located in the region of the winter curve where little thermal mass benefit is observed. Therefore, in a hot, humid climate like Miami thermal mass can result in increased consumption of energy during the cooling season. Since the cooling season is dominant in these climates, thermal mass construction should not be employed in a purely passive sense.

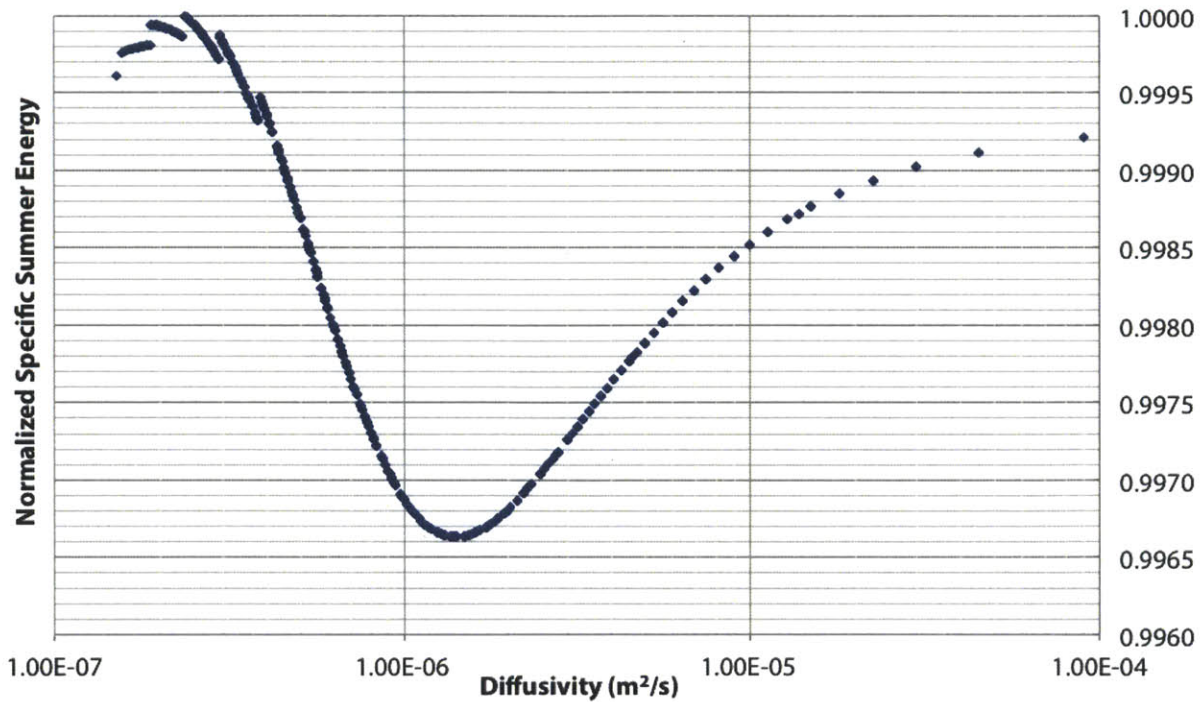


Figure 6-29 Inset of Specific Summer Energy Consumption ( $J/m^3$ ) vs Diffusivity ( $m^2/s$ ), Miami, FL

### 6.3.3 Discussion

The above results indicate that while one-dimensional transient heat transfer assumptions apply, passive thermal mass provides little energy saving benefit in many climate zones. Only San Francisco, CA of the four climates discussed had significant energy savings due to thermal mass performance, and the results of these experiments indicated that this quantity varies widely should conductivity and thickness not be optimized. The results have indicated for all climates points at which additional conductivity and wall thickness will be detrimental for thermal mass performance, indicating that in many climates there are optimum construction points with respect to these properties. In climates where thermal mass will perform effectively, these values and the principles behind them could be transferred to the design phase.

It should also be noted that, even where thermal mass does not provide a percentage savings in energy, it has been shown by the overlap of many of the curves that one may be able to achieve the same energy performance as low-mass construction by using either higher conductivities or less wall material. There is an opportunity for future work capitalizing on the potential for material reduction, reduced insulation, and/or initial cost benefits without sacrificing energy performance. These may in turn have sustainability impacts that extend beyond energy performance when considering the life-cycle assessment.

Finally, regardless of the annual performance of thermal mass, there are seasonal variations of thermal mass performance that can result in high mass performance. The result is increased savings in the off-peak season and a decrease in performance during the peak season. These seasonal variations must be analyzed closely, however, to ensure that increases do not occur in the peak season such as those observed in Miami.

## **6.4 National Results**

It becomes apparent in the study of the climates above that different climate types have different benefits from thermal mass. This section will generalize those results to the United States as a whole.

### **6.4.1 Comparison of Normalized Energy Consumption**

The normalized energy consumption curves were presented for four climates previously, and mention has been made that the ranges of their maximum values are similar across these few climates. This is, in fact, a trend that is more ubiquitous across the United States. Figure 6-30 presents the results for the 0.9 W/m-K conductivity and 0.15 m thick wall construction that have been analyzed throughout this chapter. As this figure indicates, the diffusivity at which maximum energy consumption occurs is relatively climate insensitive. In other words, for a given conductivity and thickness of construction, the construction weight of maximum energy consumption remains constant across most climates, with the exception of climates such as Miami where thermal mass is undesirable. It also suggests that there is an absolute cutoff value beyond which no thermal mass effects will be observed in the climates of interest.



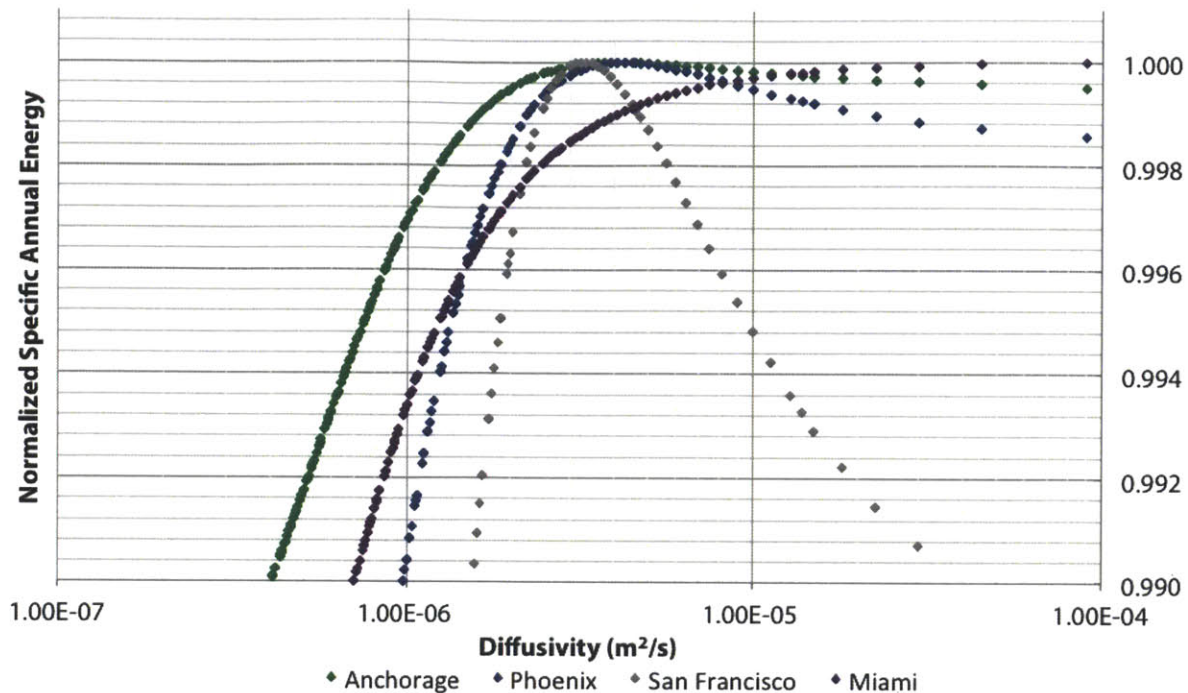


Figure 6-30 Comparison of Normalized Energy Consumption for Multiple Climates for a conductivity of 0.9 W/m-K and a thickness of 0.15 m

## 6.4.2 Mapping the Results

The first set of maps is shown in Figure 6-31 through Figure 6-33 indicating the annual, summer, and winter energy saving potential. On these figures, climates with greater than 5% energy savings have been highlighted in green. As the figures indicate, on an annual scale, thermal mass effects appear to be strongest along the coast of California, with parts of the southeast, southwest, and west also showing impacts. The smallest annual performance gain of thermal mass is located in the northeast, Alaska, Hawaii, and very extreme climates in the southern U.S. The summer impact of thermal mass is excellent for most of the northern United States, while the winter impact of thermal mass is best in the southern United States. This reinforces the notion that passive thermal mass performs better in off-peak seasons.

Looking at Figure 6-34, one can see that there are three different types of behavior observed. It appears that hot, humid climates generally have no observed maximum, whereas many other southern climates have asymptotic behavior instead of a clear maximum. Temperate climates, on the other hand, have a singular value at which maximum thermal mass potential is observed. Interestingly, it appears that the climates with the best thermal mass energy savings either obtained their optimum at a low conductivity or have excellent values at low conductivities. For instance, San Francisco peaks at a wall conductivity of 0.4 W/m-K, while Los Angeles and San Diego exceed 20% potential energy reduction by 0.3 W/m-K

and 0.4 W/m-K, respectively. This implies that these climates are excellent candidates for thermal mass construction because they take advantage of the combined effects of insulation and thermal storage.

Looking at the optimum thickness map for the 0.9 W/m-K wall in Figure 6-35, one notices that the maximum wall thickness rarely achieves the optimum thermal mass performance. In fact, the values indicated on this graph are the absolute maxima, but many of these climates achieve little additional benefit from increasing the wall section past a certain point, as shown in the individual case studies in Section 6.3.1. Therefore, this information indicates that the optimum wall thickness, as well as the optimum conductivity, can exist for a particular construction in a particular climate.

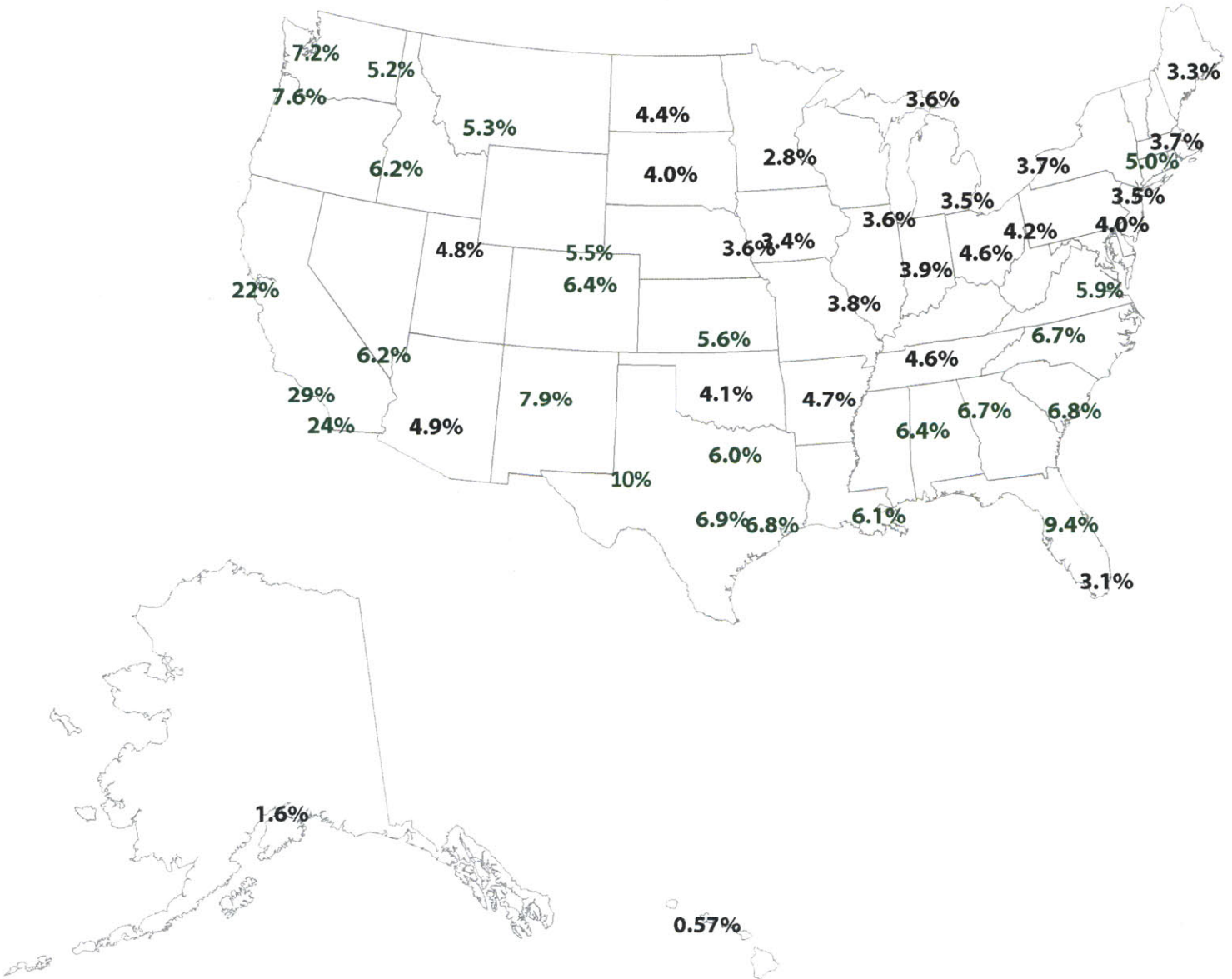


Figure 6-31 Annual Thermal Mass Impact Map, percent optimization for 0.9 W/m-K and 0.15 m wall based on 30,000 of 132,500 data points for residential construction in the United States

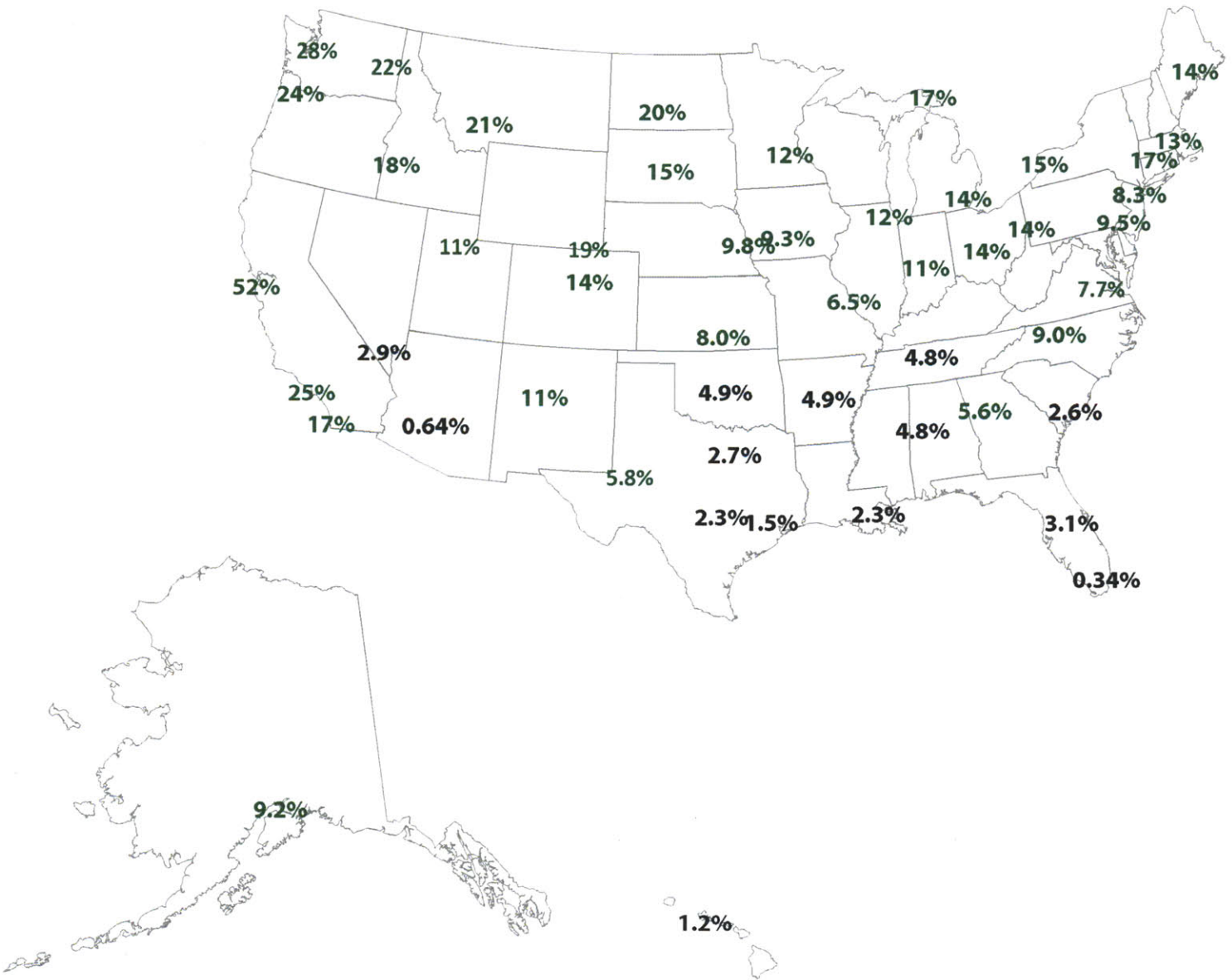


Figure 6-32 Summer Thermal Mass Impact Map, percent optimization for 0.9 W/m-K and 0.15 m wall based on 30,000 of 132,500 data points for residential construction in the United States

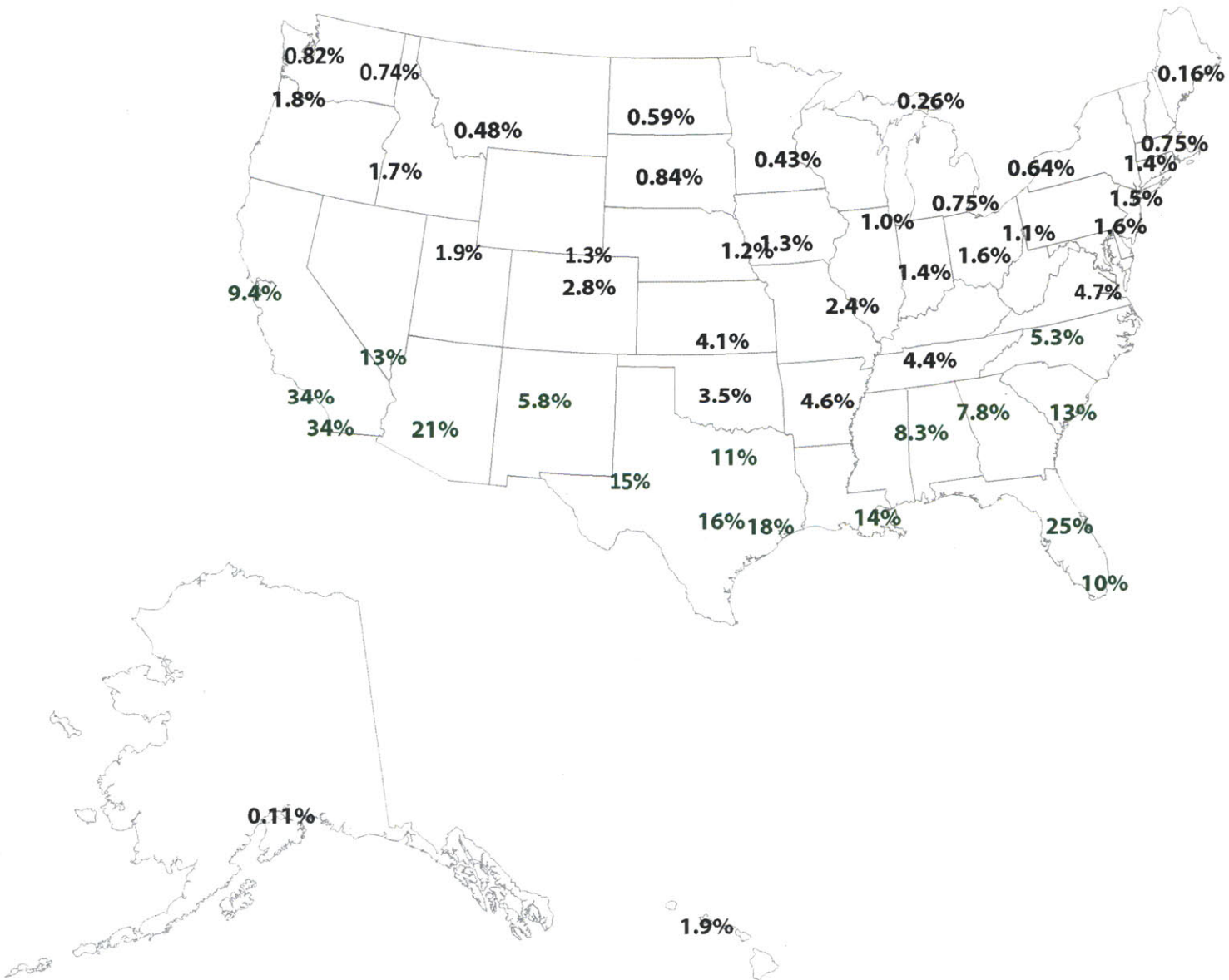


Figure 6-33 Winter Thermal Mass Impact Map, percent optimization for 0.9 W/m-K and 0.15 m wall based on 30,000 of 132,500 data points for residential construction in the United States

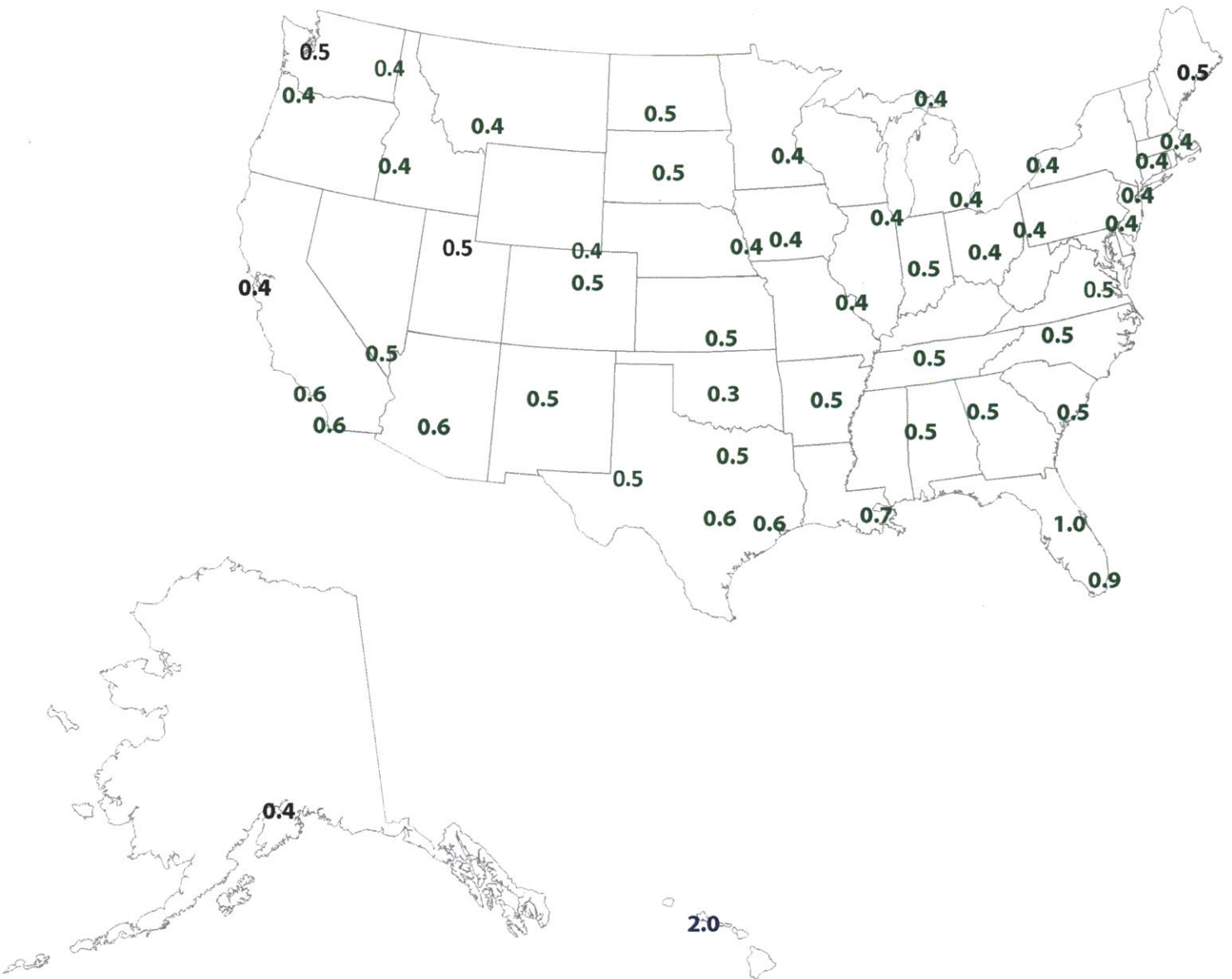


Figure 6-34 Optimum Conductivity (W/m-K) for 0.15 m wall (green locations asymptotic, blue locations increase without bound) based on 51,000 of 132,500 data points for residential construction in the United States



## 6.5 Chapter Summary

This chapter has presented an investigation of the thermal mass impacts of wall constructions for fifty United States climates. The discussion has primarily illuminated the quantitative nature of thermal mass performance, in line with the second research question. The results show that thermal mass does not perform equally in all climates and that, in some climates, it is undesirable to use high-mass wall constructions. Also, it demonstrates that thermal mass impacts are seasonal, with the best results obtained in the off-peak seasons. The results of the diffusivity experiments indicate that thermal mass performance, conductivity, and wall thickness can potentially be mutually optimized with respect to the design of a wall section to provide the best thermal mass performance for a given set of conditions. This result answers the third research question regarding optimization of material properties for thermal mass. Note that the values here are indicative only of the fixed conditions assumed in this experiment, but that values could be generated for any set of fixed parameters. In the end, the research provides a birds-eye view of the benefits of thermal mass and its potential for energy savings in the United States. The next chapter will provide the analogous investigation for the thermal mass impact of slabs as a point of comparison, to demonstrate which constructions perform better in a given climate.



# Chapter 7

## Thermal Mass of Equivalent Slabs

The previous chapter discussed the results of a study of passive thermal mass for wall systems. This section presents the results of a similar simulation experiment conducted on equivalent slabs, to answer the second and third research questions posed in Chapter 1 for the slab problem. That is, throughout the course of this investigation, the quantitative effects of energy storage within an exposed slab will be analyzed through the use of the Cube Model.

### 7.1 Introduction and Experimental Simulation Setup

Just as there is substantial interest in the use of wall sections to provide energy savings, energy storage in slabs is also of great interest to building scientists. This chapter will quantify the effects using the same method of six sub-experiments as the thermal mass studies of walls. The same explanation of the experimental setup discussed in Section 6.2 applies to this investigation, except it is the slab-on-grade parameters varied with the wall parameters constant. Otherwise, the same starting values, ending values, increments, and sub-experiments have been conducted on the slabs to provide a direct comparison between the potential of slabs to store energy versus the potential of walls to store energy.

### 7.2 Local Results

As with the previous chapter, the discussion of thermal mass of slabs will begin at the local scale before moving to the national scale. Case studies will be presented here, as before, to illuminate the key relationships of thermal mass at the individual building scale.

## 7.2.1 Diffusivity

As presented in Chapter 6, diffusivity is a singular value used to measure the thermal performance of a building. It can be interpreted as the ratio of a material's ability to transmit energy to its ability to store energy. The equation for calculating the diffusivity based on the conductivity  $\lambda$ , the mass density  $\rho$ , and the specific heat  $C_p$  of the equivalent construction is recalled:

$$a = \frac{\lambda}{\rho C_p} \quad (7-1)$$

An analysis of the diffusivity of the slab condition shows similar types of relationships to the walls. There are clear curves governing the relationship between density-specific heat and the overall energy performance. These curves are shifted based upon the conductivity and/or wall thickness of the slab. Recall from the setup of the experiment that these equivalent parameters are assumed to account for all insulating conditions and that the results have been generated using the slab preprocessor available with EnergyPlus. This preprocessor is only stable for reasonable material input values, and therefore the values on the extremes of the experiments are not available. The portions unable to be calculated become clear given that the graphs below are printed using the same horizontal axes as those in Chapter 6.

The documentation for ground temperatures for the EnergyPlus engine also indicates that only small temperature differences between indoor temperature and ground temperature should be assumed [25]. The result of this assumption is that, for certain climates, the slab should be more conductive to take advantage of this mild temperature condition, effectively utilizing the thermal mass of the earth itself. Therefore, all results depend on the validity of this preprocessor and on the soil conditions (see Appendix A for complete ground assumptions), which have been left constant for all climates.

### 7.2.1.1 San Francisco, CA - Mild, Marine Climate

San Francisco, CA, a mild climate listed as 3C, will now be analyzed with respect to its slab thermal mass performance [29]. The results for the specific annual energy consumption of a building are presented with respect to diffusivity and conductivity in Figure 7-1. This figure indicates that slabs of higher conductivity result in overall lower energy performance. Note that this is the inverse of the curve presented in Figure 6-1 for wall performance. The curve is reversed due to the impact of ground contact with the model. Considering the 0.9 W/m-K main test slab, the optimization potential of the thermal mass performance is only 4.0%; however, the overlap in energy values among the curves suggests that there is potential to optimize the performance of thermal mass with respect to conductivity in San Francisco. That is, one may be able to achieve same or better energy performance using a higher conductivity, or lower R-value insulation, through the use of mass materials.

Normalizing each conductivity curve with respect to its maximum values, the graph in Figure 7-2 is obtained. This graph indicates that there is little behavior change in thermal mass above a conductivity of 0.4 W/m-K; that is, the curves all overlap with respect to their energy savings, but the different curves still reach different minima for the range tested. The maximum values correspond to diffusivities in the range  $7E-7 \text{ m}^2/\text{s}$  to  $4E-6 \text{ m}^2/\text{s}$ , with the lower conductivities reaching maxima at lower values of diffusivity. This graph indicates that for a reasonable range of conductivities, it is difficult to achieve substantial energy savings.

Graphing the minima of the normalization curves, the information in Figure 7-3 is obtained. This graph indicates that the maximum optimization of the thermal mass of a slab occurs at 0.2 W/m-K, with the energy savings potential due to the thermal mass in the slab declining sharply after this point. This peak value for the 0.15 m thick slab can readily be converted to an R-value of  $0.75 \text{ m}^2\text{-K/W}$  ( $4.26 \text{ hr-ft}^2\text{-}^\circ\text{F/Btu}$ ) [86]. As can be seen in the graph the energy savings reported in Figure 7-1 due to higher conductivities in contact with the mild ground temperatures are not due to thermal mass effects in the slab but rather the impact of the conductivity itself. The peak energy savings from the experiments common to all conductivities is 5.4%. Note that this savings is much lower than the peak energy savings attributed to thermal mass effects in wall systems.

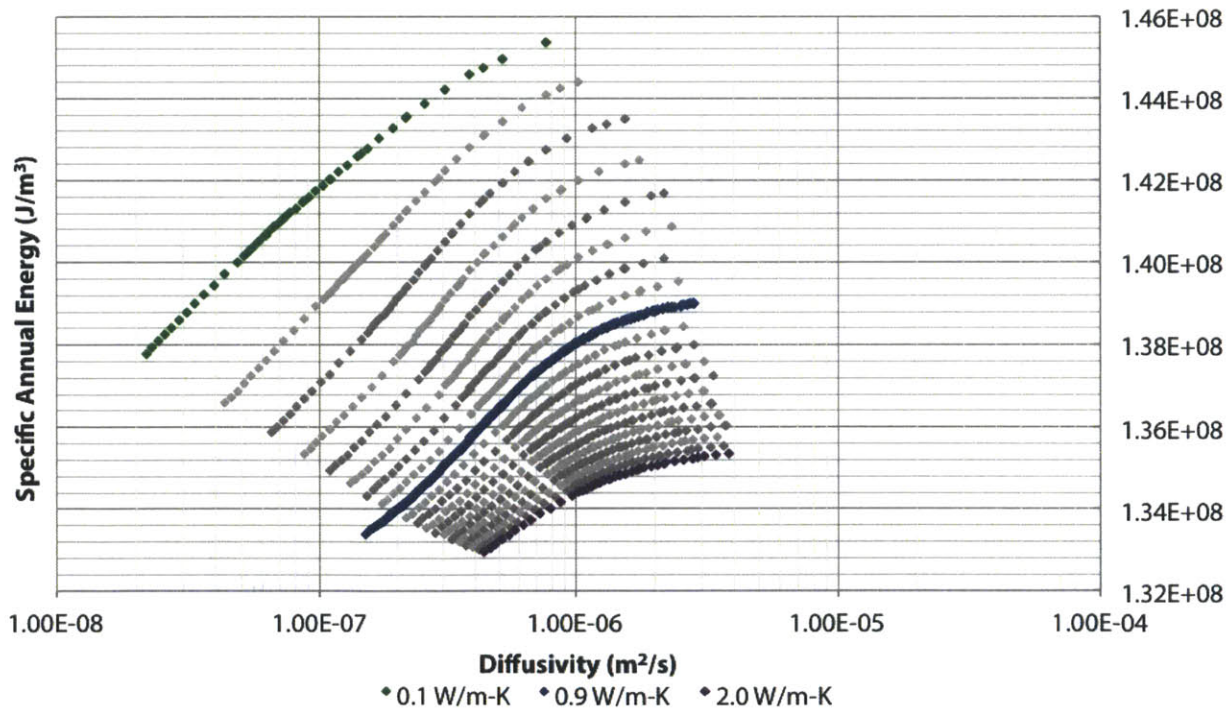


Figure 7-1 Specific Annual Energy Consumption ( $\text{J}/\text{m}^3$ ) vs Diffusivity ( $\text{m}^2/\text{s}$ ) and Conductivity ( $\text{W}/\text{m-K}$ ), San Francisco, CA

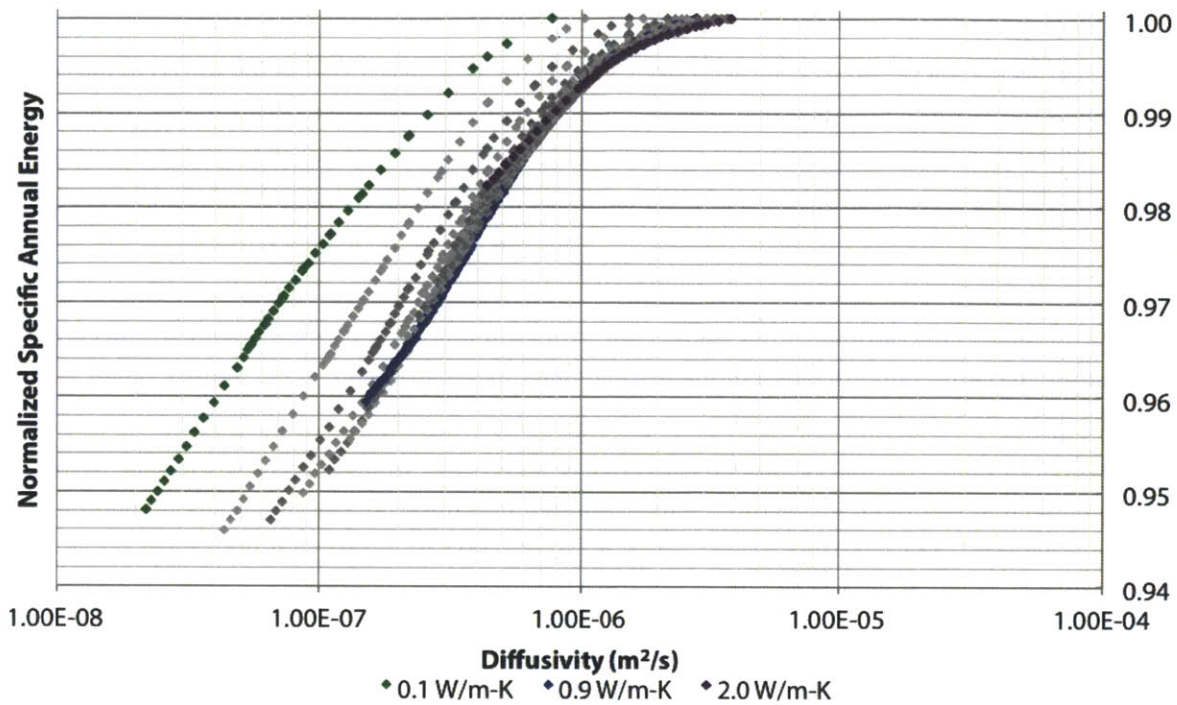


Figure 7-2 Normalized Specific Annual Energy Consumption vs Diffusivity ( $m^2/s$ ) and Conductivity ( $W/m-K$ ), San Francisco, CA

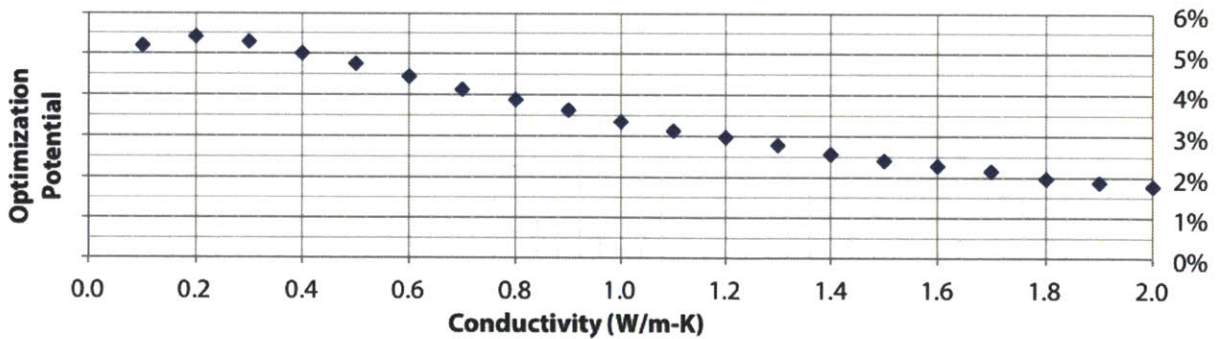


Figure 7-3 Potential Energy Savings from Thermal Mass vs Conductivity ( $W/m-K$ ), San Francisco, CA

Moving to a discussion of the relationship between slab thickness and thermal mass impacts, Figure 7-4 shows the energy consumption for a range of wall thicknesses, densities, and specific heat capacities. The thicker slab curves are all parallel, but interestingly, the curves for slabs 0.15 m and thinner do not align with the pattern. This graph shows potential for thermal mass effects to reduce operational energy when used in thicker, high-mass construction systems. The master curve for the 0.15 m slab indicates an energy-saving potential of 4.0%, with thicker constructions showing greater benefits. However, increasing thickness alone does not always benefit energy consumption; low-mass ground construction assemblies will experience higher energy consumption than their thinner counterparts.

Normalizing the curves with respect to their maxima, Figure 7-5 demonstrates that there is increased thermal mass benefit from increasing the thickness of the slab. Values reach 5.8% energy reduction through the increase of thickness in the slab section. The overlap of the curves indicates that thicker slab constructions all demonstrate roughly the same potential for thermal mass, and therefore it is the conductivity that determines if additional energy is saved through the increased depth of the slab construction. The peak energy use values lie in the small diffusivity range of  $2E-6 \text{ m}^2/\text{s}$  to  $4E-6 \text{ m}^2/\text{s}$ , indicating that for this level of conductivity that ratio of heat transmission to heat storage should be avoided in building construction, as changing the thickness will still result in high energy construction.

Looking at the optimization potential of the various wall thickness curves, presented in Figure 7-6, it becomes clear that thickening the ground construction benefits the thermal mass mechanism up to 0.35 m. Beyond that point, asymptotic behavior is observed and no additional thermal mass energy savings are shown. These results can be converted to an R-value of  $0.389 \text{ m}^2\text{-K/W}$  ( $2.21 \text{ hr-ft}^2\text{-}^\circ\text{F/Btu}$ ) [86]. This graph must be compared with Figure 7-4, which indicates that some change in wall thickness will still impact the overall energy consumption. Given the overlap of the wall thickness curves and the normalization asymptote, there is a range of thicknesses where thermal mass can be used to achieve the same or better performance as low mass construction of a different design, which allows potential benefits in constructability, cost, or preventing pollution and resource depletion.

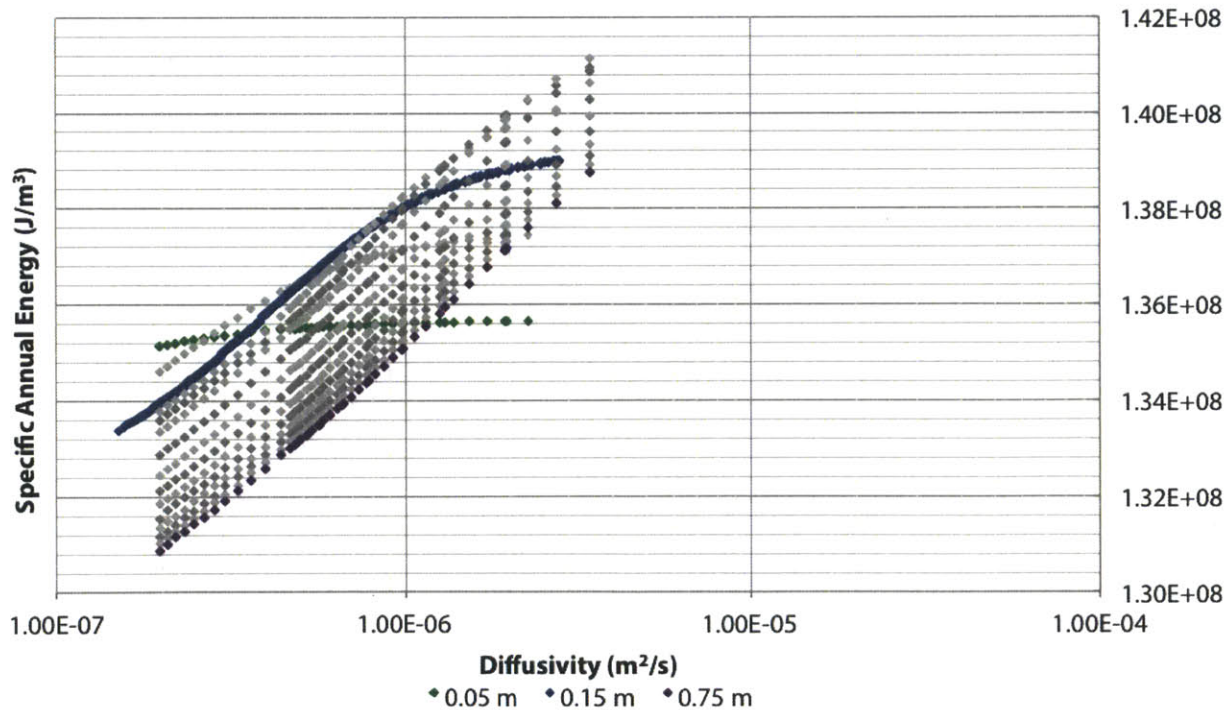


Figure 7-4 Specific Annual Energy Consumption ( $\text{J}/\text{m}^3$ ) vs Diffusivity ( $\text{m}^2/\text{s}$ ) and Slab Thickness (m), San Francisco, CA

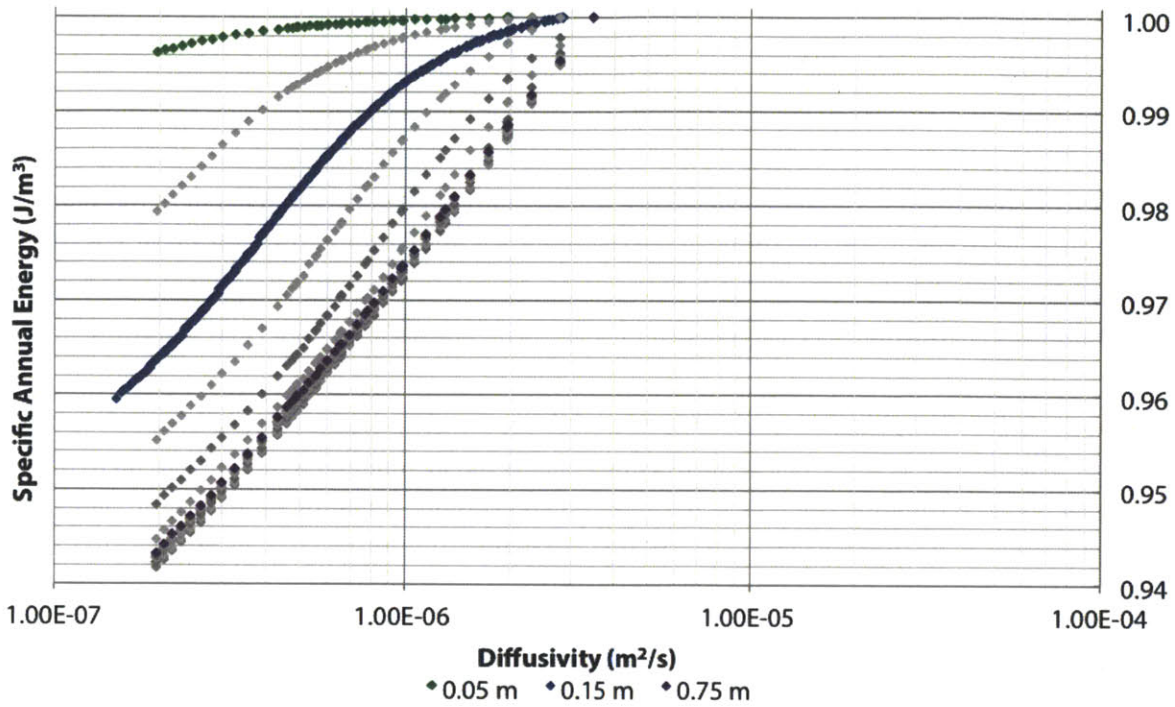


Figure 7-5 Normalized Specific Annual Energy Consumption vs Diffusivity ( $m^2/s$ ) and Slab Thickness (m), San Francisco, CA

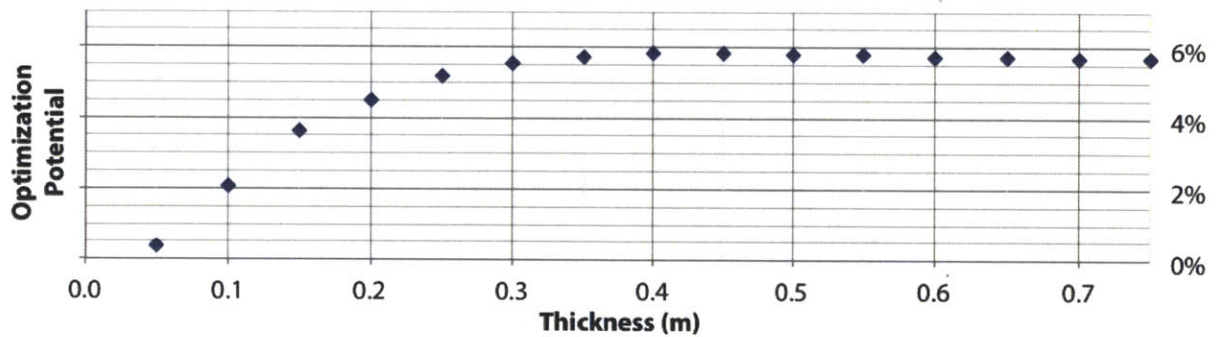


Figure 7-6 Potential Energy Savings from Thermal Mass vs Slab Thickness (m), San Francisco, CA

### 7.2.1.2 Phoenix, AZ - Hot, Dry Climate

The second case study to analyze for its slab performance is Phoenix, AZ, a hot, dry climate designated as 2B [29]. The first relationship to analyze is the relationship between diffusivity, conductivity, and specific energy consumption shown in Figure 7-7. This relationship indicates that there is very little energy savings associated with increasing the mass of the slab for a given thickness. For the 0.9 W/m-K conductivity and 0.15 m thick slab, there is a potential to save 0.9% of the annual energy consumption. Further, there is little overlap in the energy consumption of the curves, indicating that one cannot achieve the same energy performance with high mass materials versus a different conductivity and low mass

materials. In other words, the energy use with respect to slab construction in Phoenix is a function of conductivity, not thermal mass.

Normalizing the energy consumption curves with respect to their maxima, Figure 7-8 indicates that for the slab thickness tested, no value of conductivity improves the thermal mass performance of the slab beyond 1%. The maxima of energy consumption occur at diffusivities of between  $7E-7 \text{ m}^2/\text{s}$  and  $4E-6 \text{ m}^2/\text{s}$  similarly to San Francisco, with lower conductivities peaking at lower values of diffusivity. This leads to the interesting observation that this pattern of peak energy consumption versus diffusivity mirrors the one from the wall thermal mass discussion even though the overall energy consumption versus conductivity graph is the inverse of the one presented for walls (see Figure 6-8). This indicates that, while the relationship of conductivity to energy consumption is sensitive to outside conditions, the relationship between diffusivity and thermal mass potential is relatively insensitive to these fluctuations.

Looking at the graph of the potential optimization with respect to conductivity shown in Figure 7-9, the potential to optimize thermal mass peaks at  $0.3 \text{ W/m-K}$ , which corresponds to an R-value of  $0.5 \text{ m}^2\text{-K/W}$  ( $2.84 \text{ hr-ft}^2\text{-}^\circ\text{F/Btu}$ ) [86]. The trend shows that as conductivity increases, the ability of thermal mass in the slab construction to be optimized decreases by a factor of two. It is important to recall that for the ground conditions tested, the overall potential is quite low in Phoenix. Therefore, while the conductivity-driven thermal mass curve indicates a particular conductivity, the overall energy results presented in Figure 7-7 suggest that higher conductivities would result in lower energy consumption.

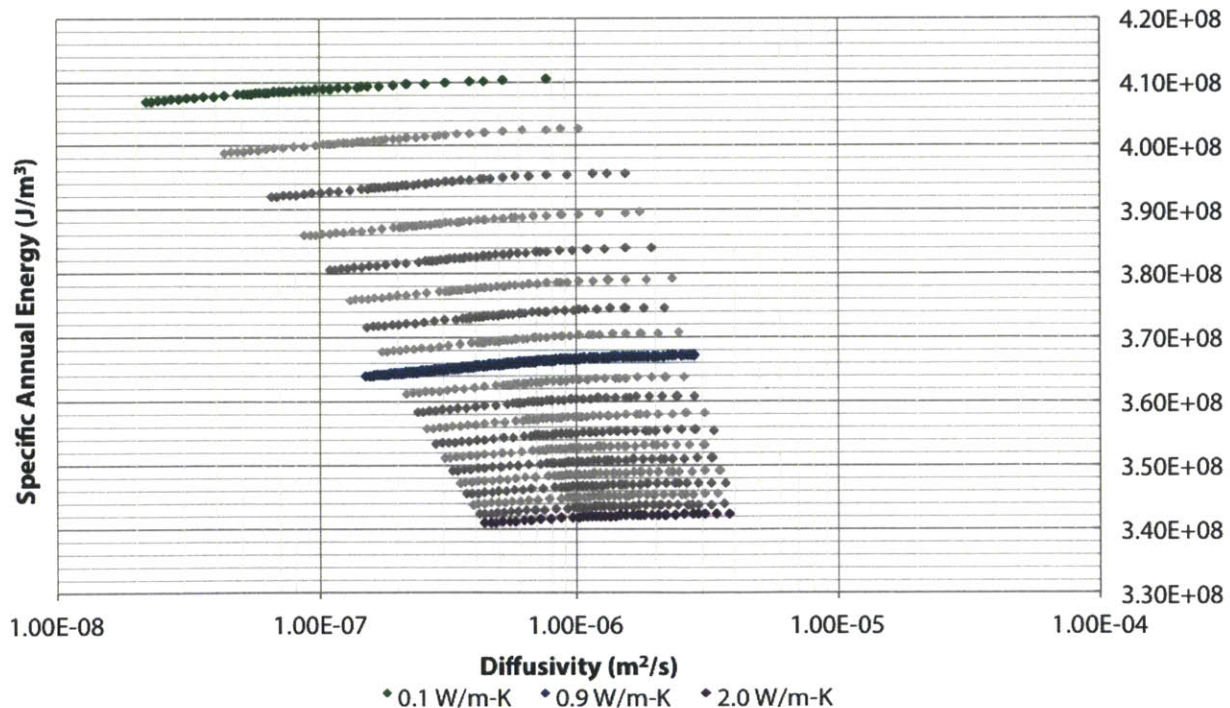


Figure 7-7 Specific Annual Energy Consumption ( $\text{J/m}^3$ ) vs Diffusivity ( $\text{m}^2/\text{s}$ ) and Conductivity ( $\text{W/m-K}$ ), Phoenix, AZ

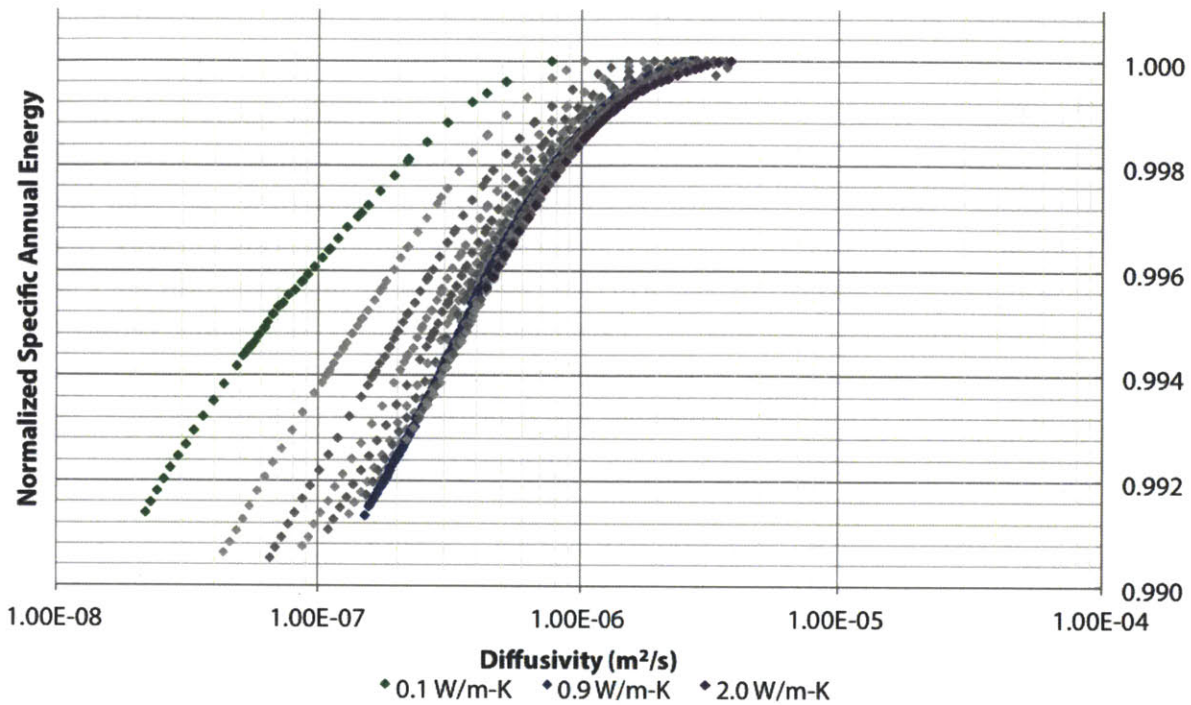


Figure 7-8 Normalized Specific Annual Energy Consumption vs Diffusivity ( $m^2/s$ ) and Conductivity ( $W/m-K$ ), Phoenix, AZ

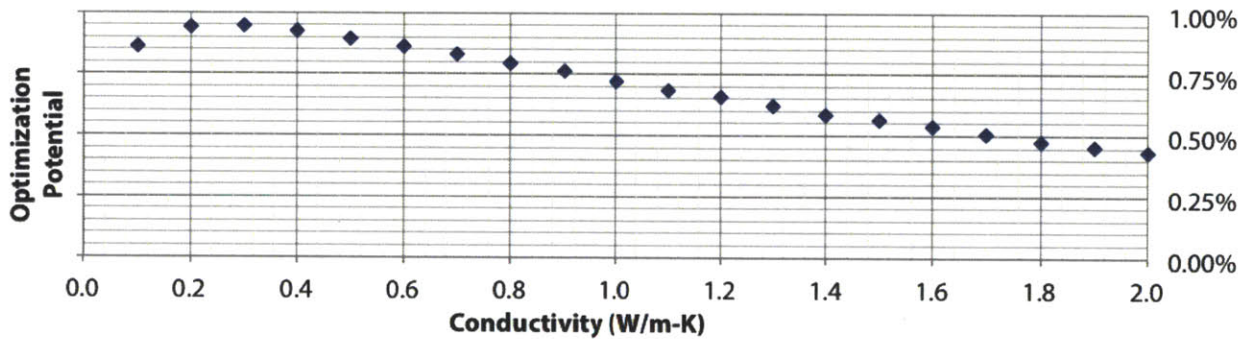


Figure 7-9 Potential Energy Savings from Thermal Mass vs Conductivity ( $W/m-K$ ), Phoenix, AZ

Looking instead at the relationship between thermal mass and material thickness, there is a clear trend shown in Figure 7-10 that thicker slab materials have worse energy consumption in Phoenix. This trend is in stark contrast to the trends in San Francisco and in the wall thermal mass data. This would indicate that the same type of information visible in the energy consumption versus conductivity data: the ground conditions calculated are mild enough for them to act as a stabilizing force on the building. This would indicate a potential to consider optimizing the use of the soil mass below the building rather than constructing a thicker slab to reduce energy consumption. Further, increasing the mass of the constructed material above ground also does little to improve energy consumption. Slabs greater than 0.25 m thick are



required for high-mass materials to achieve the same or better energy consumption as their thinner low-mass counterparts.

Normalizing the energy consumption curves for Figure 7-11, it can be seen that for slabs thicker than 0.25 m, roughly the same thermal mass behavior is observed. Peak energy consumption occurs at diffusivities of  $1\text{E-}6\text{ m}^2/\text{s}$  to  $4\text{E-}6\text{ m}^2/\text{s}$ , with maxima occurring at lower diffusivities for thinner slabs. Very thin slabs show much less optimization potential than thicker slabs, but the overall magnitude of the potential for optimization just exceeds 1%. This indicates that increasing slab thickness for the purpose of thermal mass benefits would be unwise, especially in consideration of the results of Figure 7-10. It can be seen that thicker constructions are generally consuming more energy and the impact of thermal mass is relatively minor for this climate.

Finally, the graph of the optimization potential versus wall thickness in Figure 7-12 suggests that there is an asymptotic behavior with respect to improving thermal mass performance for sections thicker than 0.30 m. This thickness corresponds to an R-value of  $0.333\text{ m}^2\text{-K/W}$  ( $1.89\text{ hr-ft}^2\text{-}^\circ\text{F/Btu}$ ) [86]. Beyond this point, thermal mass results do not improve substantially and do not justify additional expense. Especially in consideration of the overall energy consumption, it would be unwise to exceed this value. Finally, noting the increase in energy consumption from thicker slabs, it is unwise to build with thicker slabs than required by structural or code requirements in this climate.

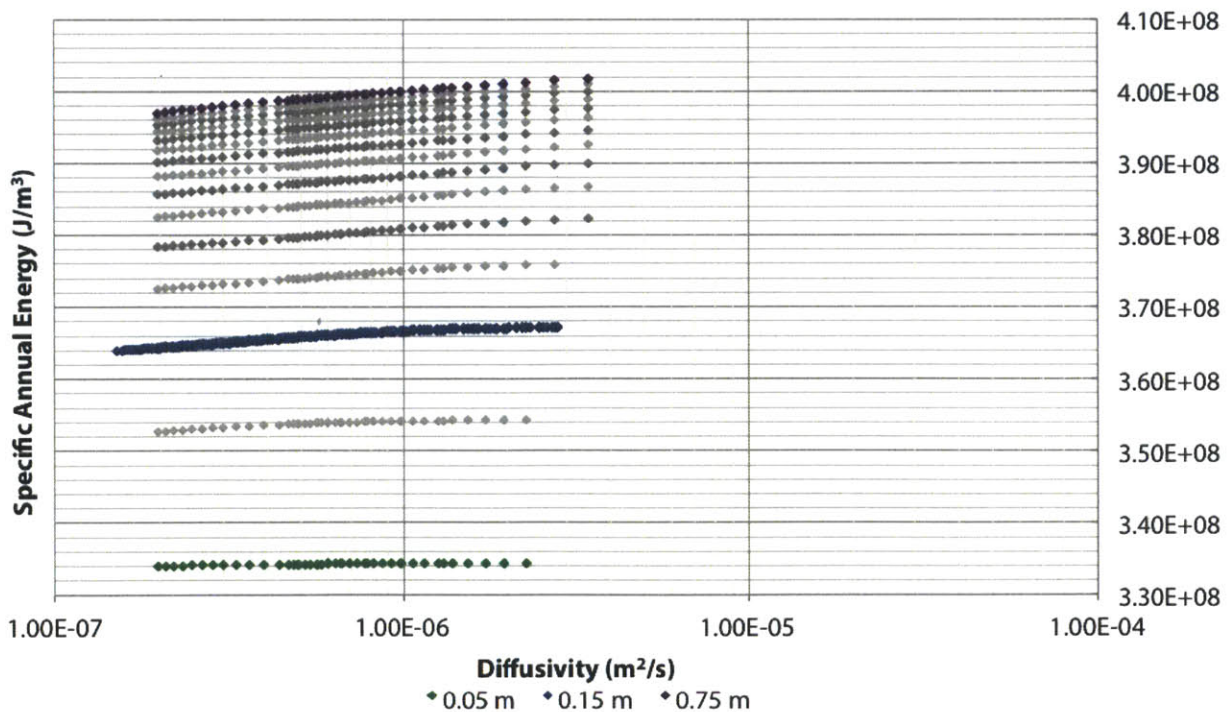


Figure 7-10 Specific Annual Energy Consumption ( $\text{J/m}^3$ ) vs Diffusivity ( $\text{m}^2/\text{s}$ ) and Slab Thickness (m), Phoenix, AZ

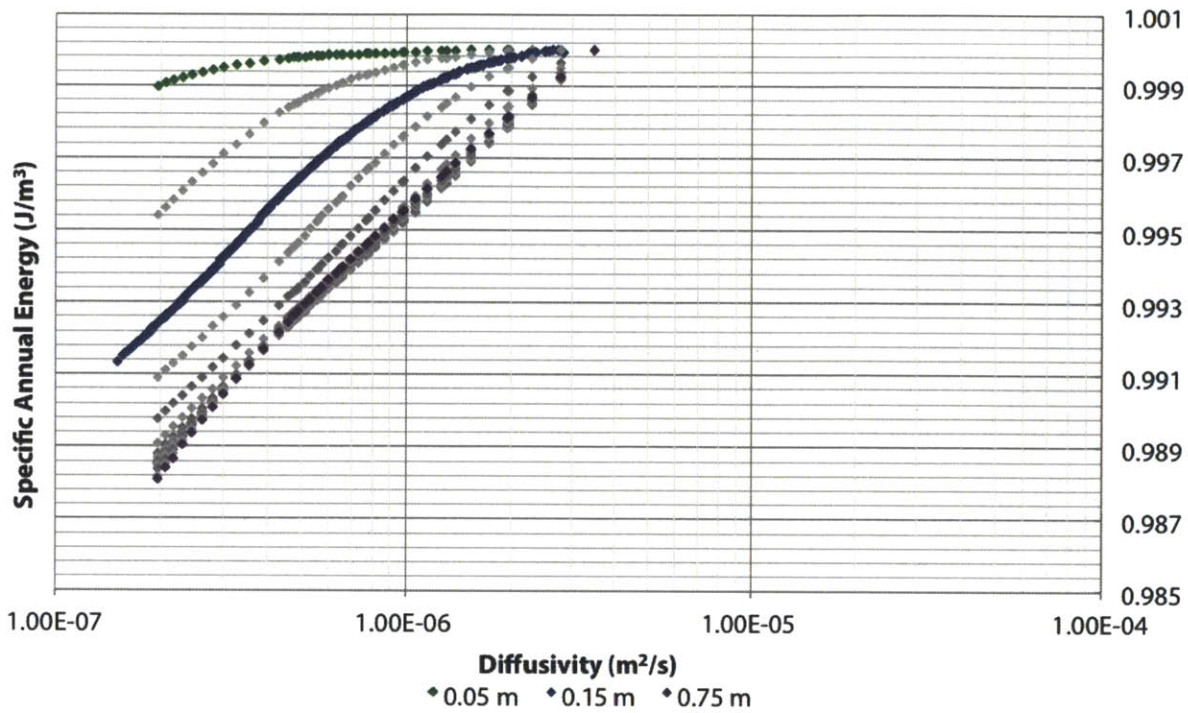


Figure 7-11 Normalized Specific Annual Energy Consumption vs Diffusivity ( $m^2/s$ ) and Slab Thickness (m), Phoenix, AZ

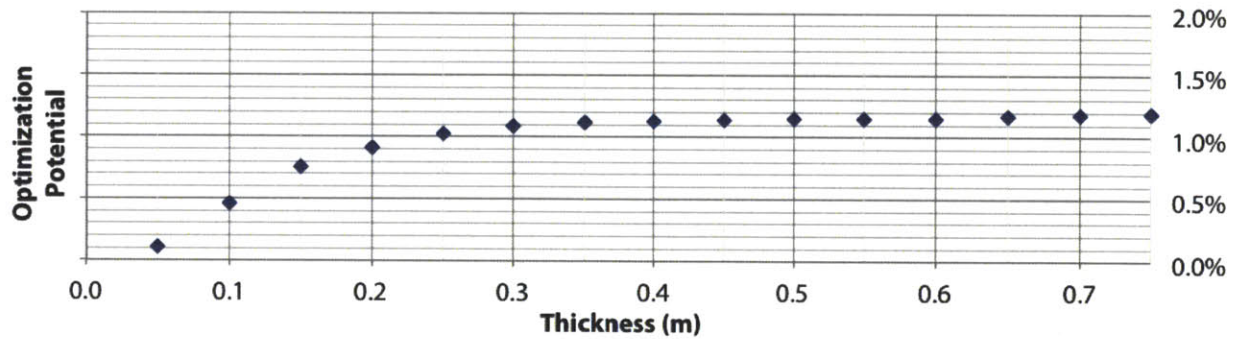


Figure 7-12 Potential Energy Savings from Thermal Mass vs Slab Thickness (m), Phoenix, AZ

### 7.2.1.3 Miami, FL - Hot, Humid Climate

The thermal mass benefit for slab construction in Miami, FL, climate zone 1A, will now be addressed [29]. The graph of the specific energy consumption versus diffusivity is presented for the range of conductivity values in Figure 7-13. The graph indicates that higher conductivities result in lower overall energy consumption of the structure, continuing the trend of strong dependency between slab energy consumption and the EnergyPlus ground temperature assumptions. The energy consumption curves over the range of densities and specific heat values are relatively flat, and there is little overlap between one

value of conductivity and another. For instance, the potential savings for the 0.9 W/m-K and 0.15 m slab is 0.60%. This indicates that it is likely not possible to use thermal mass impacts to achieve the same performance as a slab section with a higher conductivity value. In other words, this graph indicates that energy consumption is primarily conductivity driven in Miami, FL.

Normalizing the energy consumption, the curves in Figure 7-14 indicate that there is very little difference in the behavior of thermal mass past around 0.4 W/m-K. In addition, the curves between 0.9 W/m-K and 2.0 W/m-K are nearly indistinguishable. The normalized energy curves show maximum energy consumption at diffusivities between  $9E-7 \text{ m}^2/\text{s}$  and  $4E-6 \text{ m}^2/\text{s}$ , with the peak energy consumption occurring at lower diffusivities for lower values of thermal conductivity. This graph also indicates that for the range of conductivities tested, there is no ability to optimize thermal mass to an energy savings greater than 1%.

Looking finally at the relationship between optimization potential and thermal conductivity shown in Figure 7-15, it is apparent that higher values of conductivity exhibit lower potential for energy savings due to changes in material weight. The optimum conductivity from this graph is 0.2 W/m-K, corresponding to a slab-section R-value of  $0.75 \text{ m}^2\text{-K/W}$  ( $4.26 \text{ hr}\text{-ft}^2\text{-}^\circ\text{F/Btu}$ ) [86]. However, the results from Figure 7-13 must be recalled in this case; since energy consumption increases with lower conductivity for the assumptions in this model, it would be impractical to optimize thermal mass at the expense of additional energy consumption.

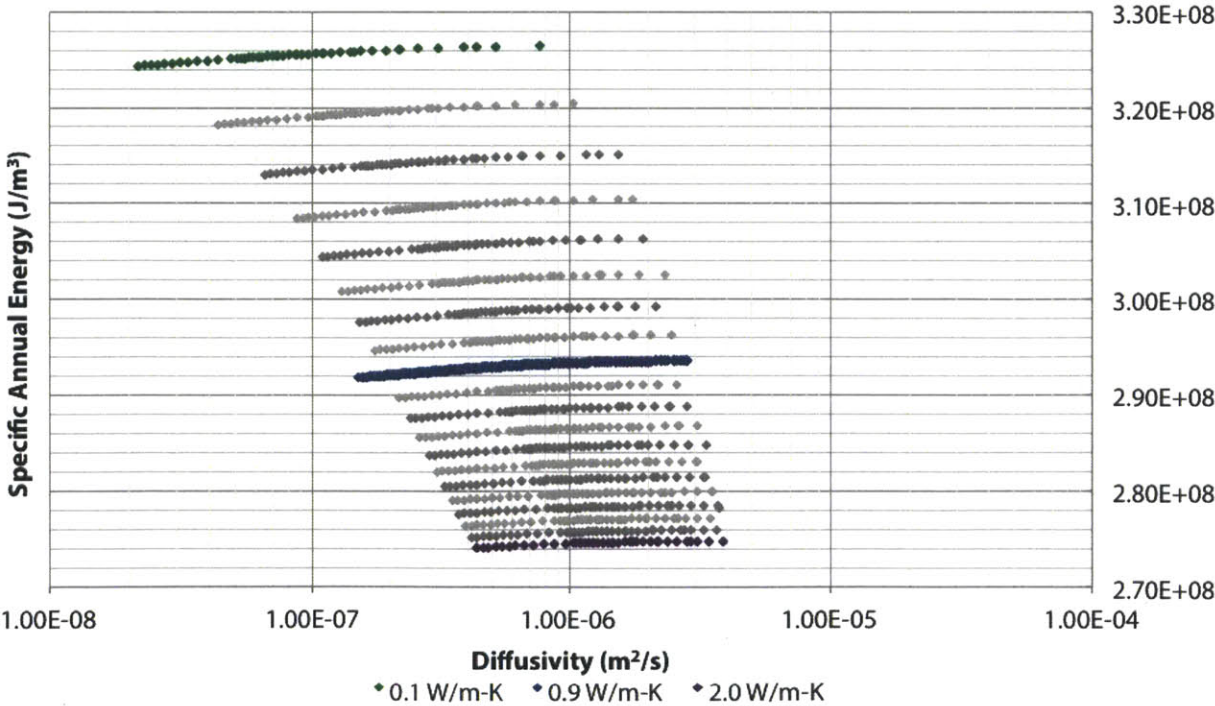


Figure 7-13 Specific Annual Energy Consumption ( $\text{J}/\text{m}^3$ ) vs Diffusivity ( $\text{m}^2/\text{s}$ ) and Conductivity ( $\text{W}/\text{m}\text{-K}$ ), Miami, FL

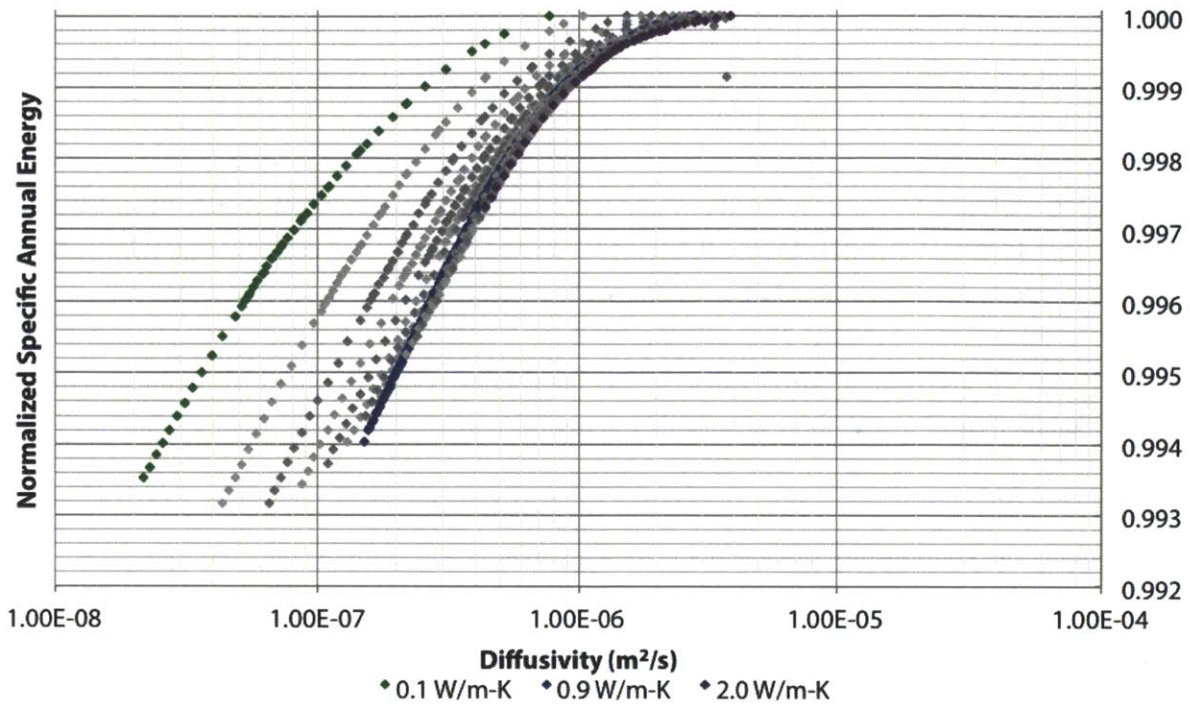


Figure 7-14 Normalized Specific Annual Energy Consumption vs Diffusivity ( $m^2/s$ ) and Conductivity ( $W/m-K$ ), Miami, FL

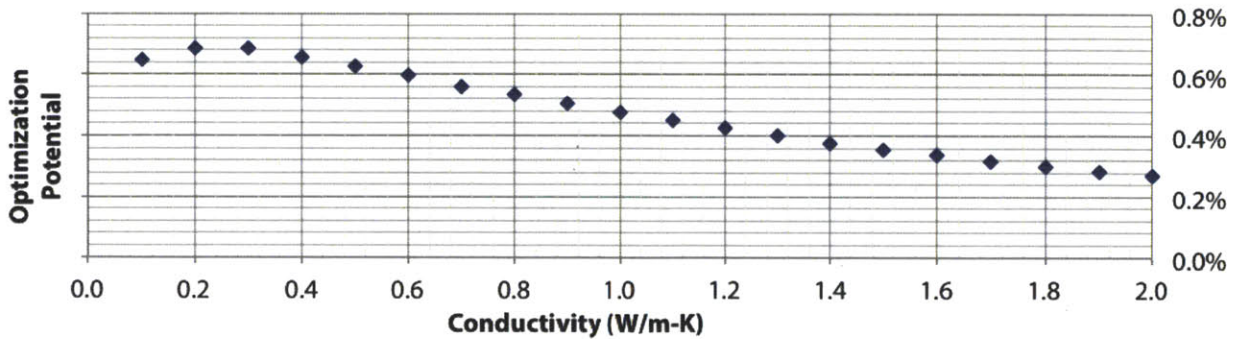


Figure 7-15 Potential Energy Savings from Thermal Mass vs Conductivity ( $W/m-K$ ), Miami, FL

Moving to a discussion of the relationships with respect to material thickness, Figure 7-16 shows that thicker slabs consume more energy than thinner slabs in a hot, humid climate. Also, there is little overlap in the curves until one reaches the performance of the thickest slabs. This means that unless one of these very thick slab constructions is used in the design of the building, there is no opportunity to use thermal mass as a means to achieve the same energy performance as a lower curve value. The thickness results thus concur with the conductivity results, indicating that neither thickness nor conductivity changes allow Miami to be a thermal mass driven climate.

Normalizing the specific energy consumption curves with respect to their maxima, Figure 7-17 shows that thicker slabs do have a greater potential for overall energy savings than thinner slabs, as a result of thermal mass effects. The curves reach their maxima between diffusivities of  $1\text{E-}6 \text{ m}^2/\text{s}$  and  $4\text{E-}6 \text{ m}^2/\text{s}$ , with thinner slabs hitting their maxima at lower values of conductivity. However, noting the quantities on the y-axis it becomes apparent that no increase of thickness can generate more than 1% energy savings in this climate. When considered in combination with the results of Figure 7-16, it becomes apparent that designing a slab for thermal mass optimization in Miami would be unwise from an overall energy consumption standpoint.

Looking at the potential energy consumption savings versus thickness shown in Figure 7-18, it can be seen that the benefit of increasing slab thickness, even from a thermal mass perspective alone, diminishes after around 0.40 m. This presents the clearest picture that optimizing thickness of a construction will not generate better thermal mass results for this climate. When considered along with the overall energy results, the combination of the slim performance of thermal mass and the energy savings generated from using thinner constructions suggest that thickness should also be optimized with respect to energy transmission, not energy storage.

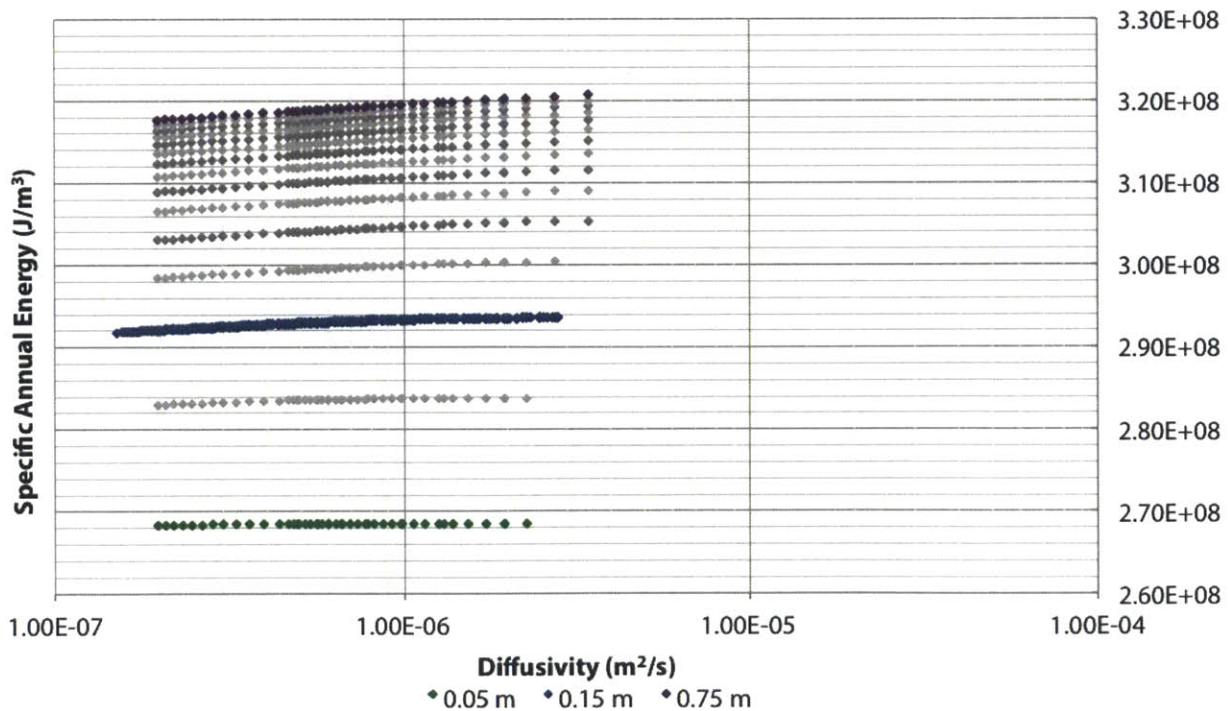


Figure 7-16 Specific Annual Energy Consumption ( $\text{J}/\text{m}^3$ ) vs Diffusivity ( $\text{m}^2/\text{s}$ ) and Slab Thickness (m), Miami, FL

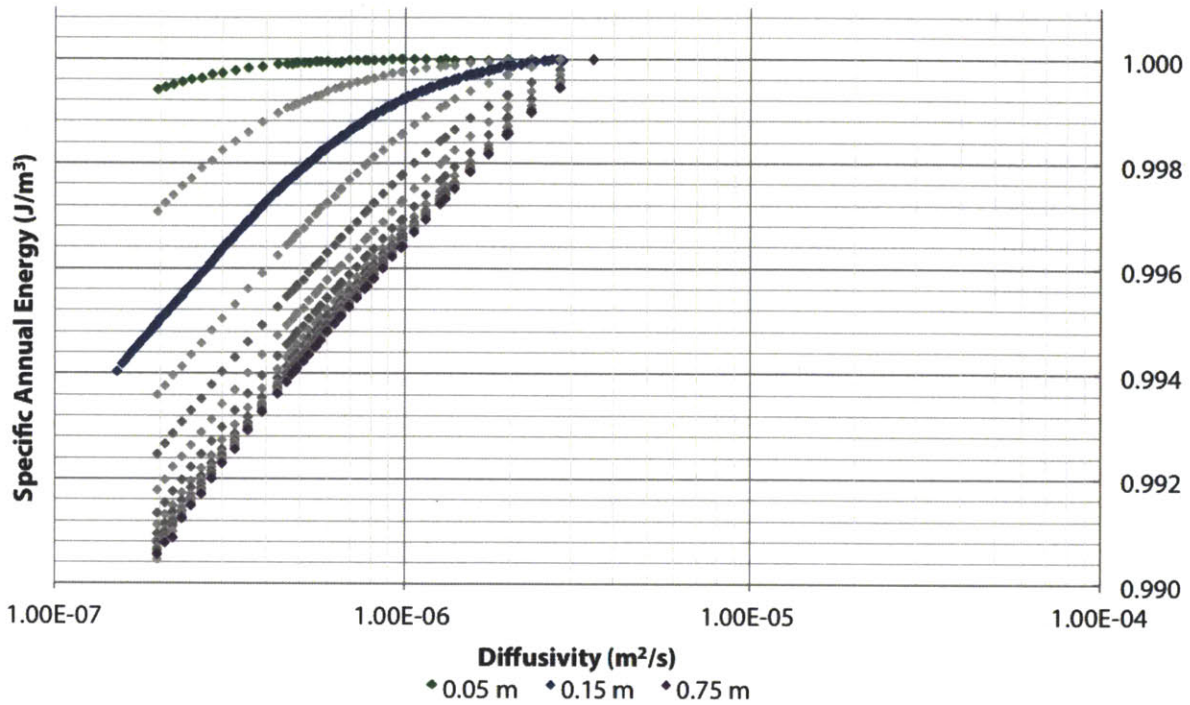


Figure 7-17 Normalized Specific Annual Energy Consumption vs Diffusivity ( $\text{m}^2/\text{s}$ ) and Slab Thickness (m), Miami, FL

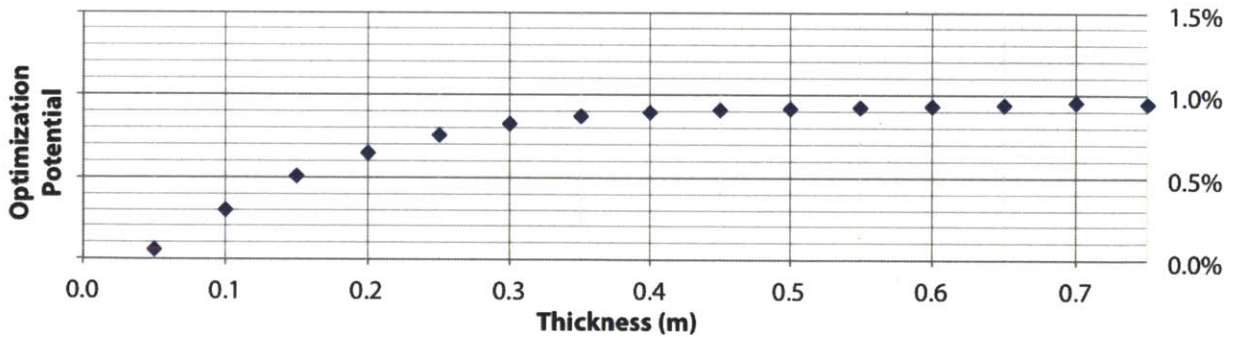


Figure 7-18 Potential Energy Savings from Thermal Mass vs Slab Thickness (m), Miami, FL

#### 7.2.1.4 Anchorage, AK - Cold Climate

The final climate to consider for thermal mass effects in slabs is Anchorage, AK, designated as climate zone 7 by the IECC [29]. The relationship between specific energy consumption, diffusivity, and conductivity is presented in Figure 7-19. The graph indicates that, similar to the assumptions for other slabs, the higher conductivity curves result in lower energy consumption in the system. There are diminishing returns from continuing to optimize conductivity, with the greater gains occurring at the lowest conductivity values. For the  $0.9 \text{ W/m-K}$  and  $0.15 \text{ m}$  master curve, there is a potential energy

savings of 0.30%. Thus for the flat curves in Anchorage, there is little benefit from optimizing thermal mass. Instead it appears that conductivity should be optimized for greater energy savings.

Normalizing the energy consumption for each curve with respect to its maximum, Figure 7-20 demonstrates that the change in energy savings follows the same trend for conductivities above 0.4 W/m-K. The maxima fall in a similar range to the other climates, with diffusivities ranging from  $9E-7$   $m^2/s$  to  $4E-6$   $m^2/s$ . Unlike other climates, the thermal mass performance of lower conductivities appears to be much more effective than higher conductivities. Thus, thermal mass and conductivity are at their respective optima at opposite ends of the conductivity values tested, likely explaining the poor performance of the property in this test.

Viewing the relationship between optimization potential and conductivity shown in Figure 7-21, it is clear that thermal mass performance drops rapidly in a cold climate with the increase in conductivity. In Anchorage, the best potential for thermal mass performance at 0.1 W/m-K, the lowest conductivity tested. While the overall ability to optimize energy performance never exceeds 0.50% in this climate, the trend indicates that thermal mass must be coupled with insulation in order to even reach that value. Still, in the light of the absolute magnitude of the energy savings, the overall resulting performance is rather trivial and conductivity of the slab should be optimized instead.

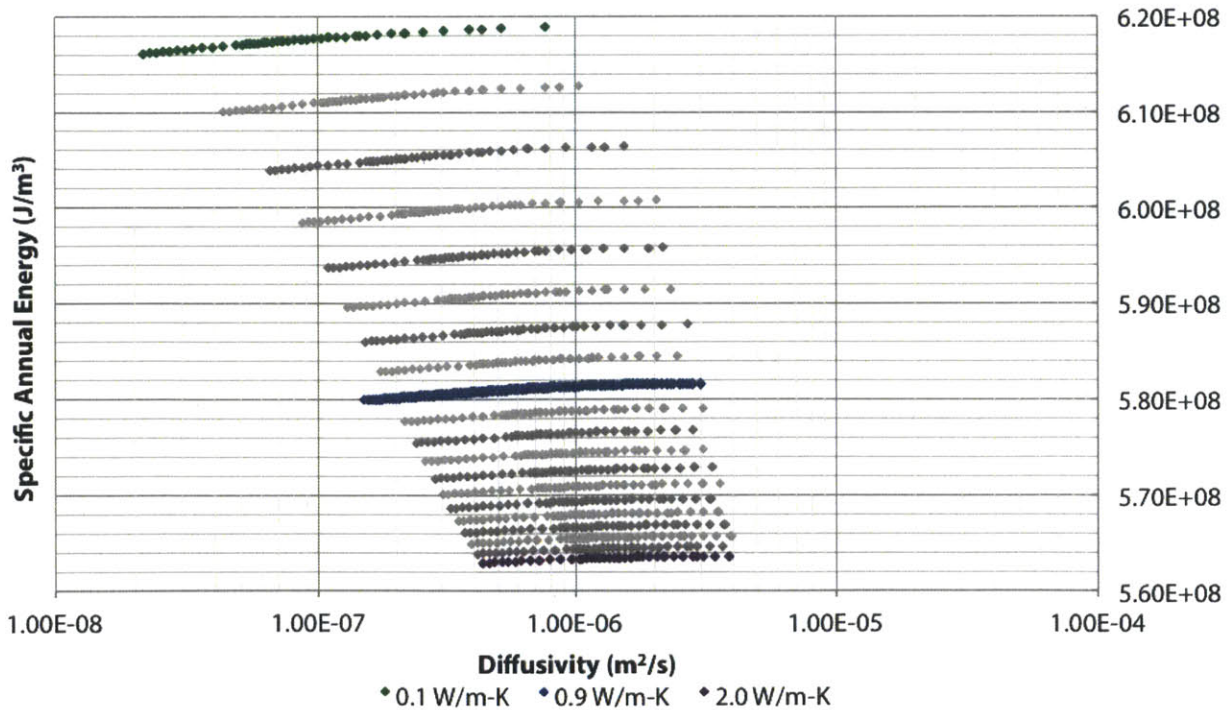


Figure 7-19 Specific Annual Energy Consumption ( $J/m^3$ ) vs Diffusivity ( $m^2/s$ ) and Conductivity (W/m-K), Anchorage, AK

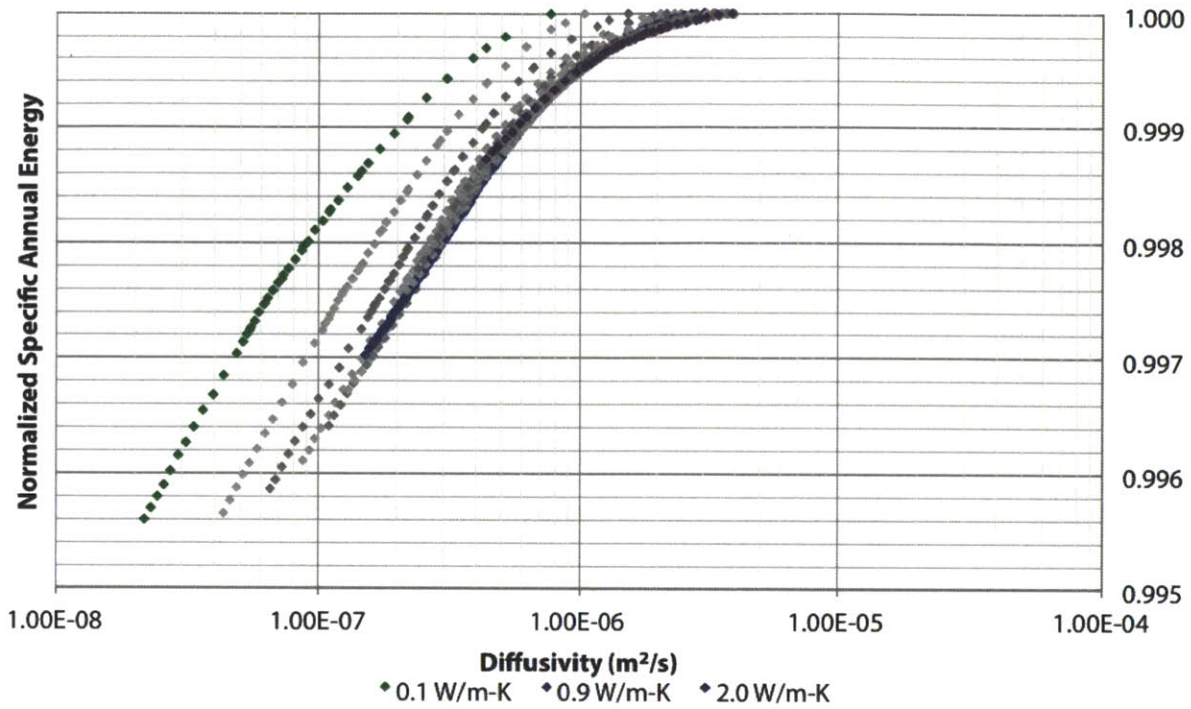


Figure 7-20 Normalized Specific Annual Energy Consumption vs Diffusivity ( $m^2/s$ ) and Conductivity (W/m-K), Anchorage, AK

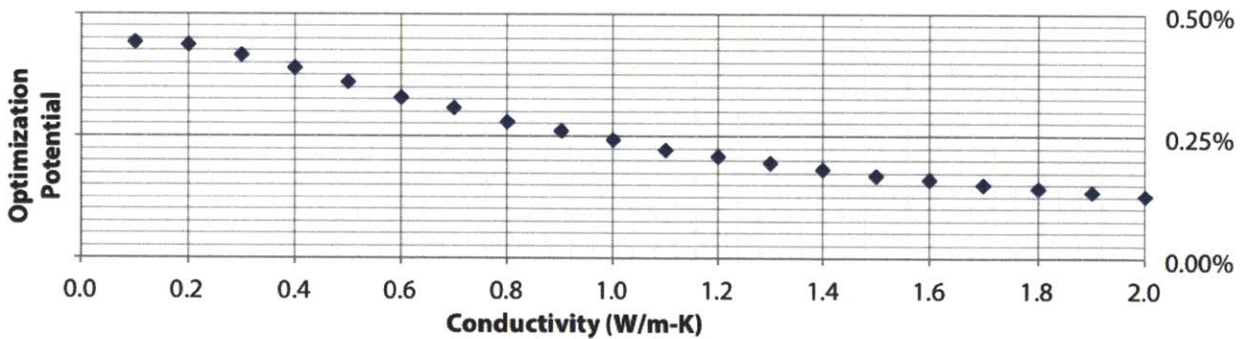


Figure 7-21 Potential Energy Savings from Thermal Mass vs Conductivity (W/m-K), Anchorage, AK

Moving to the relationships between specific annual consumption, diffusivity, and slab thickness, the overall energy consumption results presented in Figure 7-22 demonstrate that thinner slabs result in buildings that consume less energy. The curves representing the thinner slabs are well-spaced, while the curves for the thicker constructions show overlap in energy values. This suggests that for thinner slabs there is no opportunity to optimize thermal mass for equivalent performance of a different slab geometry. In contrast, for thicker slab constructions there is such a potential, allowing building scientists to perform such an optimization if thicker slab-on-grade construction is required for other (i.e. structural) considerations.



Normalizing the energy consumption curves with respect to their maxima, it is apparent from Figure 7-23 that thicker slabs have a greater potential for optimizing thermal mass than thinner slabs, in agreement with the results from other climate types. The maximum energy consumption occurs at diffusivities between  $1\text{E-}6 \text{ m}^2/\text{s}$  and  $4\text{E-}6 \text{ m}^2/\text{s}$ , with the thinner slabs reaching peak energy consumption at lower diffusivities. Finally, unlike many of the other climates studied, there is less overlap in the normalized curves, which indicates that the trends of thermal mass are continually changing for Anchorage.

Finally, studying the optimization potential of the thermal mass component shown in Figure 7-24, one can see that the percentage of energy savings is strictly increasing with slab thickness and does not show any asymptotic behavior. Therefore, in climates like Anchorage the tendency of energy consumption to improve with slab thickness matches the conventional wisdom of using very thick constructions to achieve thermal mass benefits. However, the overall magnitude of energy savings never exceeds 1%, which demonstrates that the energy use of buildings is dominated by slab conductivity as opposed to slab thermal mass in this climate.

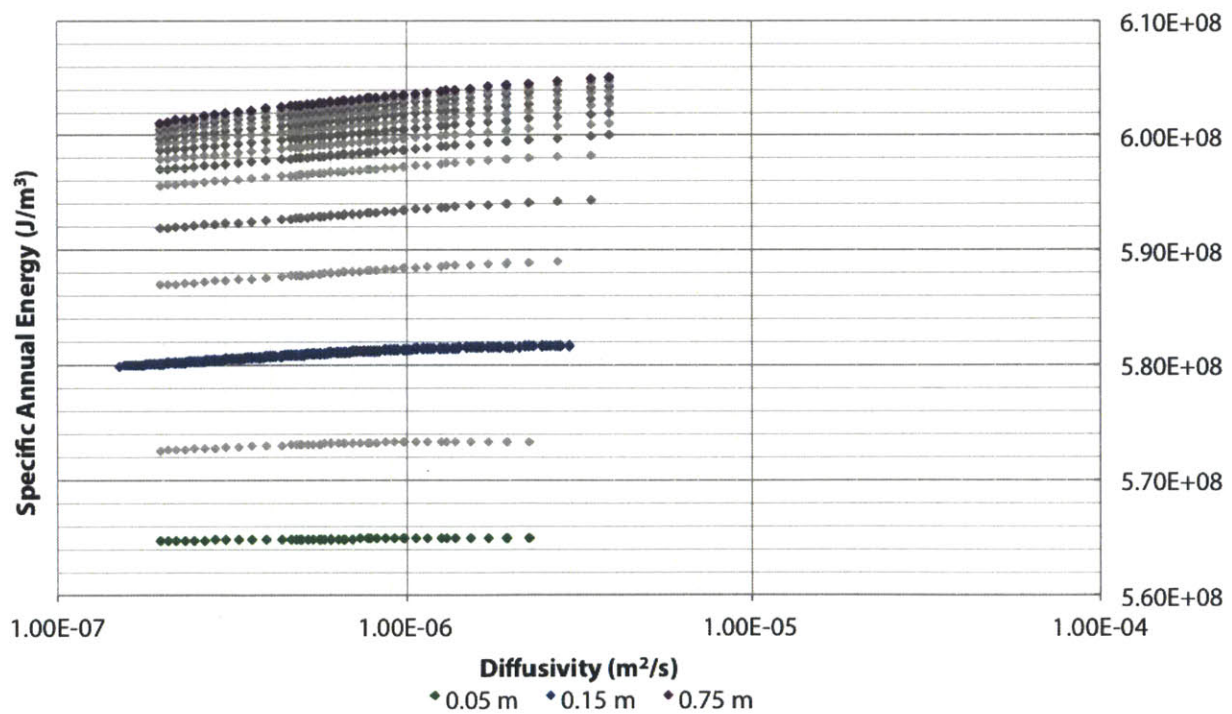


Figure 7-22 Specific Annual Energy Consumption (J/m<sup>3</sup>) vs Diffusivity (m<sup>2</sup>/s) and Slab Thickness (m), Anchorage, AK

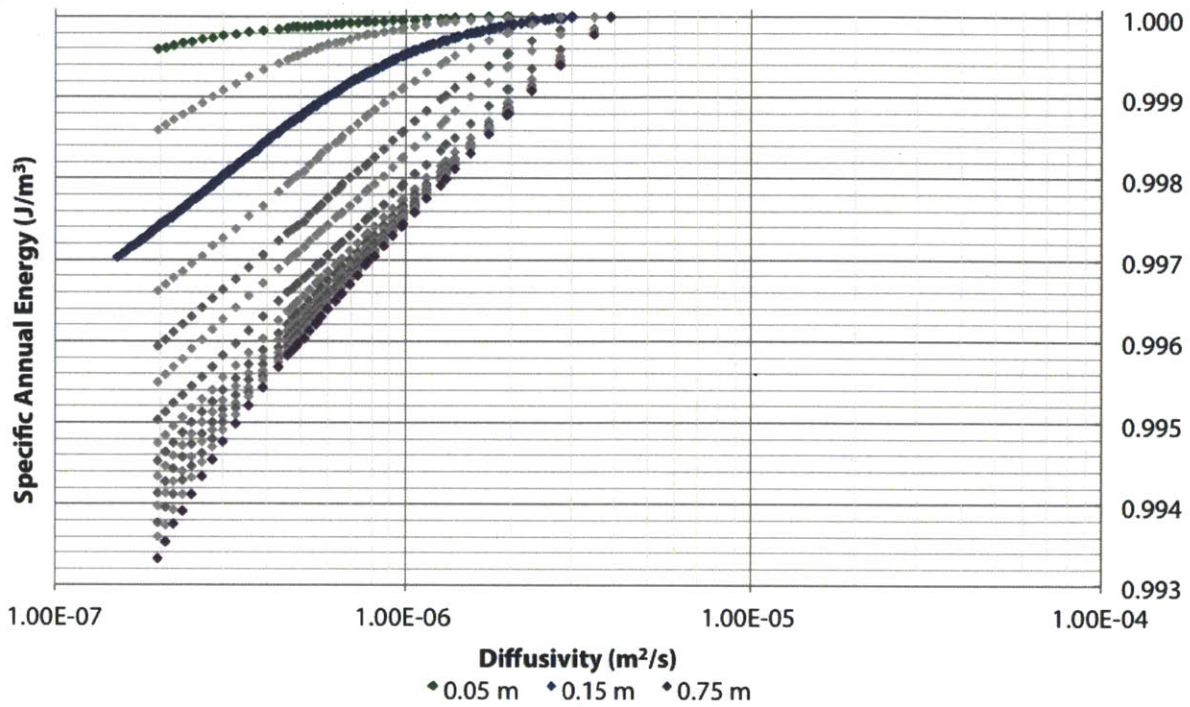


Figure 7-23 Normalized Specific Annual Energy Consumption vs Diffusivity ( $m^2/s$ ) and Slab Thickness (m), Anchorage, AK

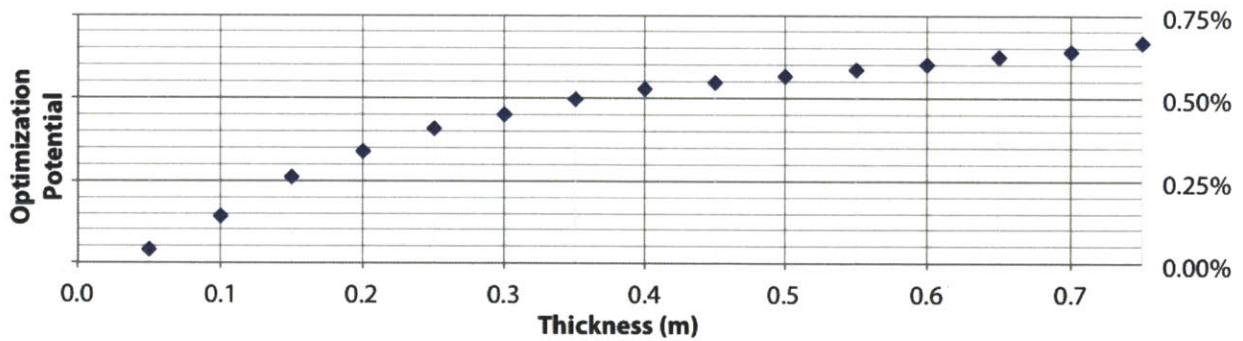


Figure 7-24 Potential Energy Savings from Thermal Mass vs Slab Thickness (m), Anchorage, AK

## 7.2.2 Seasonal Effects of Thermal Mass

At this point, all results presented for the energy consumption of buildings have referenced the annual consumption of buildings as a result of thermal mass changes in the slab. However, since thermal mass is a seasonally dependent phenomenon, this section will reference the diffusivity curve for 0.9 W/m-K and 0.15 m slab construction for the summer, winter, and annual performance. For the purpose of this investigation, summer is considered April through September while winter is considered October through March. The results for the four climates discussed in this chapter are presented in Figure 7-25 through

Figure 7-28. In general, the graphs indicate that summer and winter thermal mass have similar trends but different magnitudes of those trends.

Looking at thermal mass performance of the four climates, only San Francisco shows better summer performance of slab thermal mass. The trends in San Francisco demonstrate that there is excellent summer performance but marginal winter performance. In contrast, Phoenix, Miami, and Anchorage all show better winter performance of the phenomenon. In Phoenix and Miami this is likely due to overheating potentials in these climates. In Anchorage, the thermal mass benefit improves likely because of the contrast between extreme outdoor temperatures, mild under-slab temperatures, and the indoor air temperature. That is, ground contact with mild temperatures has an additional stabilizing effect in this extreme climate.

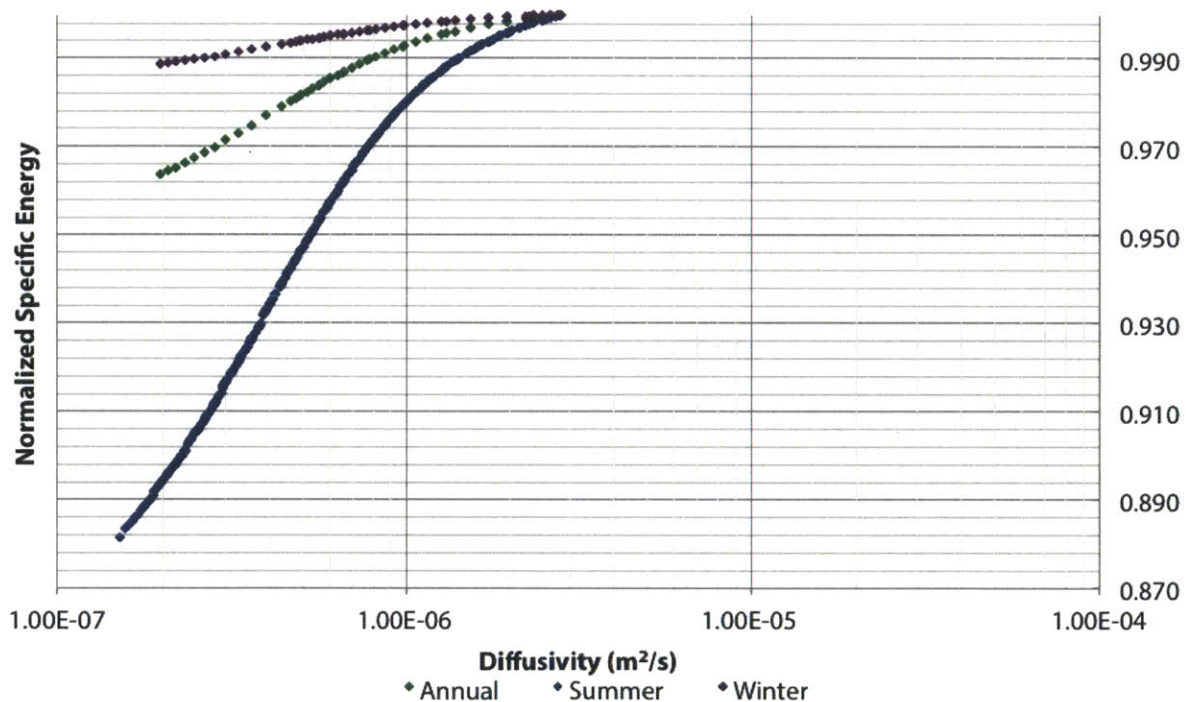


Figure 7-25 Specific Energy Consumption (J/m<sup>3</sup>) vs Diffusivity (m<sup>2</sup>/s) by Season, San Francisco, CA

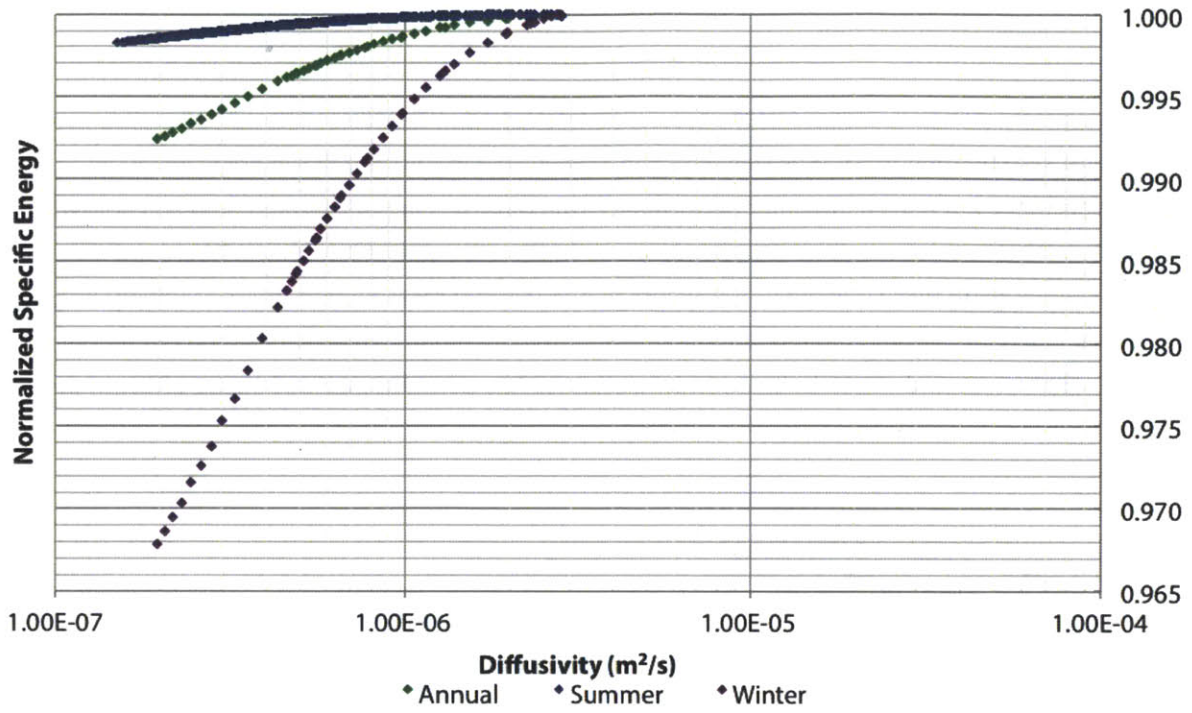


Figure 7-26 Specific Energy Consumption ( $J/m^3$ ) vs Diffusivity ( $m^2/s$ ) by Season, Phoenix, AZ

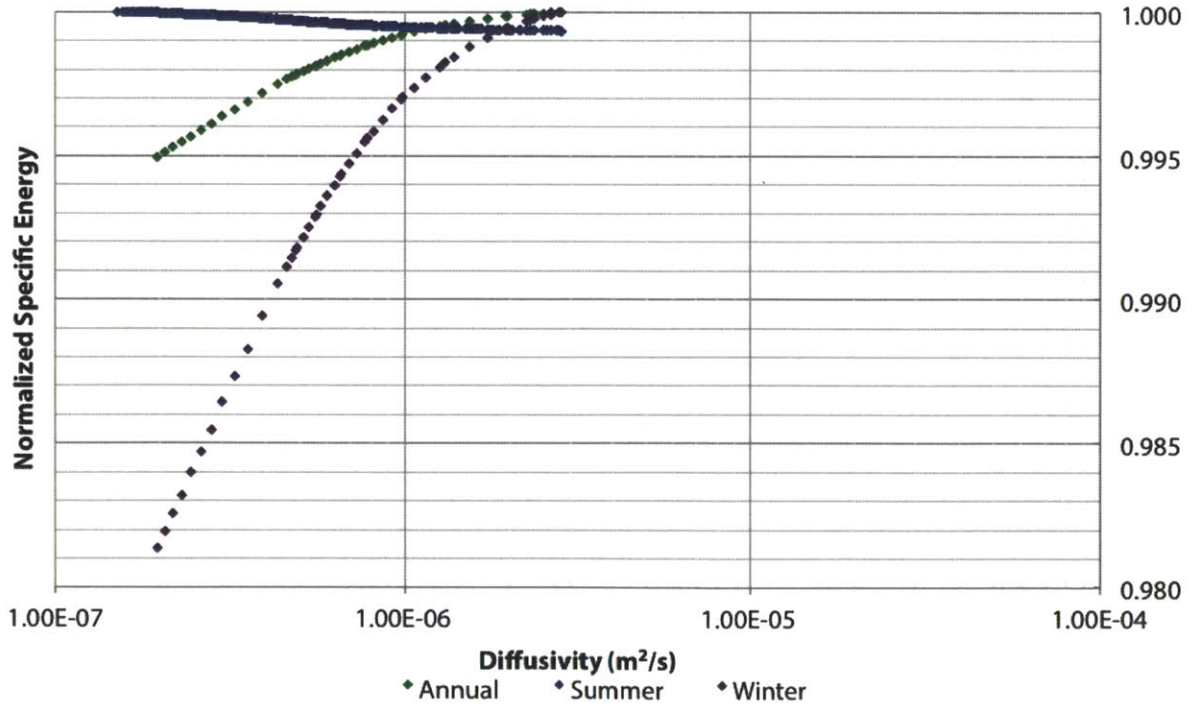


Figure 7-27 Specific Energy Consumption ( $J/m^3$ ) vs Diffusivity ( $m^2/s$ ) by Season, Miami, FL

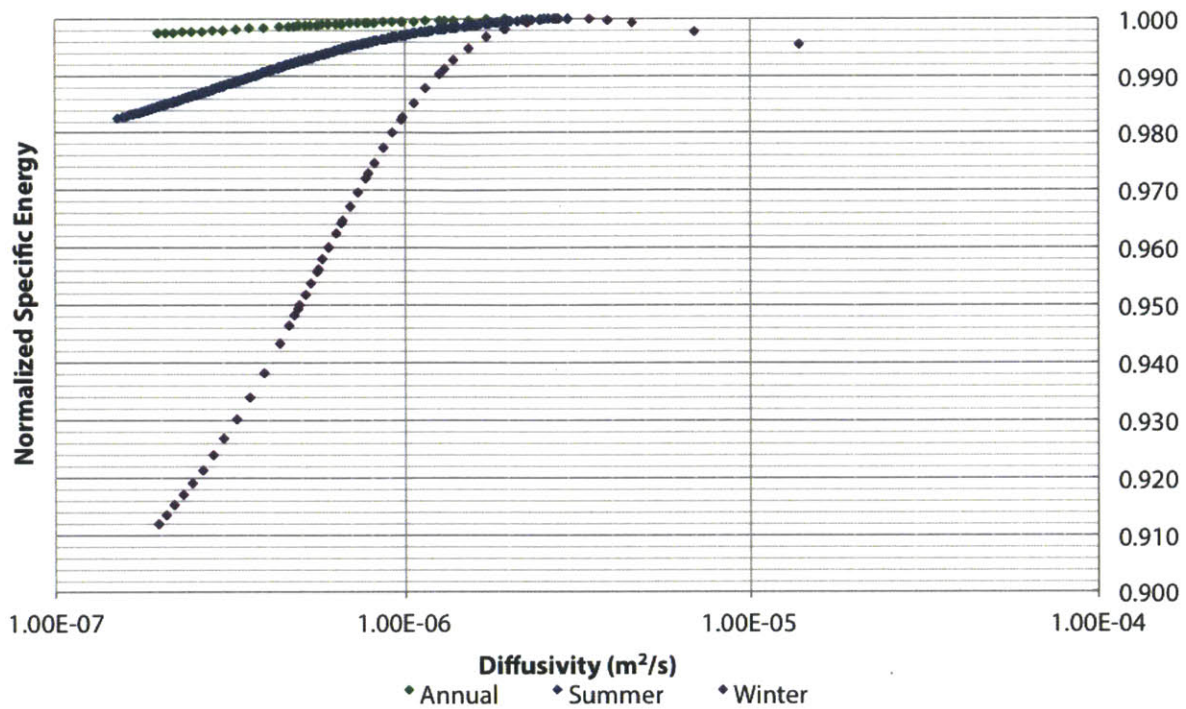


Figure 7-28 Specific Energy Consumption (J/m<sup>3</sup>) vs Diffusivity (m<sup>2</sup>/s) by Season, Anchorage, AK

Looking at the inset of the Miami summer energy consumption curve shown in Figure 7-29, it is clear that increases in material weight have a negative effect on energy consumption. That is, the best energy performance is obtained through the use of the lightest weight slab constructions. This graph clearly demonstrates the inverse effect of storing energy in a cooling climate, where additional energy storage can even hinder the performance of the building. Therefore, these results seem to indicate that slab thermal mass effects in Miami are undesirable due to the predominance of the cooling season on the use of the building.

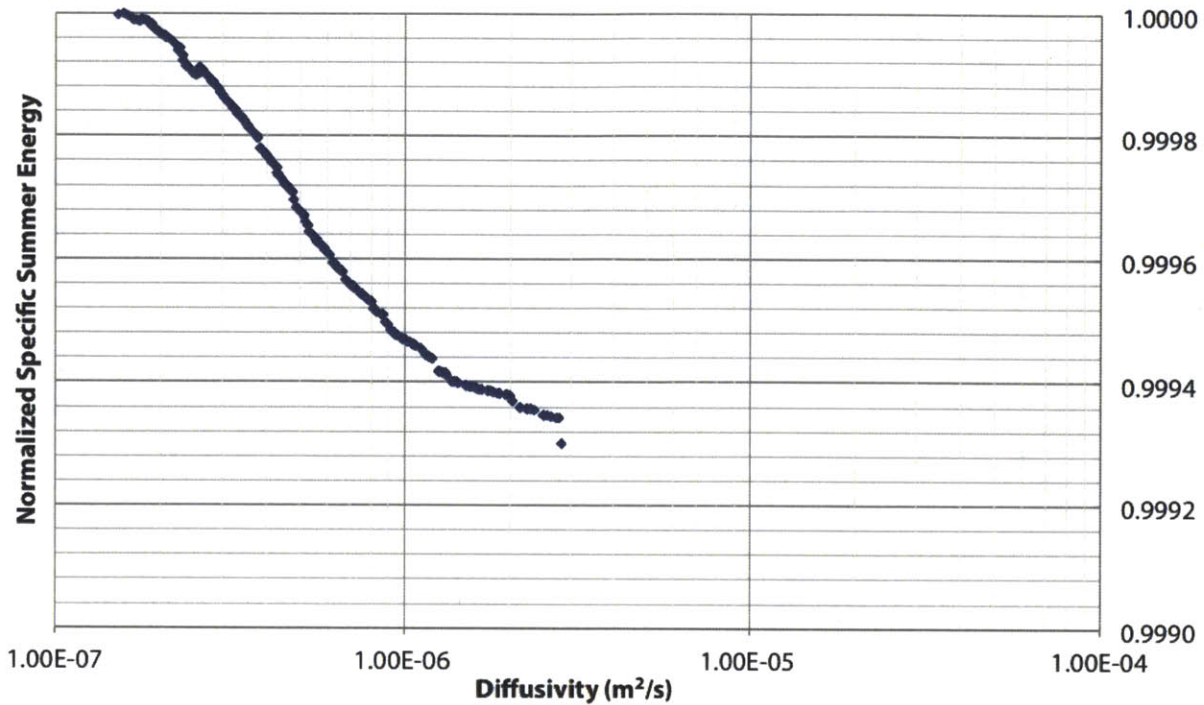


Figure 7-29 Inset of Specific Summer Energy Consumption (J/m<sup>3</sup>) vs Diffusivity (m<sup>2</sup>/s), Miami, FL

### 7.2.3 Discussion

The results for thermal mass performance of slabs indicate that the potential energy savings for the climates studied above are lower than the potential observed in the wall results. It should be noted, however, that these results are also highly assumption dependent. For instance, this model reflects the BAHSP benchmark home which has low percentages of windows. By lowering the available solar radiation to the slab it is possible that the material is not activated to its full capacity. Second, the model is highly dependent on ground assumptions as explained at the beginning of Section 7.2. Most of the materials achieve their optimum thermal mass performance at low conductivities, but the ground assumptions indicated that low conductivities used more energy. The data show an alignment of the aims of conductivity reduction and thermal mass optimization. Finally, seasonal results suggest that winter has stronger thermal mass performance than summer in all climates except San Francisco, CA. This indicates that in Anchorage, there is better thermal mass performance on the peak season and this results in much higher energy savings.

## 7.3 National Results

Moving from the discussion of four climates to the national scale, the remainder of the fifty climate

regions have been analyzed. These results indicate that there are trends both in the normalized consumption of building energy across the United States and in the overall performance of thermal mass by geographic region.

### 7.3.1 Comparison of Normalized Energy Consumption

Throughout the discussion of slab thermal mass in this chapter, the ranges of the maximum normalized energy consumption for the curve have been presented. In Figure 7-30, the graph shows that in three of the climates, there is roughly the same diffusivity at which the maximum value occurs. The hot, humid climate of Miami is the exception to this rule, which suggests that perhaps climates which suffer negative impacts from thermal mass do not exhibit in this trend. Otherwise, these results show that for most climates, the results of maximum energy consumption for a given geometric configuration of a slab are relatively climate insensitive, allowing reasonable cutoffs above which no thermal mass effects are observed to be established. This also indicates that, while the optimum slab construction may vary by climate, the least beneficial construction configuration is relatively stable and could reasonably be avoided.

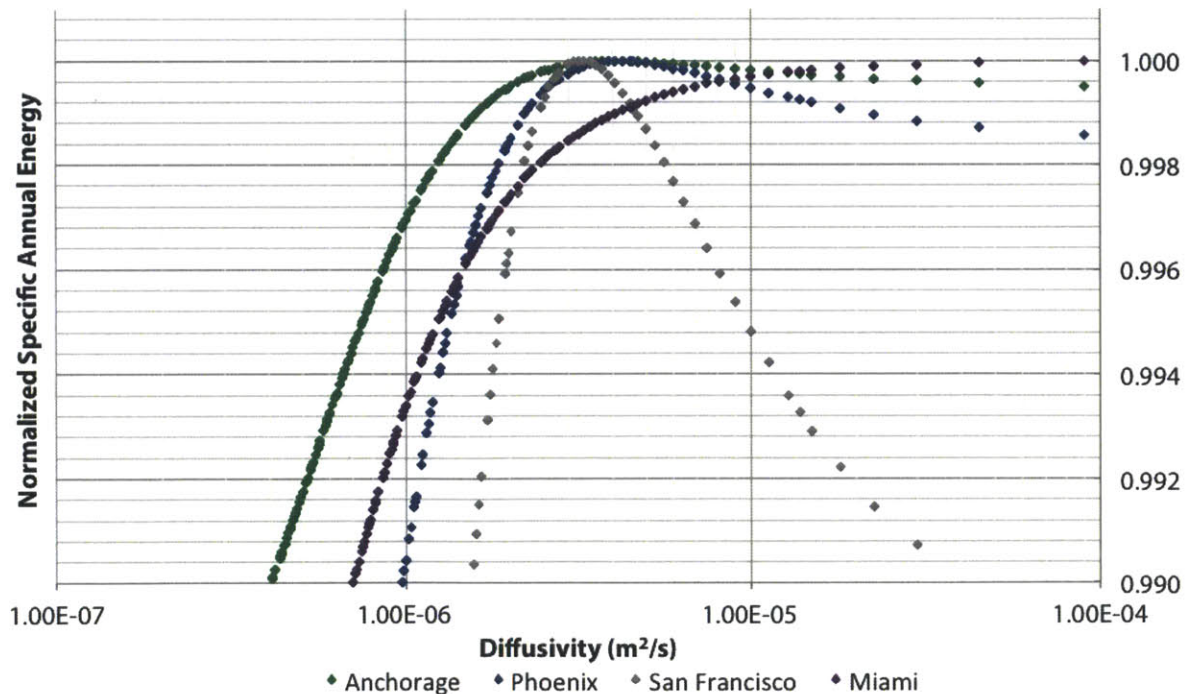


Figure 7-30 Comparison of Normalized Energy Consumption for Multiple Climates for a conductivity of 0.9 W/m-K and a thickness of 0.15 m

### 7.3.2 Mapping the Results

The results for the fifty climates are presented on maps of the United States to provide a visual representation of the impact of thermal mass and the efforts to optimize its construction. For the annual results presented in Figure 7-31, it is clear that only the coast of California shows reasonable energy savings as a result of the use of slab thermal mass. Similarly for the summer and winter results shown in Figure 7-32 and Figure 7-33, respectively, the cities on the coast of California change magnitudes of performance benefit but are generally the best location for the use of the thermal mass of slabs. These results indicate that it takes a reasonably mild climate for buildings to take advantage of passive thermal mass of a slab-on-grade construction.

The optimum conductivity value for the 0.15 m slab is much more stable than the conductivity values observed for walls. As can be seen in Figure 7-34, all of the values range from 0.1 W/m-K to 0.3 W/m-K. This indicates that, should thermal mass of the slab itself have any benefit, it should be substantially isolated from the ground condition. While the values for overall energy consumption indicated that less insulation should be used under the slab, a recommendation that may be suspect in light of conventional building wisdom, it is the optimization map that demonstrates the potential benefit of isolating the slab from the ground condition for the purpose of thermal mass use.

The optimum thickness for a 0.9 W/m-K slab shows one of two general behavioral patterns, as shown in Figure 7-35. The thickness behavior shows that for climates where thermal mass is ineffective, the results reach maxima toward the higher thicknesses of slabs. In contrast, in climates where thermal mass is more effective the slabs reach their peak at lower thicknesses. This is likely also a result of the impact of the mild climate and ground contact effects; it is sensible in these mild climates to allow the stable ground temperatures to couple with the interior of the building.



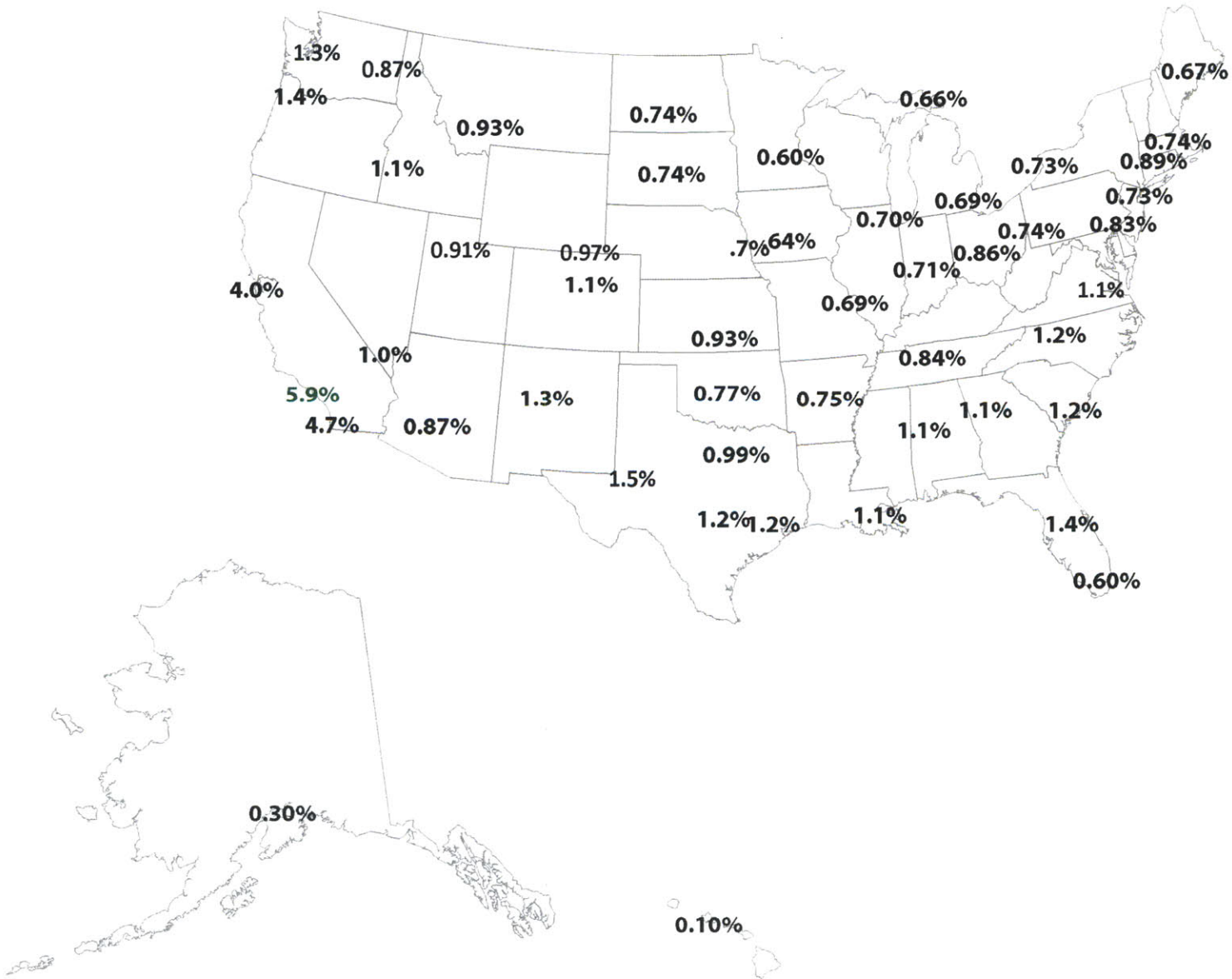


Figure 7-31 Annual Thermal Mass Impact Map, percent optimization for 0.9 W/m-K and 0.15 m slab based on 30,000 of 132,500 data points for residential construction in the United States

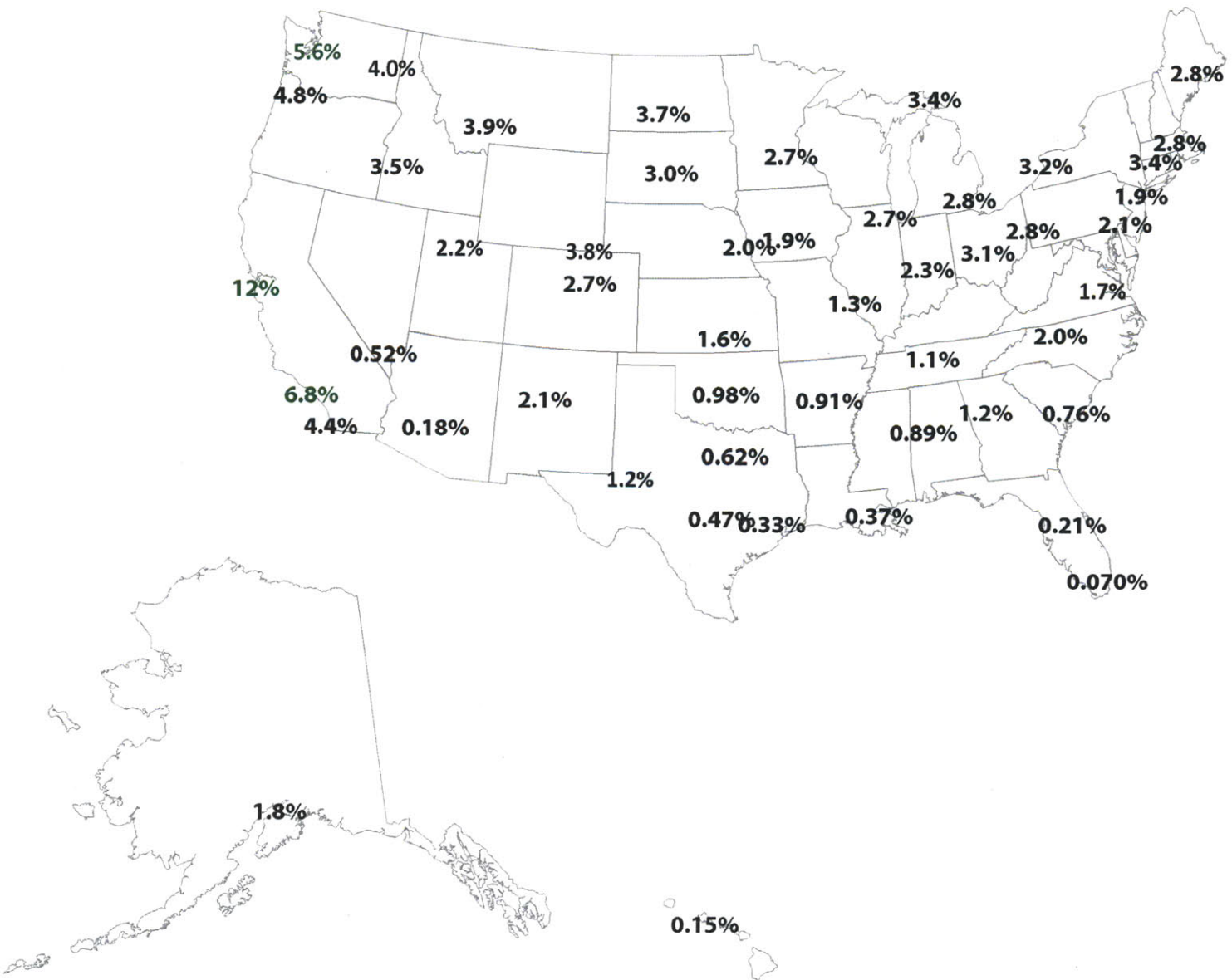


Figure 7-32 Summer Thermal Mass Impact Map, percent optimization for 0.9 W/m-K and 0.15 m slab based on 30,000 of 132,500 data points for residential construction in the United States

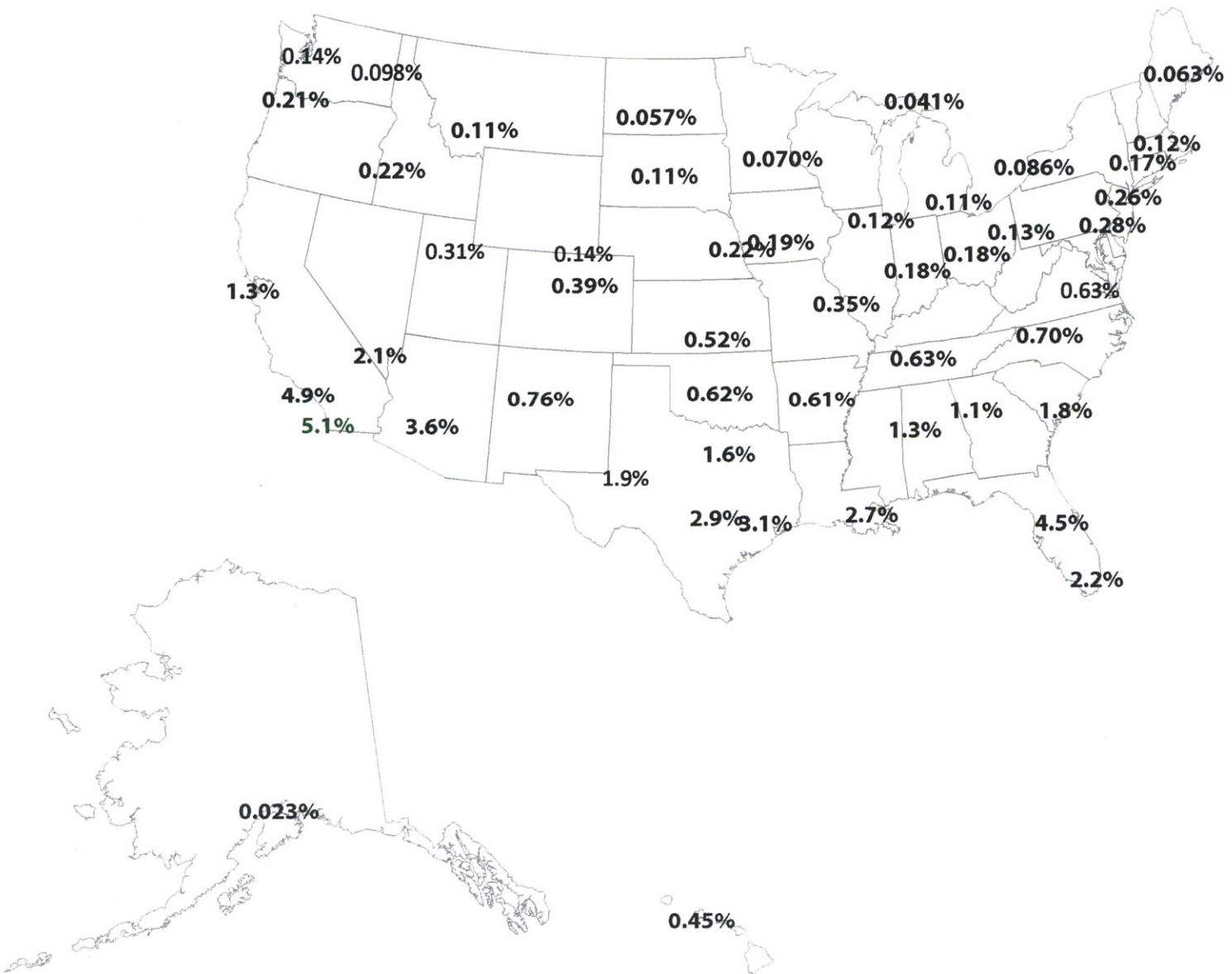


Figure 7-33 Winter Thermal Mass Impact Map, percent optimization for 0.9 W/m-K and 0.15 m wall based on 30,000 of 132,500 data points for residential construction in the United States

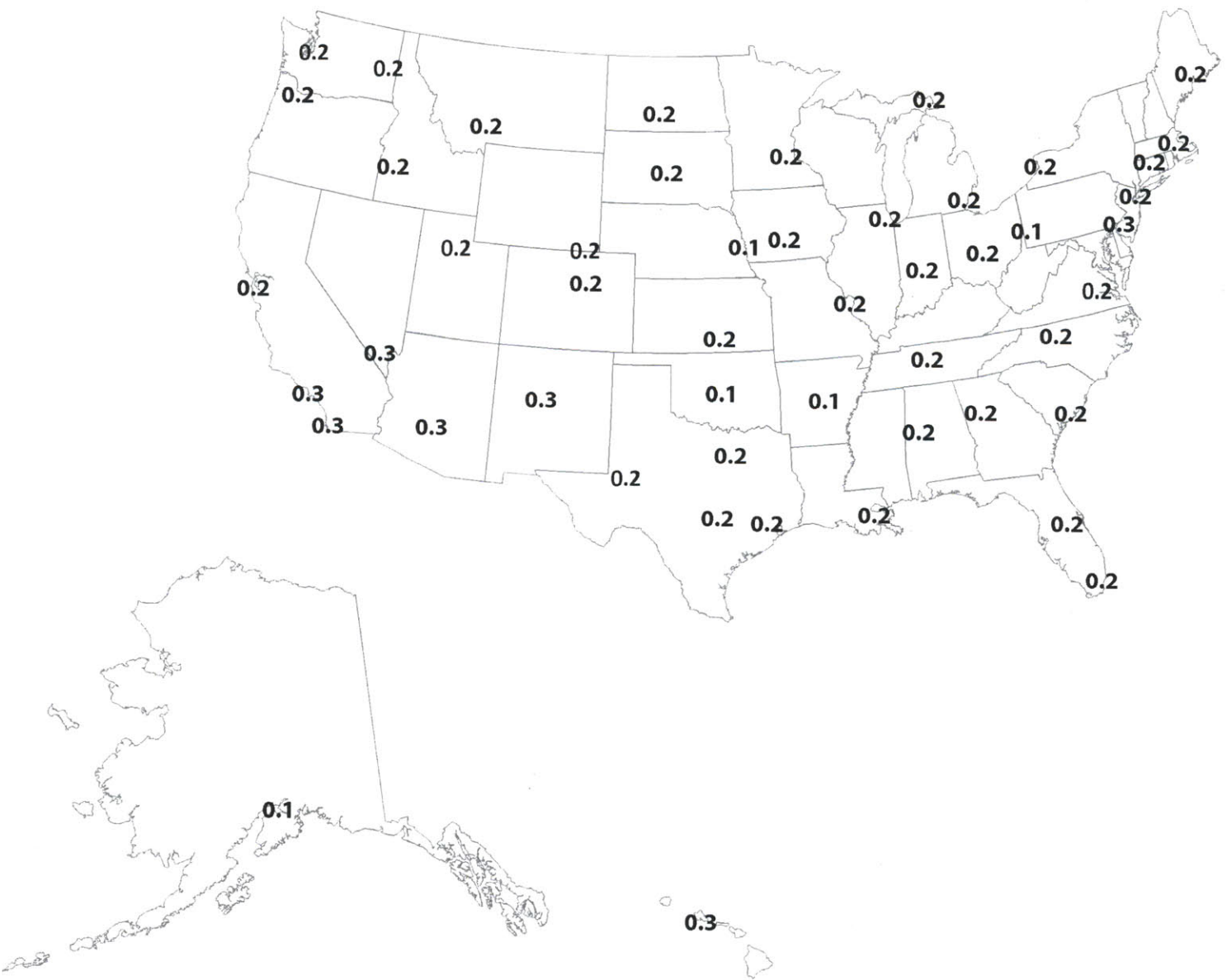


Figure 7-34 Optimum Conductivity (W/m-K) for 0.15 m slab (green locations asymptotic, blue locations increase without bound) based on 51,000 of 132,500 data points for residential construction in the United States



## 7.4 Chapter Summary

The presentation of the results of thermal mass in slab-on-grade construction has answered the second research question by indicating that slab performance is inferior to wall performance in passive construction. The best climates are located in California, similarly to wall construction, but with much lower potential of optimization of energy consumption. As discussed in this chapter, these slab-on-grade results are highly sensitive to the ground contact assumptions, many of which are inherent to EnergyPlus. The results suggested that, in answer to the third research question regarding optima, higher conductivities and thicker sections provided better performance due to the ability to use the moderated ground temperatures to stabilize the internal building temperature. This seems to defy conventional wisdom in the construction of insulated ground contact, leading one to question whether the energy modeling of slab contact in EnergyPlus is accurately capturing all possible effects. Thus, it becomes clear from this analysis that either (1) slab thermal mass provides little benefit due to the ground contact condition, or (2) present energy modeling tools do not accurately predict the ground contact condition. The remainder of this thesis will test the sensitivity of wall and slab data to infiltration and geometry effects.

**Part IV**

**Sensitivity Analysis**

**of Thermal Mass Results**

# Chapter 8

## Infiltration

Infiltration is the exchange of air between the indoor and outdoor environments through the building envelope in an uncontrolled manner. This phenomenon functions as a mechanism of heat loss or heat gain and is responsible for a substantial component of energy usage. As a result, strict building codes and voluntary initiatives such as Passive House seek to limit the uncontrolled exchange of air with the outdoor surroundings by favoring mechanical ventilation and tight building construction [87]. However, the literature review indicates that passive air movement is responsible for night cooling and can have a positive benefit on thermal mass performance. To address this consideration and answer the fourth research question regarding the interrelationship of thermal mass with other building parameters, a study of infiltration will be conducted. It will be determined if minimizing infiltration provides the best overall energy consumption when combined with a high-mass construction. The goal is to provide evidence as to whether infiltration is an essential component in activating thermal mass or if the two phenomena are not interacting in a significant way.

### 8.1 Experimental Simulation Setup

Infiltration is a subject widely studied and discussed in other research initiatives. This work will only present results for infiltration as it relates to the benefit of thermal mass on energy consumption. To this end, different levels of allowable infiltration will be modeled for a variety of material weights to determine the relationship between the two considerations. Infiltration will be modeled at five different levels to determine whether the change has an impact on the ability to activate thermal mass. The infiltration levels, presented in Table 8-1, are based off of design initiatives and legal standards. These standards measure infiltration as the parameter  $ACH_{50}$ , which is the infiltration rate measured in performance tests. Specifically, a door blower test pressurized at 50 Pascals is used to verify that



the air exchange rate is below the targeted limit from Table 8-1 [29]. This test is then converted to the unpressurized infiltration rate, known as ACH without a subscript, by dividing the  $ACH_{50}$  by 20 [63].

Table 8-1 Levels of Infiltration According to Different Standards

Infiltration Level Description	Infiltration Limit ( $ACH_{50}$ )
Passive House Standard [87]	0.6 / h
German Legal Limit for Buildings with Mechanical Ventilation [88]	1.5 / h
International Energy Conservation Code 2012 (Climates 1+2, Climates 3-8) [29]	3.0 / h, 5.0 / h
International Energy Conservation Code 2009 [89]	7.0 / h

For each level of infiltration, an experiment will be conducted simultaneously varying density and specific heat capacity in different climate conditions. The wall system and slab system will be varied separately to determine the impact of infiltration on the thermal mass potential of each envelope element. The experiment will be conducted similarly to those experiments in Chapter 6 and Chapter 7. The values of wall thickness and conductivity will be set at the Cube Model standard (solid concrete) of 0.15 m and 0.9 W/m-K. The values for specific heat and density will be varied across 100 experiments per infiltration level. The experiment setup for the varying parameters is presented in Table 8-2.

Table 8-2 Ranges and Increments for Infiltration Study

Parameter	Minimum Value	Maximum Value	Increment
Density	300 kg/m <sup>3</sup>	3000 kg/m <sup>3</sup>	300 kg/m <sup>3</sup>
Specific Heat Capacity	200 J/kg-K	2000 J/kg-K	200 J/kg-K

## 8.2 Results

The results of this study indicate that there is a small impact on thermal mass performance from the infiltration rate for a building. The following analysis will present the information for the four climates analyzed in Chapter 6 and Chapter 7: San Francisco, Phoenix, Miami, and Anchorage.

### 8.2.1 San Francisco, CA - Mild, Marine Climate

The results for the overall energy consumption and the normalized energy consumption versus infiltration and wall diffusivity are shown in Figure 8-1. The overall energy results support the conventional wisdom that tighter construction results in lower energy consumption. In addition, it is evident from the graph

that there is overlap between the infiltration component and the thermal mass component of energy savings. In other words, one could use high mass construction in San Francisco, CA to achieve greater energy savings that improving the air-tightness of construction. Normalizing the energy consumption for each infiltration rate by its maximum, it is clear from the figure that there is significant overlap in the normalized curves for light- and medium-weight construction. Only at the highest mass, or lowest diffusivities, is the normalized savings potential different for the different infiltration rates. For the heavy-weight construction, lower infiltration rates provide better thermal mass performance.

Looking at the overall and normalized energy consumption results for slabs in San Francisco shown in Figure 8-2, the results indicate similar trends in the saving potential of air-tightness but less overlap among the energy values spanned by the curves. As a result, only very high mass construction of slabs could be used to achieve the same energy performance as a higher infiltration rate. This is due to the smaller potential energy savings of thermal mass for slabs for San Francisco. Normalizing the energy consumption, it is clear that the energy consumption trend remains the same for slabs as for walls. In other words, there is little change in the master curve for the section describing lightweight materials, but there is a slight difference toward smaller values of diffusivity. This demonstrates the trend that tighter construction results in greater slab thermal mass performance.

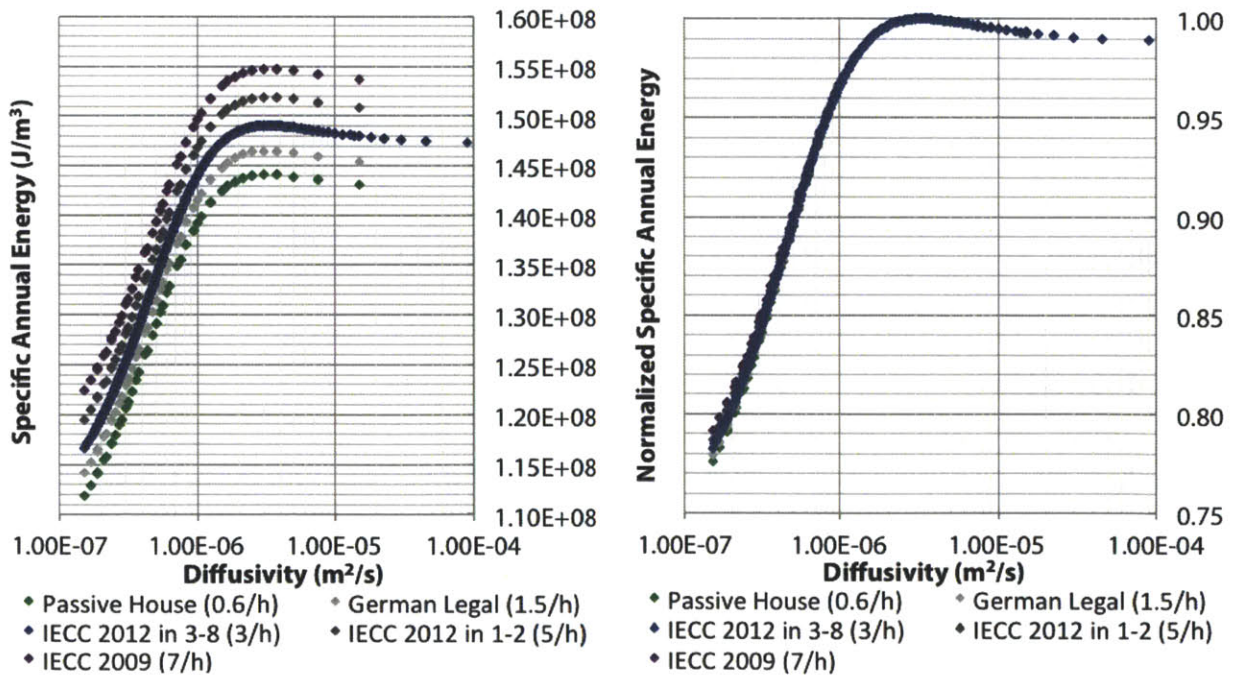


Figure 8-1 Specific Annual Energy Consumption (J/m<sup>3</sup>) vs Wall Diffusivity (m<sup>2</sup>/s) and Infiltration (1/h), left, and Normalized Specific Annual Energy Consumption vs Wall Diffusivity (m<sup>2</sup>/s) and Infiltration (1/h), right, San Francisco, CA

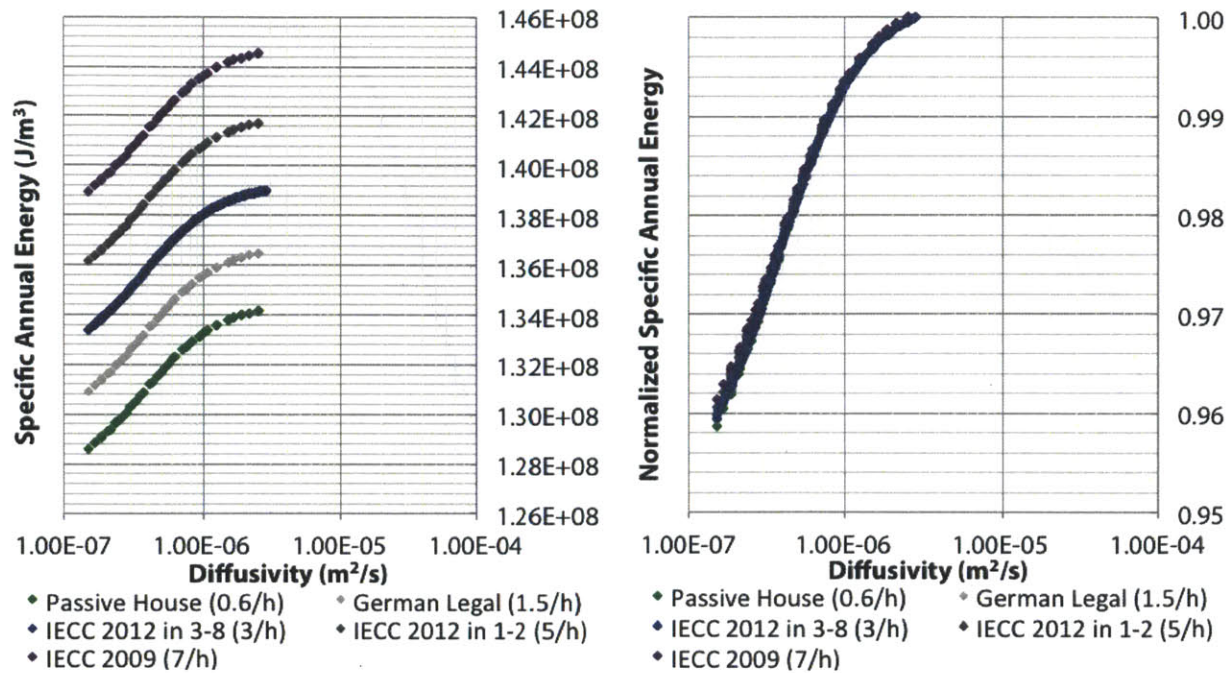


Figure 8-2 Specific Annual Energy Consumption ( $J/m^3$ ) vs Slab Diffusivity ( $m^2/s$ ) and Infiltration (1/h), left, and Normalized Specific Annual Energy Consumption vs Slab Diffusivity ( $m^2/s$ ) and Infiltration (1/h), right, San Francisco, CA

### 8.2.2 Phoenix, AZ - Hot, Dry Climate

The annual energy consumption per volume and normalized consumption for wall diffusivity and infiltration is found in Figure 8-3. This figure shows that buildings with higher infiltration rates consume more energy. However, it suggests that even in Phoenix, shown to have lower thermal mass performance, there is significant overlap in the energy curves. This allows a construction project to achieve the same or better energy performance as tighter construction by using the energy savings of the walls' thermal mass. Normalizing the consumption it is clear that the potential savings from thermal mass is similar for all infiltration rates. In other words, infiltration and thermal mass are essentially independent in this climate.

Moving to the overall and normalized energy consumption for slab diffusivity and infiltration presented in Figure 8-4, the results demonstrate the same relationship between airtight construction and overall energy consumption. There is much less overlap in the curves for slab thermal mass in Phoenix, suggesting that very high mass construction would be needed to achieve the performance of a looser construction. The normalized results show that there is substantial overlap among the thermal mass curves on a relative scale. Therefore, the trend between infiltration and thermal mass of slabs is relatively insignificant compared to the magnitudes of energy consumption considered.

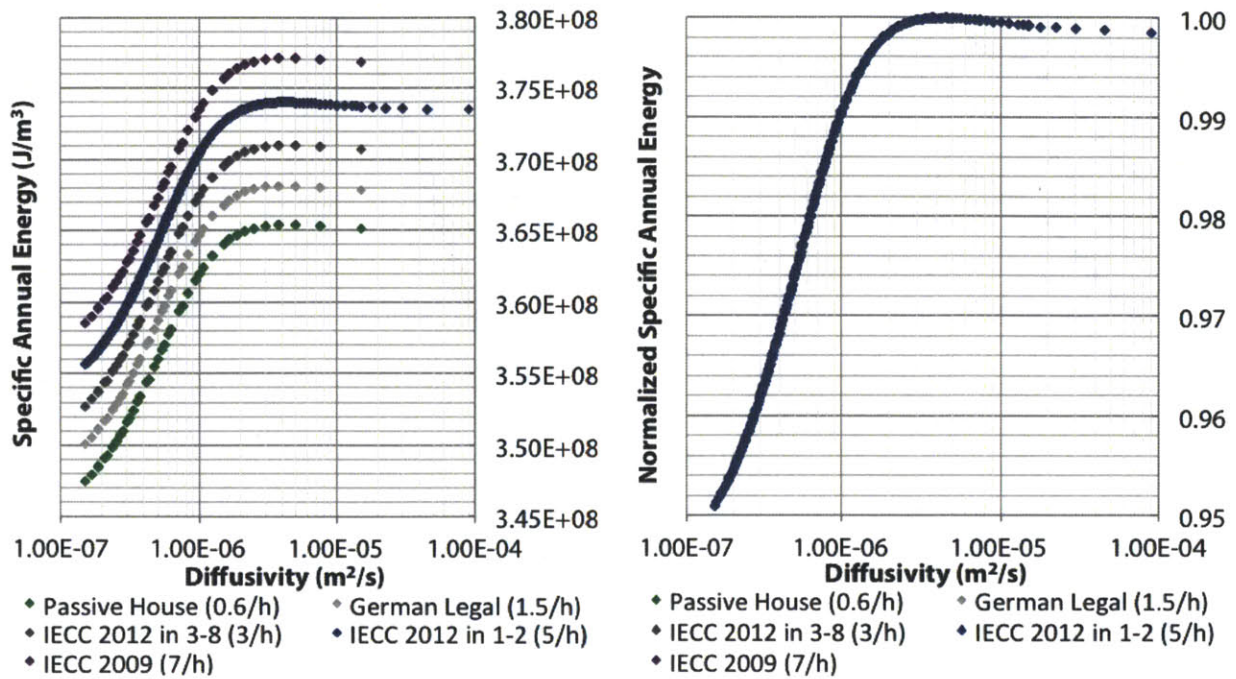


Figure 8-3 Specific Annual Energy Consumption (J/m<sup>3</sup>) vs Wall Diffusivity (m<sup>2</sup>/s) and Infiltration (1/h), left, and Normalized Specific Annual Energy Consumption vs Wall Diffusivity (m<sup>2</sup>/s) and Infiltration (1/h), right, Phoenix, AZ

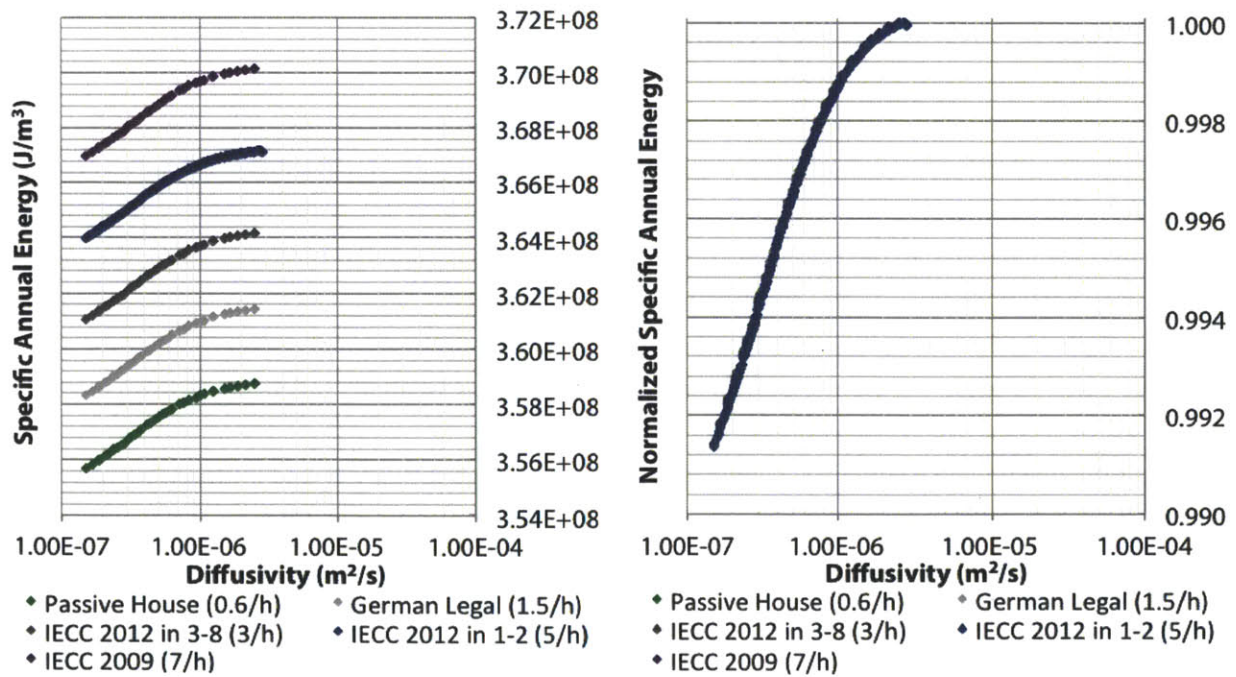


Figure 8-4 Specific Annual Energy Consumption (J/m<sup>3</sup>) vs Slab Diffusivity (m<sup>2</sup>/s) and Infiltration (1/h), left, and Normalized Specific Annual Energy Consumption vs Slab Diffusivity (m<sup>2</sup>/s) and Infiltration (1/h), right, Phoenix, AZ

### 8.2.3 Miami, FL - Hot, Humid Climate

The results for the overall energy consumption and normalized consumption for wall thermal mass in Figure 8-5 indicate that increased infiltration results in an increase in energy consumption. It is notable in the overall results diagram that the curves are more loosely spaced than the results for walls in San Francisco or Phoenix (compare with Figure 8-1 and Figure 8-3), suggesting that there is a similar impact on overall energy consumption for either improving the air tightness by one standard or moving toward a high-mass material. The normalized results show that there is similar thermal mass performance for all values of infiltration, with little difference in the shape of the curve or the overall amount of optimization.

The results for the overall and normalized energy consumption for slab thermal mass in Miami are shown in Figure 8-6. These graphs show the same trend of increasing air-tightness resulting in decreasing energy consumption. However, the thermal mass component is sufficiently small to minimize any overlap between the curves. This suggests that infiltration has a greater impact on overall energy consumption than the thermal mass component of the slab. Normalizing these energy consumption values, it is clear that the Passive House standard still exhibits the best thermal mass performance, though the difference is only notable for the heaviest constructions. Overall magnitudes of energy savings are somewhat limited; as a result thermal mass makes an insubstantial contribution to energy savings for all tested infiltration levels.

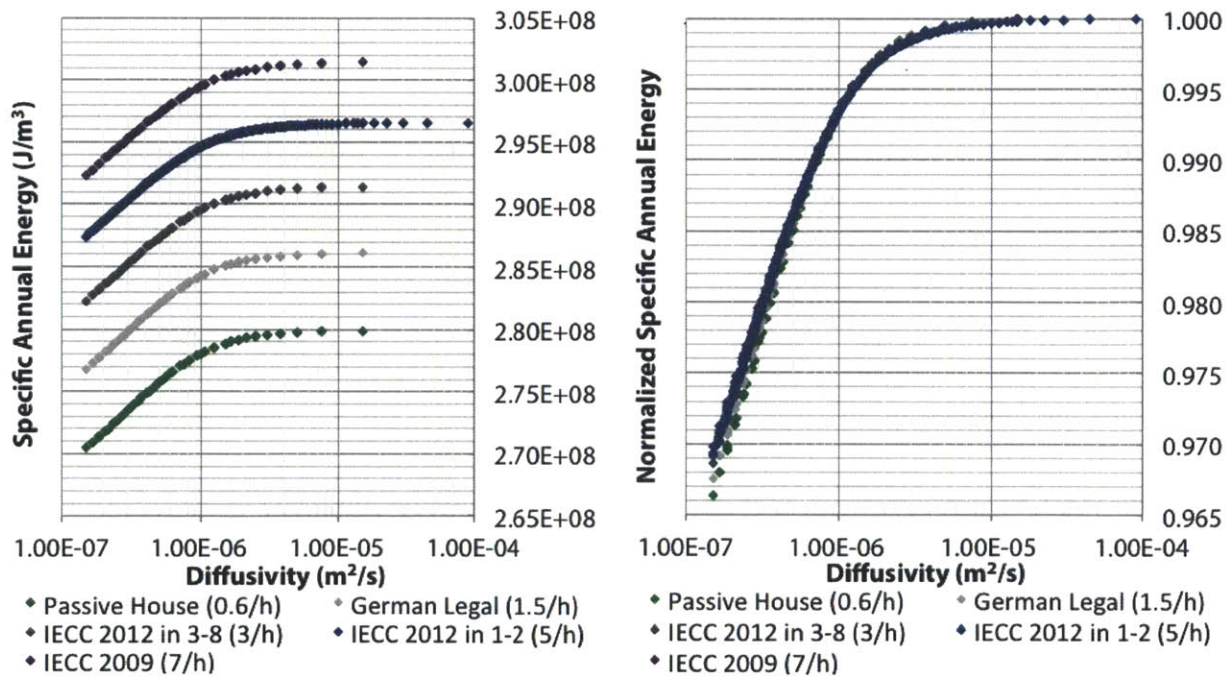


Figure 8-5 Specific Annual Energy Consumption ( $J/m^3$ ) vs Wall Diffusivity ( $m^2/s$ ) and Infiltration (1/h), left, and Normalized Specific Annual Energy Consumption vs Wall Diffusivity ( $m^2/s$ ) and Infiltration (1/h), right, Miami, FL

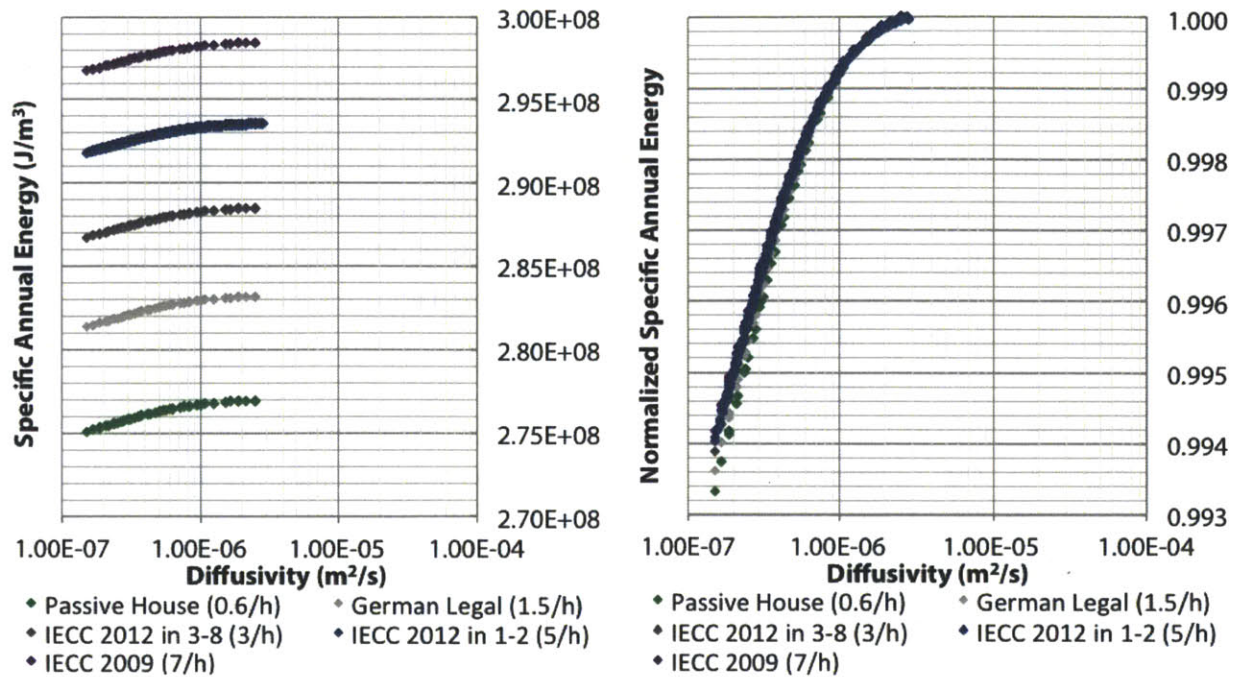


Figure 8-6 Specific Annual Energy Consumption (J/m<sup>3</sup>) vs Slab Diffusivity (m<sup>2</sup>/s) and Infiltration (1/h), left, and Normalized Specific Annual Energy Consumption vs Slab Diffusivity (m<sup>2</sup>/s) and Infiltration (1/h), right, Miami, FL

## 8.2.4 Anchorage, AK - Cold Climate

The results for wall thermal mass in Anchorage illustrated in Figure 8-7 show that the trend regarding infiltration energy consumption holds. In this climate, there is a sufficiently large difference in energy consumption between infiltration levels. As a result, the change in energy consumption from infiltration is on the same order of magnitude as the difference from the thermal mass. The normalized energy consumption shows that low infiltration rates have a greater percentage optimization than high infiltration rates. The curves show substantial overlap for low-mass constructions, suggesting that the only key difference is in the heaviest building materials. Also, this shows that there is no trade-off between thermal mass and airtight construction.

The results for slab thermal mass for Anchorage shown in Figure 8-8 demonstrate that the impact of infiltration on energy consumption is much greater than the impact of thermal mass. This is evident by the large gaps between the curves. It is also clear from the diagram that tighter construction will result in lower energy consumption. In the normalized curve, the results are very similar for all rates of infiltration. There is a slight improvement of thermal mass performance for the tighter construction. Together these results indicate that decisions made with regard to infiltration will not negatively impact slab thermal mass performance.

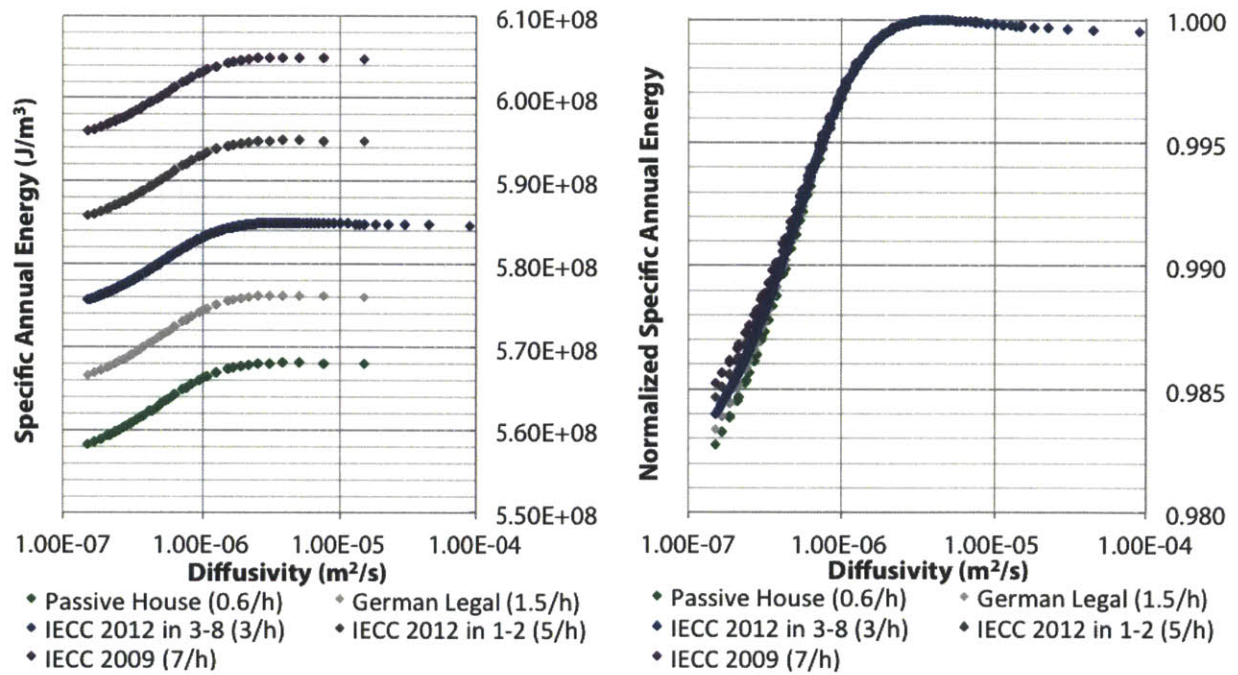


Figure 8-7 Specific Annual Energy Consumption ( $J/m^3$ ) vs Wall Diffusivity ( $m^2/s$ ) and Infiltration (1/h), left, and Normalized Specific Annual Energy Consumption vs Wall Diffusivity ( $m^2/s$ ) and Infiltration (1/h), right, Anchorage, AK

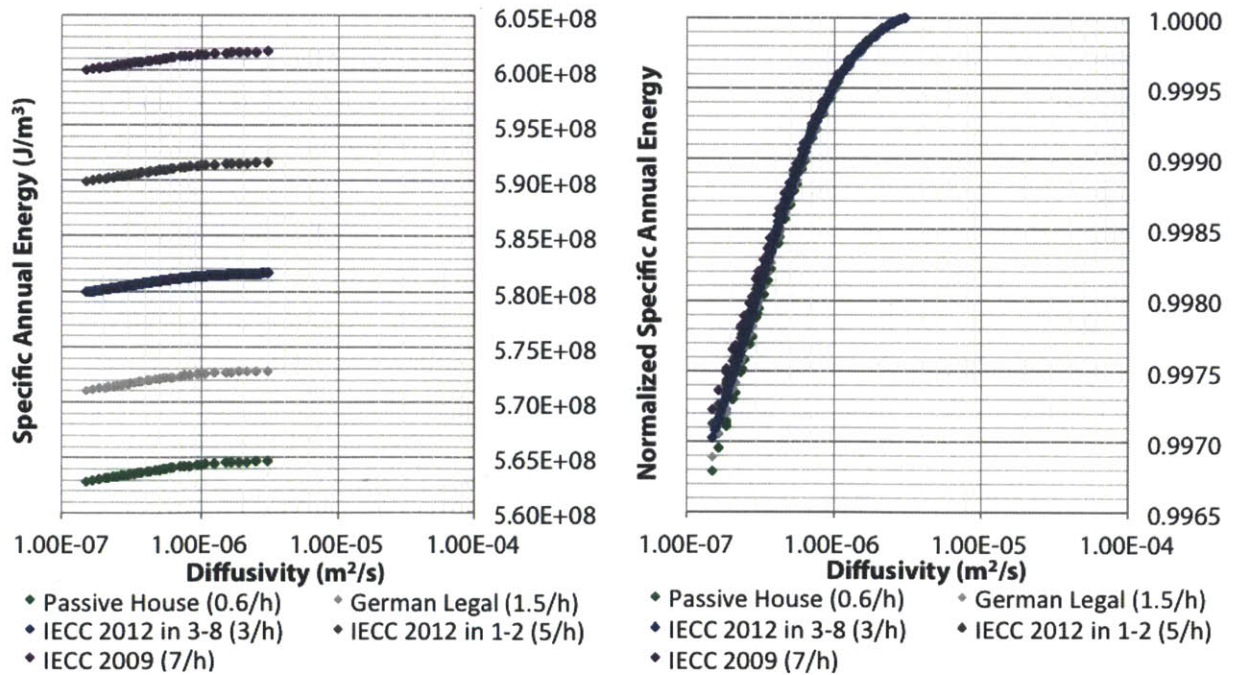


Figure 8-8 Specific Annual Energy Consumption vs Slab Diffusivity ( $m^2/s$ ) and Infiltration (1/h), left, and Normalized Specific Annual Energy Consumption vs Slab Diffusivity ( $m^2/s$ ) and Infiltration (1/h), right, Anchorage, AK

## 8.2.5 Optimization and National Scale

Figure 8-9 provides the optimization results versus infiltration for walls and slabs. These results demonstrate the potential to change thermal mass performance for the four climates discussed in the previous sections. For most climates, the energy saving potential does change by air infiltration rate; lower infiltration rates show better optimization potential of thermal mass. The results for walls show the strongest improvement in San Francisco. In this climate, a double dividend in energy savings between optimum passive thermal mass and optimum air-tightness can be achieved for high performance construction. The results in Phoenix are linearly related with a near-zero slope. This suggests that infiltration would not need to be considered in Phoenix. The optimization for Miami and Anchorage is very shallow but follows the same trend as San Francisco. For these climates, the benefit of tighter construction on thermal mass is present but does not result in substantial improvement.

The graph for thermal mass of slabs shown in the right diagram of Figure 8-9 demonstrates that the trends are similar but the magnitudes are smaller. As a result, even in San Francisco the increase in energy performance due to airtight construction is minimal. For the other three climates, the change in airtightness results in no significant change in thermal mass performance. Therefore, for slab thermal mass, the benefit of tighter construction is primarily in the energy savings from reducing infiltration, not the savings from better thermal mass performance.

The trends on the national scale, presented in Figure 8-10 and Figure 8-11, are generally similar to the results presented above. The trends of lower energy consumption and higher thermal mass performance for tighter construction hold. The only strong exception to this rule, of the fifty climates, run is Los Angeles, CA. This climate shows an improvement to thermal mass performance at higher infiltration rates. The resulting increase in thermal mass performance corresponds to an additional 1% of overall energy consumption. While this is a notable increase, it is marginal compared to the energy difference between an  $ACH_{50}$  of 7 and the lower values. The other exception is Phoenix, whose graphs shown in Figure 8-9 demonstrate that the optimization curve is flat enough for the exception to be neglected. Therefore, the national data do not negate the general result that infiltration and thermal mass are optimized together by decreasing the infiltration rate for the home.



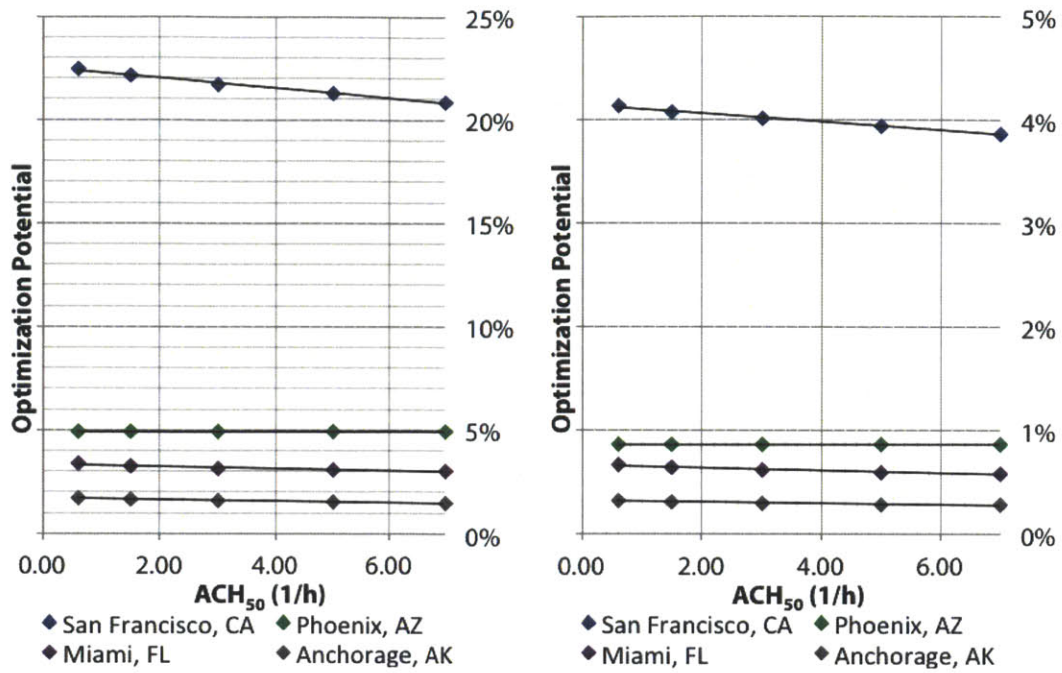


Figure 8-9 Potential Energy Savings from Thermal Mass vs Infiltration (1/h), Walls (left) and Slabs (right)

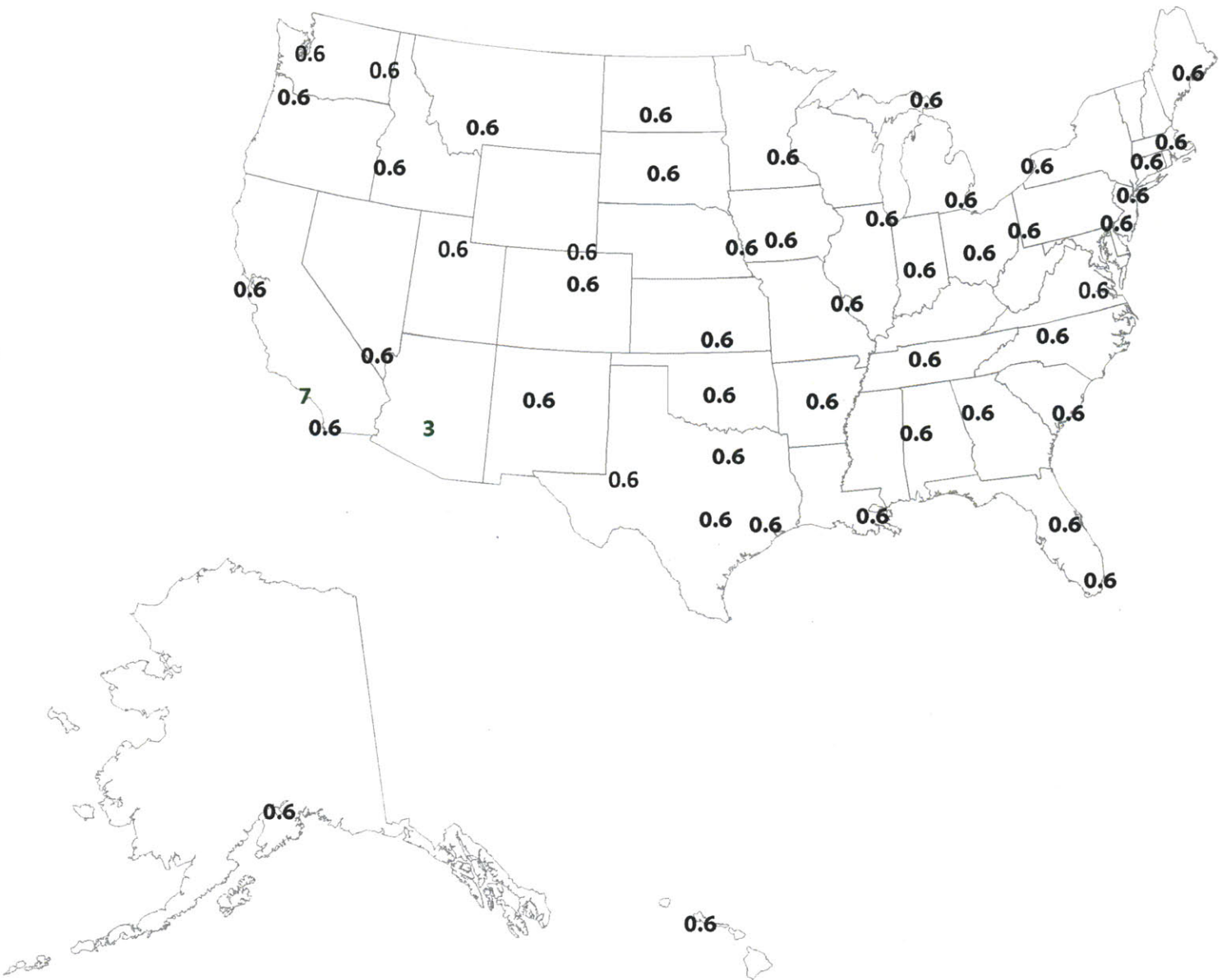


Figure 8-10 Optimum Infiltration (1/h) for 0.9 W/m-K, 0.15 m thick wall (green locations do not optimize at 0.6/h) based on 25,000 data points for residential construction in the United States

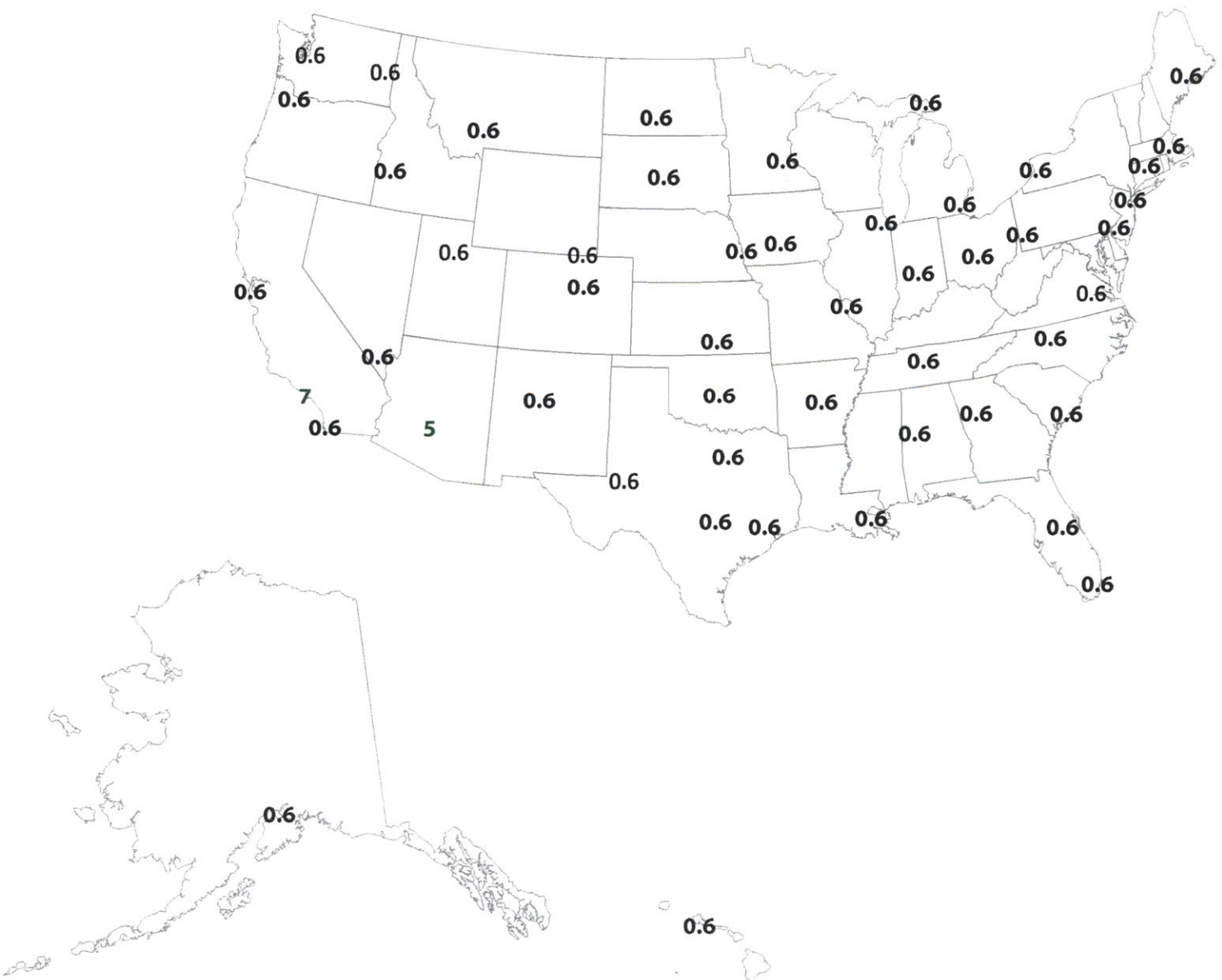


Figure 8-11 Optimum Infiltration (l/h) for 0.9 W/m-K, 0.15 m thick slab (green locations do not optimize at 0.6/h) based on 25,000 data points for residential construction in the United States

## 8.3 Chapter Summary

This chapter indicates that relationship between thermal mass and infiltration is not entirely independent and that there is no perceivable trade-off between thermal mass and air-tight construction. For most climates, the best performance occurs at the lowest infiltration rates. A few climates break the trend by showing little correlation or reversed trends. In all of these climates and infiltration cases, either thermal mass performance is small, essentially constant, or much greater than the variation achieved through infiltration changes. In no climate does infiltration make the difference between excellent thermal mass performance and poor thermal mass performance.

Finally, it should be noted that there is often overlap in the overall energy consumption of buildings with regard to their thermal mass potential. This shows the important notion that thermal mass can achieve greater or equal energy savings to reducing infiltration in some climates. Such a trait is significant considering the reliability of thermal mass as a property. That is, a building designed with high mass materials is likely to be constructed as such, whereas a building designed with a low infiltration rate may or may not achieve that standard in building performance tests. Finally, it is notable that infiltration does not hinder thermal mass performance substantially in the range of relevant building codes. However, the negative slope on thermal mass potential suggests that very leaky buildings (an  $ACH_{50}$  of much higher than 7) will likely suffer a loss of thermal mass performance.

# Chapter 9

## Geometry Effects

All previous experiments for the development of thermal mass relationships have included a fixed geometry of the cube, namely 10 m x 10 m x 4 m. The fourth research question addresses the sensitivity of thermal mass results to basic geometry factors. This section will determine how changes in attic condition, internal slabs, basement condition, height, plan dimensions, and glazing percentage impact the overall thermal mass potential of the structure. In the end, it will be determined if geometry impacts are significant to the benefit of thermal mass.

### 9.1 Experimental Simulation Setup

Each simulation experiment discussed in this chapter has unique parameters to its experimental setup that will be discussed individually, but all of the experiments maintain a few constant parameters. The goal of each experiment is to generate similar thermal mass master curves as those in Part III (see for instance Figure 6-1, Figure 6-2, Figure 7-1, and Figure 7-2). Therefore, in all of the experiments the conductivity and material thickness are fixed at 0.9 W/m-K and 0.15 m, respectively. In addition, each experiment uses the same variable parameters for determining the thermal mass of the construction in question, shown in Table 9-1. Finally, each experiment will test the impact of the new assumption on both wall and slab thermal mass performance in order to determine if the effect is significant or can be neglected in the understanding of the phenomenon.

Table 9-1 Ranges and Increments for Geometry Studies

Parameter	Minimum Value	Maximum Value	Increment
Density	300 kg/m <sup>3</sup>	3000 kg/m <sup>3</sup>	300 kg/m <sup>3</sup>
Specific Heat Capacity	200 J/kg-K	2000 J/kg-K	200 J/kg-K

## 9.2 Incorporating the Attic

During the calibration analysis, the building feature found to have the greatest impact on matching the overall energy consumption was the attic. However, such a study does not provide information as to whether the consideration of this geometric feature is essential to understanding thermal mass. For simplicity of the main thermal mass data set, the attic was omitted from the building geometry. This experiment will determine whether the attic contributes substantially to either wall or slab thermal mass performance. To conduct the analysis, an unconditioned attic of 0.5 m has been modeled on top of the standard 10 m by 10 m by 4 m cube, which has been shown through the calibration analysis to be a reasonable normalized height of an attic.

### 9.2.1 San Francisco, CA - Mild, Marine Climate

The annual energy consumption per volume and normalized consumption for the single cube and building with attic have been shown in Figure 9-1. The overall energy diagram demonstrates the attic results in a substantial change in overall magnitude of energy consumption for all values of construction weight, reinforcing the calibration result. The normalized consumption diagram demonstrates the impact on thermal mass from the resulting change in the building condition. It can be seen that the inclusion of the attic greatly reduces the overall percentage of energy reduction possible for the single-family home as a result of thermal mass performance. The potential energy savings has been reduced from 22% to 14%. However, as the first graph shows, the decrease in overall consumption suggests that the attic has an overall positive impact on the energy consumption as a buffering space. The combination of high mass construction and an attic can be used to achieve maximum energy performance. Finally, it is clear that the attic is an important consideration in determining if wall thermal mass is effective for a given building.

The results for the slab thermal mass master curve for specific annual energy consumption and normalized energy consumption are shown in Figure 9-2. This graph also shows the strong decrease in overall energy consumption of the building due to the incorporation of the attic regardless of weight of construction. The normalized energy consumption shows that, with the incorporation of the attic, slab thermal mass savings have dropped below 2% annual energy consumption. This result indicates that the presence of an attic may inhibit slab thermal mass from providing significant energy saving potential.

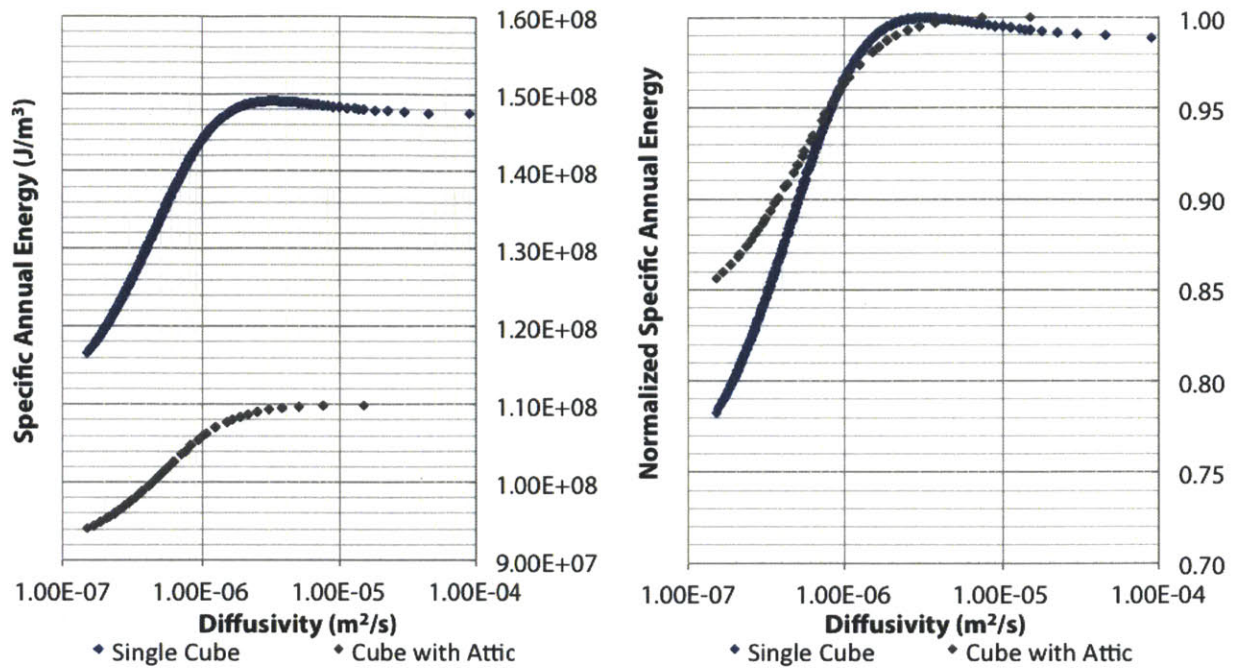


Figure 9-1 Specific Annual Energy Consumption (J/m³) vs Wall Diffusivity (m²/s) and Attic Condition, left, and Normalized Specific Annual Energy Consumption vs Wall Diffusivity (m²/s) and Attic Condition, right, San Francisco, CA

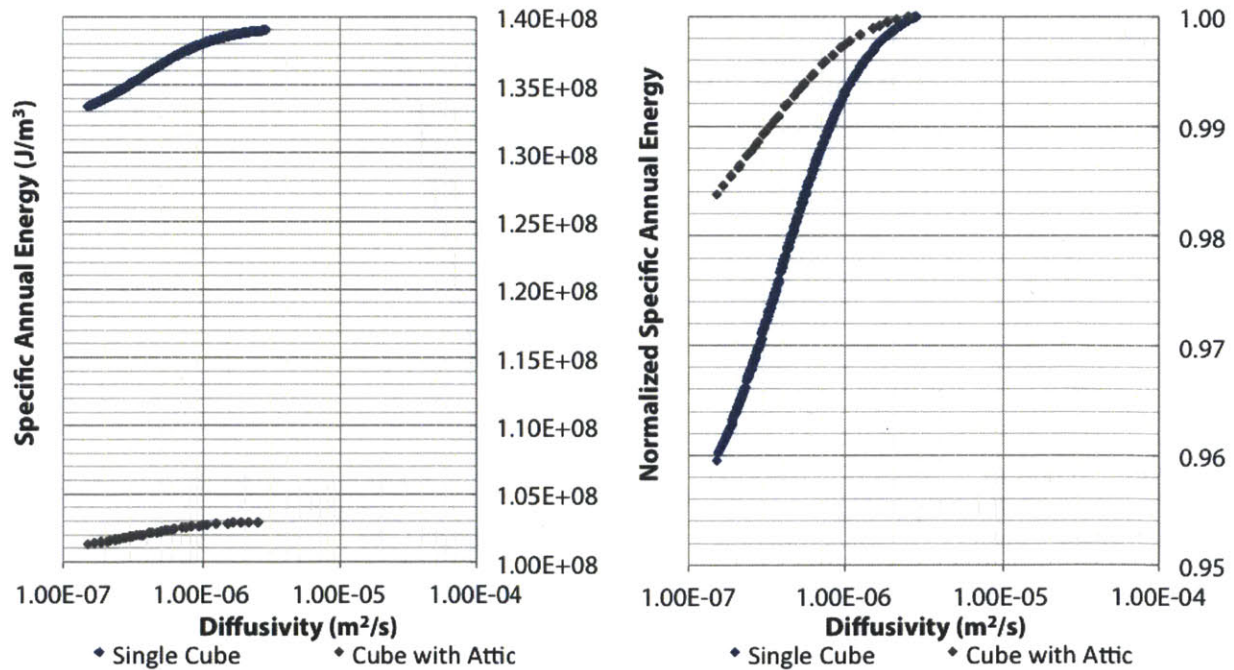


Figure 9-2 Specific Annual Energy Consumption (J/m³) vs Slab Diffusivity (m²/s) and Attic Condition, left, and Normalized Specific Annual Energy Consumption vs Slab Diffusivity (m²/s) and Attic Condition, right, San Francisco, CA

## 9.2.2 Phoenix, AZ - Hot, Dry Climate

The specific annual energy consumption and normalized annual energy consumption for Phoenix, AZ and wall thermal mass performance are shown in Figure 9-3. The overall annual energy consumption shows that the attic is responsible for significant overall reduction of energy consumption in this climate as well, as shown in the calibration study of Phoenix. For the normalized energy consumption, it is clear that thermal mass performance has dropped to 3.4% annual savings, a much smaller amount than indicated for the basic cube model. The sharp decline in overall energy performance suggests that an attic benefits energy perspective even though it lessens the performance of thermal mass.

The specific annual energy consumption and normalized consumption for slab thermal mass performance are shown in Figure 9-4. Once again, the attic makes the impact of decreasing both overall energy performance and thermal mass performance. The reduced annual energy consumption savings is 0.4%, indicating that there is little benefit to the use of slab thermal mass in a building with an attic in Phoenix. The graph also indicates that this is not a substantial change from the original thermal mass results; slab thermal mass is not an effective parameter to optimize in Phoenix with or without an attic.

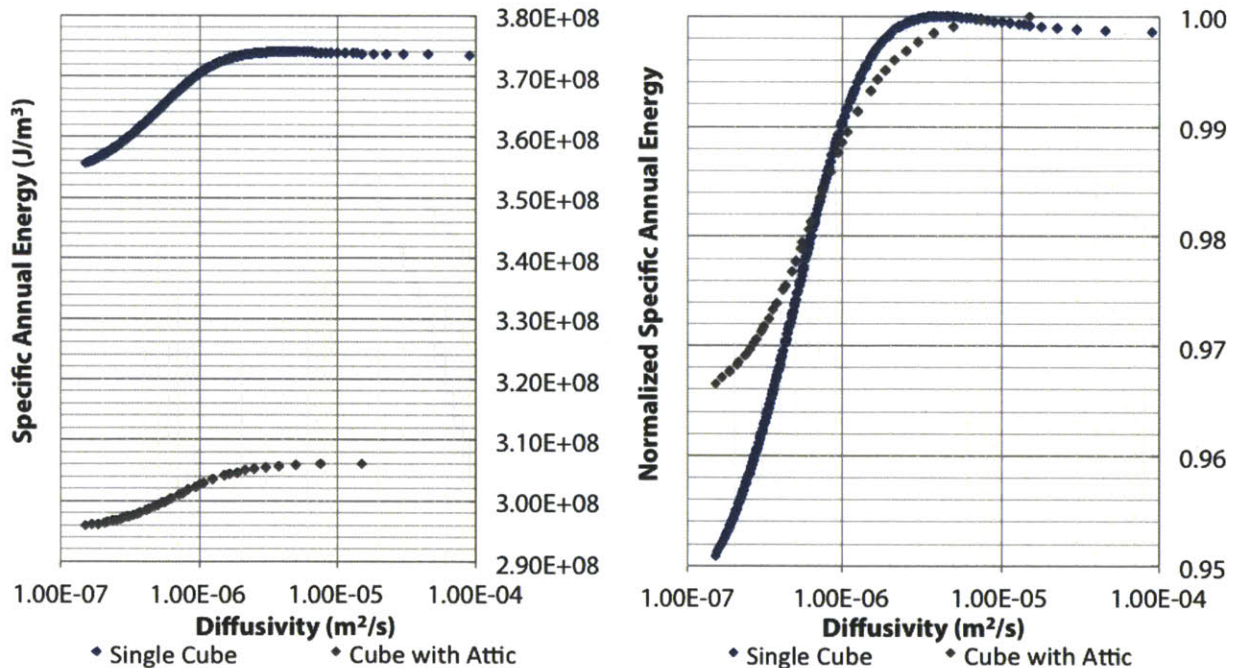


Figure 9-3 Specific Annual Energy Consumption ( $J/m^3$ ) vs Wall Diffusivity ( $m^2/s$ ) and Attic Condition, left, and Normalized Specific Annual Energy Consumption vs Wall Diffusivity ( $m^2/s$ ) and Attic Condition, right, Phoenix, AZ



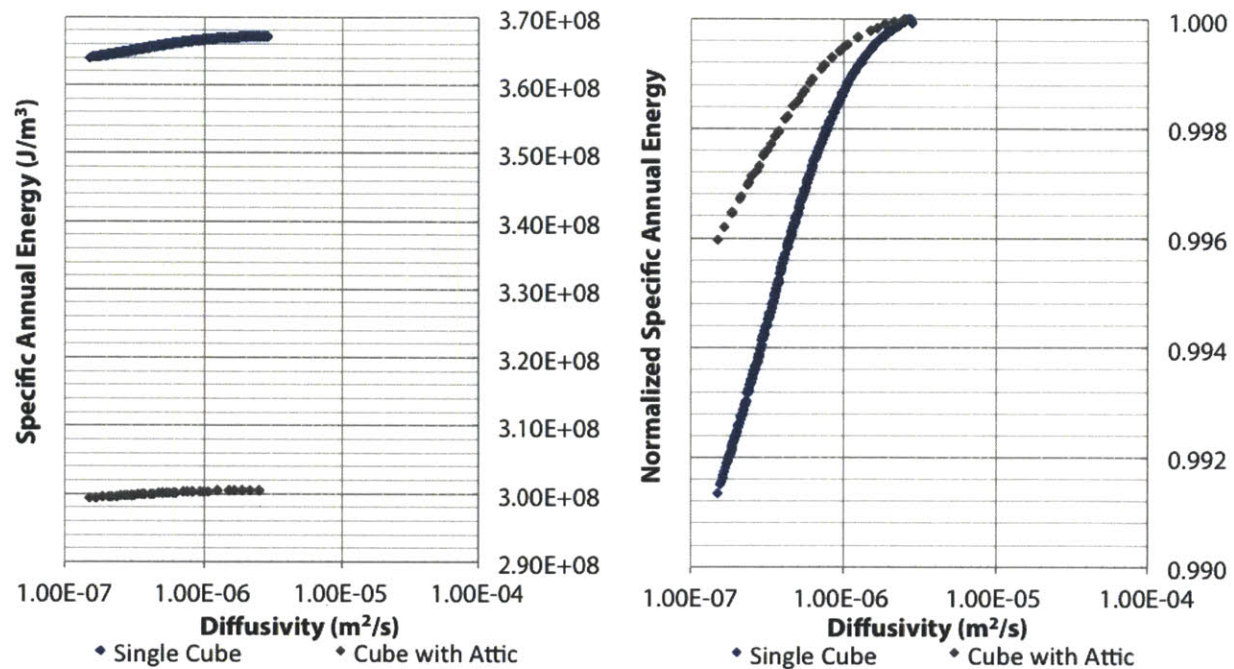


Figure 9-4 Specific Annual Energy Consumption ( $J/m^3$ ) vs Slab Diffusivity ( $m^2/s$ ) and Attic Condition, left, and Normalized Specific Annual Energy Consumption vs Slab Diffusivity ( $m^2/s$ ) and Attic Condition, right, Phoenix, AZ

### 9.2.3 Miami, FL - Hot, Humid Climate

The results for the annual energy consumption per volume and normalized energy consumption for Miami, FL and wall thermal mass are presented in Figure 9-5. This annual energy consumption shows a similar trend to the other climates, but the impact on the thermal mass performance is much smaller in Miami. With an attic, there is still 2.5% annual energy savings compared with 3.1% without the attic. This is a much smaller decrease in performance than observed in other climates, suggesting that the impact of the attic is not fixed in all climates. Still, the results suggest that the thermal mass performance of walls in Miami is not responsible for substantial energy savings in the presence or absence of an attic.

The results for the specific annual energy consumption and normalized values for slab thermal mass are graphed in Figure 9-6. While the attic results in the same decrease in energy performance, the normalized results show that the impact of thermal mass on energy consumption is low for both the cube with an attic and the cube without an attic. With a potential energy savings of 0.32% for the cube with an attic, slab thermal mass is insignificant with regard to other factors impacting overall energy consumption, such as the reduction from the incorporation of the attic itself.

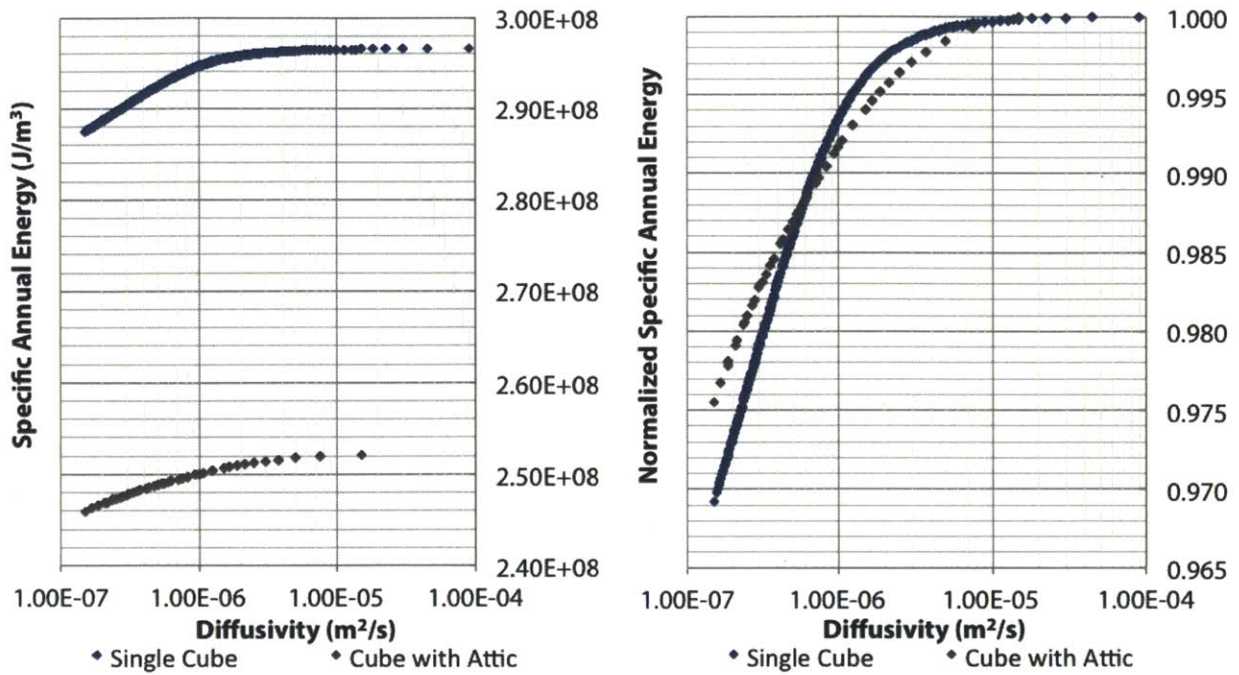


Figure 9-5 Specific Annual Energy Consumption (J/m³) vs Wall Diffusivity (m²/s) and Attic Condition, left, and Normalized Specific Annual Energy Consumption vs Wall Diffusivity (m²/s) and Attic Condition, right, Miami, FL

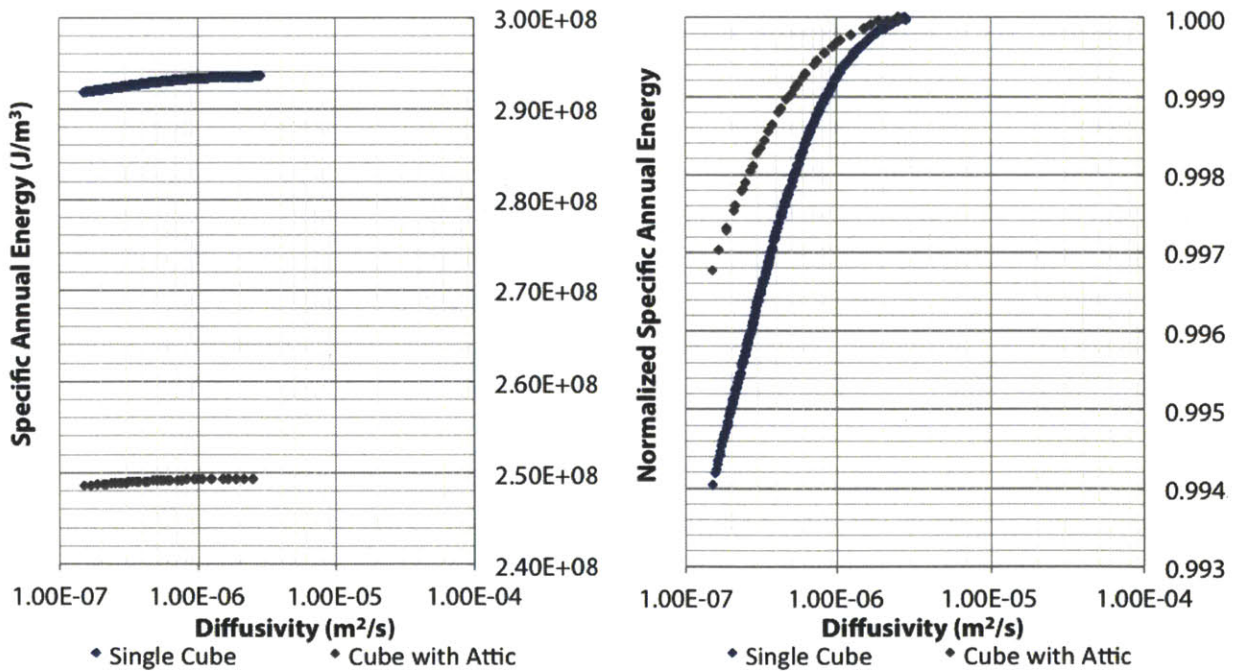


Figure 9-6 Specific Annual Energy Consumption (J/m³) vs Slab Diffusivity (m²/s) and Attic Condition, left, and Normalized Specific Annual Energy Consumption vs Slab Diffusivity (m²/s) and Attic Condition, right, Miami, FL

### 9.2.4 Anchorage, AK - Cold Climate

The results for specific annual energy consumption and normalized consumption for wall thermal mass are shown in Figure 9-7. These results demonstrate that the impact of the attic shows a sharp reduction in energy consumption in keeping with the results from other climates. The benefit of thermal mass from walls drops below 1% annual energy savings for the attic condition, indicating that the already modest savings in Anchorage are reduced further as a result of the attic condition.

The results for slab thermal mass for the annual consumption per volume and normalized consumption are presented in Figure 9-8. These results indicate that the overall energy reduction from the attic condition is significant. However, as can be seen in the normalized plot, the magnitude of energy savings for both the cubes with and without the attic is minimal. Therefore, energy saving strategies such as the use of an attic would result in far greater savings than the incorporation of high mass systems in this climate.

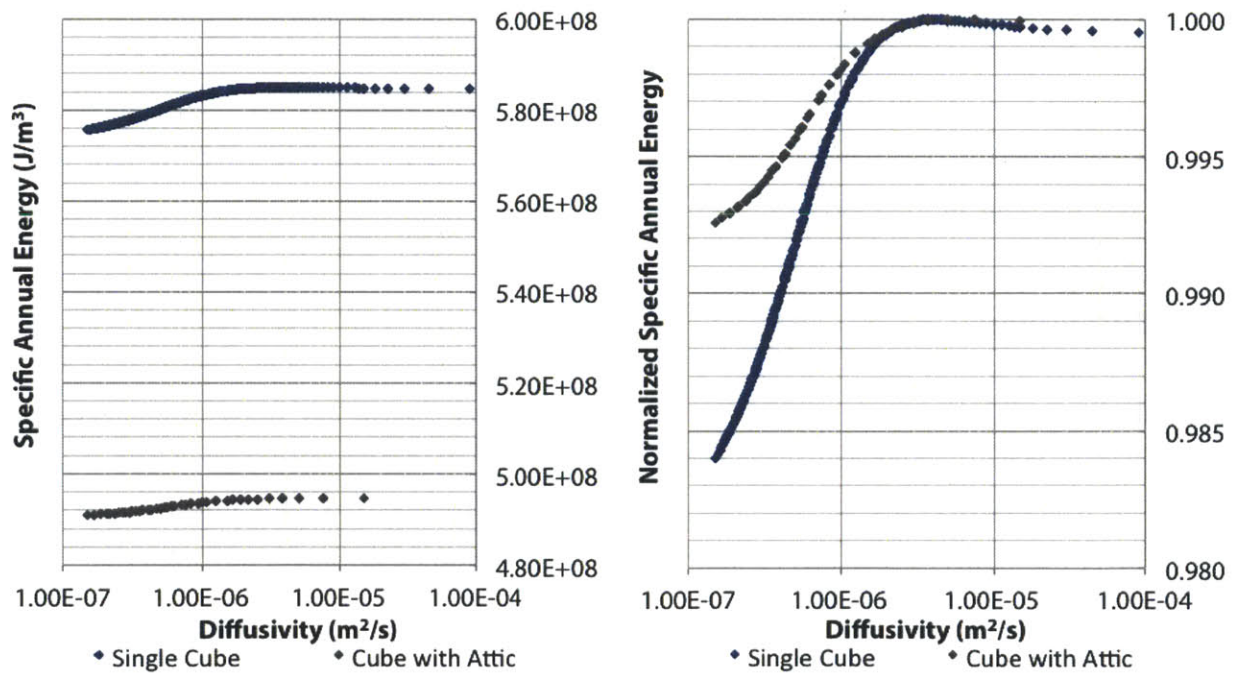


Figure 9-7 Specific Annual Energy Consumption ( $J/m^3$ ) vs Wall Diffusivity ( $m^2/s$ ) and Attic Condition, left, and Normalized Specific Annual Energy Consumption vs Wall Diffusivity ( $m^2/s$ ) and Attic Condition, right, Anchorage, AK

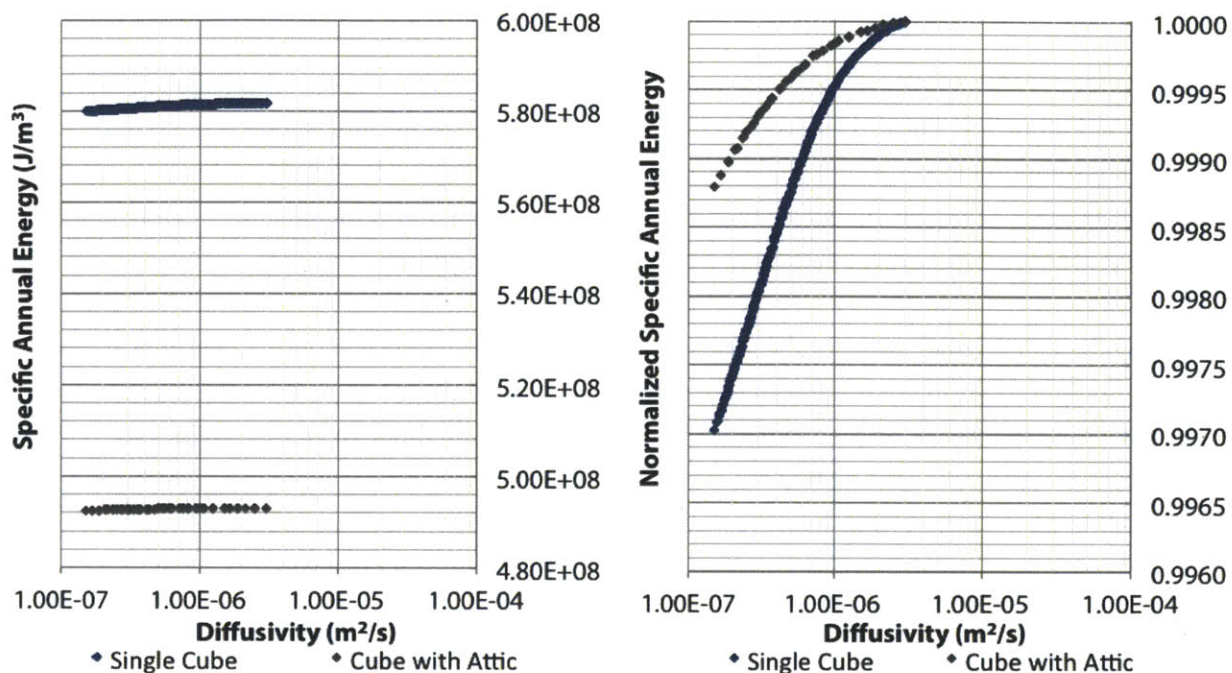


Figure 9-8 Specific Annual Energy Consumption (J/m³) vs Slab Diffusivity (m²/s) and Attic Condition, left, and Normalized Specific Annual Energy Consumption vs Slab Diffusivity (m²/s) and Attic Condition, right, Anchorage, AK

### 9.2.5 Discussion

The results of this analysis show consistent trends across all climates tested. The attic condition results in lower overall energy consumption in the building. However, it also lowers the impact of both wall and slab thermal mass performance for a building. Thermal mass performance has a lower impact on energy consumption in all climates than the use of an attic, indicating that it would be unwise to omit an attic for the sake of better thermal mass performance.

## 9.3 Testing Internal Slabs

Internal slabs were found during the calibration experiment to be relatively unimportant to the overall use of energy in the building. To verify that this impact does not affect the potential to optimize thermal mass of either walls or slabs, the model has been tested with an internal slab. The internal slab is assumed to cover the entire floor area and be constructed of the same test material used for all other constructions, as set by the Cube Model assumptions. Since this material has the properties of brut concrete, it will test whether a high-mass construction inside the cube interacts with the thermal mass performance of either the slab or the wall mass.

### 9.3.1 San Francisco, CA - Mild, Marine Climate

The results for the annual energy consumption per volume and the normalized energy consumption for wall thermal mass are shown in Figure 9-9. The overall energy consumption suggests that there is significant overlap among the energy consumption levels of a building with and without an internal slab. There is an intersection point near the maximum energy consumption. For constructions with high thermal mass, there is lower energy consumed without the presence of the heavyweight internal construction. The normalized energy consumption suggests that less overall energy reduction is observed for the cube with the internal slab. The combination of these results would imply the design consideration that heavyweight internal constructions do not benefit wall thermal mass performance in this climate region.

The results for the specific energy consumption and normalized consumption for slab thermal mass have been presented in Figure 9-10. These results indicate that the building with an internal slab uses more energy than buildings without an internal slab for the entire range of material properties. In addition, the normalized energy consumption suggests that the ability to optimize thermal mass with the presence of an internal slab decreases to 1.7%, much lower than the thermal mass performance of the slab without the internal partition. Therefore, this result indicates that the presence of a heavy internal slab is not recommended for optimum performance of the thermal mass of the slab.

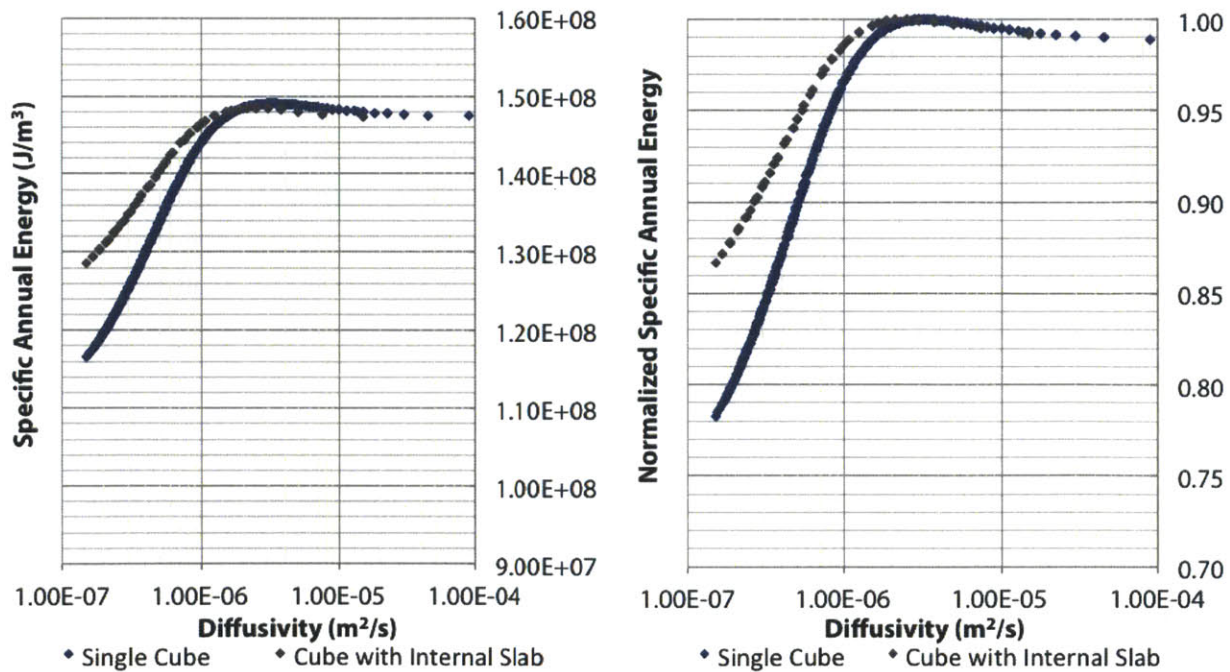


Figure 9-9 Specific Annual Energy Consumption (J/m³) vs Wall Diffusivity (m²/s) and Internal Slab, left, and Normalized Specific Annual Energy Consumption vs Wall Diffusivity (m²/s) and Internal Slab, right, San Francisco, CA

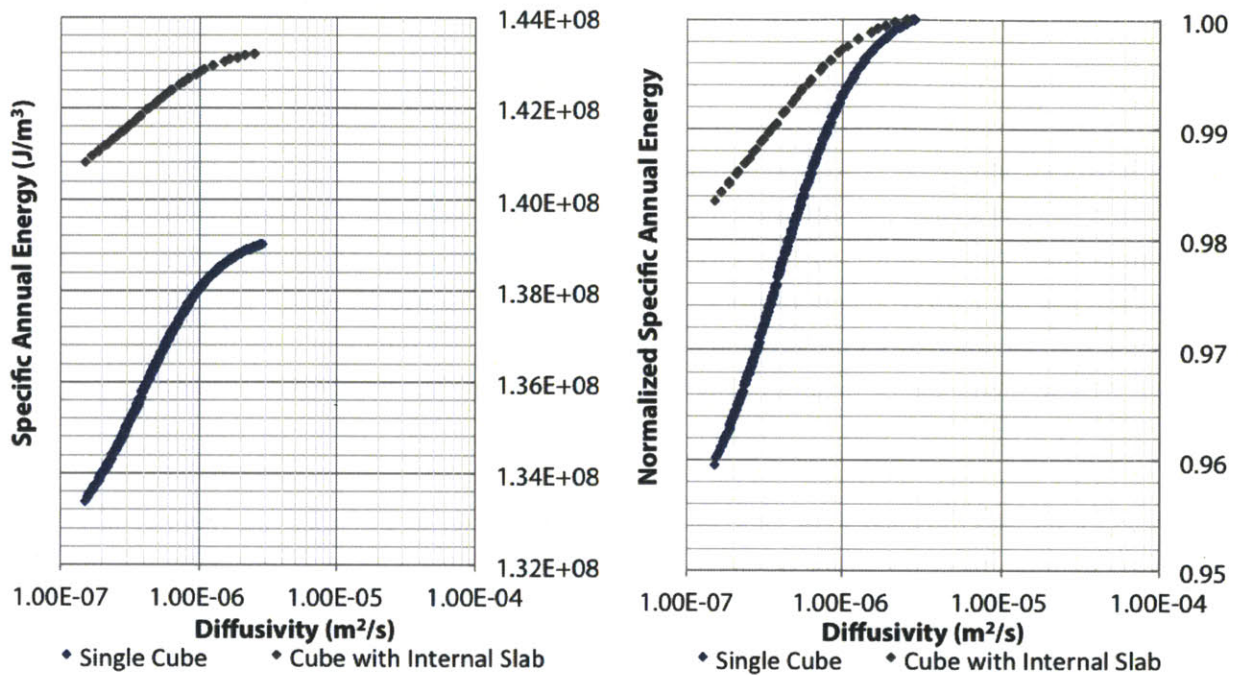


Figure 9-10 Specific Annual Energy Consumption ( $J/m^3$ ) vs Slab Diffusivity ( $m^2/s$ ) and Internal Slab, left, and Normalized Specific Annual Energy Consumption vs Slab Diffusivity ( $m^2/s$ ) and Internal Slab, right, San Francisco, CA

### 9.3.2 Phoenix, AZ - Hot, Dry Climate

The results for the annual energy consumption per volume and normalized consumption for wall thermal mass are shown in Figure 9-11. The results suggest that the cube with the internal slab uses more overall energy than the cube without this construction. In addition, the results of the normalized curve show a reduction in wall thermal mass performance to a savings of 2.4% for the heaviest wall constructions. The conclusion to be drawn from the combination of these results is that heavy internal slabs reduce the thermal mass performance of walls in Phoenix.

Looking at the specific annual energy consumption and normalized consumption for slab thermal mass in Figure 9-12, it is clear that the internal slab causes a similar shift in overall energy consumption of the building. The normalized results reinforce the notion that the presence of an internal slab will further reduce the impact of using a slab-on-grade in a thermal mass capacity in this climate. The data indicate that buildings with internal slabs have poor performance in Phoenix with regard to slab thermal mass.

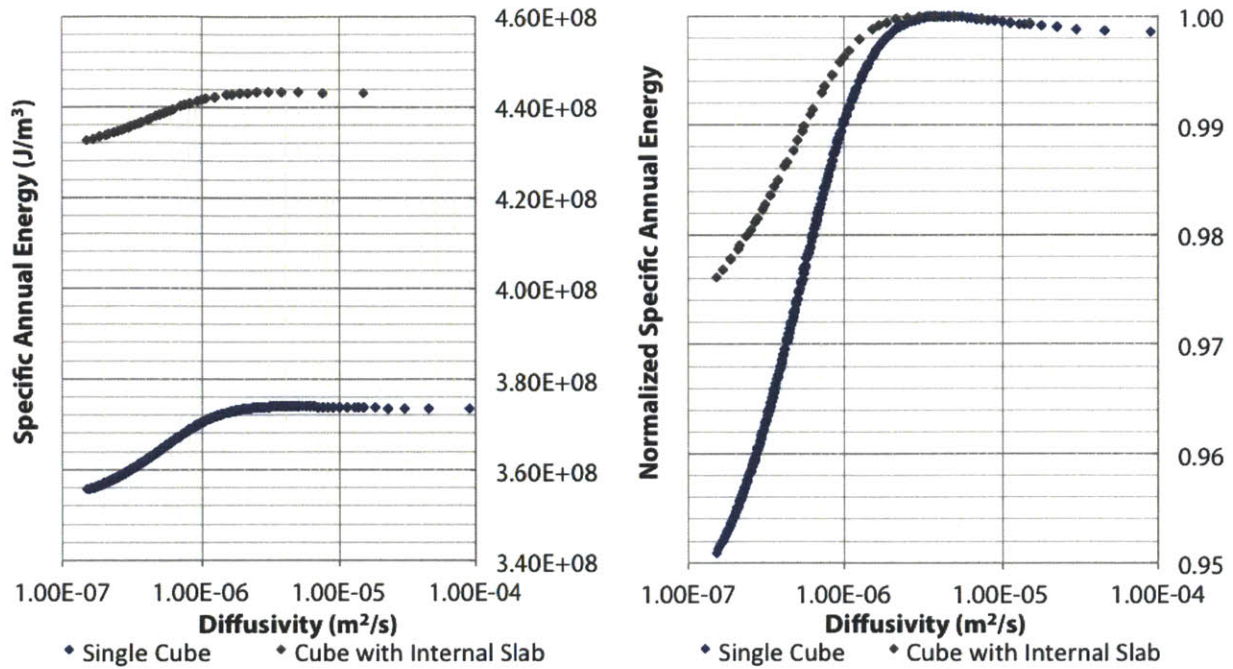


Figure 9-11 Specific Annual Energy Consumption ( $J/m^3$ ) vs Wall Diffusivity ( $m^2/s$ ) and Internal Slab, left, and Normalized Specific Annual Energy Consumption vs Wall Diffusivity ( $m^2/s$ ) and Internal Slab, right, Phoenix, AZ

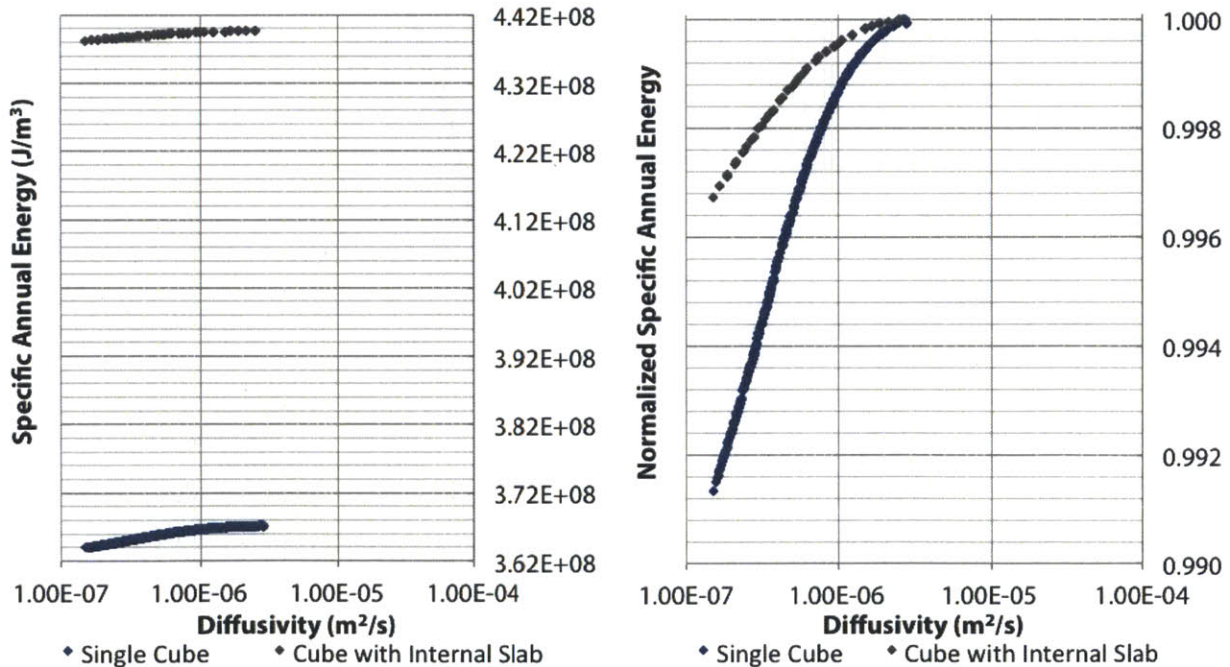


Figure 9-12 Specific Annual Energy Consumption ( $J/m^3$ ) vs Slab Diffusivity ( $m^2/s$ ) and Internal Slab, left, and Normalized Specific Annual Energy Consumption vs Slab Diffusivity ( $m^2/s$ ) and Internal Slab, right, Phoenix, AZ

### 9.3.3 Miami, FL - Hot, Humid Climate

The thermal mass performance of walls measured in specific annual consumption and normalized consumption is presented in Figure 9-13. The results suggest that the annual consumption increases with the addition of the internal slab and that the percentage optimization decreases. Since thermal mass of walls had poor performance in Miami for the basic cube, these results only reinforce the notion that thermal mass in a building with heavy-weight interior constructions will have even less impact.

Similar results for thermal mass of slabs shown in Figure 9-14 demonstrate the same impact on overall energy consumption as a result of the internal slab. The normalized results show a decrease in energy savings from thermal mass; however, the slim energy savings for the basic cube suggest that this result will not substantially impact the choice to construct with a given material in this climate. Therefore, the impact of the interior slab on energy performance is much greater than the impact of the thermal mass of the slab.

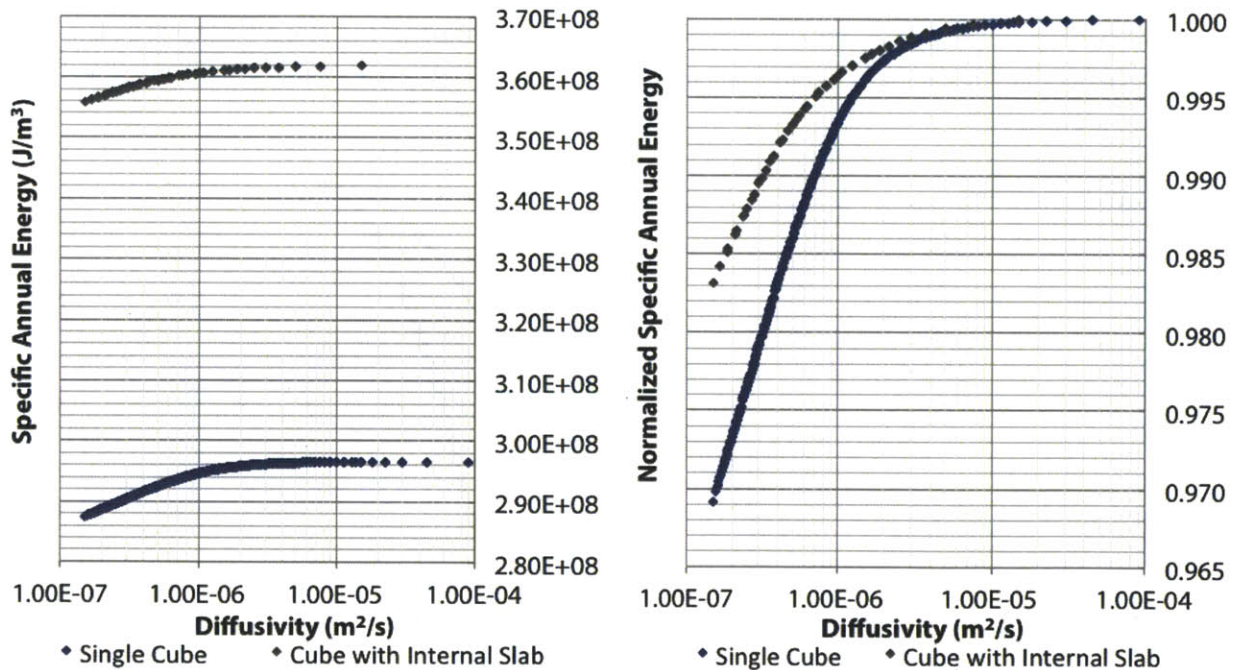


Figure 9-13 Specific Annual Energy Consumption (J/m<sup>3</sup>) vs Wall Diffusivity (m<sup>2</sup>/s) and Internal Slab, left, and Normalized Specific Annual Energy Consumption vs Wall Diffusivity (m<sup>2</sup>/s) and Internal Slab, right, Miami, FL



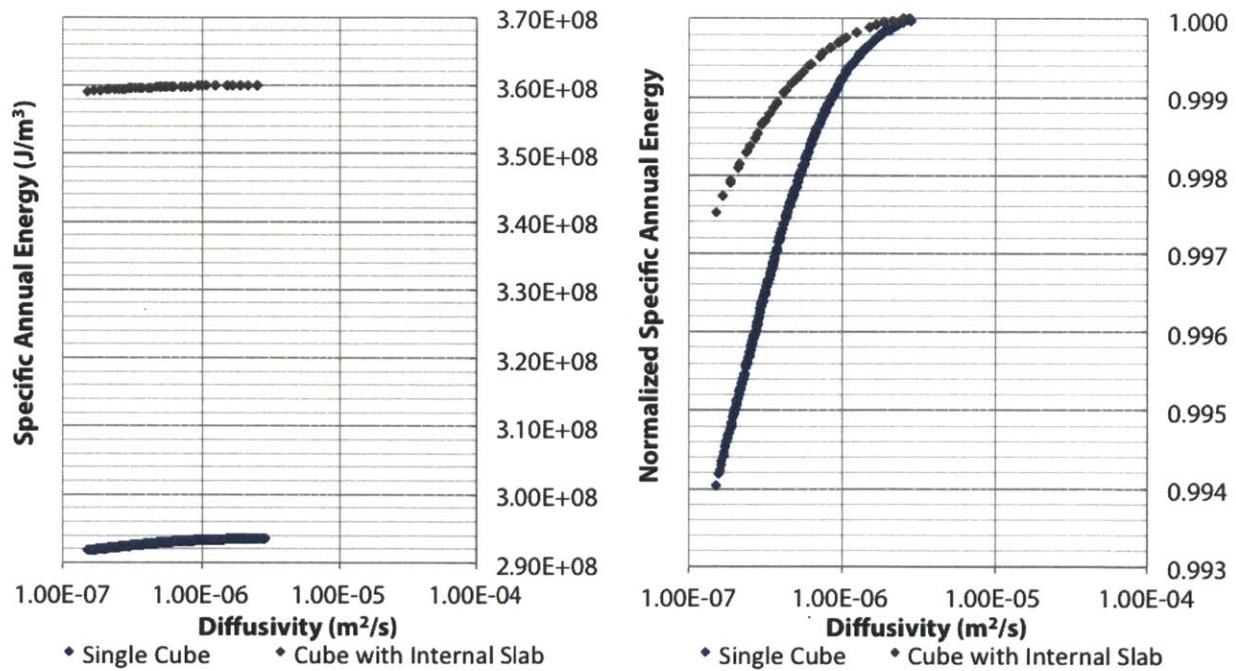


Figure 9-14 Specific Annual Energy Consumption (J/m<sup>3</sup>) vs Slab Diffusivity (m<sup>2</sup>/s) and Internal Slab, left, and Normalized Specific Annual Energy Consumption vs Slab Diffusivity (m<sup>2</sup>/s) and Internal Slab, right, Miami, FL

### 9.3.4 Anchorage, AK - Cold Climate

The specific annual energy consumption and the normalized values for wall thermal mass and Anchorage, AK are shown in Figure 9-15. The results show that the introduction of the internal slab results in increased overall energy consumption of the model. There is no overlap in the curves, so the impact of wall thermal mass cannot mitigate this increase. The normalized energy consumption curves demonstrate that thermal mass energy savings drop below 1% annually for the cube with the internal slab, suggesting that heavy internal constructions hinder the performance of the thermal mass of walls.

Looking at the energy consumption and its normalization for slab thermal mass in Figure 9-16, it is evident that similar trends of increased energy consumption from the internal construction and decreased normalized potential are seen. The graph indicates that slab thermal mass performance with an internal slab construction is just over 0.1%, suggesting that it should not be considered as a source of substantial energy savings in this climate.

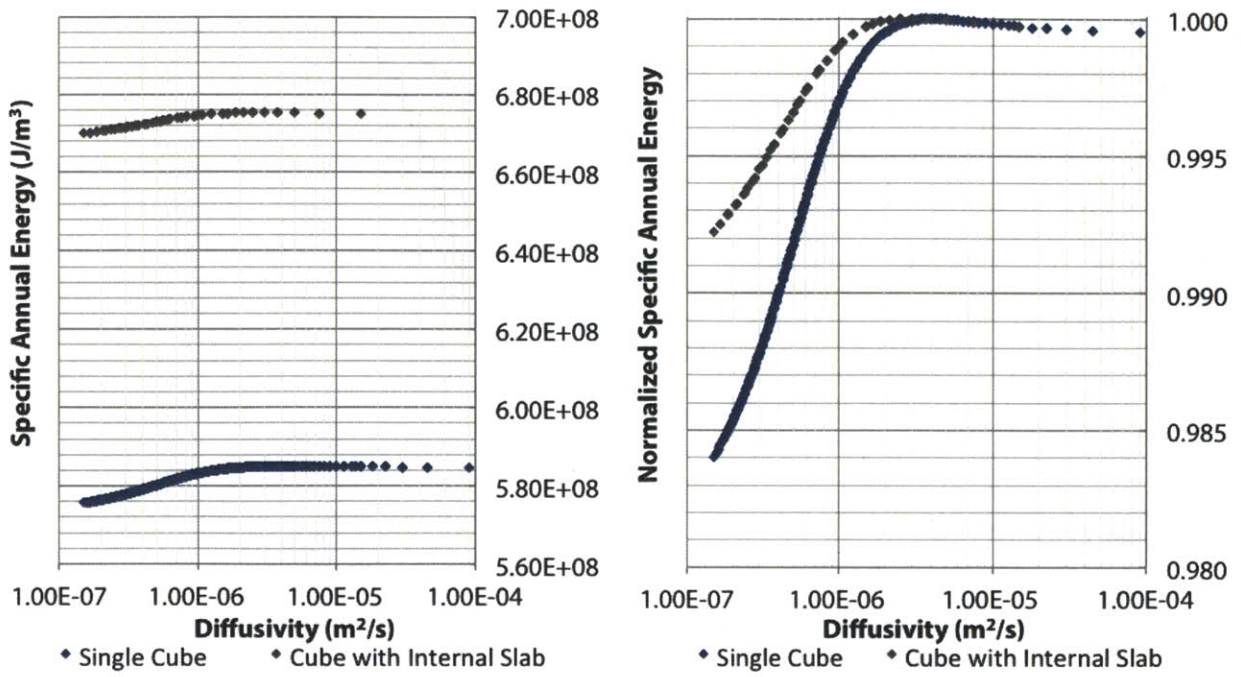


Figure 9-15 Specific Annual Energy Consumption (J/m<sup>3</sup>) vs Wall Diffusivity (m<sup>2</sup>/s) and Internal Slab, left, and Normalized Specific Annual Energy Consumption vs Wall Diffusivity (m<sup>2</sup>/s) and Internal Slab, right, Anchorage, AK

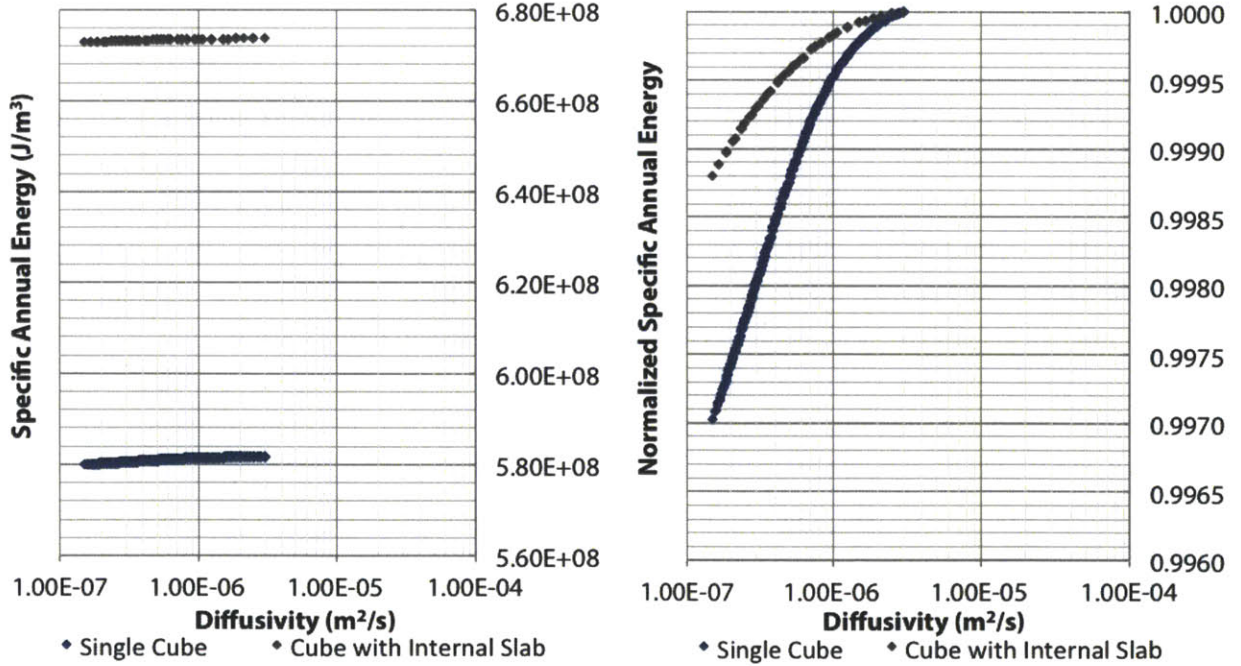


Figure 9-16 Specific Annual Energy Consumption (J/m<sup>3</sup>) vs Slab Diffusivity (m<sup>2</sup>/s) and Internal Slab, left, and Normalized Specific Annual Energy Consumption vs Slab Diffusivity (m<sup>2</sup>/s) and Internal Slab, right, Anchorage, AK

### **9.3.5 Discussion**

The results consistently show that internal slabs have a negative effect on both wall and slab thermal mass in all climates. This suggests that lightweight or minimal constructions should be used in a building with high mass constructions expected to perform in a given climate. These results could either indicate that there is an interaction of thermal mass components with one another or that there is a negative impact of adding too many high-mass components in a given building. Such speculation into the reasons for this behavior would need to be verified with a refined approach.

## **9.4 Modeling the Basement**

The ground assumption of the model is key in studying thermal mass, particularly the thermal mass impact of the slab. Since the ground floor slab is the parameter that was studied, changing the ground condition to a basement removes the ground contact with the surface that is modeled. This experiment tests the impact on thermal mass of the basement condition for both walls and slabs. In addition, it tests whether there is a difference between a conditioned or an unconditioned basement on the impact of thermal mass. For the purpose of the experiment, a 2.5 m basement of the same footprint of the building has been modeled and assumed to be completely below grade.

### **9.4.1 San Francisco, CA - Mild, Marine Climate**

The results for the specific annual energy consumption and normalized consumption for San Francisco and wall thermal mass are shown in Figure 9-17. The results show similar energy consumption magnitudes for the unconditioned basement and the slab-on-grade. The conditioned basement shows a lower energy consumption per volume because the ground contact results stabilizes the basement temperature. As a result, it works to lower the average conditioning energy per volume. Note that there is additional conditioned volume which will result in additional absolute energy consumption. The normalized results suggest that the thermal mass performance is greatest for the slab-on-grade, followed by the unconditioned basement. This trend suggests that the basement condition lowers the performance of wall thermal mass in this climate.

The results for slab thermal mass for annual energy consumption per volume and normalized consumption are shown in Figure 9-18. The energy consumption of the unconditioned basement is higher than the slab-on-grade while the energy consumption for the conditioned basement is lower. The overlap between the slab-on-grade and basement curves indicates that thermal mass can result in additional energy savings over the change of ground condition. The normalized energy results show that the basement condition improves thermal mass performance of the slab. The unconditioned basement has the best performance,

followed by the conditioned basement and slab-on-grade. Therefore, constructions without direct ground contact can be used for better thermal mass performance than those with ground contact. For the construction without ground contact, there is a substantial improvement in mass which can justify the added material. For ground contact conditions, the continuity of the system with the ground condition, by definition including high-mass soil, results in minimal improvement to energy consumption from the addition of mass into the system.

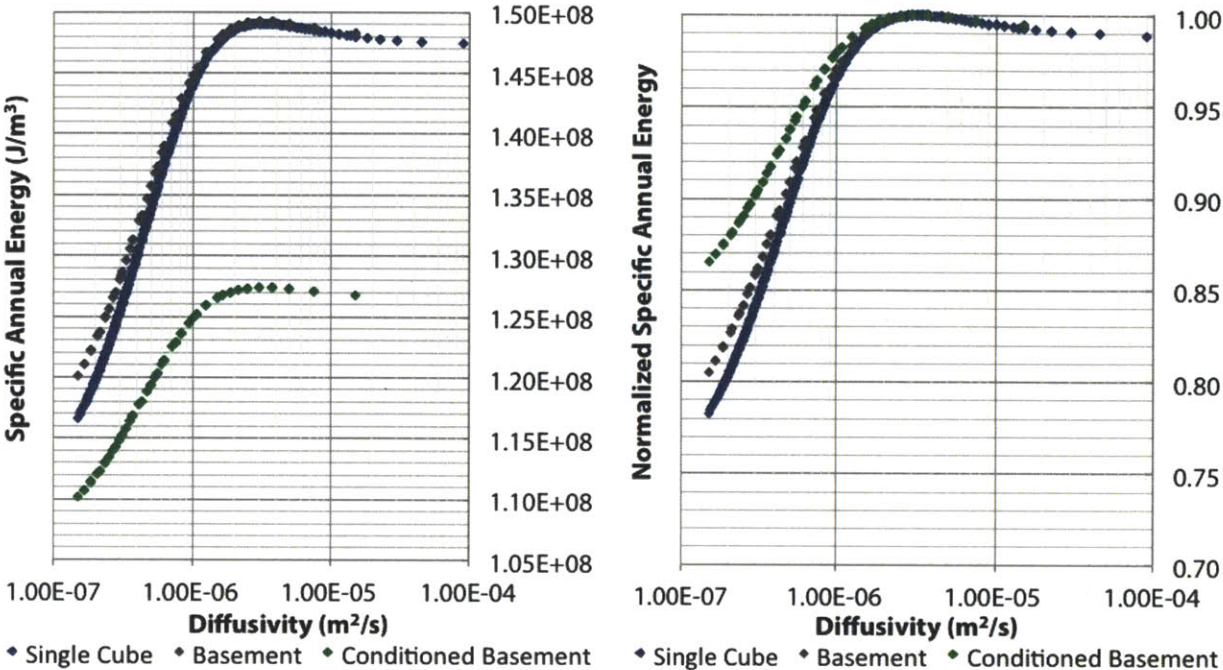


Figure 9-17 Specific Annual Energy Consumption (J/m<sup>3</sup>) vs Wall Diffusivity (m<sup>2</sup>/s) and Basement Condition, left, and Normalized Specific Annual Energy Consumption vs Wall Diffusivity (m<sup>2</sup>/s) and Basement Condition, right, San Francisco, CA

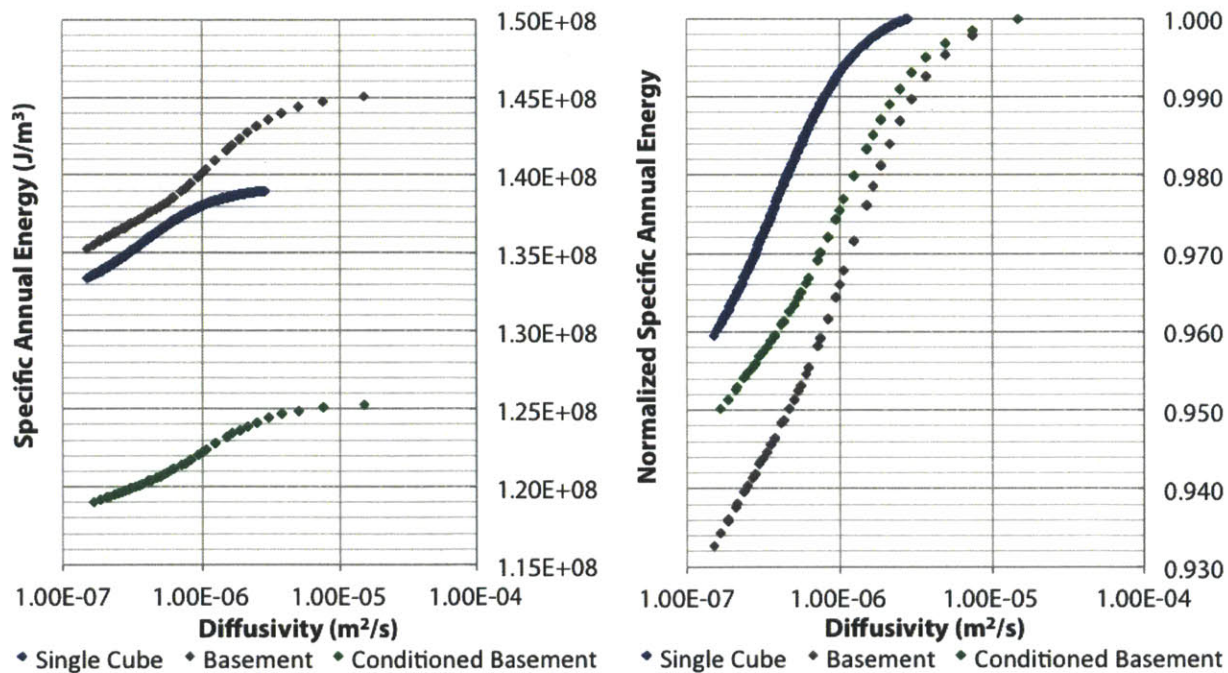


Figure 9-18 Specific Annual Energy Consumption ( $J/m^3$ ) vs Slab Diffusivity ( $m^2/s$ ) and Basement Condition, left, and Normalized Specific Annual Energy Consumption vs Slab Diffusivity ( $m^2/s$ ) and Basement Condition, right, San Francisco, CA

### 9.4.2 Phoenix, AZ - Hot, Dry Climate

Figure 9-19 presents the results for the annual energy consumption per volume and normalized consumption for wall thermal mass in Phoenix, AZ. These results suggest that there is a clear increase in energy between slab-on-grade and unconditioned basement. In contrast, there is a decrease in energy between slab-on-grade and conditioned basement when scaled by conditioned volume. There is a slight overlap in the curves for an unconditioned basement and a slab-on-grade, indicating that high-mass wall construction with a basement uses similar energy to lightweight construction and slab-on-grade. The normalized energy consumption suggests that the best wall performance exists for slab-on-grade construction, with unconditioned and conditioned basements trailing in that order. Given the relationship between overall energy consumption and the normalized results, from the perspective of wall thermal mass it is best to construct with slab-on-grade in Phoenix.

The slab results for specific annual energy consumption and its normalization are shown in Figure 9-20. The same order of the curves of overall energy consumption is observed, but the amount of thermal mass optimization is lower. As a result, there is no overlap among the curves and clear differences in the energy consumption by foundation type. The normalized results suggest that there is more potential to optimize the conditioned basement, followed closely by the unconditioned basement. This is the reverse

of the trend observed in San Francisco. Since the specific energy decreases and the thermal mass potential increases, one can capitalize on conditioned basement space to provide additional efficiency. However, it should be recalled that the increase in conditioned volume for the basement may result in additional energy demands not offset by thermal mass performance.

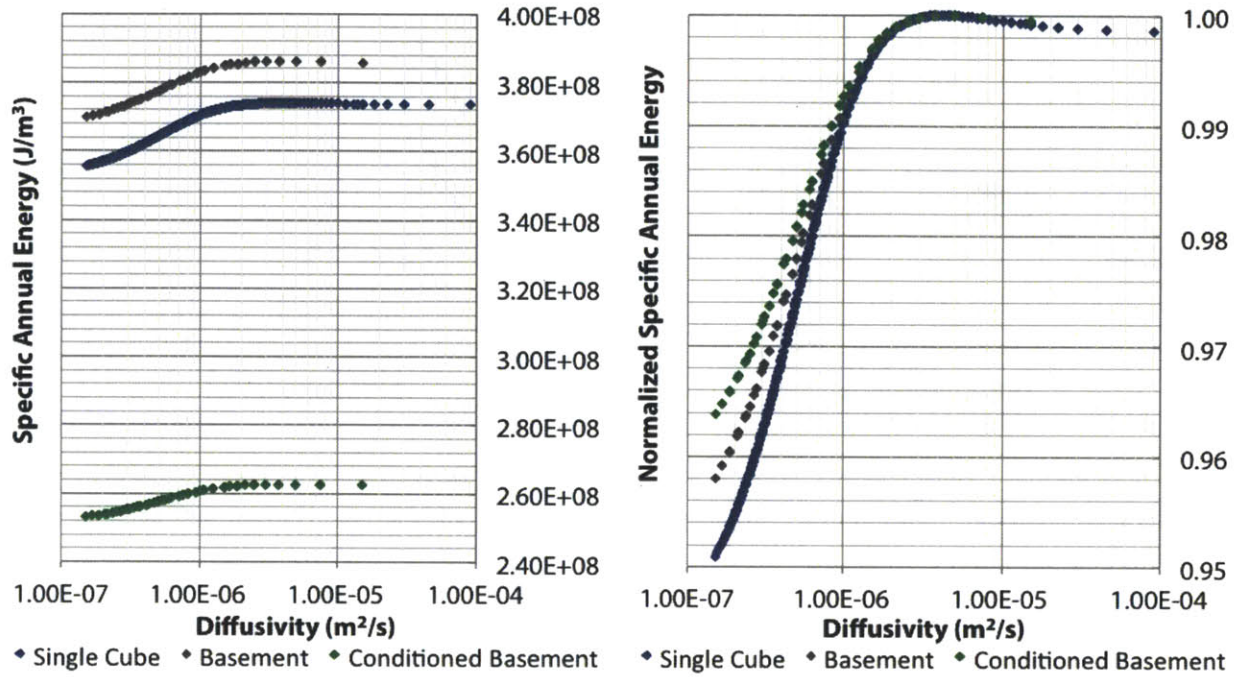


Figure 9-19 Specific Annual Energy Consumption (J/m³) vs Wall Diffusivity (m²/s) and Basement Condition, left, and Normalized Specific Annual Energy Consumption vs Wall Diffusivity (m²/s) and Basement Condition, right, Phoenix, AZ

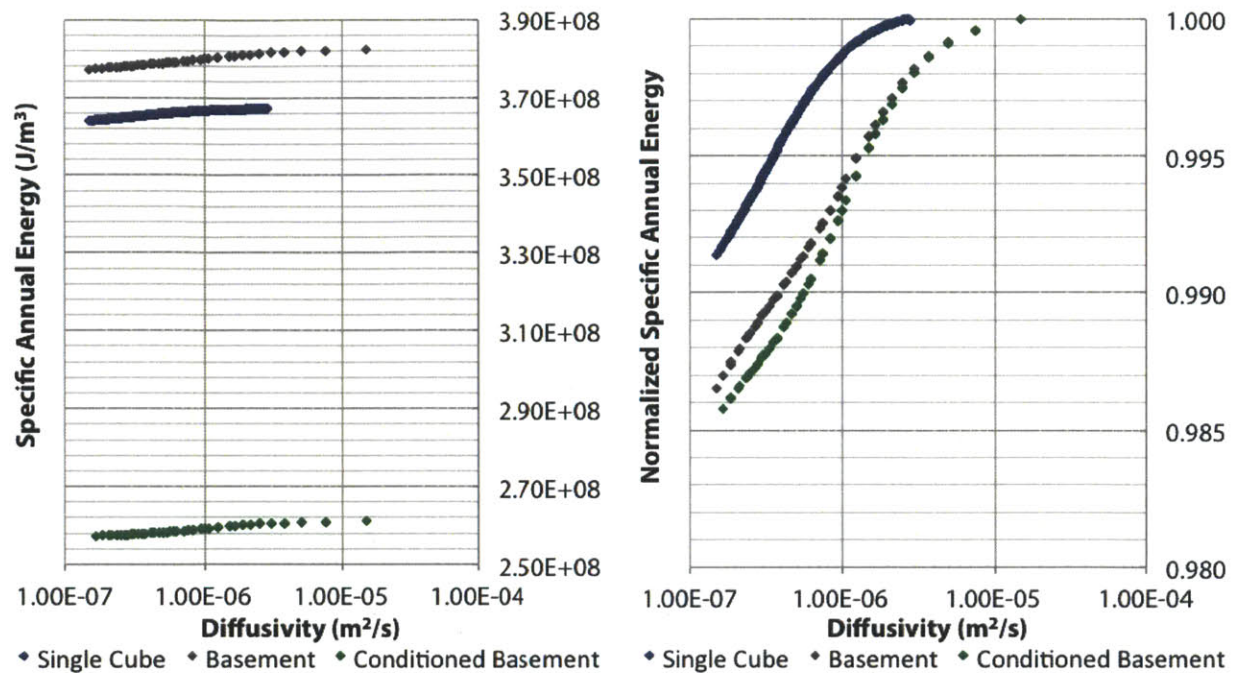


Figure 9-20 Specific Annual Energy Consumption (J/m<sup>3</sup>) vs Slab Diffusivity (m<sup>2</sup>/s) and Basement Condition, left, and Normalized Specific Annual Energy Consumption vs Slab Diffusivity (m<sup>2</sup>/s) and Basement Condition, right, Phoenix, AZ

### 9.4.3 Miami, FL - Hot, Humid Climate

The energy consumption per volume and normalized energy consumption for wall thermal mass and Miami are shown in Figure 9-21. The results suggest the same trend in overall energy consumption as the previous climates discussed, with conditioned basement lowest and unconditioned basement highest. There is no overlap in the overall energy consumption of the different construction types. The normalized energy consumption shows slab-on-grade construction has the best thermal mass performance and the conditioned basement has the worst. The combination of these results suggests that slab-on-grade construction is best for performance of wall thermal mass but not specific annual consumption.

Looking at the same relationships for slab thermal mass in Figure 9-22, the same order of energy curves is shown for the magnitude of energy consumption as expected for the same climate. The normalized energy consumption indicates that thermal mass performance is best in the conditioned basement condition and worst in the slab-on-grade condition. With consideration of the overall magnitudes, it seems that the ground condition has a much greater impact on energy consumption than the thermal mass performance of the slab. This means that specific energy consumption should be considered over slab thermal mass for the determination of the basement impact.

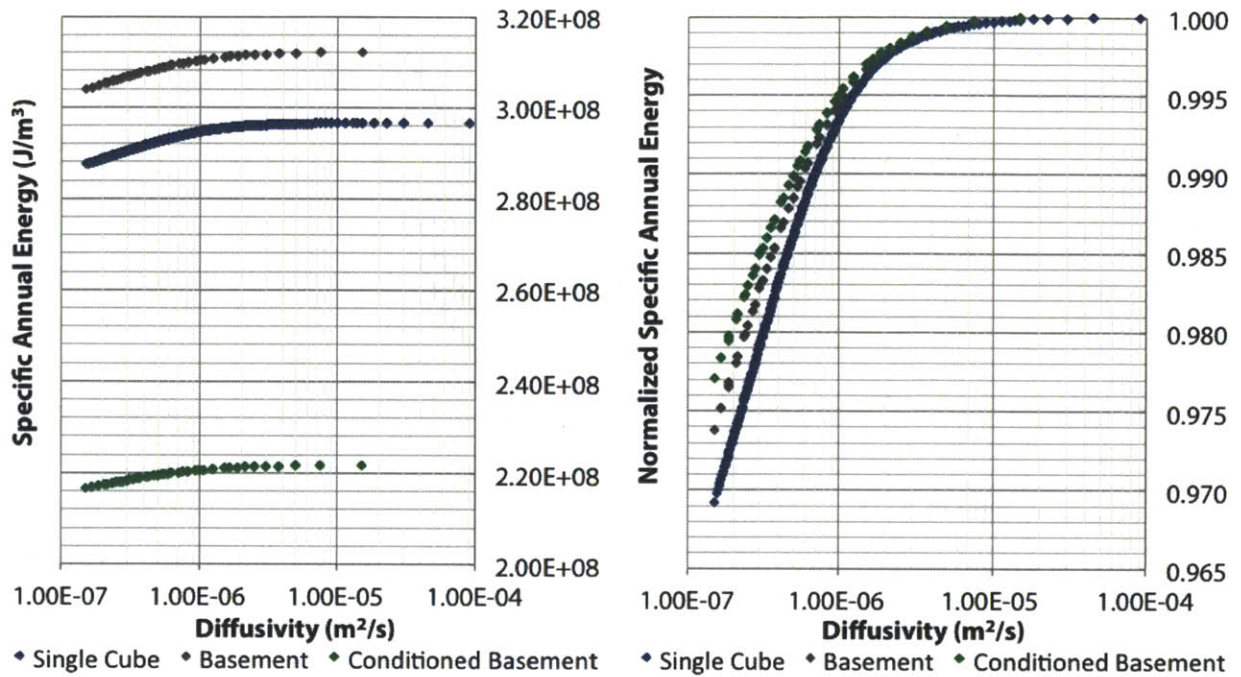


Figure 9-21 Specific Annual Energy Consumption ( $J/m^3$ ) vs Wall Diffusivity ( $m^2/s$ ) and Basement Condition, left, and Normalized Specific Annual Energy Consumption vs Wall Diffusivity ( $m^2/s$ ) and Basement Condition, right, Miami, FL

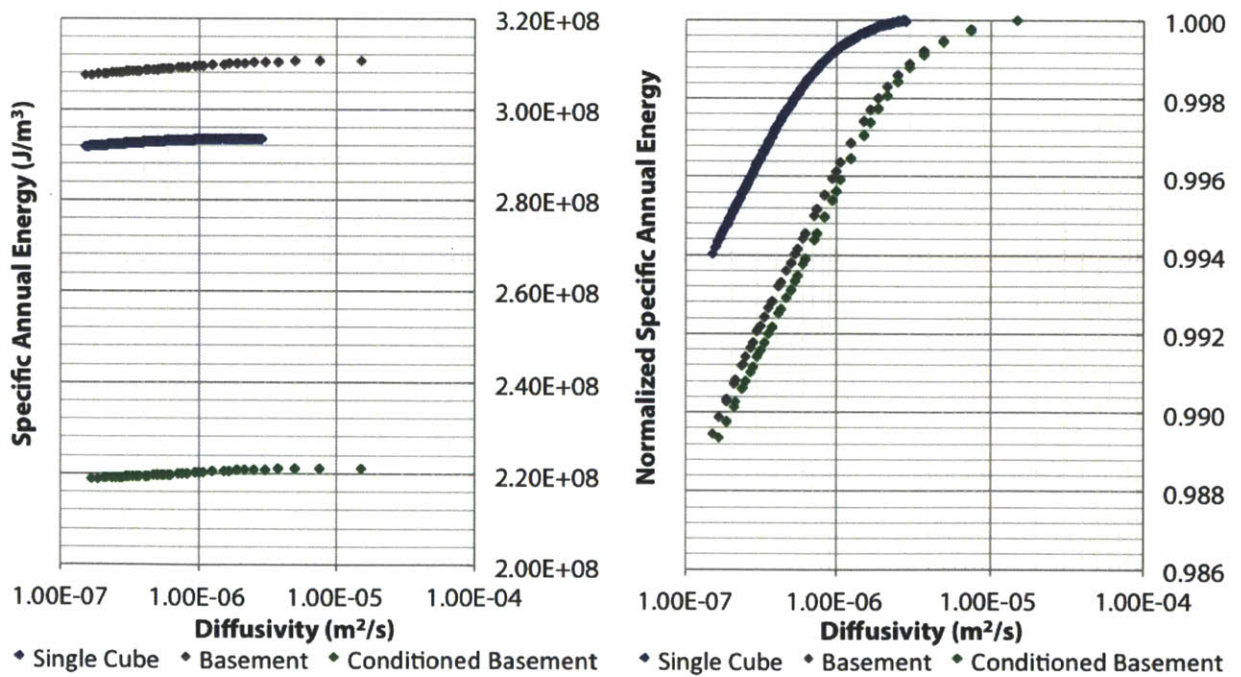


Figure 9-22 Specific Annual Energy Consumption ( $J/m^3$ ) vs Slab Diffusivity ( $m^2/s$ ) and Basement Condition, left, and Normalized Specific Annual Energy Consumption vs Slab Diffusivity ( $m^2/s$ ) and Basement Condition, right, Miami, FL



### 9.4.4 Anchorage, AK - Cold Climate

Figure 9-23 shows the specific annual energy consumption and its normalization for wall thermal mass performance in Anchorage. In consideration of overall energy consumption of the building, it is clear that the greatest energy is used by the unconditioned basement and the least energy is used by the conditioned basement. The normalized results suggest that the slab-on-grade has the best performance and the conditioned basement has the worst. Thermal mass is at its optimum for slab-on-grade construction, while the specific consumption is optimized for the conditioned basement. Given the small impact of thermal mass, the optimization of specific consumption would have greater impact.

The results for specific annual energy consumption and normalized consumption for slab thermal mass are presented in Figure 9-24. The same trend in overall energy consumption as the wall thermal mass is noted, which is to be expected for the same climate. The normalized values show that the unconditioned basement has the best thermal mass performance and the slab-on-grade has the worst performance. The actual energy saved for all ground conditions is minor in comparison with energy change from changing the foundation type. This suggests that modifying the foundation type will not result in strong improvements in thermal mass performance.

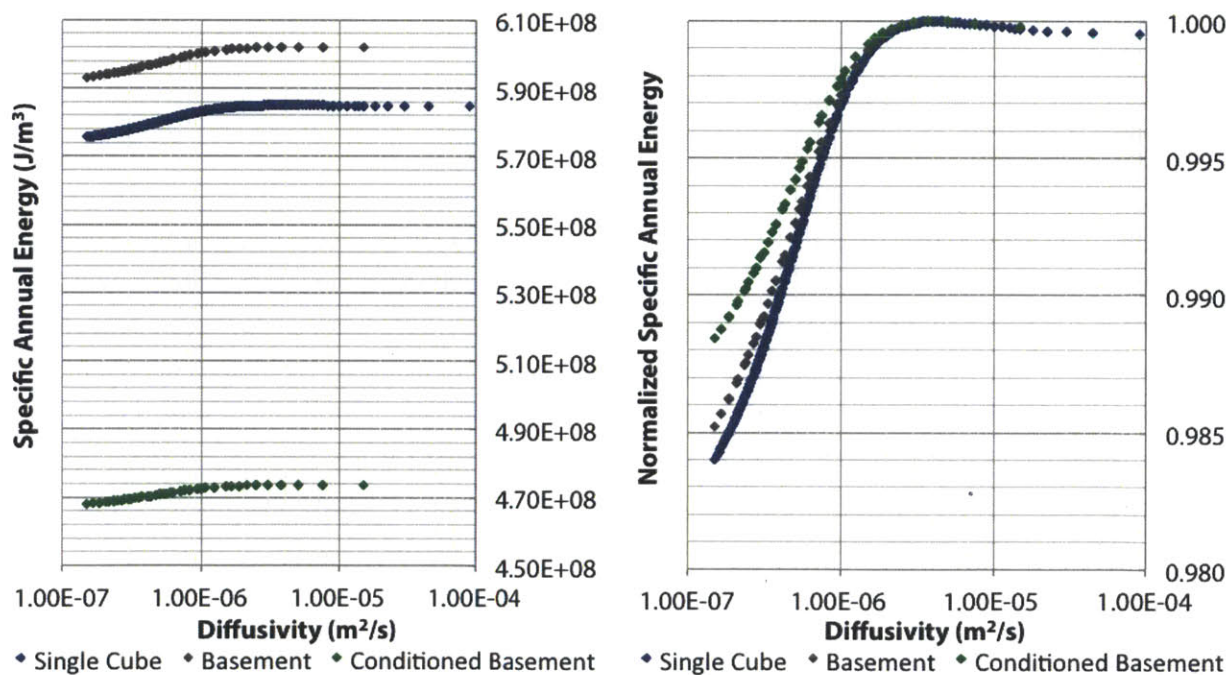


Figure 9-23 Specific Annual Energy Consumption (J/m<sup>3</sup>) vs Wall Diffusivity (m<sup>2</sup>/s) and Basement Condition, left, and Normalized Specific Annual Energy Consumption vs Wall Diffusivity (m<sup>2</sup>/s) and Basement Condition, right, Anchorage, AK

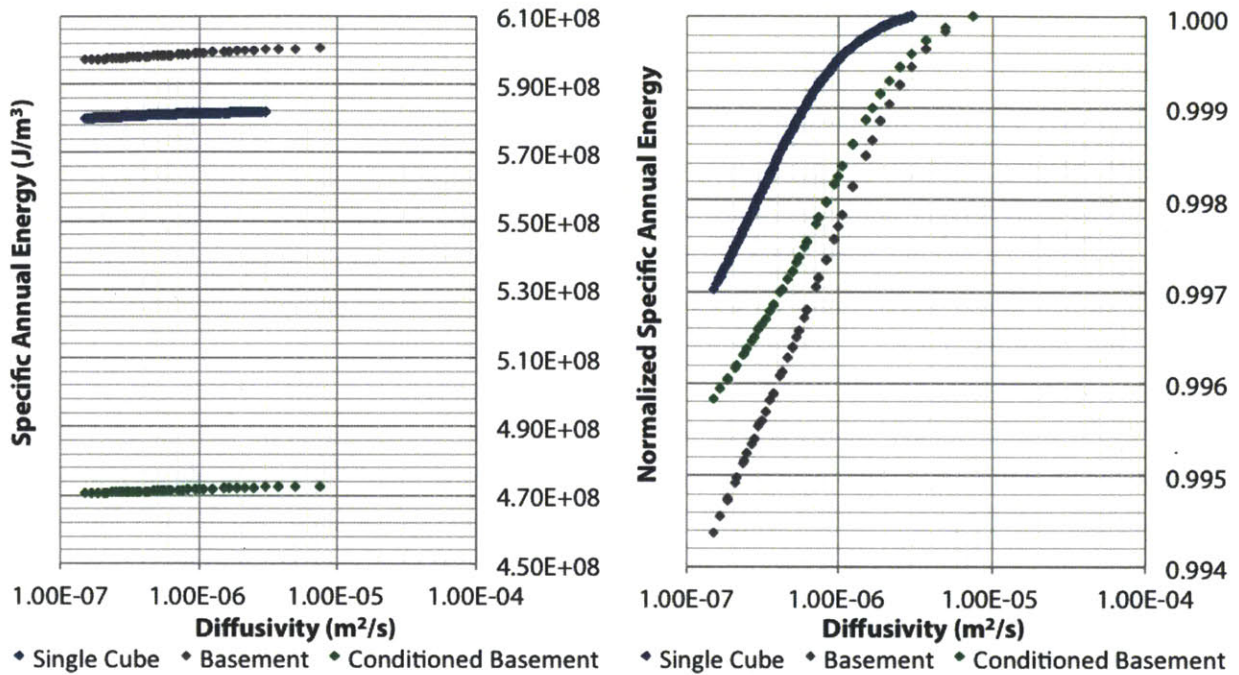


Figure 9-24 Specific Annual Energy Consumption ( $J/m^3$ ) vs Slab Diffusivity ( $m^2/s$ ) and Basement Condition, left, and Normalized Specific Annual Energy Consumption vs Slab Diffusivity ( $m^2/s$ ) and Basement Condition, right, Anchorage, AK

### 9.4.5 Discussion

The results of the comparison of ground conditions show that in all climates considered, conditioned basement construction uses the least specific energy and the unconditioned basement uses the most specific energy. The normalized energy results suggest that wall thermal mass performance is always best for slab-on-grade construction. Slab thermal mass shows best performance for the basement condition, though whether the conditioned or unconditioned basement has the best performance varies. The net result is that buildings which must have a basement may have greater benefits from slab thermal mass than those predicted in the main slab chapter, while buildings using wall thermal mass will have the best performance in the slab-on-grade condition.

## 9.5 Height Effects

The previous sections tested the impact of changing the nature of the geometry or boundary conditions of the geometry. This section will test changes to the size and shape of the cube itself. The height of the cube will be varied to determine the impact on thermal mass performance. To this end, one experiment will increase the cube height while maintaining the floor area constant, while a second experiment will

increase the height while maintaining the volume constant. Cube heights of 6 m and 8 m have been compared against the 4 m baseline cube assumption.

### **9.5.1 San Francisco, CA - Mild, Marine Climate**

The results for the wall diffusivity and both annual energy consumption per volume and normalized energy consumption are shown in Figure 9-25. The results show that buildings where the height alone was increased consume less energy per volume, whereas cubes with the same volume and increased height consume close to the same energy at high mass construction and greater energy at low mass construction. Looking at the normalized relationships, it is clear that increasing height will result in some increased performance of wall thermal mass while the volume-constant increase of height results in a greater increase. Therefore, taller buildings of more compact floor plan have better performance of wall thermal mass.

Looking at the equivalent results for slab thermal mass in Figure 9-26, there is much less overlap among the curves for overall energy consumption, with the exception of the 10x10x4m cube and the 8.16x8.16x6m cube. This indicates that, at constant volume, moderate increases in height benefit specific consumption for lightweight construction but larger increases have the opposite effect. The cubes at constant floor plan and increased height use less energy per volume. Normalizing these results, it is clear that slab thermal mass suffers worse performance for taller buildings, with the constant volume experiment showing a sharper decline in performance than the constant floor plan. Thus, taller buildings show worse performance of slab thermal mass.

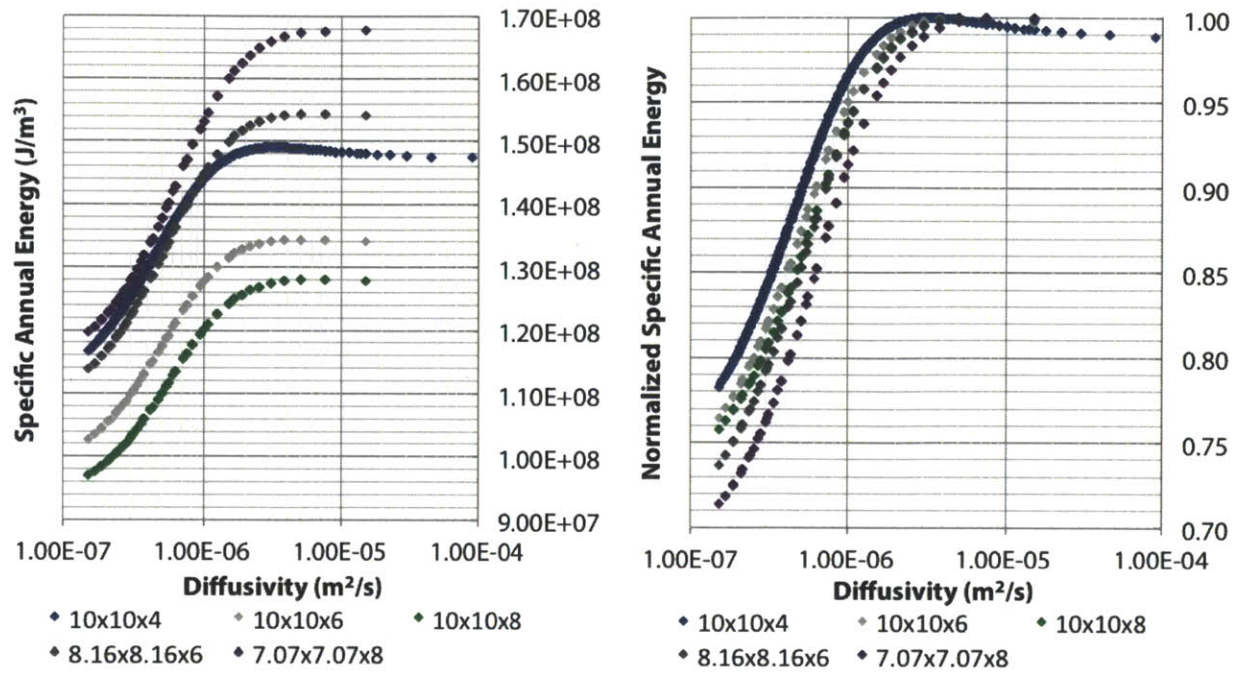


Figure 9-25 Specific Annual Energy Consumption ( $J/m^3$ ) vs Wall Diffusivity ( $m^2/s$ ) and Building Height (m), left, and Normalized Specific Annual Energy Consumption vs Wall Diffusivity ( $m^2/s$ ) and Building Height (m), right, San Francisco, CA

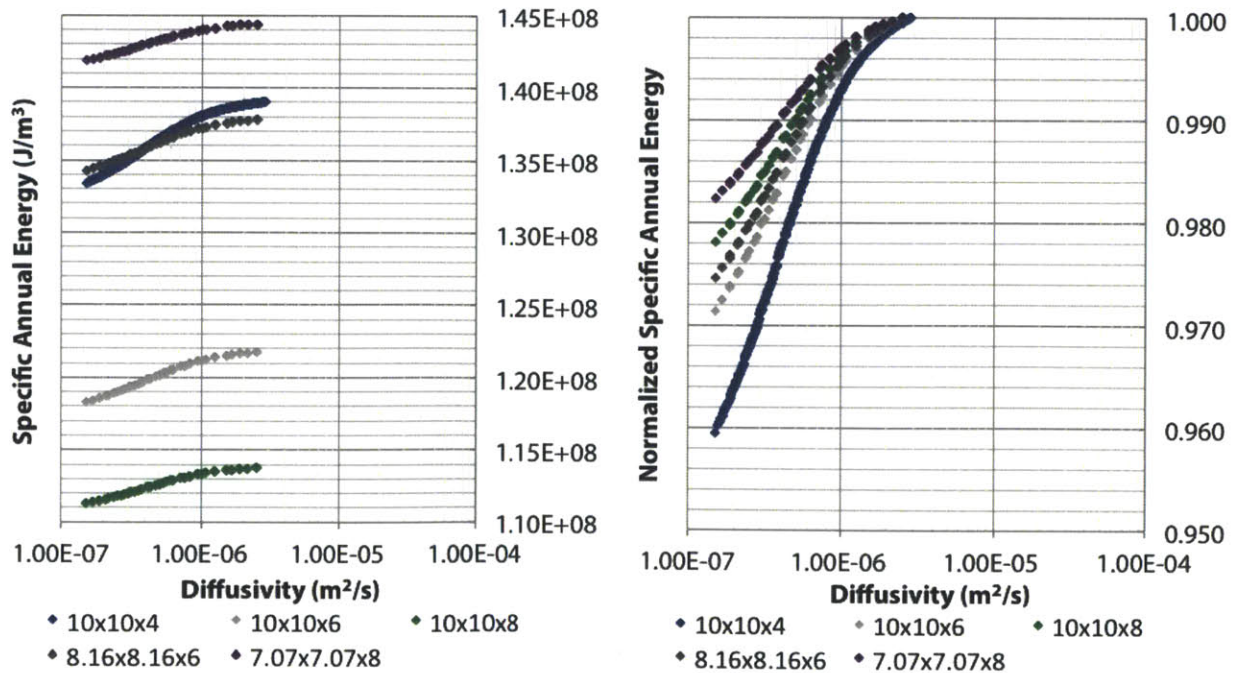


Figure 9-26 Specific Annual Energy Consumption ( $J/m^3$ ) vs Slab Diffusivity ( $m^2/s$ ) and Building Height (m), left, and Normalized Specific Annual Energy Consumption vs Slab Diffusivity ( $m^2/s$ ) and Building Height (m), right, San Francisco, CA

## 9.5.2 Phoenix, AZ - Hot, Dry Climate

The results for wall thermal mass for overall and normalized energy consumption are shown in Figure 9-27. These results show lower energy consumption per volume for all configurations increasing the height, but with the order of these configurations not progressing as consistently as San Francisco (compare with Figure 9-25). This indicates that there may be an optimum aspect ratio for a constant volume, as the tallest cube uses more energy than the middle cube but less than the baseline experiment. The normalized results suggest that the original cube configuration has the poorest performance of thermal mass, with changes in height alone resulting in some increase and changes in both height and footprint showing the greatest improvement. Since the height effect also decreases energy consumption in Phoenix, optimizing wall thermal mass can be obtained by increasing the building height at constant volume.

Looking at the annual energy consumption per volume and its normalized quantities for slab thermal mass in Figure 9-28, the same vertical order of overall energy consumption curves is observed, as would be expected for the same climate condition. The overlap of the curves is very minor, suggesting that thermal mass cannot be used to achieve the same performance as another geometrical configuration. The thermal mass normalization graph indicates that the best performance is from the baseline cube, with increases in height and compactness reducing the effectiveness of slab thermal mass. Given the decrease in overall energy per volume in relation to the magnitude of potential energy savings from thermal mass, it may be prudent to optimize the aspect ratio for a quantity other than slab thermal mass.

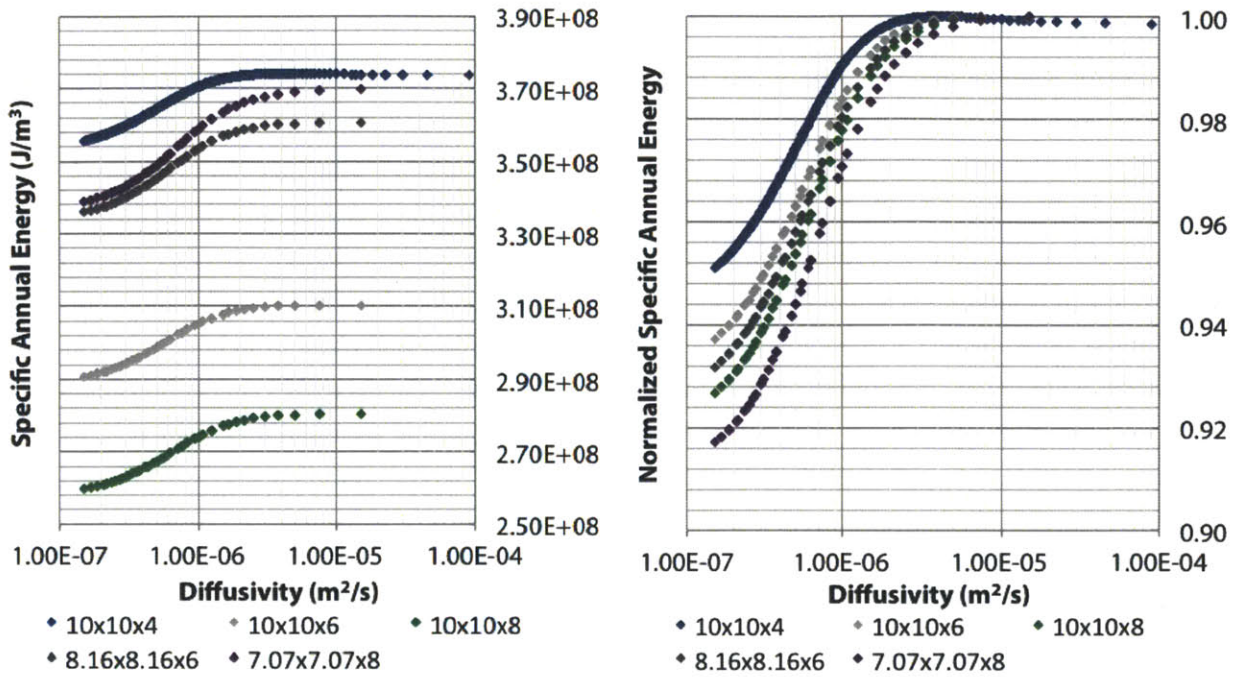


Figure 9-27 Specific Annual Energy Consumption (J/m<sup>3</sup>) vs Wall Diffusivity (m<sup>2</sup>/s) and Building Height (m), left, and Normalized Specific Annual Energy Consumption vs Wall Diffusivity (m<sup>2</sup>/s) and Building Height (m), right, Phoenix, AZ

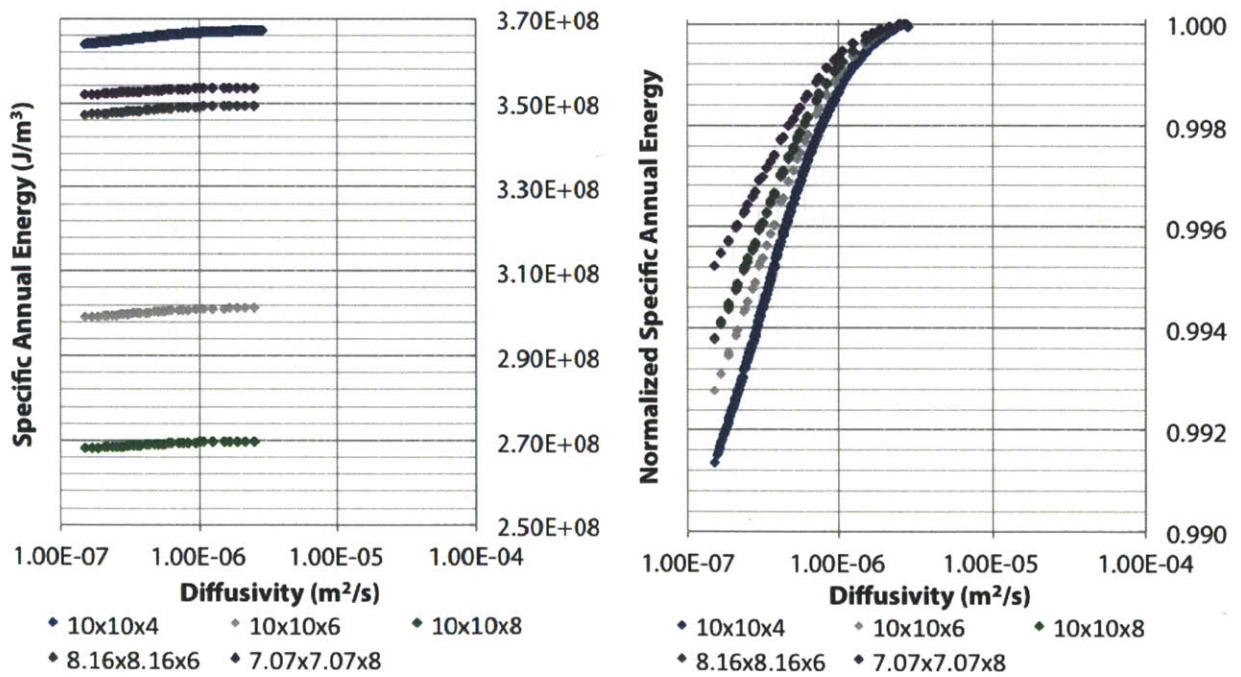


Figure 9-28 Specific Annual Energy Consumption (J/m<sup>3</sup>) vs Slab Diffusivity (m<sup>2</sup>/s) and Building Height (m), left, and Normalized Specific Annual Energy Consumption vs Slab Diffusivity (m<sup>2</sup>/s) and Building Height (m), right, Phoenix, AZ

### 9.5.3 Miami, FL - Hot, Humid Climate

The results for annual and normalized energy consumption per volume for wall thermal mass are presented in Figure 9-29. These results suggest that energy consumption per volume decreases for taller construction, more for taller buildings of the same footprint than taller buildings of the same volume. The results for the performance of thermal mass indicate that thermal mass has a much greater impact for taller buildings; the tallest, most compact cube shows nearly double the thermal mass savings of the baseline cube. This indicates that in Miami, changing the aspect ratio of building construction may make the difference between effective and ineffective wall thermal mass performance employed in the passive sense.

Likewise, the results for slab thermal mass are presented in Figure 9-30. While showing the same overall trend in energy consumption magnitudes, the small overlap of the curves due to minimal slab thermal mass performance in Miami indicates that thermal mass is not much of a deciding factor for overall energy consumption. The normalized energy consumption shows that increasing the height decreases slab thermal mass performance, as does decreasing the footprint of the building. Since all magnitudes of energy impact are low, this result suggests that aspect ratio cannot be used to improve thermal mass performance of slabs in Miami.

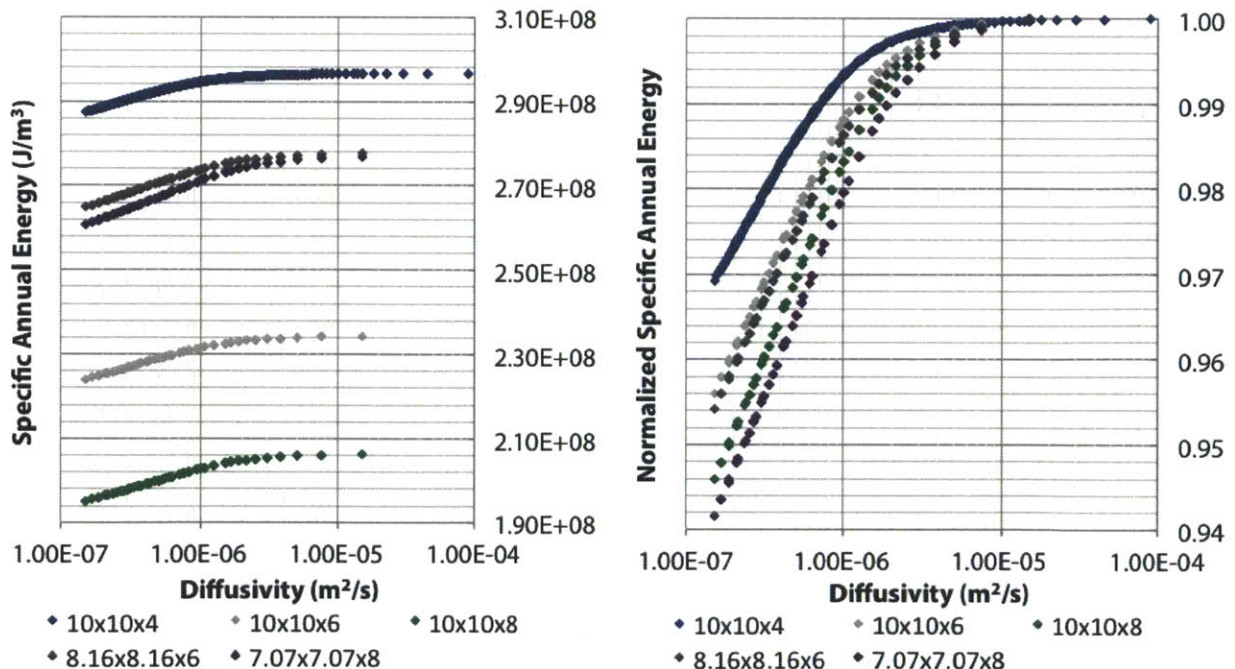


Figure 9-29 Specific Annual Energy Consumption ( $J/m^3$ ) vs Wall Diffusivity ( $m^2/s$ ) and Building Height (m), left, and Normalized Specific Annual Energy Consumption vs Wall Diffusivity ( $m^2/s$ ) and Building Height (m), right, Miami, FL

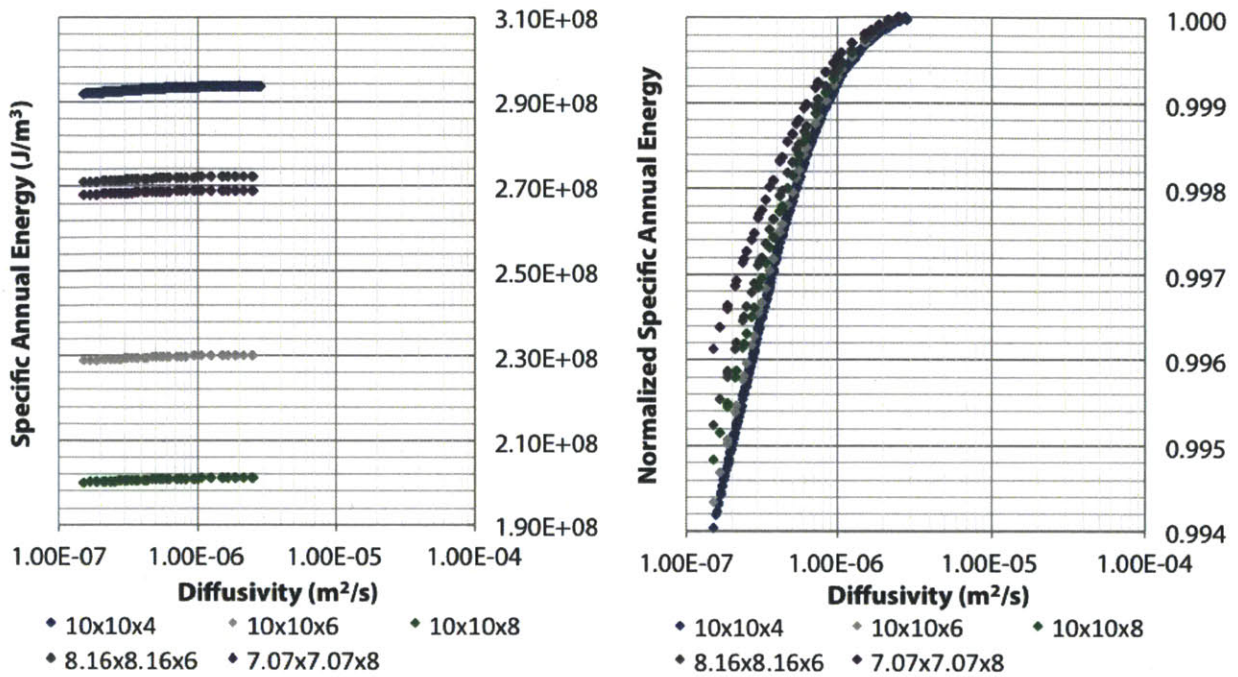


Figure 9-30 Specific Annual Energy Consumption ( $J/m^3$ ) vs Slab Diffusivity ( $m^2/s$ ) and Building Height (m), left, and Normalized Specific Annual Energy Consumption vs Slab Diffusivity ( $m^2/s$ ) and Building Height (m), right, Miami, FL

### 9.5.4 Anchorage, AK - Cold Climate

The results for annual and normalized energy consumption for wall thermal mass in Anchorage are shown in Figure 9-31. These results suggest that changes in height for the same volume show much smaller changes in overall specific energy consumption than changes in height for the same footprint. Looking at the normalized results, increasing the height at the same footprint shows some improvement and increasing the height at constant volume shows additional improvement over the baseline case. While the overall energy savings are still somewhat modest, it indicates that aspect ratio plays a role in wall thermal mass performance in Anchorage.

Similar results for slab thermal mass are presented in Figure 9-32. The results show that there is less energy consumption per volume for increased height for constant volume experiments to a point before rising again. In contrast, all increases in volume for the same footprint show decreases in overall consumption. The normalized results show that the baseline cube has the best performance of slab thermal mass, suggesting that wider, flatter buildings are a better design type for the phenomenon. Since the overall benefit of slab thermal mass is minor in this climate, however, it is unwise to optimize solely for its improvement.



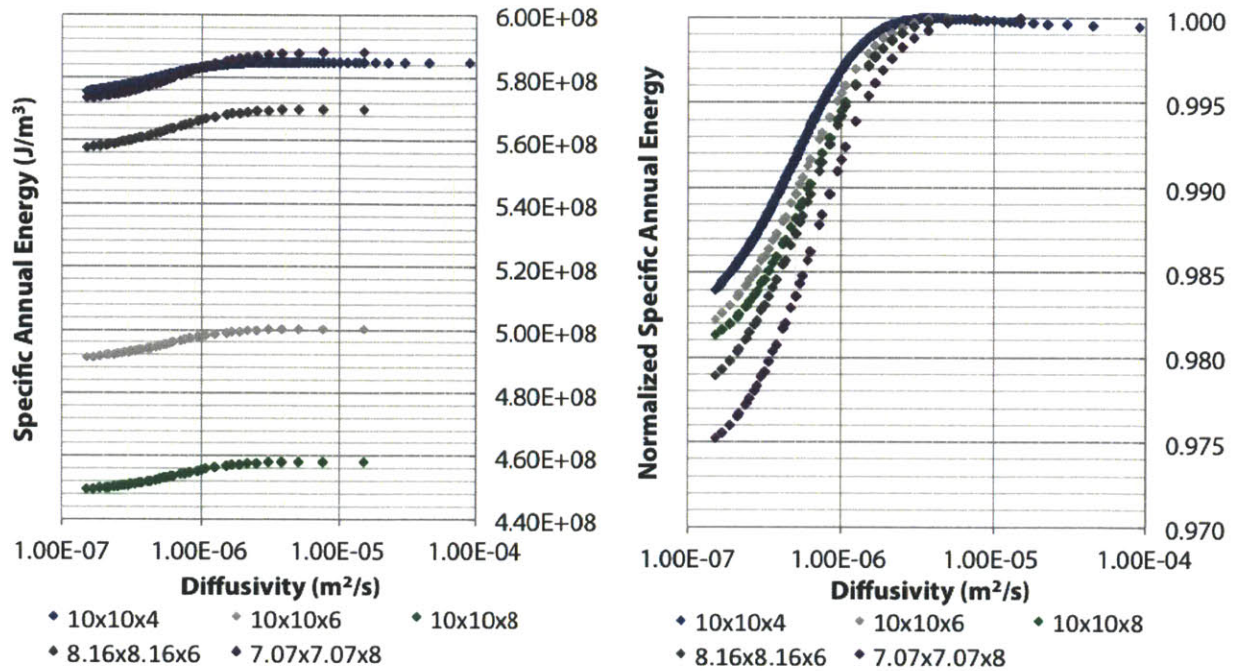


Figure 9-31 Specific Annual Energy Consumption ( $J/m^3$ ) vs Wall Diffusivity ( $m^2/s$ ) and Building Height (m), left, and Normalized Specific Annual Energy Consumption vs Wall Diffusivity ( $m^2/s$ ) and Building Height (m), right, Anchorage, AK

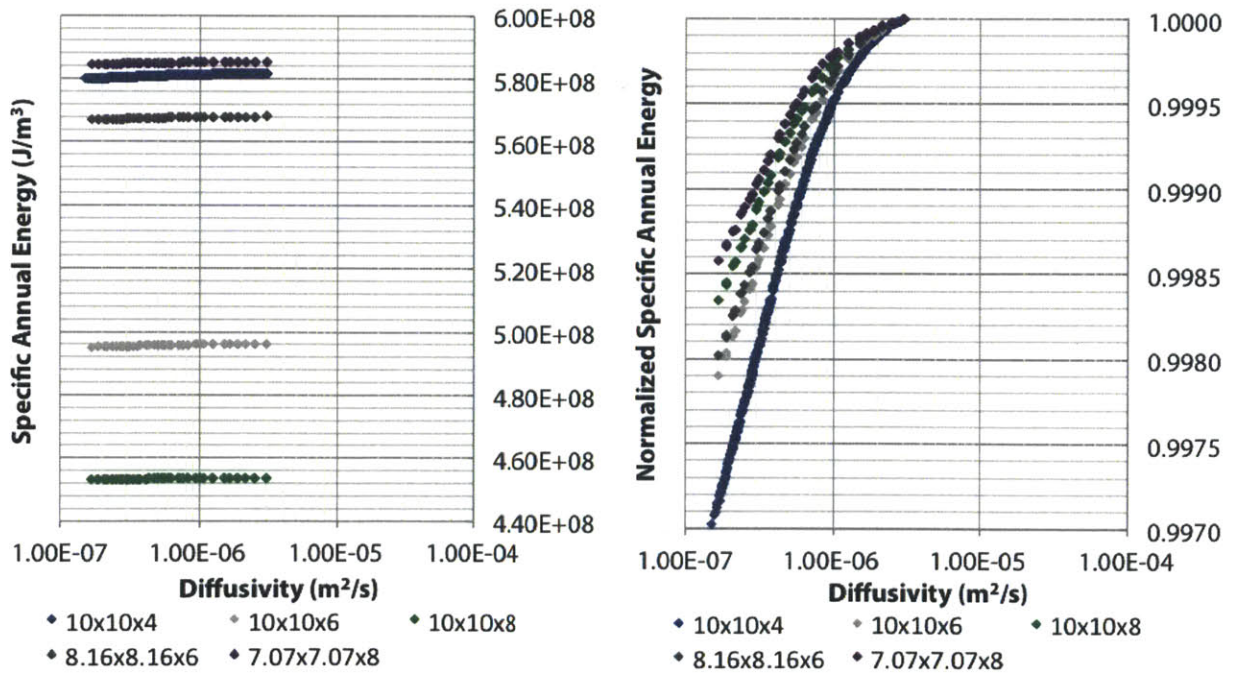


Figure 9-32 Specific Annual Energy Consumption ( $J/m^3$ ) vs Slab Diffusivity ( $m^2/s$ ) and Building Height (m), left, and Normalized Specific Annual Energy Consumption vs Slab Diffusivity ( $m^2/s$ ) and Building Height (m), right, Anchorage, AK

### 9.5.5 Discussion

The results above indicate that there is benefit for increasing height for improved performance of wall thermal mass but not of slab thermal mass. Further analysis of the trends of optimization suggests that there are two different relationships versus aspect ratio: one for constant footprint and one for constant volume. Figure 9-33 shows the relationship for constant footprint, which provides verification that there is same or better performance for taller buildings for wall thermal mass and a decline for slab thermal mass. Figure 9-34 shows the same trends for constant volume but the effect is amplified so that the effect occurs with a steeper slope in both cases. Therefore, changing aspect ratio will provide similar results to thermal mass regardless of the experiment, but the constant volume experiments provide sharper increases for wall thermal mass.

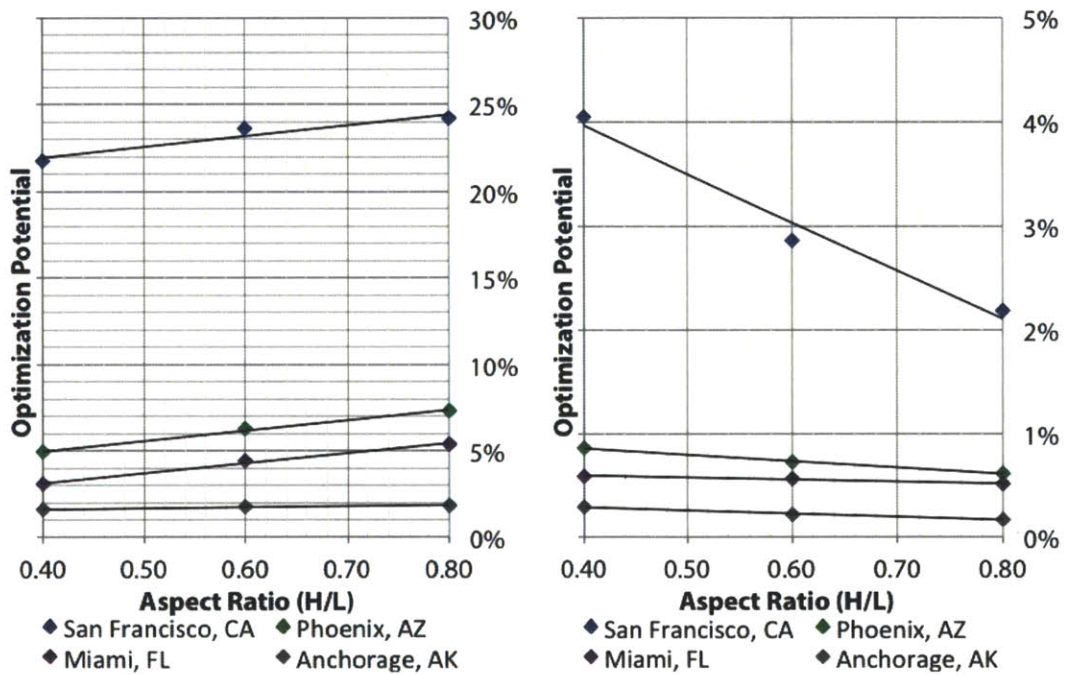


Figure 9-33 Potential Energy Savings from Thermal Mass vs Building Height (m), Constant Footprint, Walls (left) and Slabs (right)

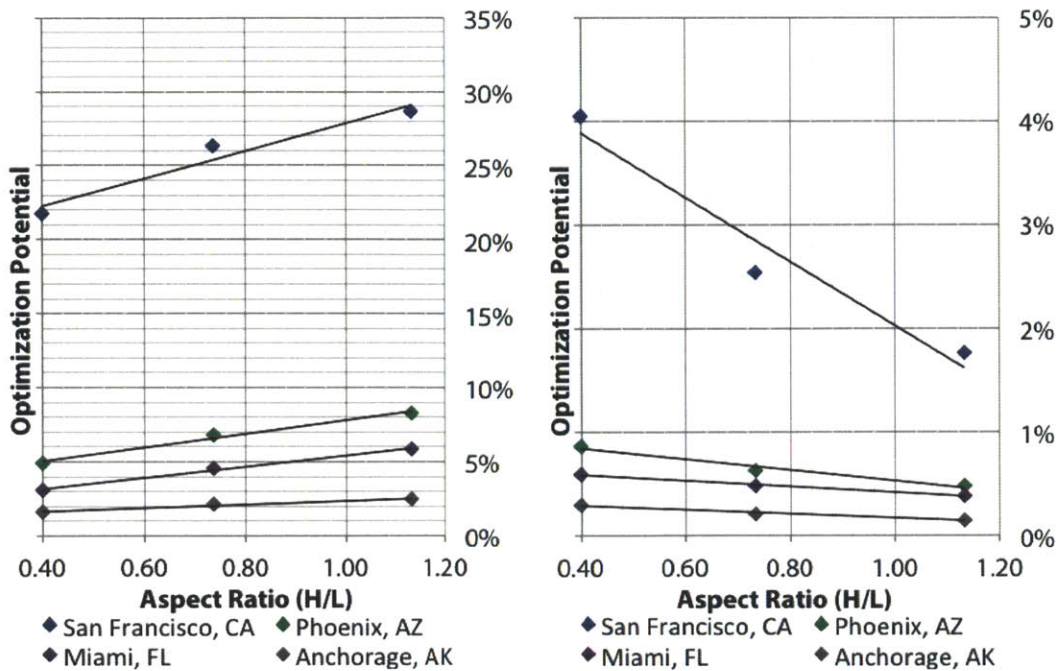


Figure 9-34 Potential Energy Savings from Thermal Mass vs Building Height (m), Constant Volume, Walls (left) and Slabs (right)

## 9.6 Plan Aspect Ratio Effects

In addition to the height of the cube, it is important to study whether changing the cube into a rectangular building that is either aligned N-S or E-W will benefit the impact of thermal mass on the construction. Therefore, in addition to the 10 m by 10 m cube, a 13.33 m by 7.5 m cube and a 20 m by 5 m cube have been modeled in both directions. For the purpose of this discussion, a cube aligned N-S has its long dimension in this direction, meaning the faces on the north and south of the building are shorter than the east-west faces. A cube aligned E-W has the opposite geometric configuration.

### 9.6.1 San Francisco, CA - Mild, Marine Climate

The results for annual energy consumption per volume and normalized consumption are shown in Figure 9-35. This diagram indicates that the lowest overall energy consumption is for the cube plan, while increasingly rectangular buildings will result in higher overall energy consumption. There is great overlap in the thermal mass curve, meaning that high mass construction can be used to obtain the energy performance of a more square building in cases where the form is dictated by other concerns. The ability to optimize thermal mass performance, as indicated by the normalized energy consumption, provides evidence that there is little cross-correlation between the plan aspect ratio and the thermal mass potential

savings. The buildings with slightly better performance are the ones that are the least square regardless of orientation, which likely suggests that these are surface area driven phenomena.

The similar results for the slab thermal mass are shown in Figure 9-36. The order of the energy consumption curves is the same, but the distance between the curves has increased while the amount of energy savings from thermal mass has decreased. This suggests that long, narrow buildings of either orientation would have definitively worse energy performance than any weight construction in a more square form factor. The normalized results show that the square structure has the best slab thermal mass performance, with the performance of the more narrow construction forms lagging behind. The combination of these two results suggests that buildings as square as possible are most effective in reducing energy consumption, with or without the use of slab thermal mass.

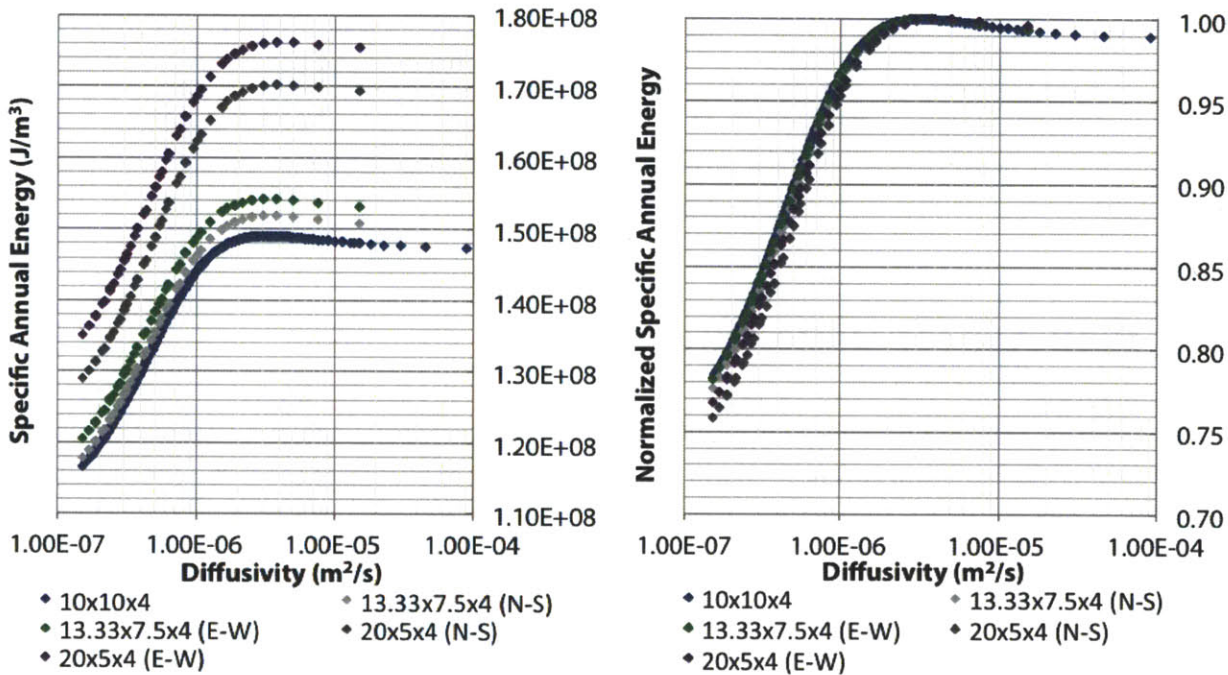


Figure 9-35 Specific Annual Energy Consumption ( $J/m^3$ ) vs Wall Diffusivity ( $m^2/s$ ) and Plan Aspect Ratio, left, and Normalized Specific Annual Energy Consumption vs Wall Diffusivity ( $m^2/s$ ) and Plan Aspect Ratio, right, San Francisco, CA

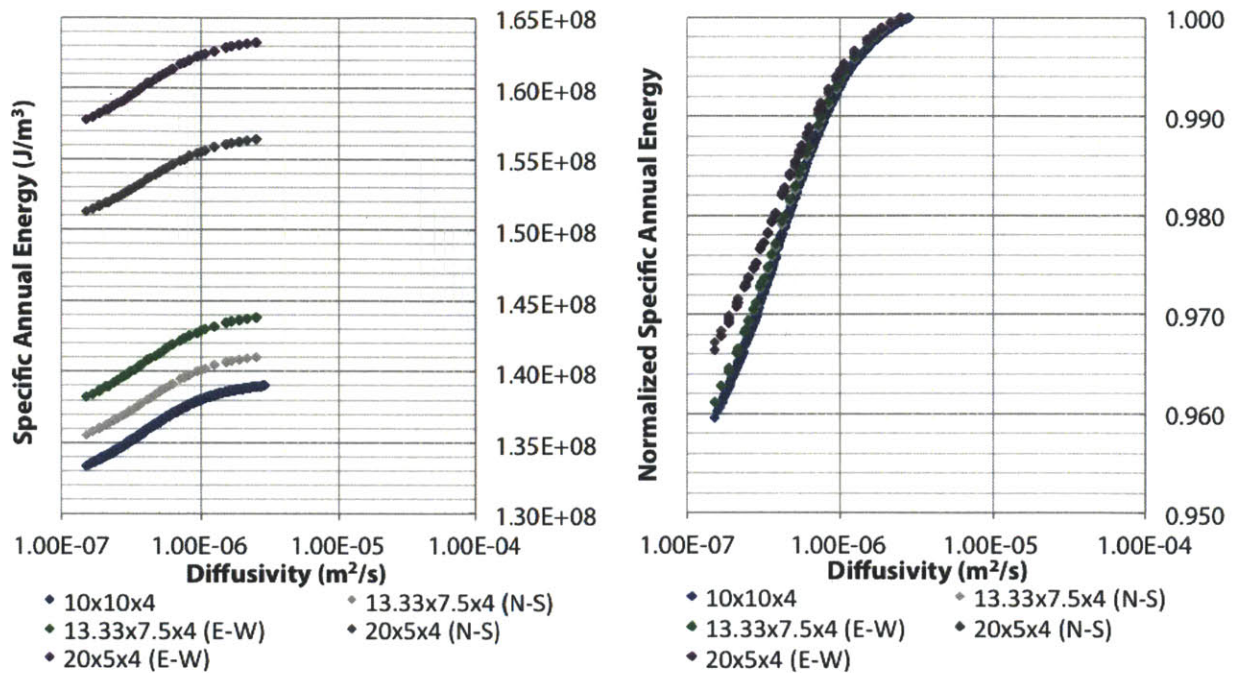


Figure 9-36 Specific Annual Energy Consumption ( $J/m^3$ ) vs Slab Diffusivity ( $m^2/s$ ) and Plan Aspect Ratio, left, and Normalized Specific Annual Energy Consumption vs Slab Diffusivity ( $m^2/s$ ) and Plan Aspect Ratio, right, San Francisco, CA

### 9.6.2 Phoenix, AZ - Hot, Dry Climate

The results for the annual energy and normalized energy consumption for wall thermal mass are shown in Figure 9-37. The results suggest that, like San Francisco, buildings that have less equal dimensions in their sides consume more energy per volume. Buildings aligned N-S consume less energy than buildings aligned E-W. From the normalized energy consumption, it is clear that the long building aligned N-S has the best thermal mass performance, followed by a cluster of the other buildings. Still, since this construction uses more energy than the more compact buildings, a reason other than simply thermal mass construction would be necessary to justify the construction type.

Moving on to the relationships for slab thermal mass in Figure 9-38, it can be seen that the same trends exist with regard to which geometry uses the lowest amount of energy. The small amount of optimization potential of thermal mass shows little overlap in the curves. The normalized relationships also suggest that there is a cluster of performance for all buildings other than the longest E-W oriented building, which shows the worst performance. The magnitude of energy savings further suggests that thermal mass optimization with respect to slabs will obtain less energy savings than deciding form from other considerations.

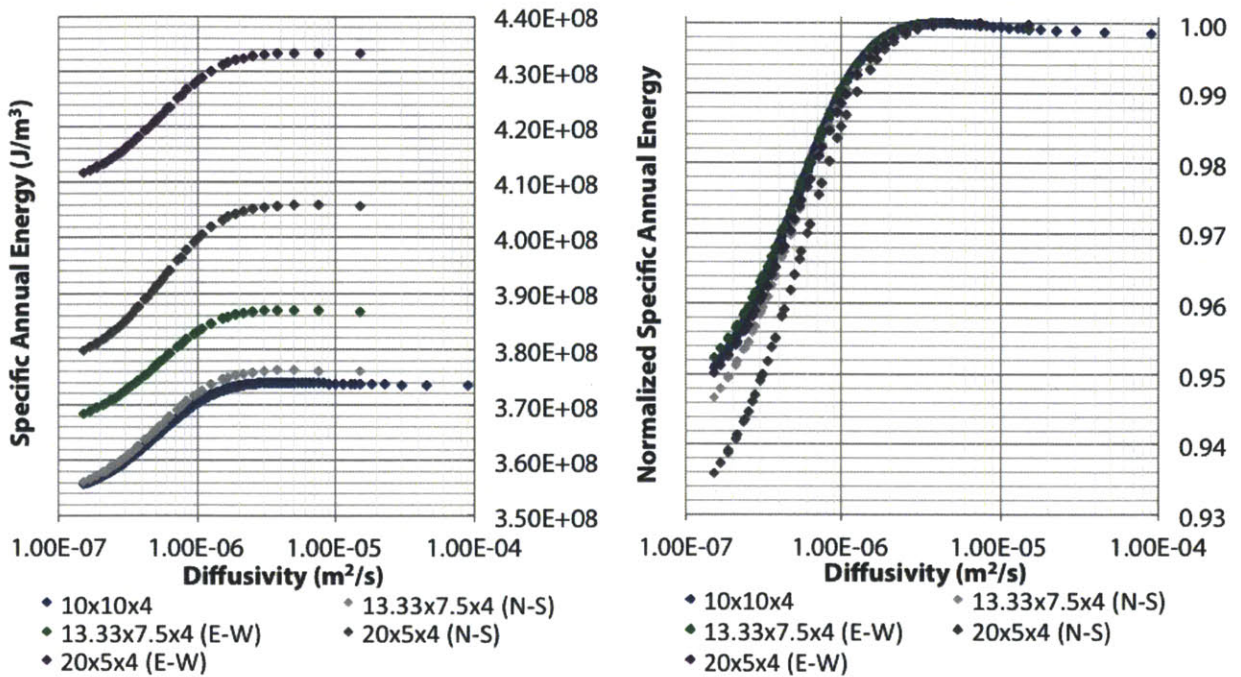


Figure 9-37 Specific Annual Energy Consumption (J/m<sup>3</sup>) vs Wall Diffusivity (m<sup>2</sup>/s) and Plan Aspect Ratio, left, and Normalized Specific Annual Energy Consumption vs Wall Diffusivity (m<sup>2</sup>/s) and Plan Aspect Ratio, right, Phoenix, AZ

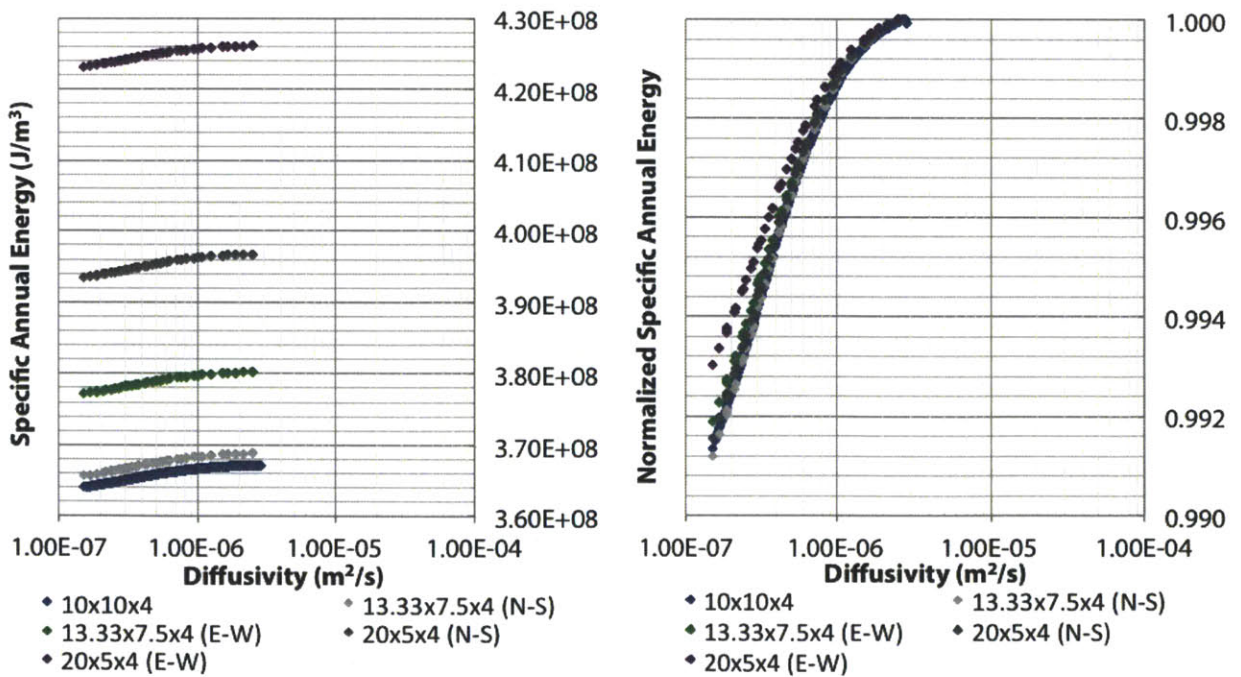


Figure 9-38 Specific Annual Energy Consumption (J/m<sup>3</sup>) vs Slab Diffusivity (m<sup>2</sup>/s) and Plan Aspect Ratio, left, and Normalized Specific Annual Energy Consumption vs Slab Diffusivity (m<sup>2</sup>/s) and Plan Aspect Ratio, right, Phoenix, AZ

### 9.6.3 Miami, FL - Hot, Humid Climate

The results for annual energy consumption and normalized consumption for Miami in Figure 9-39 demonstrate that the E-W oriented buildings still consume more energy than the N-S buildings, with the square building using the least energy per volume. The results of the normalization show that long N-S oriented buildings have the best performance, followed by long E-W buildings and trailed by the more square aspect ratios. Still, the magnitude of energy savings does not increase substantially to warrant orienting a building with respect to its plan aspect ratio for wall thermal mass.

The results for slab thermal mass shown in Figure 9-40 similarly show the trend that E-W oriented construction is more energy consuming. The normalized results, however, show that all thermal mass optimization curves have the same shape and magnitude. This indicates that there is little to no benefit of changing the plan aspect ratio with regard to slab thermal mass. Thus, the building should be oriented based on other considerations.

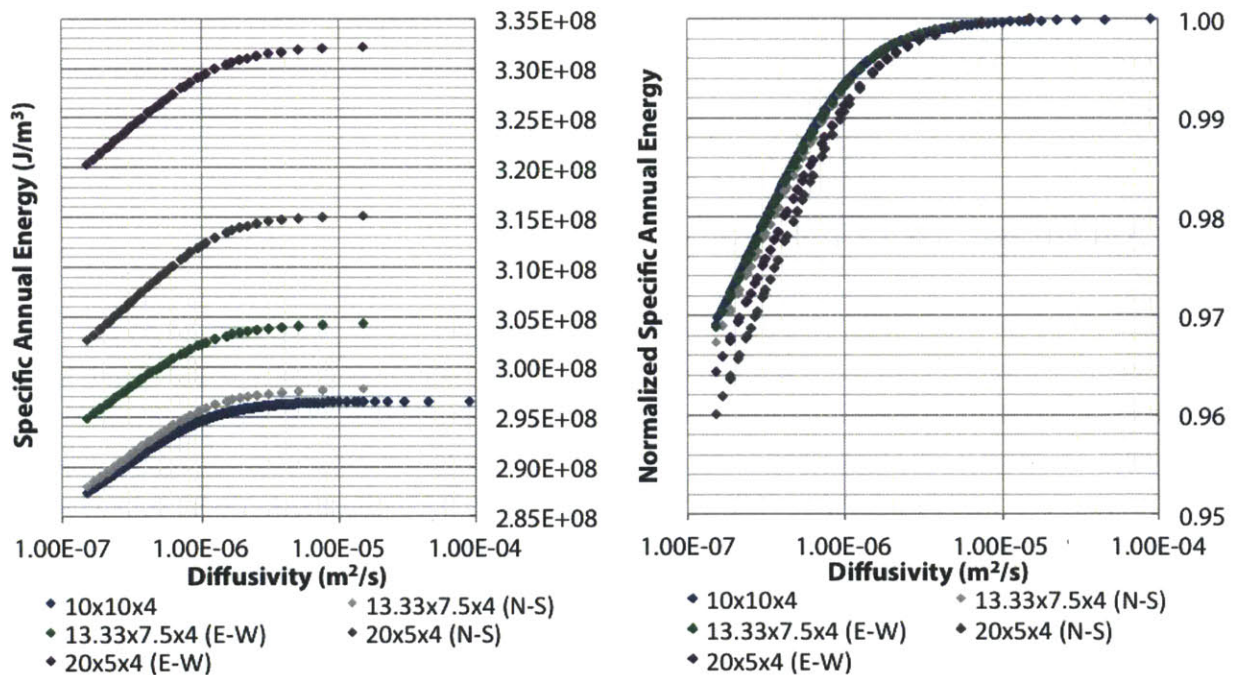


Figure 9-39 Specific Annual Energy Consumption (J/m<sup>3</sup>) vs Wall Diffusivity (m<sup>2</sup>/s) and Plan Aspect Ratio, left, and Normalized Specific Annual Energy Consumption vs Wall Diffusivity (m<sup>2</sup>/s) and Plan Aspect Ratio, right, Miami, FL

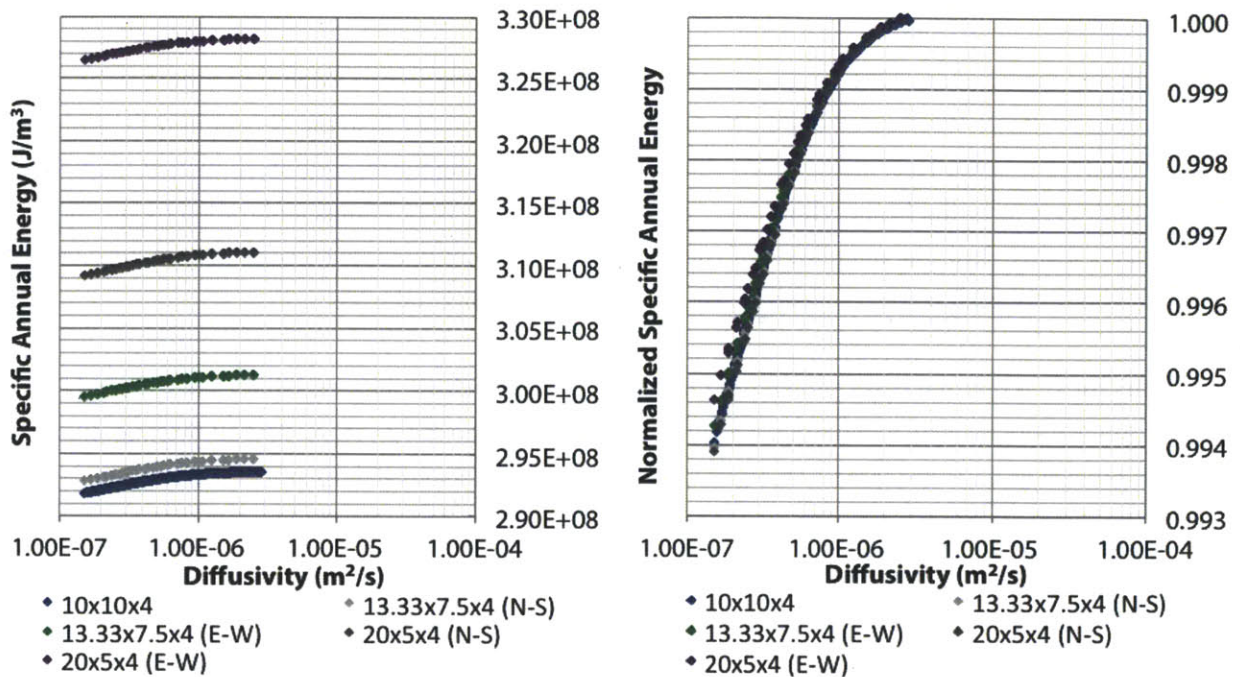


Figure 9-40 Specific Annual Energy Consumption ( $J/m^3$ ) vs Slab Diffusivity ( $m^2/s$ ) and Plan Aspect Ratio, left, and Normalized Specific Annual Energy Consumption vs Slab Diffusivity ( $m^2/s$ ) and Plan Aspect Ratio, right, Miami, FL

### 9.6.4 Anchorage, AK - Cold Climate

The annual energy consumption and normalized consumption results for wall thermal mass and Anchorage are shown in Figure 9-41. Buildings aligned E-W consume more energy, as seen in all previous climates. Thermal mass is relatively constant among all geometries, with the best thermal mass performance observed for the longest building aligned E-W. Since the overall energy savings of wall thermal mass is minor in this climate and that geometry consumes the most energy, it is clear that building orientation should not be decided on thermal mass criteria in this climate.

The results for slab thermal mass are presented in Figure 9-42, which demonstrates the same trend in overall energy consumption. However, the normalized energy consumption suggests that longer buildings have worse slab thermal mass performance than their square counterparts regardless of the building orientation. Still, the magnitude of energy savings indicates that it is unwise to consider slab thermal mass in the orientation decision for the building in Anchorage.



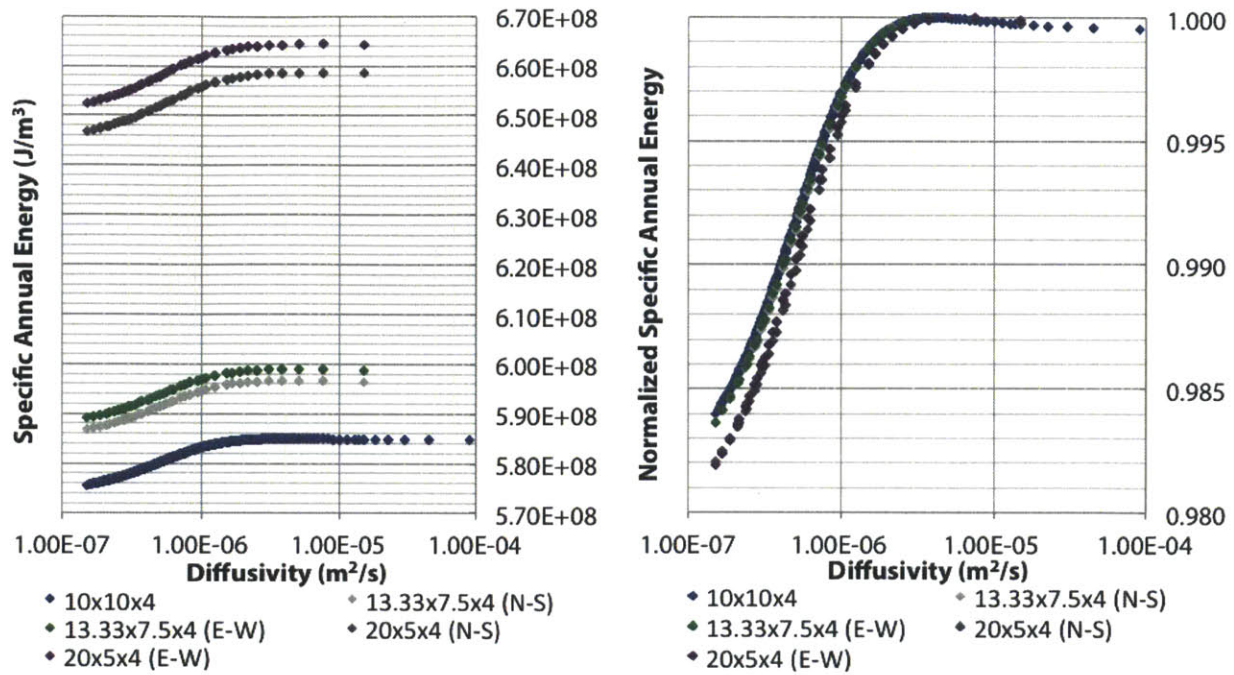


Figure 9-41 Specific Annual Energy Consumption (J/m<sup>3</sup>) vs Wall Diffusivity (m<sup>2</sup>/s) and Plan Aspect Ratio, left, and Normalized Specific Annual Energy Consumption vs Wall Diffusivity (m<sup>2</sup>/s) and Plan Aspect Ratio, right, Anchorage, AK

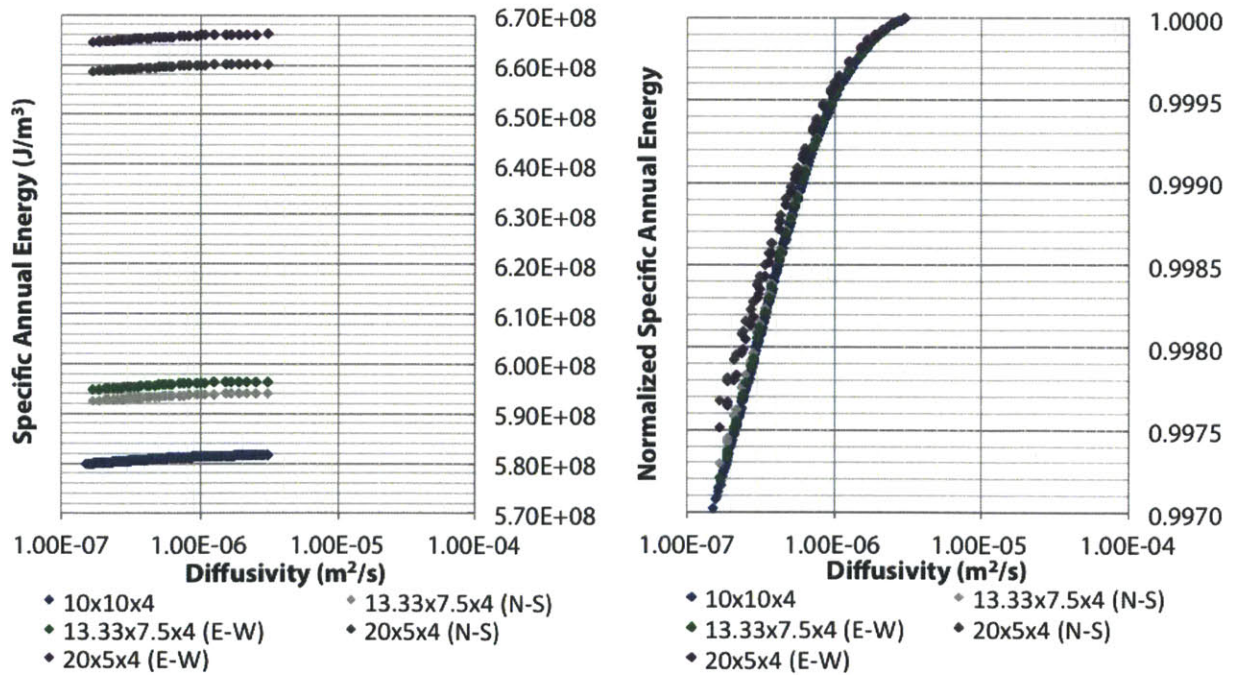


Figure 9-42 Specific Annual Energy Consumption (J/m<sup>3</sup>) vs Slab Diffusivity (m<sup>2</sup>/s) and Plan Aspect Ratio, left, and Normalized Specific Annual Energy Consumption vs Slab Diffusivity (m<sup>2</sup>/s) and Plan Aspect Ratio, right, Anchorage, AK

### 9.6.5 Discussion

The ability to optimize thermal mass performance has a connection to the aspect ratio of the building plan. All buildings aligned E-W consume more energy than buildings aligned N-S. When looking at the trends for thermal mass optimization potential for buildings aligned N-S in Figure 9-43 and E-W in Figure 9-44, it is evident that there are steeper slopes in the N-S diagrams for wall thermal mass. For slab thermal mass, the slopes are steeper in the E-W direction. This means that there is more thermal mass benefit from moving away from the square configuration through a N-S orientation for wall thermal mass. The best optimization of slab thermal mass is a square system. This is consistent with the individual results presented in the previous sub-sections.

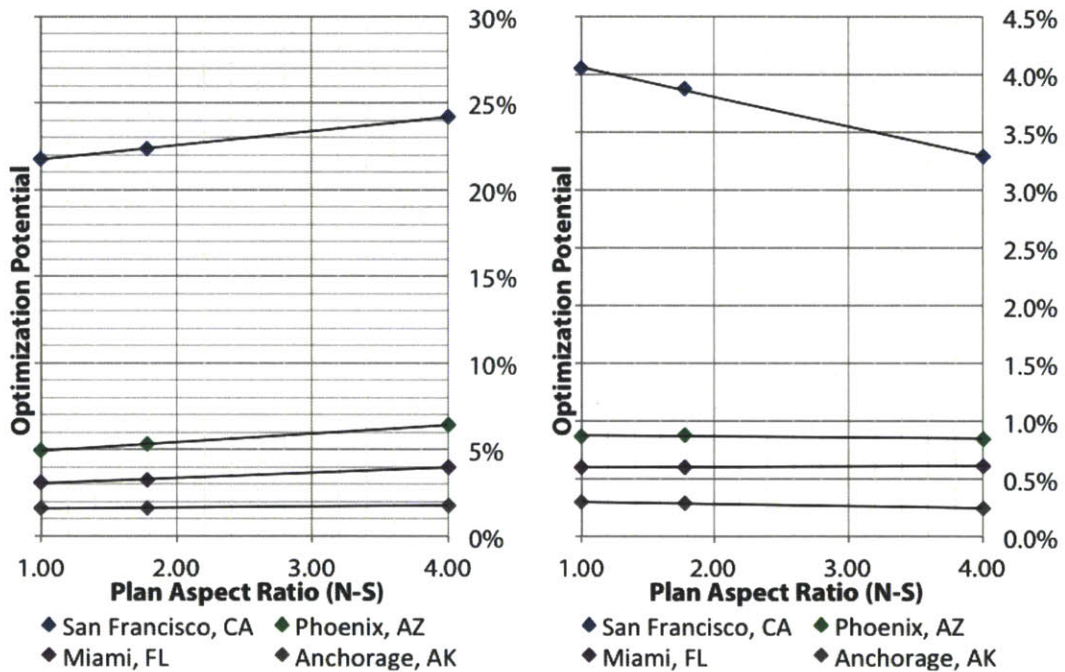


Figure 9-43 Potential Energy Savings from Thermal Mass vs N-S Plan Aspect Ratio, Walls (left) and Slabs (right)

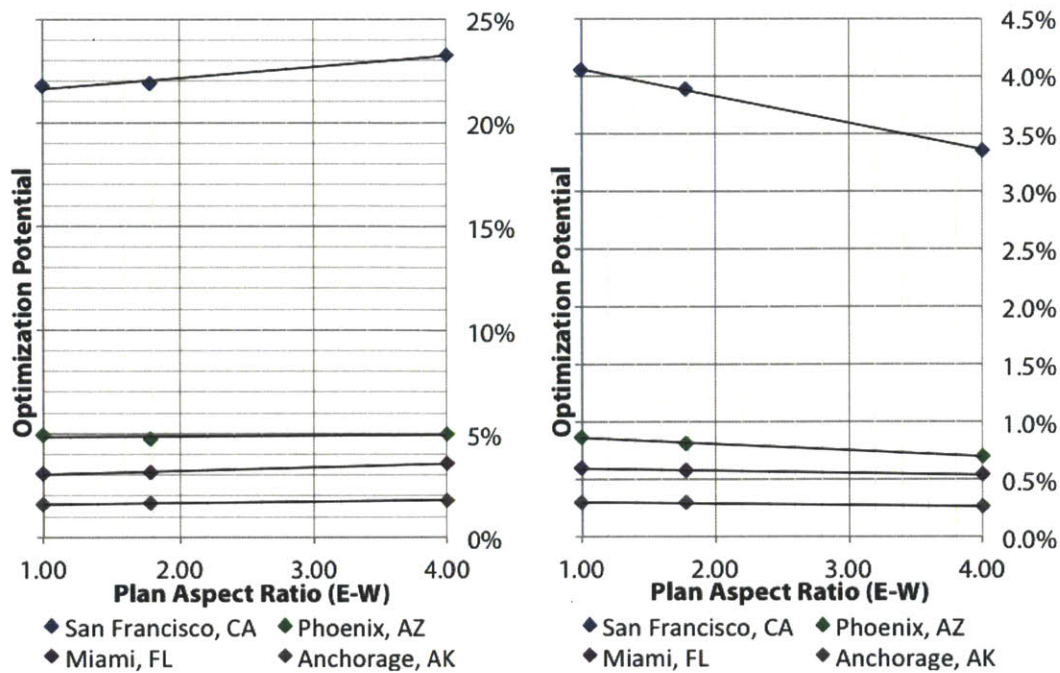


Figure 9-44 Potential Energy Savings from Thermal Mass vs E-W Plan Aspect Ratio, Walls (left) and Slabs (right)

## 9.7 Glazing Percentage Effects

The final geometry parameter is the glazing percentage and its impact on passive thermal mass performance. The standard window percentage tested is 15%. To determine if there is a benefit to different window percentages, 5% and 25% will be tested as points of comparison for considering the relative impact of solid material and openings. All other parameters remain constant, and the results for the four climates considered are presented for the remainder of this section.

### 9.7.1 San Francisco, CA - Mild, Marine Climate

The results for the density-specific heat master curve for thermal mass performance of walls are plotted versus diffusivity for the annual energy consumption per volume and normalized consumption in Figure 9-45. These results indicate that energy consumption decreases as window percentage increases. However, the overall energy savings from thermal mass, as shown in the normalized consumption, indicates that there is little impact on the thermal mass performance for most of the normal range of diffusivity values. For very low diffusivities, there is slightly improved performance shown through increasing window percentage.

Looking at the impact on the thermal mass performance of slabs for the overall energy consumption and normalized energy consumption in Figure 9-46, there is a similar trend in the overall energy savings as a result of increasing window percentage. However, the normalized curves demonstrate that the energy savings from thermal mass decrease slightly for higher percentages of windows. The results lead to the conclusion that the energy savings attributed to changing window percentage is due to factors other than the energy storage in the slab system. One example of a contributing factor is the increase of solar radiation in the system working to the advantage of building conditioning.

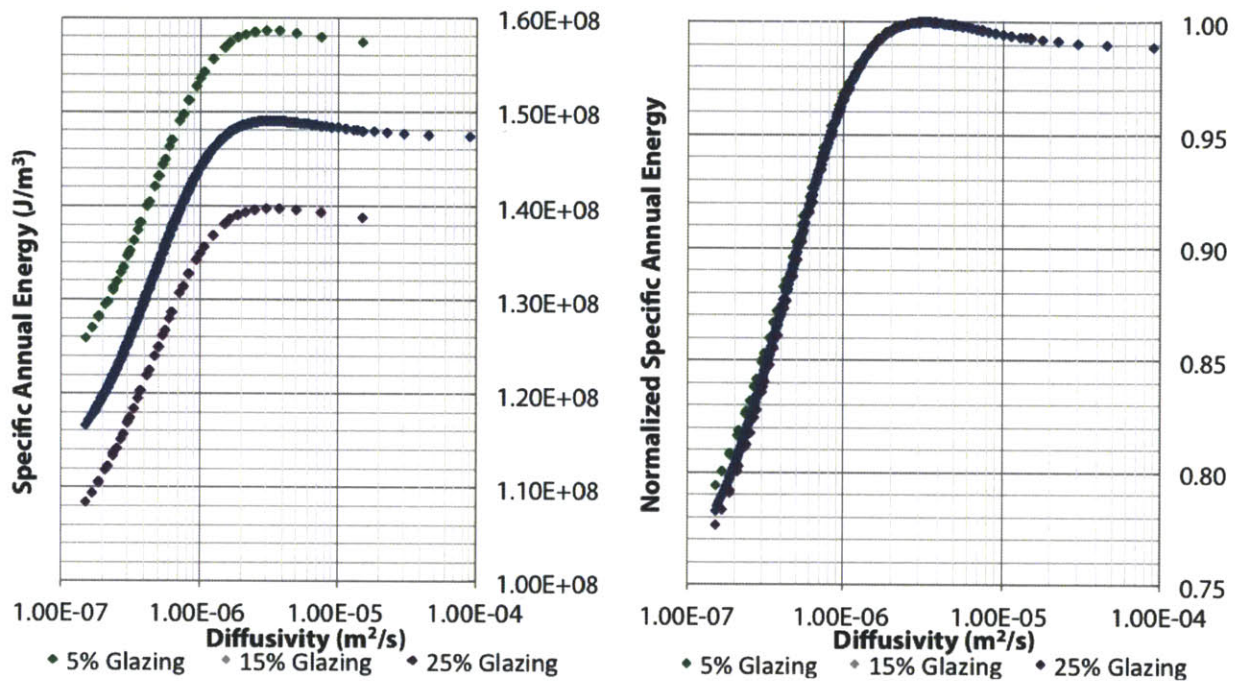


Figure 9-45 Specific Annual Energy Consumption (J/m<sup>3</sup>) vs Wall Diffusivity (m<sup>2</sup>/s) and Glazing Percentage, left, and Normalized Specific Annual Energy Consumption vs Wall Diffusivity (m<sup>2</sup>/s) and Glazing Percentage, right, San Francisco, CA

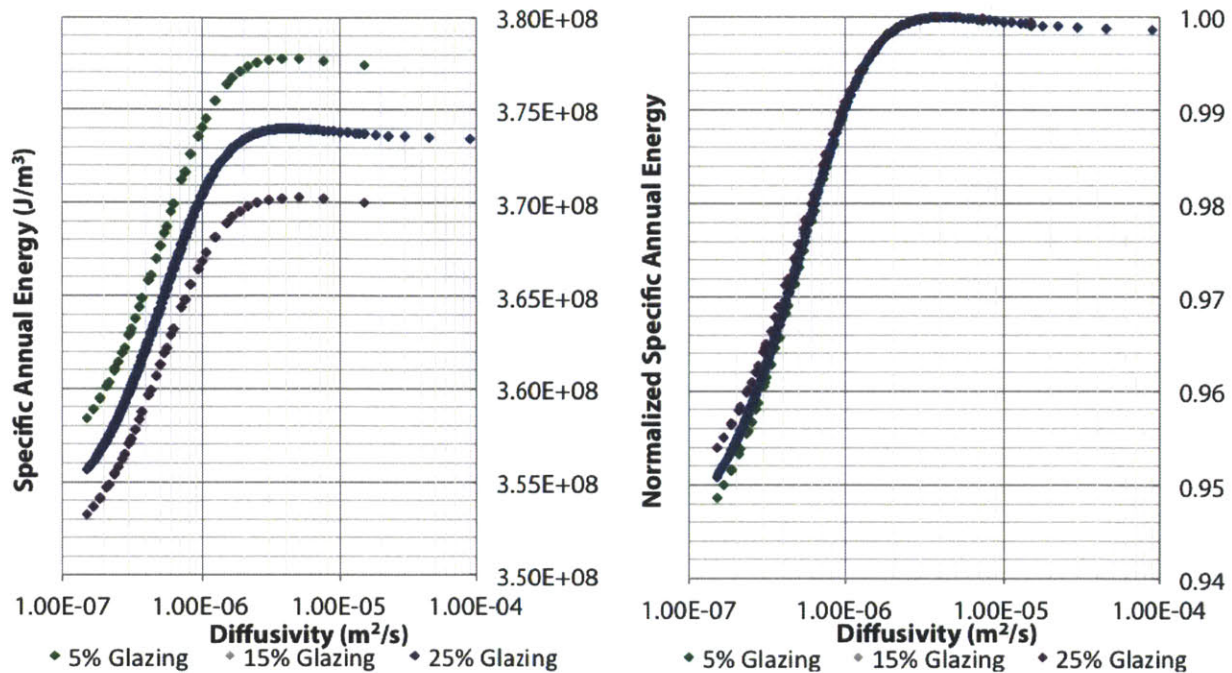


Figure 9-46 Specific Annual Energy Consumption (J/m<sup>3</sup>) vs Slab Diffusivity (m<sup>2</sup>/s) and Glazing Percentage, left, and Normalized Specific Annual Energy Consumption vs Slab Diffusivity (m<sup>2</sup>/s) and Glazing Percentage, right, San Francisco, CA

### 9.7.2 Phoenix, AZ - Hot, Dry Climate

The specific annual energy consumption and normalized energy curves for the performance of thermal mass in walls are shown in Figure 9-47. These results indicate that buildings with higher glazing percentage consume more energy than buildings with lower glazing percentages, in contrast with the results from San Francisco. The results also suggest that there is substantial overlap among the curves, meaning that the thermal mass component of the building is responsible for a greater energy contribution than the change in glazing percentage in this range. The normalized energy curves indicate that buildings with lower window percentages have greater potential for wall thermal mass optimization. Since the thermal mass trend and the overall energy trend align, the results indicate that lower window percentages are better for Phoenix.

Moving toward the slab thermal mass data presented in Figure 9-48, the same trend in energy consumption is seen as for wall thermal mass, which is logical given that these results are for the same climate. However, the smaller overlap suggests that the impact of window glazing is stronger than the impact of slab thermal mass on the overall energy consumption of the building. The normalized energy results suggest that lower glazing amounts still result in better thermal mass energy savings, indicating that it is wise to select lower glazing amounts in Phoenix from a slab thermal mass perspective.

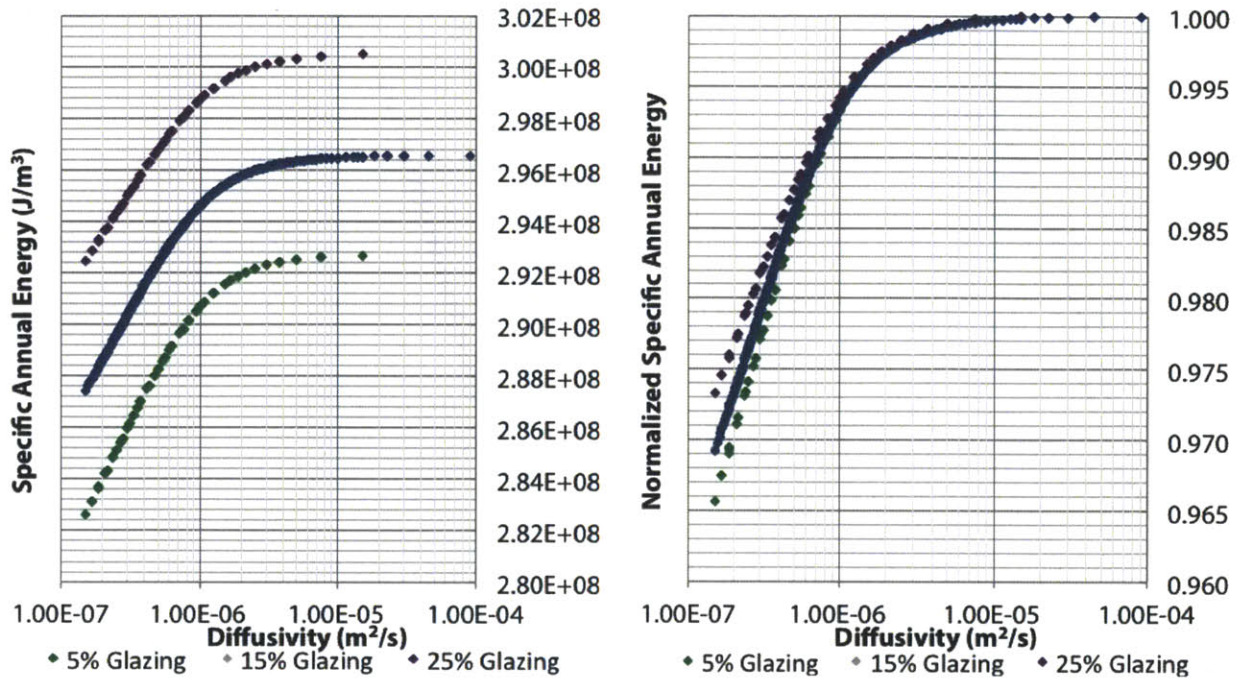


Figure 9-47 Specific Annual Energy Consumption (J/m<sup>3</sup>) vs Wall Diffusivity (m<sup>2</sup>/s) and Glazing Percentage, left, and Normalized Specific Annual Energy Consumption vs Wall Diffusivity (m<sup>2</sup>/s) and Glazing Percentage, right, Phoenix, AZ

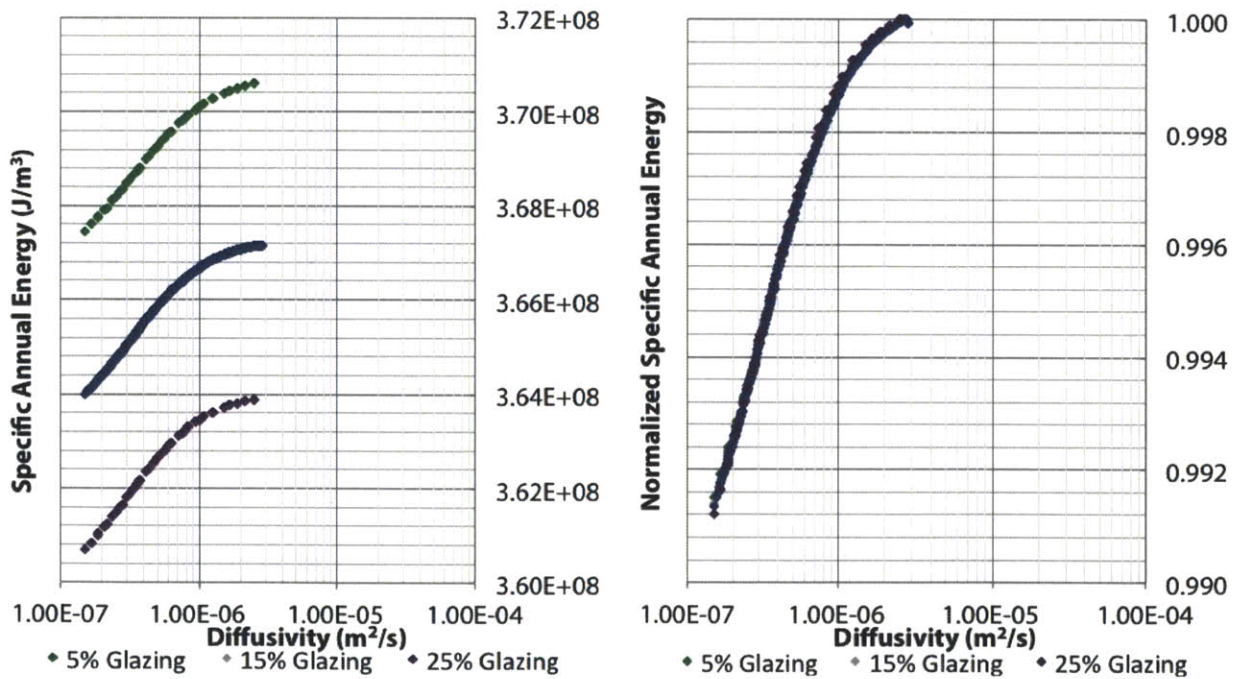


Figure 9-48 Specific Annual Energy Consumption (J/m<sup>3</sup>) vs Slab Diffusivity (m<sup>2</sup>/s) and Glazing Percentage, left, and Normalized Specific Annual Energy Consumption vs Slab Diffusivity (m<sup>2</sup>/s) and Glazing Percentage, right, Phoenix, AZ

### 9.7.3 Miami, FL - Hot, Humid Climate

The results for specific annual energy consumption and its normalized values for wall thermal mass are shown in Figure 9-49. Lower energy consumption is observed for smaller glazing percentages in Miami, but there is significant overlap between the curves. This indicates that the impact of thermal mass outweighs the energy differences from increasing the glazing percentage. The normalized energy consumption shows that the best thermal mass performance is seen in the smallest glazing percentage, which suggests that lower glazing amounts provide better energy performance and thermal mass performance in this climate.

The results for slab thermal mass in Figure 9-50 show that there is no overlap between the thermal mass curves in Miami. The trend of increased energy consumption for increased glazing percentage holds true for these results as well. The normalized diagram suggests that the benefit of thermal mass for slabs is roughly constant for Miami across the glazing percentages. Since the magnitude of savings is very low, it is sensible to optimize building performance for considerations other than slab thermal mass.

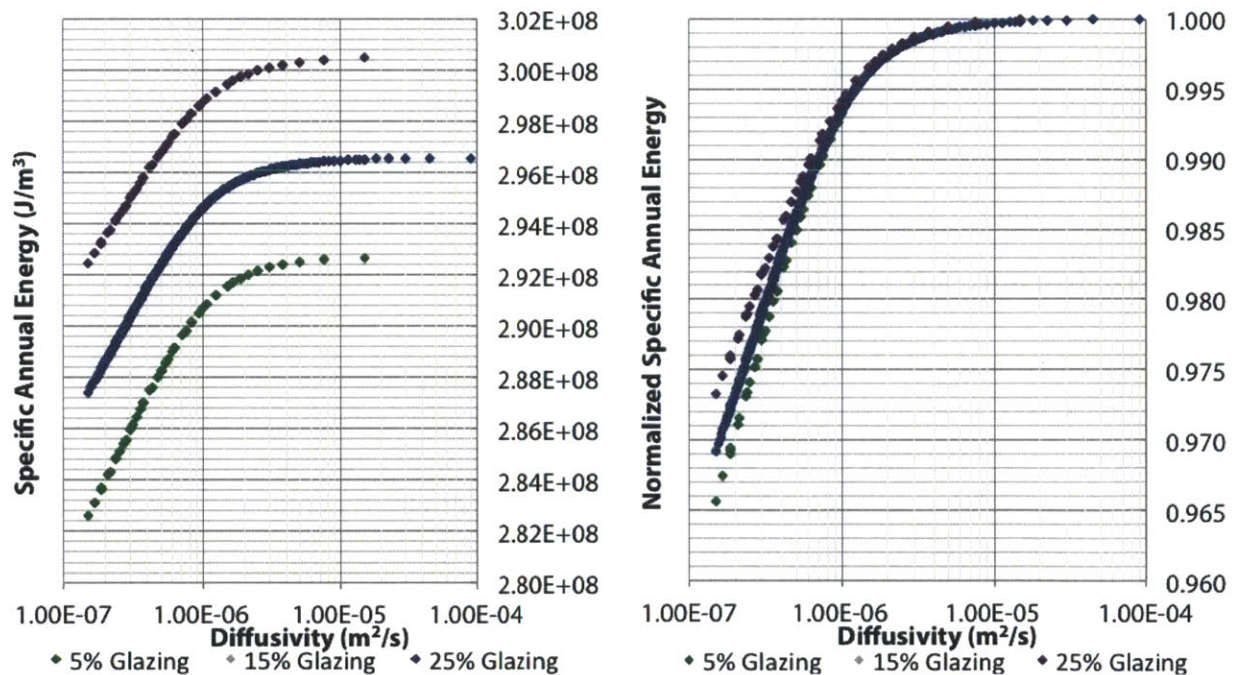


Figure 9-49 Specific Annual Energy Consumption ( $J/m^3$ ) vs Wall Diffusivity ( $m^2/s$ ) and Glazing Percentage, left, and Normalized Specific Annual Energy Consumption vs Wall Diffusivity ( $m^2/s$ ) and Glazing Percentage, right, Miami, FL

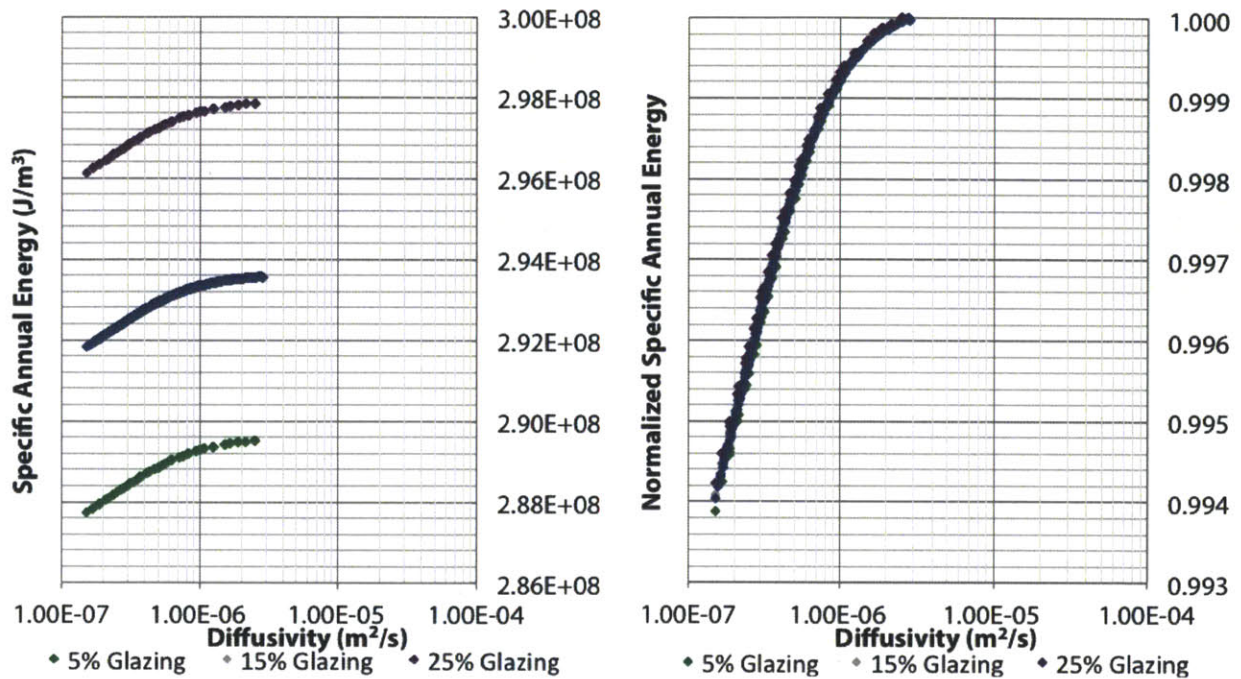


Figure 9-50 Specific Annual Energy Consumption ( $J/m^3$ ) vs Slab Diffusivity ( $m^2/s$ ) and Glazing Percentage, left, and Normalized Specific Annual Energy Consumption vs Slab Diffusivity ( $m^2/s$ ) and Glazing Percentage, right, Miami, FL

### 9.7.4 Anchorage, AK - Cold Climate

The specific annual energy consumption and normalized energy consumption are shown in Figure 9-51 for wall thermal mass in Anchorage, AK. These results indicate that less energy is consumed as glazing percentage increases. Also, there is no overlap between the curves, indicating that the impact of glazing percentage is stronger than the impact of thermal mass. The normalized consumption curves show that there is better performance from thermal mass for higher glazing percentages. The overall magnitude of energy saved is low, but there is alignment between thermal mass optimization and overall energy reduction, suggesting that there is no trade-off to be made.

The same results for slab thermal mass are presented in Figure 9-52. These results showcase the minimal impact of varying the mass of slab construction in this climate. There is no overlap in energy consumption curves and the least consumption occurs at higher window percentages. The normalized energy consumption curves demonstrate that the greatest thermal mass advantage is present from the highest window percentages, demonstrating an alignment between total consumption and thermal mass performance.



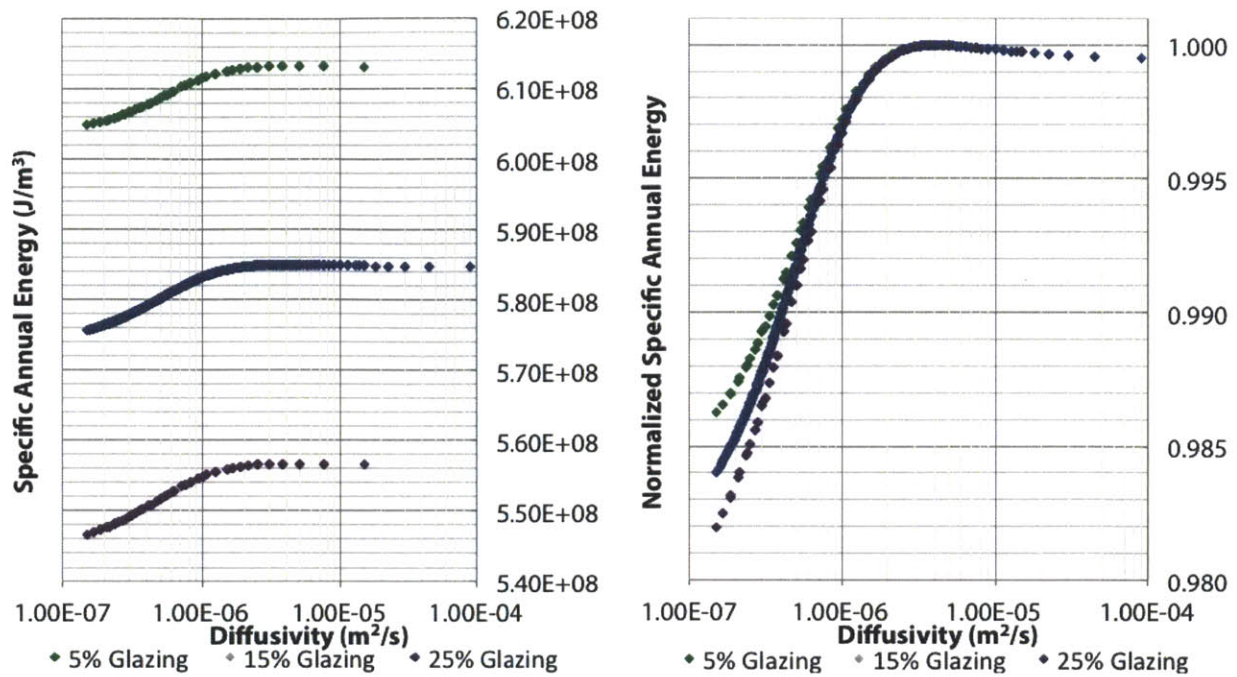


Figure 9-51 Specific Annual Energy Consumption (J/m<sup>3</sup>) vs Wall Diffusivity (m<sup>2</sup>/s) and Glazing Percentage, left, and Normalized Specific Annual Energy Consumption vs Wall Diffusivity (m<sup>2</sup>/s) and Glazing Percentage, right, Anchorage, AK

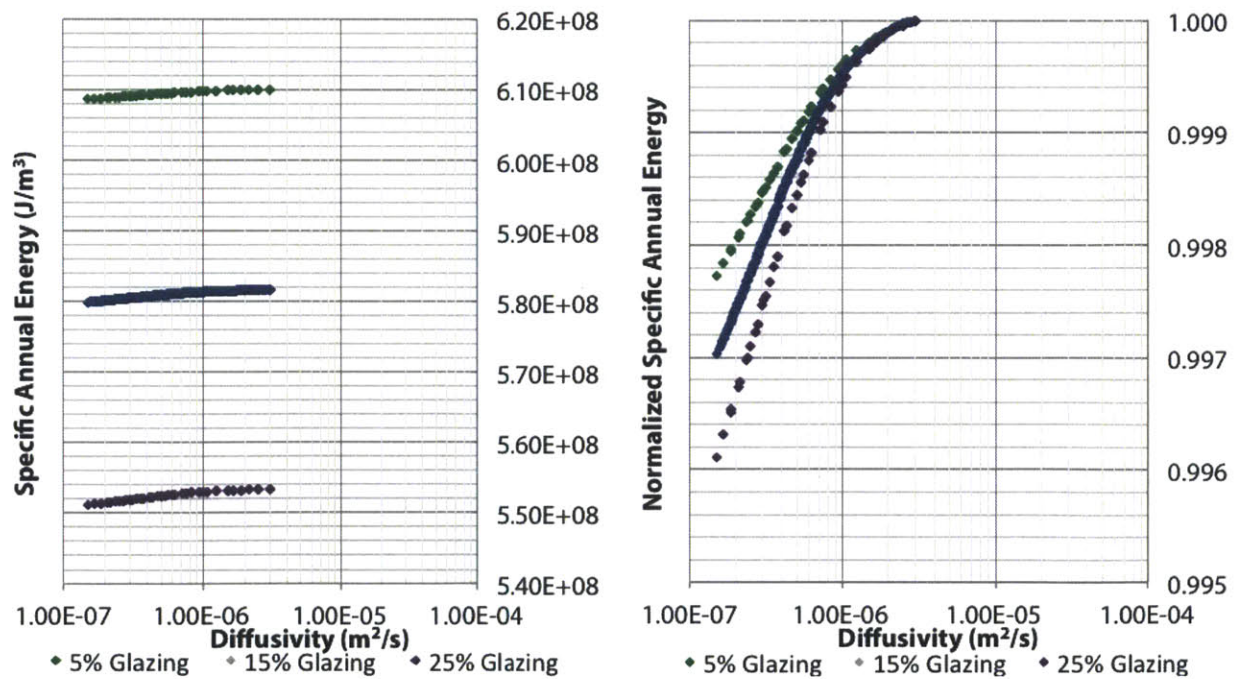


Figure 9-52 Specific Annual Energy Consumption (J/m<sup>3</sup>) vs Slab Diffusivity (m<sup>2</sup>/s) and Glazing Percentage, left, and Normalized Specific Annual Energy Consumption vs Slab Diffusivity (m<sup>2</sup>/s) and Glazing Percentage, right, Anchorage, AK

### 9.7.5 Discussion

The results for the total energy show that more energy is consumed for larger glazing percentages in warm climates, while less energy is consumed for mild and cold climates. The effect on the optimization of thermal mass is best illustrated in Figure 9-53. San Francisco and Anchorage show improvements in thermal mass performance as a result of adding glazing while Miami and Phoenix show reductions. This indicates that the decision to include glazing to benefit thermal mass is a highly climate dependent one.

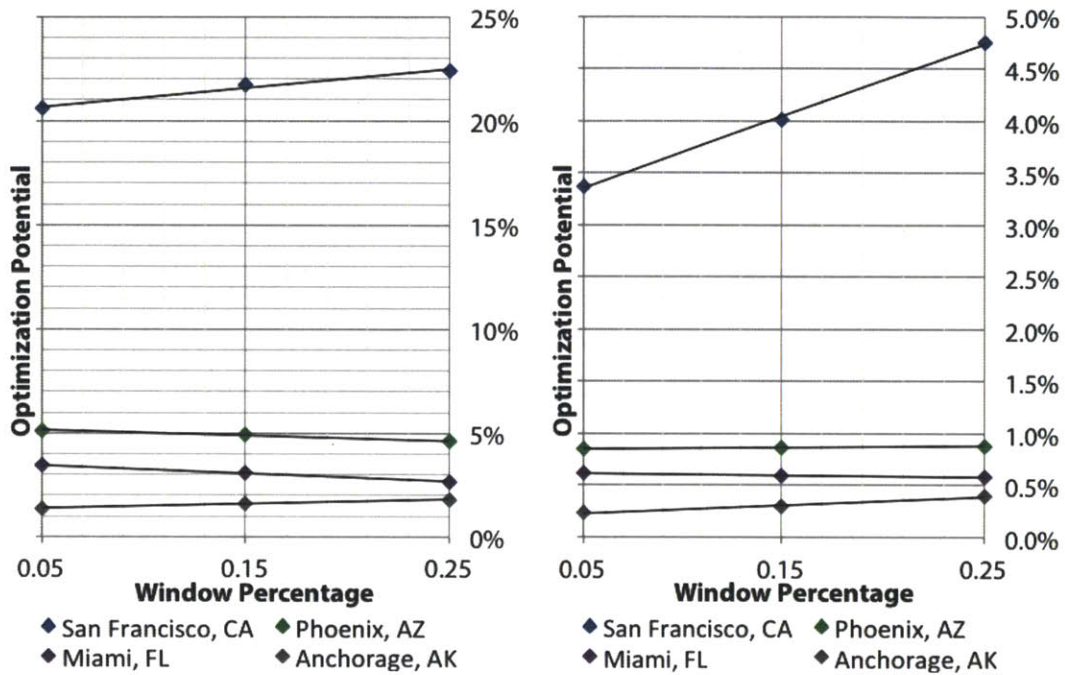


Figure 9-53 Potential Energy Savings from Thermal Mass vs Window Percentage, Walls (left) and Slabs (right)

## 9.8 Chapter Summary

This chapter has presented the relationship between thermal mass and different geometry effects to answer the research question addressing thermal mass sensitivity. The results indicate that attics and internal slabs show negative performance results while basements can improve slab thermal mass to the detriment of wall thermal mass. Generally taller buildings have better wall thermal mass performance and worse slab thermal mass performance, while square plans have the optimum energy and thermal mass use. Finally, adding windows helps in mild and cold climates while it hinders performance in warm climates. In the end, these trends indicate that, while there are means of optimizing thermal mass construction, none of these trends indicated that poor thermal mass climates would become substantially better with these improvements. Therefore, geometry sensitivity will only impact marginal and good thermal mass climates.

**Part V**  
**Conclusion**

# Chapter 10

## Conclusion

This report has analyzed the impact of thermal mass from the perspective of the Cube Model. The work presented has considered the previous scholarship, the development and testing of the model, its use to analyze thermal mass, and the sensitivity of the thermal mass relationships presented. Data analysis has provided the answers to the research questions presented in Chapter 1 as well as provide opportunities for future investigation.

### 10.1 Main Findings

In Chapter 1 of this report, a research approach is presented to target the energy savings from thermal mass performance in single-family residential homes. To focus the study, four research questions were presented as key to the understanding of the problem:

1. How can the complexity of a building be reduced while maintaining similar results to a full energy model?
2. From a quantitative perspective, what is thermal mass? Of the main thermal properties of a material (thickness, conductivity, density, specific heat), which have the greatest impact on energy consumption by climate?
3. How can thermal mass of an envelope construction be optimized? Does the optimization change when considering walls versus slabs?
4. How do other parameters (infiltration, geometry) impact the thermal mass performance of a residence?

The first question addresses the potential for reduction of building specifics in energy modeling while still providing reasonable predictions. The report developed the Cube Model as a means of addressing this goal. The model has simplified geometry and envelope parameters while adjusting the fixed parameters to modeling standards and building code. The calibration analysis verified the envelope and geometry reductions as a viable means of reducing the building problem. The calibration and validation to a full energy model demonstrates that the model obtains similar energy results to a full energy model provided the assumptions, geometry, and boundary conditions are sufficiently calibrated. This discovery shows the validity of using early breadboard design tools with minimal specific parameters to generate energy results for comparison and discussion of design alternatives.

The second question provides the impetus for the specific application of the Cube Model. The model can be used to generate scaling relationships for a variety of parameters as shown in the versatility analysis. Still, it has primarily been used to discuss the impact of thermal mass performance on building energy consumption. Thermal mass has been quantified through the use of diffusivity; these relationships illuminated the presence of a master curve for thermal mass. The master curve is governed by changes in density and specific heat. Conductivity and thickness of material provided changes in the overall energy use patterns for residential construction.

Furthermore, this report illustrated the benefit of thermal mass across the nation. The normalized energy consumption for a wall of given thickness and conductivity can be used to determine the percent energy savings possible from increasing thermal mass of a wall section through the range of realistic values. The base case of brut concrete has been used as an example to generate energy saving values. The results show that in many regions of the United States, wall thermal mass can be used to save more than 5% of annual energy consumption. In contrast, the energy savings only exceed 5% for slab thermal mass on the west coast. In all climates, the energy benefits from thermal mass of walls exceed those found from slabs.

The third question addressed the potential to optimize thermal mass performance for both the wall and slab condition. This question has been used to move beyond the amount of energy saved to determine how the properties of a wall or slab should be changed. The results indicated that the optimum conductivity for construction materials is much lower than brut concrete, allowing for the use of insulation in constructions without compromising thermal mass performance. The analysis of wall thickness indicated that for many climates, there is an asymptotic behavior with regard to the benefits of thermal mass. In other words, there are limited benefits of increasing the thickness of construction with regard to energy storage. In some climates, the energy savings from thermal mass decreases beyond a certain wall thickness. Slab thickness showed less asymptotic behavior and suggested that thicker slabs can be used to benefit performance.

The fourth question addressed the sensitivity of the thermal mass results with respect to infiltration and geometry effects, two of the key assumptions for the thermal mass analysis. The relationship between thermal mass performance and infiltration suggested that in almost all climates tested, tighter construction

resulted in greater thermal mass savings in addition to the energy savings from reducing infiltration. Also, in climates where thermal mass performs well, it provided greater magnitudes of energy savings than further restricting infiltration. Finally, in the few climates where the trend was reversed there was a maximum improvement of only 1% annual energy consumption.

All geometry effects had an impact on the thermal mass performance of the building. The results indicated that buildings with attics and internal slabs show worse thermal mass performance than the counterparts without these features. In addition, while the attic reduced overall consumption the internal slab increased consumption. The incorporation of a basement condition instead of a slab-on-grade showed diminished thermal mass performance from walls and increased performance from slabs. However, depending on the climate this increase may not be sufficient to justify the cost or extra energy from the basement condition. Still, in buildings where basements are required for design reasons it is important to recognize that the thermal mass of the ground floor slab is higher than that predicted by slab thermal mass maps.

Changes to the geometry of the cube itself showed that taller buildings with smaller, square footprints had the best performance of wall thermal mass to the slight disadvantage of slab thermal mass. Glazing percentage showed better thermal mass performance in the configuration where less energy is consumed from an overall standpoint, suggesting that a co-optimized situation could result. In the end, all of these geometry effects can be used to ensure maximum thermal mass performance, but the effects generally did not turn poor performing climates (<5% annual savings) into better performing locations (>5% annual savings).

With the answers to the four primary research questions provided, this report has provided a broad view representation of the impact of thermal mass through the analysis of over 270,000 full building simulations. Such analysis has provided a survey of the driving factors of thermal mass and key parameters which might affect its performance. It has been shown that thermal mass should be considered in select climates, to the extent where its energy savings may be greater than other energy efficiency choices such as infiltration. The results suggest an optimum for thermal mass based on many parameters, possibly tuned to each building by climate. The determination of the exact optimum point is beyond the scope of this report.

## **10.2 Implications for Building Design**

While the exact optimum is beyond the scope of this report, the results have implications on the design of single-family residential homes. The master curves and the sensitivity analyses provide key recommendations for building design, which will be considered in this section.

Assuming that the designer chose to optimize wall thermal mass, then the design should have a compact plan, accounting for additional required conditioned area by using vertical additions, either in a basement or in an additional story. The amount of glazing must be determined based on climate; temperate climates benefit from additional glazing while warm climates benefit from additional mass material. Ideally, wall thermal mass performs best in buildings with lightweight interior constructions, no attic condition, and slab-on-grade construction. However, many of these structures reduce the overall energy consumption of the building. The infiltration target rate should be set at the smallest amount feasible for the project. Finally, the optimum conductivities and thicknesses provided in Chapter 6 could be used as a starting point for designing the envelope.

Now assuming the designer chose to optimize slab thermal mass, the use of a basement resulted in the strongest improvement in slab performance. In other words, it is sensible to optimize the thermal mass of interior horizontal constructions rather than those in contact with the ground. Still, attics and internal slabs should be avoided. The less compact geometries showed slightly better performance, suggesting that slab thermal mass optimization problems should be flatter with a larger floor plan than the wall thermal mass counterparts. Glazing should be increased in temperate climates and decreased in warm climates. The infiltration rate should be minimized. Finally, the optimum conductivities and thicknesses provided in Chapter 7 could be used to start the slab design.

Note, however, that not all of these features would need to be incorporated. The purpose of Part IV is not only to demonstrate the impact of infiltration and geometry on thermal mass performance but to also demonstrate the sensitivity. For instance, many design decisions regarding the floor plan and massing had less impact on thermal mass performance than the presence of an adjacent unconditioned volume. Therefore, some or all of the dimension parameters could be set with regard to optimizing the energy performance of the whole building or to optimizing other design considerations. In contrast, incorporation of the attic and high-mass constructions resulted in much greater changes in the thermal mass performance of the building. For instance, in some climates, thermal mass benefits could move from substantial to insubstantial should the building design contain an attic. Note that this distinction depends both on the individual climate and on the designers' minimum acceptable energy savings for the use of thermal mass.

## **10.3 Future Work**

One goal for future work is to determine an optimum for thermal mass performance. The experiments of this work have suggested that such optima exist. Future work could use the key parameters to generate a more exact understanding of the location of the optima, as well as expand the parameter space to consider a more refined approach. Parameters suggested from the literature review in Chapter 2 such as ventilation

and location of thermal mass in the wall section design would be key considerations to consider in a future approach.

Secondly, there is an opportunity to consider thermal mass in the larger scale of life cycle assessment. For instance, in the analysis of trends in conductivity, thickness, and infiltration especially, there is substantial overlap in energy consumption between changes in values. This indicates that same or better energy performance can be obtained by using thermal mass materials as by using other strategies of energy reduction. Even where the energy savings may not be justifiable alone, material reduction, insulation savings, and/or initial cost benefits could provide positive impacts on building sustainability. These may have impacts at other points in the life cycle of a building that would be worth exploring in a full assessment of material pathways.

Thirdly, in the process of optimization there is potential for testing the assumptions of EnergyPlus with respect to building energy prediction. This could include validating with case study buildings. Such an analysis could be used to determine the significance of limitations in EnergyPlus with respect to conduction and ground contact. Modifications could then be made to the model to address any discrepancies found.

Fourthly, there is an opportunity for future work in showing the relationship between these results and other building typologies. Multi-family and commercial construction bring a wider variety of assumptions, loading conditions, and material choices; the impact of these options on the performance of thermal mass would be useful knowledge. In addition, movement toward neighborhood and regional planning modes through the development of lattices of simplified models could be used to determine how multiple systems interact. These interactions may affect decisions in building and planning.

Finally, an opportunity for future work exists in moving the results toward the design phase. While the Cube Model has illuminated relationships for energy consumption that were previously unreported from the literature surveyed, it is also clear that additional realism would be useful in further addressing the design space. Considerations such as building systems, active controls, constructability, and other notions of sustainable and high-performance construction would be advisable considerations in the preparation of design recommendations.



**Part VI**  
**Appendices**

# **Appendix A**

## **Detailed Model Assumptions**

This appendix provides additional input values and key EnergyPlus assumptions that were omitted from Chapter 3 for brevity. While these assumptions do not impact the theory of the Cube Model, they are necessary to understand the magnitudes of the results.

### **A.1 Input Parameters for Cube Model**

The idealized cube model has a total of 41 direct input parameters that modify the EnergyPlus code. Parameters include a basic building description of length, width, height, and volume, with only three of the four being unique parameters. Volume constraints and plan ratio constraints provide additional geometry control. The thickness, conductivity, density, and specific heat are modeled for seven input materials: wall, floor, roof, basement slab, basement wall, attic floor, and interior slab. Note that in a basic cube, only the wall, floor, and roof materials are employed. The infiltration rate as air changes per hour is specified. The ground condition, basement height, basement conditioning, attic condition, attic height, and number of slabs provide access to the advanced cube features. Note that internal slabs have been modeled as internal mass only. The input values are specified in Table A-1.

Table A-1 Input Parameters for Cube Model

Length	Roof Thickness	Attic Density
Width	Roof Conductivity	Attic Specific Heat
Height	Roof Density	Interior Slab Thickness
Volume	Roof Specific Heat	Interior Slab Conductivity
Volume Constraint	Basement Wall Thickness	Interior Slab Density
Plan Aspect Ratio Constraint	Basement Wall Conductivity	Interior Slab Specific Heat
Wall Thickness	Basement Wall Density	Infiltration Rate
Wall Conductivity	Basement Wall Specific Heat	Ground Condition
Wall Density	Basement Slab Thickness	Basement Height
Wall Specific Heat	Basement Slab Conductivity	Basement Conditioning
Floor Thickness	Basement Slab Density	Attic Condition
Floor Conductivity	Basement Slab Specific Heat	Attic Height
Floor Density	Attic Thickness	Number of Internal Slabs
Floor Specific Heat	Attic Conductivity	

## A.2 Calculated Parameters for Cube Model

In addition to the inputs described above, the program determines many resulting inputs automatically to improve result accuracy. The following descriptions determine the types of calculations imposed on the system.

### A.2.1 Window Parameter Values

Weather conditions, latitude, longitude, and elevation are set by EnergyPlus weather file information [23]. Climate conditions are used to set the window parameters through the use of IECC 2012 data and county information for the meter location from the U.S. Census Bureau [29][90]. The window properties used are presented in Table A-2 based on the climate zones presented in Table 3-7.

Table A-2 Code Required Construction Inputs by Climate Zone [29]

Climate Zone	U-Factor	Solar Heat Gain Coefficient (SHGC)	Visible Transmittance (VT)
1	0.50	0.25	0.60
2	0.40	0.25	0.60
3	0.35	0.25	0.60
4A	0.35	0.40	0.60
4B	0.35	0.40	0.60
4C	0.32	0.40	0.60
5	0.32	0.40	0.60
6	0.32	0.40	0.60
7	0.32	0.40	0.60
8	0.32	0.40	0.60

### A.2.2 Surface Albedo Values

An accurate representation of surface albedo for proper ground modeling requires an understanding of the latitude dependence of the inputs. The values used for the calculations in the ground preprocessors are presented in Table A-3 [67].

Table A-3 Surface Albedo Characteristics for Ground Heat Transfer [67]

Latitude	No Snow Surface Albedo	Snow Surface Albedo
20-25 degrees	0.158	0.158
25-30 degrees	0.179	0.178
30-35 degrees	0.172	0.191
35-40 degrees	0.165	0.285
45-50 degrees	0.158	0.379
50-55 degrees	0.148	0.464
55-60 degrees	0.146	0.503
60-65 degrees	0.165	0.591
65-70 degrees	0.156	0.673

### A.2.3 Thermostat Setpoint Calculations

In addition to the determination of window properties, the procedure from BAHSP has been used to determine the thermostat setpoints from the weather files' supplementary climate data and from ASHRAE 90.1 [23][28][33]. First, the thermostat settings are determined from the temperatures averaged by

month, with 18.89°C being the dividing line between heating and cooling. Once heating is determined for temperatures below the line and cooling is used for the remainder of the year, several checks are performed on the setpoints. The heating system must be in use during December and January if the ASHRAE 99% annual threshold heating temperature is below 15°C. The cooling system must be active during July and August. Should a condition result where there are alternating periods of heating and cooling, the setpoints must be adjusted so that only one switch occurs per season. Finally, an additional month of cooling should be added to the beginning of the cooling season. Note that BAHSP also requires the availability of heating and cooling to coincide with the settings for the thermostat [28].

#### **A.2.4 Internal Load Schedules**

The internal load schedules are presented in this section. The overall annual magnitudes of energy used by the internal loads are included in Chapter 3, but these values are adjusted by the following schedules to provide the final hourly loads. The procedure for determining the loads is as follows. The annual energy consumption is divided into the proper consumption per month using the scaling factors shown in Table A-4. Once the accurate monthly consumption has been determined, the consumption is divided by the number of days in the month to obtain the daily consumption. Finally, this daily consumption is scaled by the hourly schedules and converted to watts. The daily schedule values for all loads except lighting can be found in Table A-5, while the daily loads for lighting can be found in Table A-6. The difference between the schedules in the two tables is that lighting has a unique daily schedule for each month in addition to the multiplying value shown in Table A-4 [28][62]. This procedure results in 288 schedule values per load to be input into EnergyPlus. For brevity in this appendix, the hourly and monthly factors will be represented rather than the entire expanded schedules.

Table A-4 Monthly Schedule Values for Scaling Daily BAHSP Loads [62]

	Month	Refrigerator	Range	Clothes washer	Clothes dryer	Dishwasher	Misc Electric Load
1	Jan	0.837	1.097	1.011	1.151	1.097	1.154
2	Feb	0.835	1.097	1.002	1.144	1.097	1.161
3	Mar	1.084	0.991	1.022	1.010	0.991	1.013
4	Apr	1.084	0.987	1.020	1.007	0.987	1.010
5	May	1.084	0.991	1.022	1.010	0.991	1.013
6	Jun	1.096	0.890	0.996	0.874	0.890	0.888
7	Jul	1.096	0.896	0.999	0.881	0.896	0.883
8	Aug	1.096	0.896	0.999	0.881	0.896	0.883
9	Sep	1.096	0.890	0.996	0.874	0.890	0.888
10	Oct	0.931	1.085	0.964	1.010	1.085	0.978
11	Nov	0.925	1.085	0.959	1.007	1.085	0.974
12	Dec	0.837	1.097	1.011	1.151	1.097	1.154
		12.00	12.00	12.00	12.00	12.00	12.00
	Month	Shower DHW	Bath DHW	Sinks DHW	System DHW	Lighting	
1	Jan	1.04	1.04	1.04	1.04	1.39	
2	Feb	1.05	1.05	1.05	1.04	1.10	
3	Mar	1.04	1.04	1.04	1.03	1.03	
4	Apr	1.03	1.03	1.03	1.02	0.82	
5	May	1.00	1.00	1.00	1.00	0.73	
6	Jun	0.98	0.98	0.98	0.98	0.66	
7	Jul	0.95	0.95	0.95	0.96	0.70	
8	Aug	0.94	0.94	0.94	0.95	0.79	
9	Sep	0.95	0.95	0.95	0.96	0.91	
10	Oct	0.98	0.98	0.98	0.98	1.13	
11	Nov	1.00	1.00	1.00	1.00	1.29	
12	Dec	1.03	1.03	1.03	1.02	1.44	
		12.00	12.00	12.00	12.00	12.00	

Table A-5 Daily Schedule Values for All BAHSP Loads Except Lighting [62]

Hour	People	Refrigerator	Range	Clothes Washer	Clothes Dryer	Dishwasher
1	0.061	0.040	0.007	0.009	0.010	0.015
2	0.061	0.039	0.007	0.007	0.006	0.007
3	0.061	0.038	0.004	0.004	0.004	0.005
4	0.061	0.037	0.004	0.004	0.002	0.003
5	0.061	0.036	0.007	0.007	0.004	0.003
6	0.061	0.036	0.011	0.011	0.006	0.010
7	0.061	0.038	0.025	0.022	0.016	0.020
8	0.053	0.040	0.042	0.049	0.032	0.031
9	0.025	0.041	0.046	0.073	0.048	0.058
10	0.015	0.041	0.048	0.086	0.068	0.065
11	0.015	0.040	0.042	0.084	0.078	0.056
12	0.015	0.040	0.050	0.075	0.081	0.048
13	0.015	0.042	0.057	0.067	0.074	0.041
14	0.015	0.042	0.046	0.060	0.067	0.046
16	0.015	0.042	0.057	0.049	0.057	0.036
15	0.015	0.041	0.044	0.052	0.061	0.038
17	0.018	0.044	0.092	0.050	0.055	0.038
18	0.033	0.048	0.150	0.049	0.054	0.049
19	0.054	0.050	0.117	0.049	0.051	0.087
20	0.054	0.048	0.060	0.049	0.051	0.111
21	0.054	0.047	0.035	0.049	0.052	0.090
22	0.061	0.046	0.025	0.047	0.054	0.067
23	0.061	0.044	0.016	0.032	0.044	0.044
24	0.061	0.041	0.011	0.017	0.024	0.031
	1.000	1.000	1.000	1.000	1.000	1.000

<b>Hour</b>	<b>Misc Electric Load</b>	<b>Shower DHW</b>	<b>Bath DHW</b>	<b>Sinks DHW</b>	<b>System DHW</b>
1	0.037	0.011	0.008	0.014	0.006
2	0.035	0.005	0.004	0.007	0.003
3	0.034	0.003	0.004	0.005	0.001
4	0.034	0.005	0.004	0.005	0.001
5	0.032	0.014	0.008	0.007	0.003
6	0.036	0.052	0.019	0.018	0.022
7	0.042	0.118	0.046	0.042	0.075
8	0.044	0.117	0.058	0.062	0.079
9	0.037	0.095	0.066	0.066	0.076
10	0.032	0.074	0.058	0.062	0.067
11	0.033	0.060	0.046	0.054	0.061
12	0.033	0.047	0.035	0.050	0.048
13	0.032	0.034	0.031	0.049	0.042
14	0.033	0.029	0.023	0.045	0.037
16	0.037	0.026	0.023	0.043	0.037
15	0.035	0.025	0.023	0.041	0.033
17	0.044	0.030	0.039	0.048	0.044
18	0.053	0.039	0.046	0.065	0.058
19	0.058	0.042	0.077	0.075	0.069
20	0.060	0.042	0.100	0.069	0.065
21	0.062	0.042	0.100	0.057	0.059
22	0.060	0.041	0.077	0.048	0.048
23	0.052	0.029	0.066	0.040	0.042
24	0.045	0.021	0.039	0.027	0.023
	1.000	1.000	1.000	1.000	1.000



Table A-6 Daily Schedule Values for BAHSP Lighting Loads [62]

Hour	January	February	March	April	May	June
1	0.024	0.027	0.032	0.039	0.045	0.048
2	0.014	0.016	0.019	0.024	0.027	0.029
3	0.010	0.011	0.013	0.016	0.018	0.019
4	0.010	0.011	0.013	0.016	0.018	0.019
5	0.010	0.011	0.013	0.016	0.018	0.019
6	0.010	0.012	0.014	0.017	0.019	0.020
7	0.023	0.023	0.022	0.028	0.027	0.027
8	0.047	0.046	0.039	0.052	0.045	0.043
9	0.045	0.041	0.031	0.042	0.034	0.032
10	0.023	0.020	0.016	0.020	0.018	0.018
11	0.019	0.016	0.013	0.016	0.015	0.016
12	0.019	0.016	0.013	0.016	0.015	0.015
13	0.019	0.016	0.013	0.016	0.015	0.015
14	0.019	0.016	0.013	0.016	0.015	0.015
16	0.025	0.020	0.015	0.016	0.015	0.016
15	0.020	0.017	0.013	0.016	0.015	0.015
17	0.042	0.031	0.023	0.017	0.016	0.016
18	0.078	0.060	0.046	0.023	0.020	0.020
19	0.116	0.103	0.089	0.042	0.035	0.032
20	0.123	0.132	0.133	0.083	0.070	0.062
21	0.106	0.123	0.143	0.136	0.123	0.111
22	0.089	0.102	0.120	0.147	0.161	0.161
23	0.067	0.076	0.090	0.110	0.126	0.135
24	0.046	0.053	0.063	0.076	0.088	0.094
	1.000	1.000	1.000	1.000	1.000	1.000

Hour	July	August	September	October	November	December
1	0.048	0.042	0.035	0.029	0.025	0.023
2	0.029	0.025	0.021	0.018	0.015	0.014
3	0.019	0.017	0.014	0.012	0.010	0.009
4	0.019	0.017	0.014	0.012	0.010	0.009
5	0.019	0.017	0.014	0.012	0.010	0.009
6	0.020	0.018	0.015	0.013	0.011	0.010
7	0.028	0.029	0.028	0.027	0.019	0.021
8	0.046	0.051	0.053	0.055	0.037	0.043
9	0.035	0.040	0.044	0.049	0.036	0.042
10	0.019	0.020	0.022	0.024	0.020	0.023
11	0.016	0.016	0.017	0.019	0.017	0.019
12	0.016	0.016	0.017	0.019	0.017	0.019
13	0.016	0.016	0.017	0.019	0.017	0.019
14	0.016	0.016	0.017	0.019	0.017	0.019
16	0.016	0.016	0.017	0.020	0.027	0.029
15	0.016	0.016	0.017	0.019	0.019	0.021
17	0.017	0.017	0.019	0.025	0.049	0.052
18	0.020	0.022	0.028	0.041	0.087	0.091
19	0.032	0.037	0.052	0.075	0.119	0.120
20	0.061	0.072	0.095	0.118	0.119	0.112
21	0.110	0.123	0.142	0.130	0.110	0.102
22	0.159	0.158	0.132	0.109	0.093	0.086
23	0.133	0.118	0.099	0.082	0.069	0.064
24	0.092	0.082	0.069	0.057	0.048	0.045
	1.000	1.000	1.000	1.000	1.000	1.000

### A.3 EnergyPlus Code Assumptions

In addition to the parameters that are input or calculated, there are many assumptions built directly into the EnergyPlus code, which are not changed by the user during the model simulation. It is these assumptions which allow the Cube Model to be deceptively simple; however, they greatly impact the output energy. To allow the model to produce reasonable results, nearly all of these modeling assumptions have been based on outside source material. The purpose of this section of the appendix is to detail the source materials for the assumptions in Table A-7.

Table A-7 EnergyPlus Code Assumptions

Assumption	Value	Reference or Explanation
<b>Basic Program Controls</b>		
EnergyPlus Version	7.1.0	Current at time of publication [23]
Inside Convection Algorithm	Simple	EnergyPlus default [23]
Outside Convection Algorithm	Simple Combined	EnergyPlus default [23]
Heat Balance Algorithm	Conduction Transfer Function	EnergyPlus default [26]
Zone Air Heat Balance Algorithm	Third Order Backward Difference	EnergyPlus default [26]
Timestep	6	Largest recommended [26]
Terrain	City	Representative of chosen locations
Solar Reflections	Full Interior and Exterior with Reflections	Provides advanced radiation values based on geometry [26]
<b>Material Assumptions</b>		
Material Roughness	MediumRough	EnergyPlus value for concrete [23]
Thermal Absorptance	0.90	BAHSP specification [28]
Solar Absorptance: Roof	0.75	BAHSP specification [28]
Solar Absorptance: Other	0.60	BAHSP specification [28]
Visible Absorptance: Roof	0.75	BAHSP specification [28]
Visible Absorptance: Other	0.60	BAHSP specification [28]
Window Module	Simple Glazing System	EnergyPlus module to specify code performance, not window type [26]
<b>Internal Mass Material Assumptions</b>		
Material Roughness	MediumSmooth	EnergyPlus value for wood [23]
Thickness	0.10 m	BAHSP total mass ensured [28]
Conductivity	0.15 W/m-K	ASHRAE wood data average [35]
Density	600 kg/m <sup>3</sup>	ASHRAE wood data average [35]
Specific Heat	2350 J/kg-K	ASHRAE wood data average [35]
Thermal Absorptance	0.90	EnergyPlus default [23]
Solar Absorptance	0.70	EnergyPlus default [23]
Visible Absorptance	0.70	EnergyPlus default [23]

Assumption	Value	Reference or Explanation
<b>Ground Heat Transfer Assumptions: Slab</b>		
Surface Emissivity	0.95 (snow and no snow)	Bahnfleth assumptions [65]
Surface Roughness	0.75 cm (no snow) 0.03 cm (snow)	Bahnfleth assumptions [65]
Indoor Combined Heat Transfer	6.13 W/m <sup>2</sup> -K (downward) 9.26 W/m <sup>2</sup> -K (upward)	Bahnfleth assumptions [65]
Surface Albedo	Table A-3	Kung, et al [67]
Soil Density	1200 kg/m <sup>3</sup>	Bahnfleth assumptions [65]
Soil Specific Heat	1200 J/kg-K	Bahnfleth assumptions [65]
Soil Conductivity	1.0 W/m-K	Bahnfleth assumptions [65]
Evapotranspiration	Off	Model stability
Lower Boundary Condition	Zero Flux	EnergyPlus default [23]
Ground Surface Convection	Autocalculate	EnergyPlus default [23]
Slab Insulation	Uninsulated	Insulation included in the equivalent slab properties
Slab Geometry	Equivalent slab using autogrid	EnergyPlus default based on area to perimeter ratio, set to maximum or minimum where slab geometry exceeds allowable range [23]
Domain Clearance	15 m	EnergyPlus and Bahnfleth recommendations [23][65]

Assumption	Value	Reference or Explanation
<b>Ground Heat Transfer Assumptions: Basement</b>		
Surface Emissivity	0.95 (snow and no snow)	Bahnfleth assumptions [65]
Surface Roughness	0.75 cm (no snow) 0.03 cm (snow)	Bahnfleth assumptions [65]
Indoor Heat Transfer Coefficients	Convection Only: 0.92 W/m <sup>2</sup> -K (downward) 4.04 W/m <sup>2</sup> -K (upward) 3.08 W/m <sup>2</sup> -K (horizontal) Convection and Radiation: 6.13 W/m <sup>2</sup> -K (downward) 9.26 W/m <sup>2</sup> -K (upward) 8.29 W/m <sup>2</sup> -K (horizontal)	EnergyPlus default [23]
Surface Albedo	Table A-3	Kung, et al [67]
Soil Density	1200 kg/m <sup>3</sup>	Bahnfleth assumptions [65]
Soil Specific Heat	1200 J/kg-K	Bahnfleth assumptions [65]
Soil Conductivity	1.0 W/m-K	Bahnfleth assumptions [65]
Gravel Density	2000 kg/m <sup>3</sup>	EnergyPlus default [23]
Gravel Specific Heat	720 J/kg-K	EnergyPlus default [23]
Gravel Conductivity	1.9 W/m-K	EnergyPlus default [23]
Evapotranspiration	Off	Model stability
Slab Insulation	0.01 m <sup>2</sup> -K/W	Minimum for model stability, otherwise insulation assumed part of cube model construction
Full Wall Insulation	True	Represents equal surface properties over the entire wall height
Gravel Pit Width	0.01 m	Minimum for model stability
Gravel Depth Above Slab	0.01 m	Minimum for model stability
Gravel Depth Below Slab	0.01 m	Minimum for model stability
Basement Conditioning	True	For preprocessor, necessary for incorporation into EnergyPlus [25]
Slab Geometry	Equivalent sizing using autogrid	EnergyPlus default based on area to perimeter ratio, set to maximum or minimum where geometry exceeds allowable range [23]
Domain Clearance	15 m	EnergyPlus and Bahnfleth recommendations [23][65]

<b>Assumption</b>	<b>Value</b>	<b>Reference or Explanation</b>
<b>Infiltration Assumptions</b>		
Infiltration Module	Design Flow Rate	Chosen to specify infiltration as air changes per hour only
Constant Term Coefficient	1.0	Chosen to specify infiltration as air changes per hour only
Temperature Term Coefficient	0.0	Chosen to specify infiltration as air changes per hour only
Velocity Term Coefficient	0.0	Chosen to specify infiltration as air changes per hour only
Velocity Squared Term Coefficient	0.0	Chosen to specify infiltration as air changes per hour only
<b>Ventilation Assumptions</b>		
Ventilation Module	Design Specification Outdoor Air	Chosen to specify ventilation as air changes per hour only
<b>Occupancy Load Assumptions</b>		
Fraction Sensible	0.573	BAHSP specification [28]
Fraction Radiant	0.435	ASHRAE publication [91]
<b>Lighting Load Assumptions</b>		
Fraction Radiant	0.42	EnergyPlus default [23]
Fraction Visible	0.18	EnergyPlus default [23]
Fraction Replaceable	0.00	Daylighting not considered in lighting use patterns
<b>Domestic Hot Water Assumptions</b>		
Shower Fraction Latent	0.487	BAHSP specification [28]
Shower Fraction Radiant	0.000	Engineering judgment
Shower Fraction Lost	0.000	BAHSP only specifies gains [28]
Bath Fraction Latent	0.000	BAHSP specification [28]
Bath Fraction Radiant	0.000	Engineering judgment
Bath Fraction Lost	0.000	BAHSP only specifies gains [28]
Sinks Fraction Latent	0.312	BAHSP specification [28]
Sinks Fraction Radiant	0.000	Engineering judgment
Sinks Fraction Lost	0.000	BAHSP only specifies gains [28]
System Fraction Latent	0.000	BAHSP specification [28]
System Fraction Radiant	0.000	Engineering judgment
System Fraction Lost	0.000	BAHSP only specifies gains [28]

<b>Assumption</b>	<b>Value</b>	<b>Reference or Explanation</b>
<b>Appliance Assumptions</b>		
Refrigerator Fraction Latent	0.00	BAHSP specification [28]
Refrigerator Fraction Radiant	0.00	ASHRAE publication [91]
Refrigerator Fraction Lost	0.00	BAHSP specification [28]
Clothes Washer Fraction Latent	0.00	BAHSP specification [28]
Clothes Washer Fraction Radiant	0.32	ASHRAE publication [91]
Clothes Washer Fraction Lost	0.20	BAHSP specification [28]
Clothes Dryer Fraction Latent	0.05	BAHSP specification [28]
Clothes Dryer Fraction Radiant	0.09	ASHRAE publication [91]
Clothes Dryer Fraction Lost	0.80	BAHSP specification [28]
Dishwasher Fraction Latent	0.15	BAHSP specification [28]
Dishwasher Fraction Radiant	0.36	ASHRAE publication [91]
Dishwasher Fraction Lost	0.25	BAHSP specification [28]
Range Fraction Latent	0.30	BAHSP specification [28]
Range Fraction Radiant	0.24	ASHRAE publication [91]
Range Fraction Lost	0.30	BAHSP specification [28]
Miscellaneous Electric Load Fraction Latent	0.20	BAHSP specification [28]
Miscellaneous Electric Load Fraction Radiant	0.44	ASHRAE publication [91]
Miscellaneous Electric Load Fraction Lost	0.07	BAHSP specification [28]
<b>Ideal Loads Air System Assumptions</b>		
Heating Supply Temperature	50 C	EnergyPlus default [23]
Cooling Supply Temperature	13 C	EnergyPlus default [23]
Heating Supply Humidity Ratio	0.0156	EnergyPlus default [23]
Cooling Supply Humidity Ratio	0.0077	EnergyPlus default [23]
Heating Limit	No Limit	Idealization of model
Cooling Limit	No Limit	Idealization of model
Dehumidification	Humidistat	BAHSP specification [28]
Humidification	None	BAHSP specification [28]
Demand Controlled Ventilation	None	ASHRAE 62.2 ventilation used [32]
Outdoor Air Economizer	None	EnergyPlus default [23]
Heat Recovery	None	EnergyPlus default [23]

<b>Assumption</b>	<b>Value</b>	<b>Reference or Explanation</b>
<b>Thermostat and Humidistat Assumptions</b>		
Heating Setpoint	21.67 C	BAHSP specification [28]
Cooling Setpoint	24.44 C	BAHSP specification [28]
Dehumidification Setpoint	60.0 %	BAHSP specification [28]

## **A.4 Chapter Summary**

This appendix provides additional information regarding the structure, calculations, and assumptions of the Cube Model. The assumed values have been provided in detail along with the necessary reference materials to obtain further information on the chosen values. These assumptions are essential for the verification of the work or development of any future work based on the results in this report.



# Appendix B

## References

- [1] U.S. Energy Information Administration, *2005 RECS Survey Data*, 2009. Available: <http://www.eia.gov/consumption/residential/data/2005/>.
- [2] Meritage Homes. Interview. Phoenix, AZ, February 13, 2012.
- [3] K.R. Harney. "Mortgage lenders could soon take homes' energy costs into account" *The Washington Post* (October, 2011). Available: [http://www.washingtonpost.com/realestate/mortgage-lenders-could-soon-take-homes-energy-costs-into-account/2011/10/24/gIQAyxjPPM\\_story.html](http://www.washingtonpost.com/realestate/mortgage-lenders-could-soon-take-homes-energy-costs-into-account/2011/10/24/gIQAyxjPPM_story.html).
- [4] A. Stadel, P. Gursel, and E. Masanet. Life Cycle Evaluation of Commercial Buildings: An Overview of the Berkeley Lab Building Materials Pathways (B-PATH) Model, unpublished.
- [5] U.S. Department of Energy, *Building Energy Software Tools Directory*, 2011. Available: [http://apps1.eere.energy.gov/buildings/tools\\_directory/](http://apps1.eere.energy.gov/buildings/tools_directory/).
- [6] D.B. Crawley, J.W. Hand, M. Kummert, and B.T. Griffith. *Contrasting the Capabilities of Building Energy Performance Simulation Programs*, 2005. U.S. Department of Energy. Available: [http://apps1.eere.energy.gov/buildings/tools\\_directory/pdfs/contrasting\\_the\\_capabilities\\_of\\_building\\_energy\\_performance\\_simulation\\_programs\\_v1.0.pdf](http://apps1.eere.energy.gov/buildings/tools_directory/pdfs/contrasting_the_capabilities_of_building_energy_performance_simulation_programs_v1.0.pdf).
- [7] P.A. Strachan, G. Kokogiannakis, and I.A. Macdonald. History and Development of validation with the ESP-r simulation program, 2006. *Building and Environment* 43 (4): pp. 601-609. Available: <http://strathprints.strath.ac.uk/5819/1/strathprints005819.pdf>.

- [8] D.B. Crawley, et al. EnergyPlus: An Update, presented at *SimBuild 2004: IBPSA-USA National Conference*, Boulder, CO, 2004.
- [9] U.S. Department of Energy. *Software Abstract: 000158IBMPC04 DOE2.1E-121*, 2005. Energy Science and Technology Software Center. Available: <http://www.osti.gov/estsc/details.jsp?rcdid=3543>.
- [10] J.F. Kerrisk, B.D. Hunn, N.M. Schnurr, and J.E. Moore. "The Custom Weighting-Factor Method for Thermal-Load Calculations in the DOE-2 Computer Program." Los Alamos Scientific Laboratory Report LA-UR-81-1559, 1981.
- [11] T. Maile, M. Fischer, and V. Bazjanac. "Building Energy Performance Simulation Tools - a Life-Cycle and Interoperable Perspective." Center for Integrated Facility Engineering, Stanford University, Working Paper #WP107. Available: [http://www.stanford.edu/group/CIFE/online\\_publications/WP107.pdf](http://www.stanford.edu/group/CIFE/online_publications/WP107.pdf).
- [12] R. Sullivan and F. Winkelmann. "Validation Studies of the DOE-2 Building Energy Simulation Program," Ernest Orlando Lawrence Berkeley National Laboratory, LBNL-42241, June 1998. Available: <http://www.osti.gov/energycitations/servlets/purl/6488-JT2vxB/webviewable/6488.pdf>.
- [13] S. Andolsun, C. Culp, and J. Haberl. EnergyPlus vs. DOE-2: The Effect of Ground Coupling on Heating and Cooling Energy Consumption of a Slab-on-Grade Code House in a Cold Climate, presented at *SimBuild 2010: IBPSA-USA National Conference*, New York, NY, 2010.
- [14] University of Illinois and Ernest Orlando Lawrence Berkeley National Laboratory, *EnergyPlus Engineering Reference*, May 2012. Available: <http://apps1.eere.energy.gov/buildings/energyplus/pdfs/engineeringreference.pdf>.
- [15] R.H. Henninger and M.J. Witte. *EnergyPlus Testing with Building Thermal Envelope and Fabric Load Tests from ANSI/ASHRAE Standard 140-2011: EnergyPlus Version 7.1.0.012*, 2012. U.S. Department of Energy. Available: [http://apps1.eere.energy.gov/buildings/energyplus/energyplus\\_testing.cfm](http://apps1.eere.energy.gov/buildings/energyplus/energyplus_testing.cfm).
- [16] Department of Mechanical Engineering, University of Strathclyde. *ESP-r*, 2012. Available: <http://www.esru.strath.ac.uk/Programs/ESP-r.htm>.

- [17] A.E. Nakhi. "Adaptive Construction Modelling within Whole Building Dynamic Simulation." Ph.D Thesis, University of Strathclyde, Glasgow, UK, 1995. Available: [http://www.esru.strath.ac.uk/Documents/PhD/nakhi\\_thesis.pdf](http://www.esru.strath.ac.uk/Documents/PhD/nakhi_thesis.pdf).
- [18] PASSYS-1 Project, "PASSYS. Final Report of the Simplified Design Tool Subgroup," Commission of the European Communities, Directorate General XII, report EUR 12 998 EN, 1989. Available: <http://www.buildup.eu/publications/1662>.
- [19] University of Wisconsin-Madison. *A TRAnsient SYstems Simulation Program*, 2012. Available: <http://sel.me.wisc.edu/trnsys/default.htm>.
- [20] M. Hiller, S. Holst, A.Knirsch, and M. Schuler. Trnsys 15 – A Simulation Tool for Innovative Concepts, presented at *Seventh International IBPSA Conference*, Rio de Janeiro, Brazil, 2001.
- [21] M.J. Witte, R.H. Henninger, J. Giazer, and D.B. Crawley. Testing and Validation of a New Building Energy Simulation Program, presented at *Seventh International IBPSA Conference*, Rio de Janeiro, Brazil, 2001.
- [22] E. Kossecka, J. Kosny, A. Desjarlais, and J. Christian. *Dynamic Thermal Performance and Energy Benefits of Using Massive Walls in Residential Buildings*, 2001. Oak Ridge National Labs and Polish Academy of Sciences. Available: [http://www.ornl.gov/sci/roofs+walls/research/detailed\\_papers/dyn\\_perf/](http://www.ornl.gov/sci/roofs+walls/research/detailed_papers/dyn_perf/).
- [23] EnergyPlus Energy Simulation Software version 7.1.0. US Department of Energy, 2012. Available: <http://www.energyplus.gov>.
- [24] J. Neymark, et al. IEA BESTEST In-Depth Diagnostic Cases for Ground Coupled Heat Transfer Related to Slab-On- Grade Construction. Golden, Colorado: National Renewable Energy Laboratory, 2008. In Conjunction with International Energy Agency Solar, Heating and Cooling Programme Task 34 / Energy Conservation in Buildings and Community Systems Annex 43. Available: <http://www.nrel.gov/docs/fy08osti/43388.pdf>.
- [25] University of Illinois and Ernest Orlando Lawrence Berkeley National Laboratory, *Auxiliary EnergyPlus Programs*, May 2012. Available: <http://apps1.eere.energy.gov/buildings/energyplus/pdfs/auxiliaryprograms.pdf>.
- [26] University of Illinois and Ernest Orlando Lawrence Berkeley National Laboratory, *Input/ Output Reference*, May 2012. Available: <http://apps1.eere.energy.gov/buildings/energyplus/pdfs/inputoutputreference.pdf>.

- [27] International Code Council, *2012 International Building Code*, Falls Church, VA: International Building Code, 2011. Available: <http://publicecodes.citation.com/icod/ibc/2012/>.
- [28] R. Hedron and C. Engebrecht, *Building America House Simulation Protocols*, Oak Ridge, TN: National Renewable Energy Laboratory, U.S. Department of Energy, 2010.
- [29] International Code Council, *2012 International Energy Conservation Code*, Falls Church, VA: International Code Council, 2011. Available: <http://publicecodes.citation.com/icod/iecc/2012/>.
- [30] Thermal Environmental Conditions for Human Occupation, American Society of Heating, Refrigerating and Air-Conditioning Engineers, Inc. Standard 55-2010, 2010.
- [31] American Society of Heating, Refrigerating and Air-Conditioning Engineers, Inc. *Resources and Publications: Standard 55*. Available: <http://www.ashrae.org/resources--publications/bookstore/standard-55>.
- [32] Ventilation and Acceptable Indoor Air Quality in Low-Rise Residential Buildings, American Society of Heating, Refrigerating and Air-Conditioning Engineers, Inc. Standard 62.2-2010, 2010.
- [33] Energy Standard for Buildings Except Low-Rise Residential Buildings, American Society of Heating, Refrigerating and Air-Conditioning Engineers, Inc. Standard 90.1-2010, 2010.
- [34] U.S. Department of Energy. *Building Energy Codes 101: An Introduction*, 2010. Available: <http://www.ashrae.org/standards-research--technology/standards--guidelines>.
- [35] American Society of Heating, Refrigerating and Air-Conditioning Engineers, Inc., *2009 ASHRAE Handbook - Fundamentals (SI Edition)*, Atlanta, GA: American Society of Heating, Refrigerating and Air-Conditioning Engineers, Inc., 2009.
- [36] M.G. Davies, *Building Heat Transfer*, Chichester, England: John Wiley & Sons, Ltd, 2004.
- [37] C.A. Balaras. (1996). The Role of Thermal Mass on the Cooling Load of Buildings. An Overview of Computational Methods. *Energy and Buildings* 24, pp. 1-10.
- [38] S.A. Kalogirou, G. Florides, and S. Tassou. (2002). Energy analysis of buildings employing thermal mass in Cyprus. *Renewable Energy* 27: pp. 353-368.
- [39] The Chartered Institution of Building Services Engineers London. *CIBSE Guide A: Environmental Design*. 7th edition. Norwich, UK: Page Bros (Norwich) Ltd., 2006.

- [40] J. Kosny, T. Petrie, D. Gawin, P. Childs, A. Desjarlais, and J. Christian. *Thermal Mass -- Energy Savings Potential in Residential Buildings*, 2001. Oak Ridge National Labs and Polish Academy of Sciences. Available: [http://www.ornl.gov/sci/roofs+walls/research/detailed\\_papers/thermal/](http://www.ornl.gov/sci/roofs+walls/research/detailed_papers/thermal/).
- [41] N. Chaturveti and J.E. Braun. "Analytical Tools for Dynamic Building Control." ASHRAE Report #5031-1, October 2000.
- [42] D. Bennett. *Sustainable Concrete Architecture*. London: RIBA Publishing, 2010.
- [43] E. Kossecka and J. Kosny. (2002). Influence of insulation configuration on heating and cooling loads in a continuously used building. *Energy and Buildings* 34: pp. 321-331.
- [44] H.K. Lee and J.E. Braun. (2006). An Experimental Evaluation of Demand-Limiting Using Building Thermal Mass in a Small Commercial Building. *ASHRAE Transactions* 112 (1): pp. 559-571.
- [45] K. Gregory, B. Moghtaderi, H. Sugo, and A Page (2008). Effect of thermal mass on the thermal performance of various Australian residential construction systems. *Energy and Buildings* 40: pp. 459-465.
- [46] K.H. Lee and J.E. Braun (2008). A Data-Driven Method for Determining Zone Temperature Trajectories that Minimize Peak Electrical Demand. *ASHRAE Transactions* 114 (2): pp. 1-10.
- [47] P.R. Armstrong, S.B. Leeb, and L.K. Norford (2006). Control with Building Mass – Part II: Simulation. *ASHRAE Transactions* 112 (1).
- [48] Development and Application of an Inverse Building Model for Demand Response in Small Commercial Buildings, presented at *SimBuild 2004: IBPSA-USA National Conference*, Boulder, CO, 2004.
- [49] J.E. Braun and K.H. Lee (2006). Assessment of Demand Limiting Using Building Thermal Mass in Small Commercial Buildings. *ASHRAE Transactions* 112 (1): pp. 547-558.
- [50] P. Xu and P. Haves (2006). Case Study of Demand Shifting with Thermal Mass in Two Large Commercial Buildings. *ASHRAE Transactions* 112 (1): pp. 572-580.
- [51] Lawrence Berkeley National Laboratory. "Demand Shifting with Thermal Mass in Large Commercial Buildings: Field Tests, Simulations, and Audits." LBNL-58815, January 2006.

- [52] K.R. Keeney and J.E. Braun. (1997). Application of Building Precooling to Reduce Peak Cooling Requirements. *ASHRAE Transactions 103 (1)*: pp. 463-469.
- [53] M.L. Marceau and M.G. VanGeem. "Modeling Energy Performance of Concrete Buildings for LEED-NC Version 2.2: Energy and Atmosphere Credit 1." Portland Cement Association R&D Serial No. 2880a, 2007.
- [54] U.S. Green Building Council, *What LEED Is*, 2011. Available: <http://www.usgbc.org/DisplayPage.aspx?CMSPageID=1988>.
- [55] E. Kossecka and J. Kosny. Relations between Structural and Dynamic Thermal Characteristics of Building Walls, presented at *1996 International Symposium of CIB W67 "Energy and Mass flow in the Life cycle of Buildings"*, Vienna, Austria, 1996.
- [56] E. Kossecka and J. Kosny. *Effects of Different Sequences of Materials in the Massive Walls on Energy Consumption in Continuously Used Residential Buildings*, 2001. Oak Ridge National Labs and Polish Academy of Sciences. Available: [http://www.ornl.gov/sci/roofs+walls/research/detailed\\_papers/effects/](http://www.ornl.gov/sci/roofs+walls/research/detailed_papers/effects/).
- [57] D.M. Ogoli. (2003). Predicting indoor temperatures in closed buildings with high thermal mass. *Energy and Buildings 35*: pp. 851-862.
- [58] J. Khedari, M. Rungsiyopas, R. Sarachitti, and J. Hirunlabh (2004). A new type of vented concrete block for zero cooling energy. *Building and Environment 39*: pp. 1193-1197.
- [59] H.D. Baehr and K. Stephan, *Heat and Mass Transfer*, Berlin: Springer, 2011.
- [60] P. von Böckh and T. Wetzel. *Heat Transfer: Basics and Practice*. New York: Springer, 2012.
- [61] U.S. Census Bureau. *Profile of General Population and Housing Characteristics: 2010*, 2010. Available: [http://factfinder2.census.gov/faces/tableservices/jsf/pages/productview.xhtml?pid=DEC\\_10\\_DP\\_DPDP1&prodType=table](http://factfinder2.census.gov/faces/tableservices/jsf/pages/productview.xhtml?pid=DEC_10_DP_DPDP1&prodType=table).
- [62] U.S. Department of Energy. *Building America -- Resources for Energy Efficient Homes: Analysis Spreadsheets*, 2011. Available: [http://www1.eere.energy.gov/buildings/building\\_america/analysis\\_spreadsheets.html](http://www1.eere.energy.gov/buildings/building_america/analysis_spreadsheets.html).
- [63] Energy Star Home Sealing Specification, Energy Star Version 1.0, 2001. Available: [http://www.energystar.gov/ia/home\\_improvement/home\\_sealing/ES\\_HS\\_Spec\\_v1\\_0b.pdf](http://www.energystar.gov/ia/home_improvement/home_sealing/ES_HS_Spec_v1_0b.pdf).

- [64] M. Sherman and D. Dickerhoff, "Air-Tightness of U.S. Dwellings," Lawrence Berkeley Laboratory, University of California, Berkeley, CA, LBL-35700, Aug. 1998. Available: [http://epb.lbl.gov/database/docs/leakage\\_db.pdf](http://epb.lbl.gov/database/docs/leakage_db.pdf).
- [65] W.P. Bahnfleth and C.O. Pedersen. (1990). A Three-Dimensional Numerical Study of Slab-on-Grade Heat Transfer. *ASHRAE Transactions [Online]* 96(2), pp. 61-72. Available: [http://www.engr.psu.edu/ae/faculty/bahnfleth/3D\\_numerical\\_study.pdf](http://www.engr.psu.edu/ae/faculty/bahnfleth/3D_numerical_study.pdf).
- [66] W.P. Bahnfleth, "Three-Dimensional Modelling of Heat Transfer From Slab Floors," US Army Core of Engineers Construction Engineering Research Laboratory, Champaign, IL, USACERL Technical Manuscript E-89/11, July 1989.
- [67] E.C. Kung, R.A. Bryson, and D.H. Lenschow. (1964, Dec.). Study of a Continental Surface Albedo on the Basis of Flight Measurements and Structure of the Earth's Surface Cover over North America. *Monthly Weather Review [Online]* 92, pp. 543-564. Available: <http://docs.lib.noaa.gov/rescue/mwr/092/mwr-092-12-0543.pdf>.
- [68] HercuWall. *HercuWall®: Stronger Faster Smarter*, 2012. Available: <http://www.hercuwall.com/>.
- [69] TF Forming Systems. *Technical Library: TransForm*, 2012. Available: <http://www.tfsystem.com/TechnicalLibrary/TransFormManual.aspx>.
- [70] R. Ghattas. "Wall Sections." Personal E-mail (July 17, 2012)
- [71] R. Ghattas. "Last Wall Section." Personal E-mail (July 19, 2012)
- [72] BLOCK USA. *Concrete Masonry Units Size and Shape Guide*, 2012. Available: <http://www.specblockusa.com/downloads/franklin/CMUguide.pdf>.
- [73] "Material Properties." *The Engineering Toolbox*, 2012. Available: [http://www.engineeringtoolbox.com/material-properties-t\\_24.html](http://www.engineeringtoolbox.com/material-properties-t_24.html).
- [74] Y.A. Çengel, R.H. Turner, and J.M. Cimbala, *Fundamentals of Thermal-Fluid Sciences*, New York: The McGraw-Hill Companies, 2008.
- [75] DuPont. *DuPont™ Tyvek® ThermaWrap™*, 2012. Available: [http://www2.dupont.com/Tyvek\\_Weatherization/en\\_US/products/residential/resi\\_thermawrap.html](http://www2.dupont.com/Tyvek_Weatherization/en_US/products/residential/resi_thermawrap.html).

- [76] Dow Building Solutions. *STYROFOAM™ Brand PANELMATE™*, 2012. Available: <http://building.dow.com/na/en/products/insulation/panelmateultra.htm>.
- [77] MATBASE. *DATA TABLE FOR: Polymers: Commodity Polymers: PVC soft*, 2009. Available: <http://www.matbase.com/material/polymers/commodity/soft-pvc/properties>.
- [78] J. Ochsendorf, et al, “Methods, Impacts, and Opportunities in the Concrete Building Life Cycle,” Concrete Sustainability Hub, Massachusetts Institute of Technology, Cambridge, MA, Research Report R11-01 Department of Civil and Environmental Engineering, Aug. 2011.
- [79] MIT Concrete Sustainability Hub LCAb Group, Internal Progress Memo - Single-Family Residential, unpublished.
- [80] CHI\_ICF4in\_Infil\_a\_GndTemps\_Exh100perASHRAE\_Avg.idf. Cambridge, MA: Concrete Sustainability Hub, Massachusetts Institute of Technology, unpublished.
- [81] CHI\_WOOD\_Infil\_a\_GndTemps\_Exh100perASHRAE\_Avg.idf. Cambridge, MA: Concrete Sustainability Hub, Massachusetts Institute of Technology, unpublished.
- [82] PHX\_ICF4in\_Infil\_a\_GndTemps\_Exh100perASHRAE\_Avg.idf. Cambridge, MA: Concrete Sustainability Hub, Massachusetts Institute of Technology, unpublished.
- [83] PHX\_WOOD\_Infil\_a\_GndTemps\_Exh100perASHRAE\_Avg.idf. Cambridge, MA: Concrete Sustainability Hub, Massachusetts Institute of Technology, unpublished.
- [84] A. Webb. “BAHSP Model.” Personal E-mail (June 18, 2012)
- [85] S. Kim and J. Haberl. *Detailed Analysis of the Thermal Mass Credits in a Code-Traceable DOE-2 Simulation of the 2001 IECC for a Single-Family Residence in Texas*, 2008. Energy Systems Lab, Texas A&M University. Available: <http://www-esl.tamu.edu/docs/terp/2008/ESL-HH-08-12-32.pdf>.
- [86] R. Rowlett. *How Many? A Dictionary of Units of Measurement*, 2012. The University of North Carolina at Chapel Hill. Available:<http://www.unc.edu/~rowlett/units/dictR.html>.
- [87] Passive House Institute US. *What is Passive House?*, 2011. Available: <http://www.passivehouse.us/passiveHouse/PassiveHouseInfo.html>.



- [88] H. Erhorn-Kluttig, H. Erhorn, and H. Lahmidi. "Airtightness Requirements for High Performance Building Envelopes," ASIEPI Information Paper P157, 2009. Available: <http://www.buildup.eu/publications/5656>.
- [89] International Code Council, *2009 International Energy Conservation Code*, Falls Church, VA: International Code Council, 2009. Available: <http://publicecodes.citation.com/icod/iecc/2009/>.
- [90] U.S. Census Bureau, *State & County QuickFacts*. Available: [quickfacts.census.gov](http://quickfacts.census.gov).
- [91] C.S. Barnaby, J.D. Spitler, and D. Xiao. (2005). The Residential Heat Balance Method for Heating and Cooling Load Calculations. *ASHRAE Transactions 111(1)*: pp. 308-320.